Highlights from ATLAS

LISHEP 2023: 5-10 March 2023

UERJ, Rio de Janeiro, Brasil

Marisilvia Donadelli, on behalf of the ATLAS Collaboration
University of Sao Paulo

A Toroidal LHC ApparatuS

- layered detector surrounding the interaction point: central tracker inside of a solenoid, calorimeters and an independent muon spectrometer with superconducting toroids

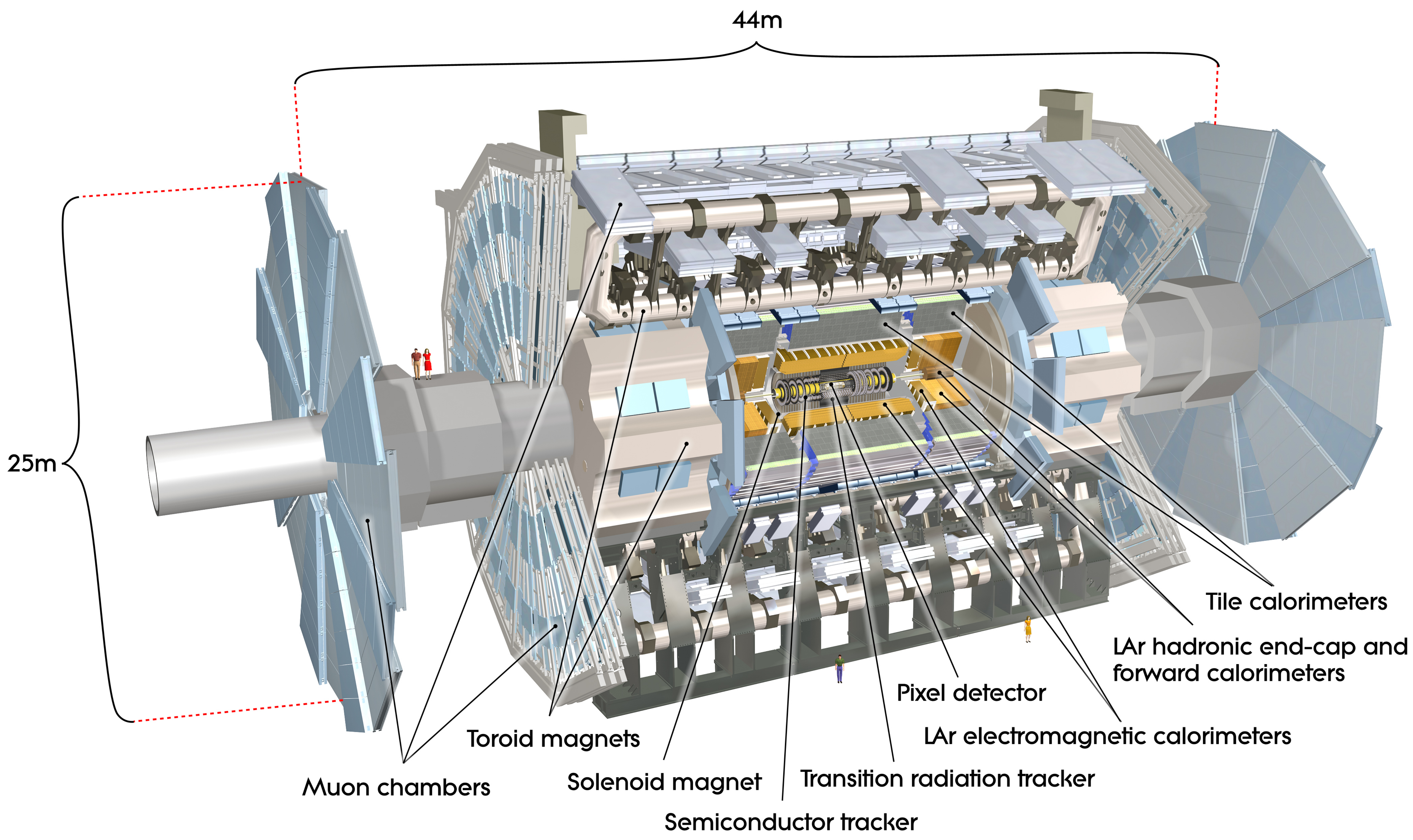

- fast triggering on interesting signatures
  - precise reconstruction of
    - collision vertices
    - photons and electrons
    - muons
    - taus
    - jets
    - missing transverse momentum
    - identification of heavy flavour jets

Performance with Run-2 data set

ATLAS Run 2 pp data set

- Run 2 (2015-2018) recorded after Run 1 data set (2010-2012)
- 95.6 % data quality efficiency
- most results in this talk: 139 fb^{-1} data for physics analysis at $\sqrt{s}$ = 13 TeV

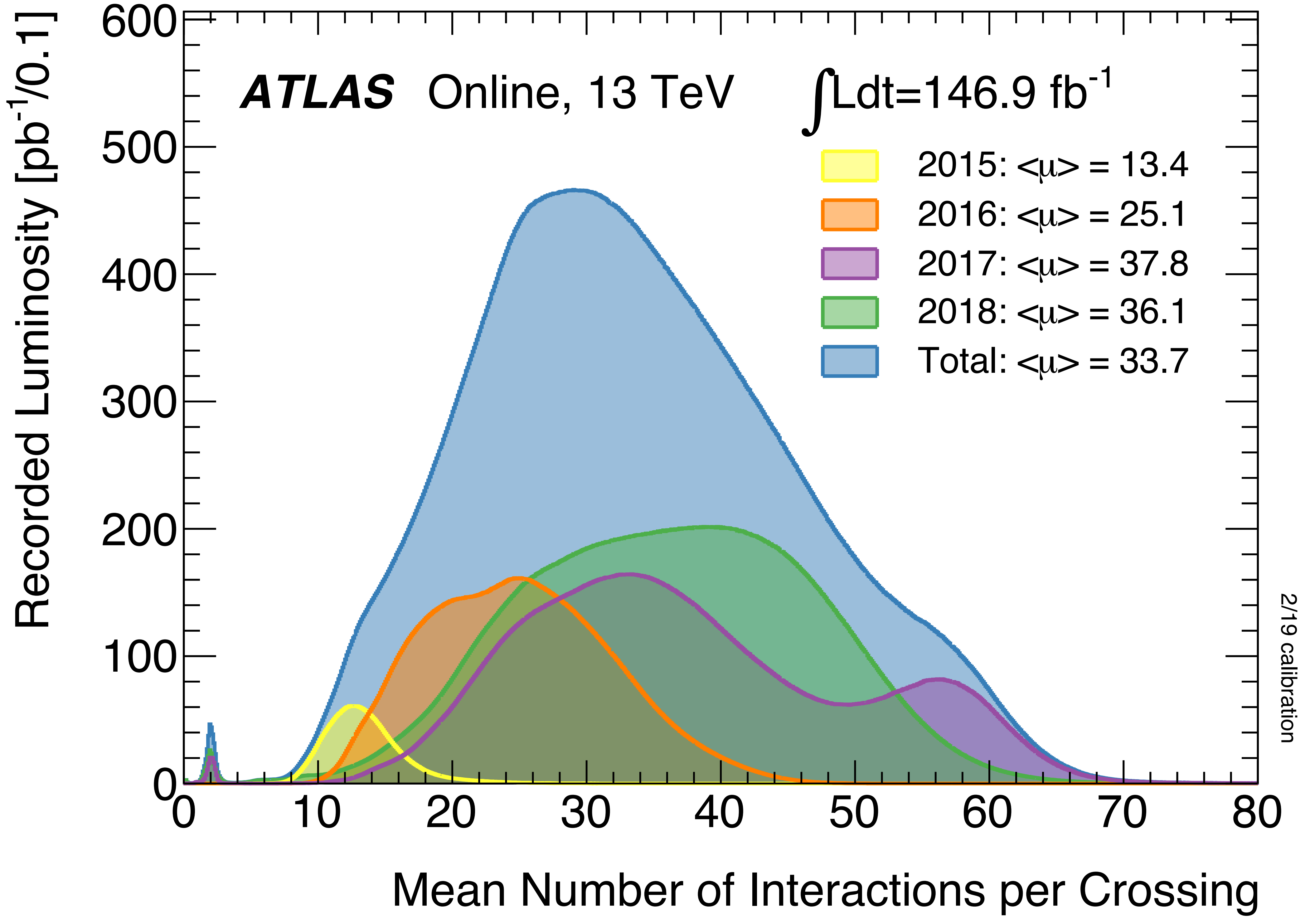

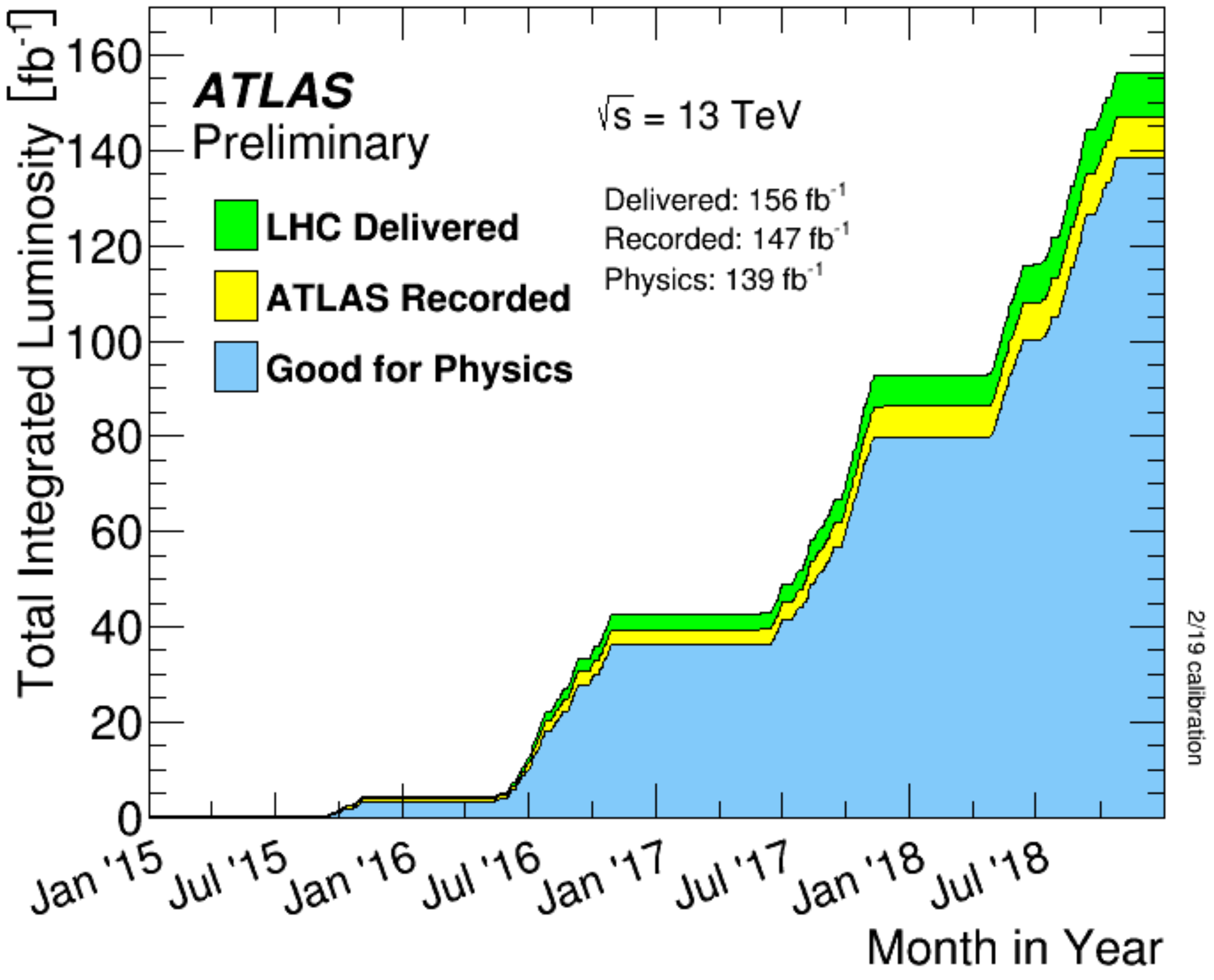

Final luminosity for Run 2 pp

NEW

- based on complimentary measurements from LUCID, Inner Detector and Calorimeters
- absolute calibration of LUCID from dedicated vdM scans each year
- final result for standard high pileup sample $\mathbf{L_{int} = 140.1 \pm 1.2\ fb^{-1}}$
- unprecedented uncertainty of **0.83%**
- 0.9% achieved by second-generation ISR experiments

[arXiv:2212.09379 (Submitted to: EPJC)](https://arxiv.org/abs/2212.09379)

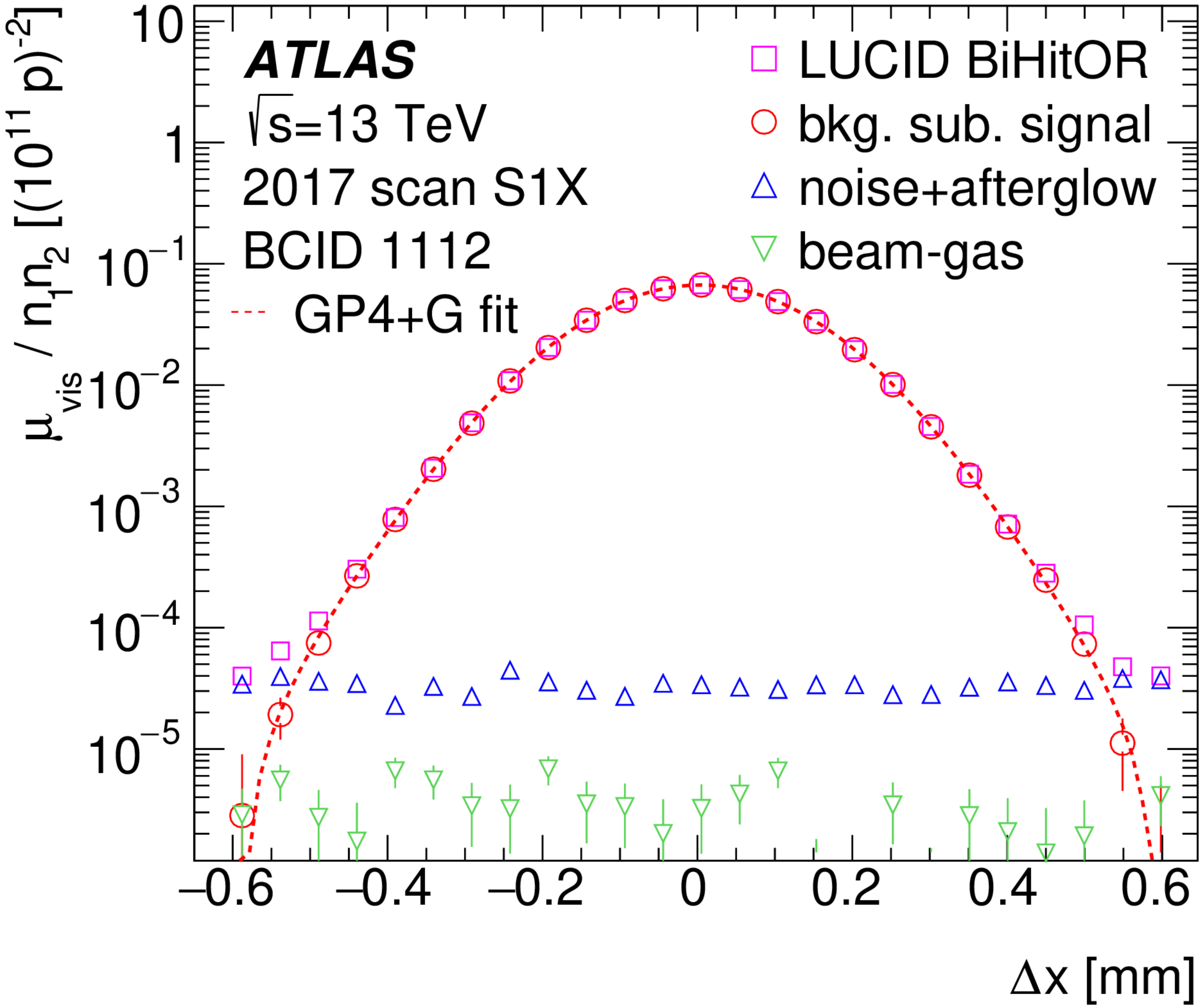

Run 2 performance highlights

- trigger algorithms and selections optimised to cope with pile-up conditions
- continuous improvements of identification and calibration of reconstructed objects

Eur. Phys. J. C 82 (2022) 223

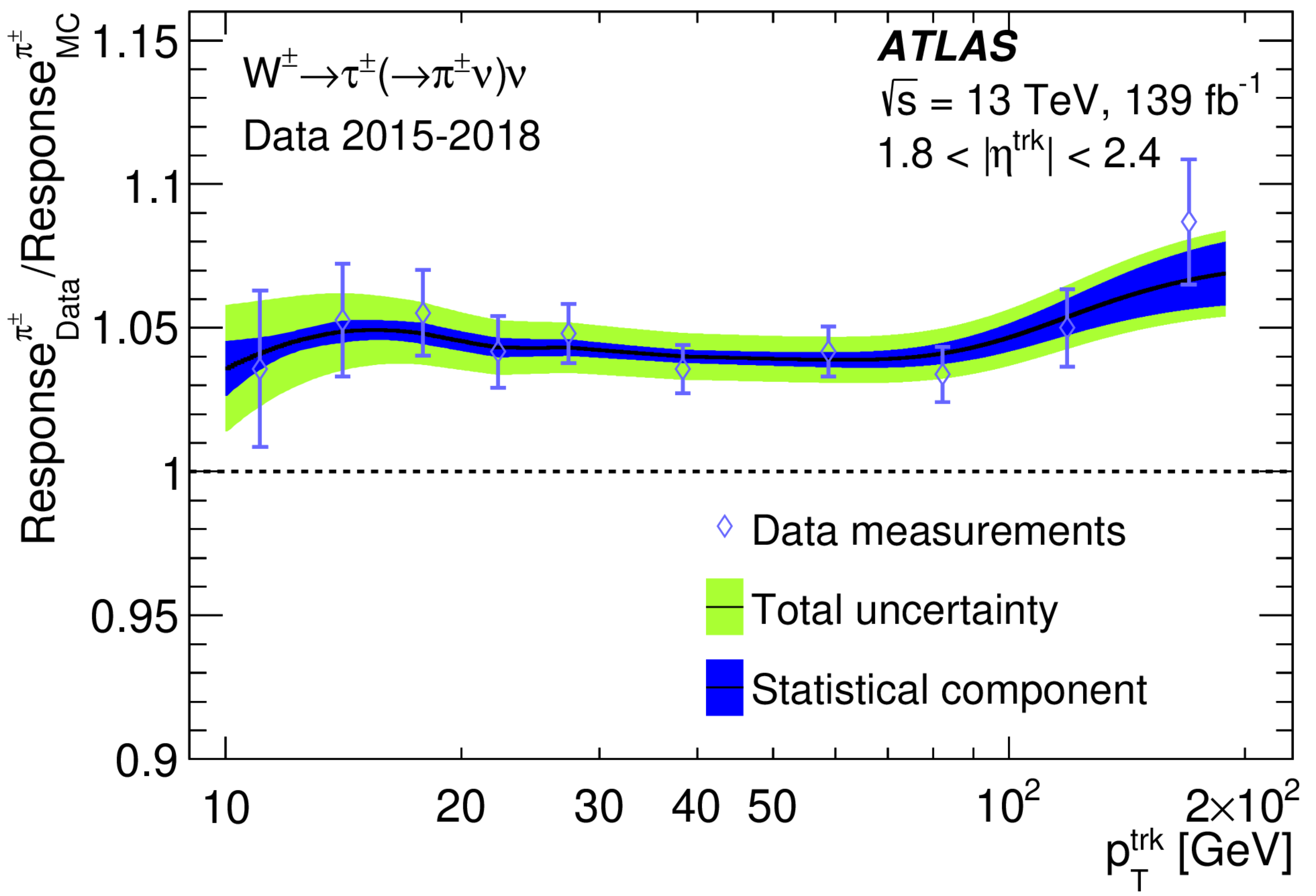

high p_T hadron calibration with $W\to\tau\to\pi$

Eur. Phys. J. C 80 (2020) 47

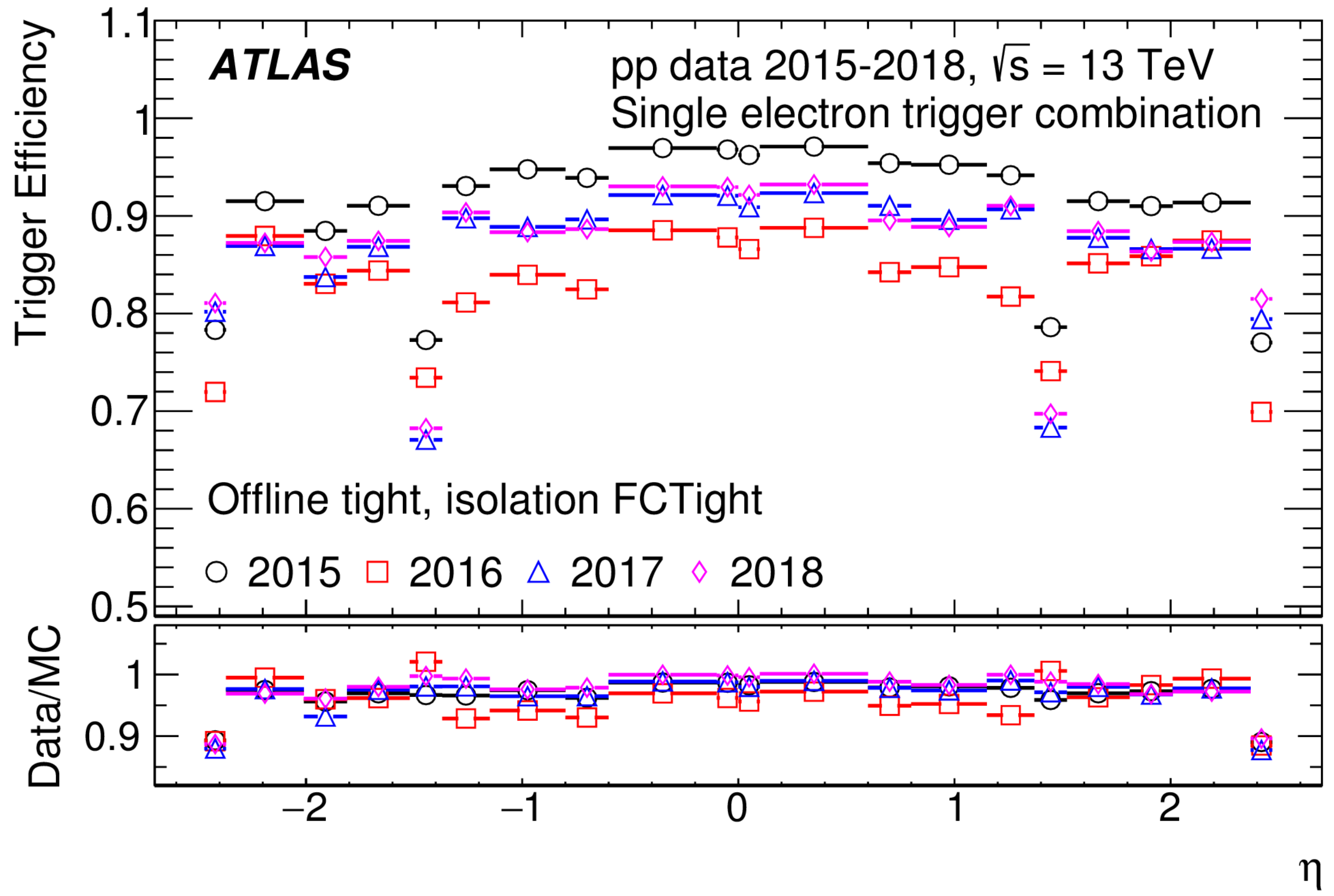

electron trigger efficiency

Eur. Phys. J. C 81 (2021) 578

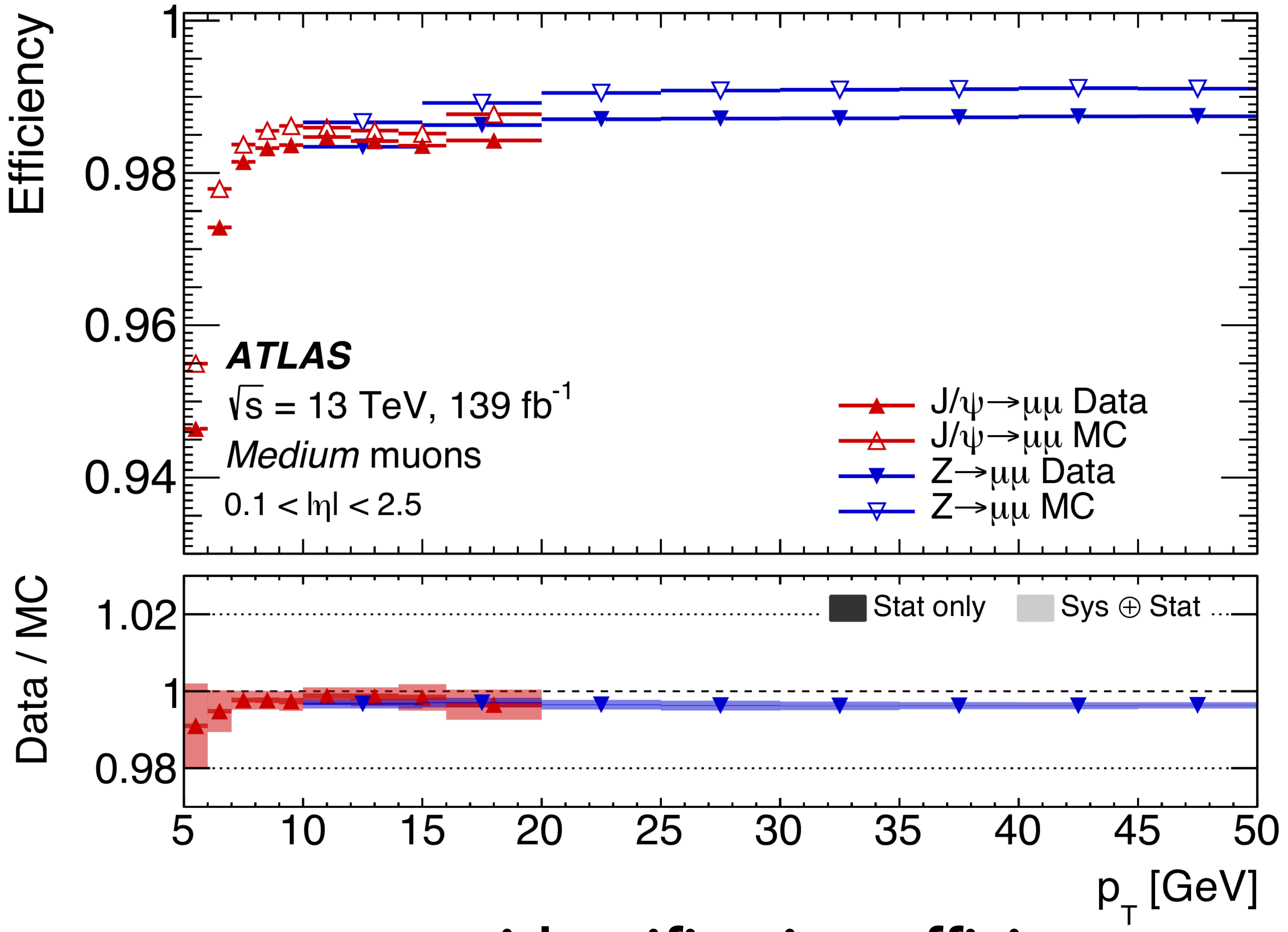

muon identification efficiency

- excellent MC modelling with correction factors (generally close to 1) measured in data

Run 2 flavour tagging

arXiv:2211.16345 (Submitted to: EPJC)

MV2: BDT combines the outputs of low-level taggers IP3D, SV1 and JetFitter

DL1r : Deep feed-forward neural network uses the same inputs and multi-dimensional outputs - P(light), P(c-jet), P(b-jet)

DL1r substantially **outperforms** all **low-level taggers** across the ε_b range!

Per-b-jet tagging efficiency increased

70% → 77%

(HH analyses example: x 2 or 4 b-jets per event)

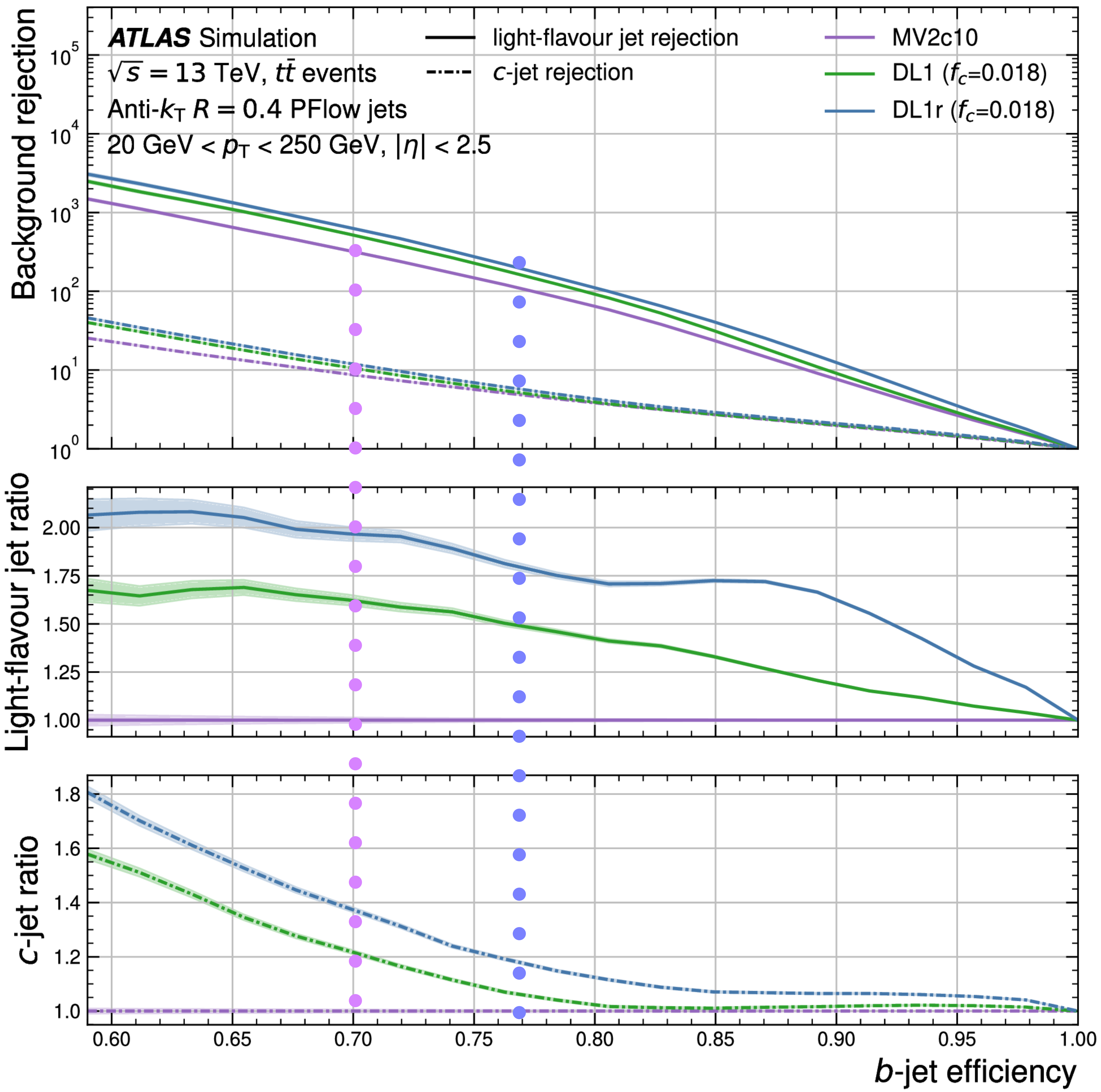

Tau identification

ATL-PHYS-PUB-2019-033

RNN

employs information from reconstructed charged-particle tracks and clusters of energy in the calorimeter associated to $\tau_{\text{had-vis}}$ candidates as well as high-level discriminating variables

Factor 2 performance improvement compared to BDT ID

Per-tau efficiency increased:

1-prong: 75% → 85%

3-prong: 60% → 75%

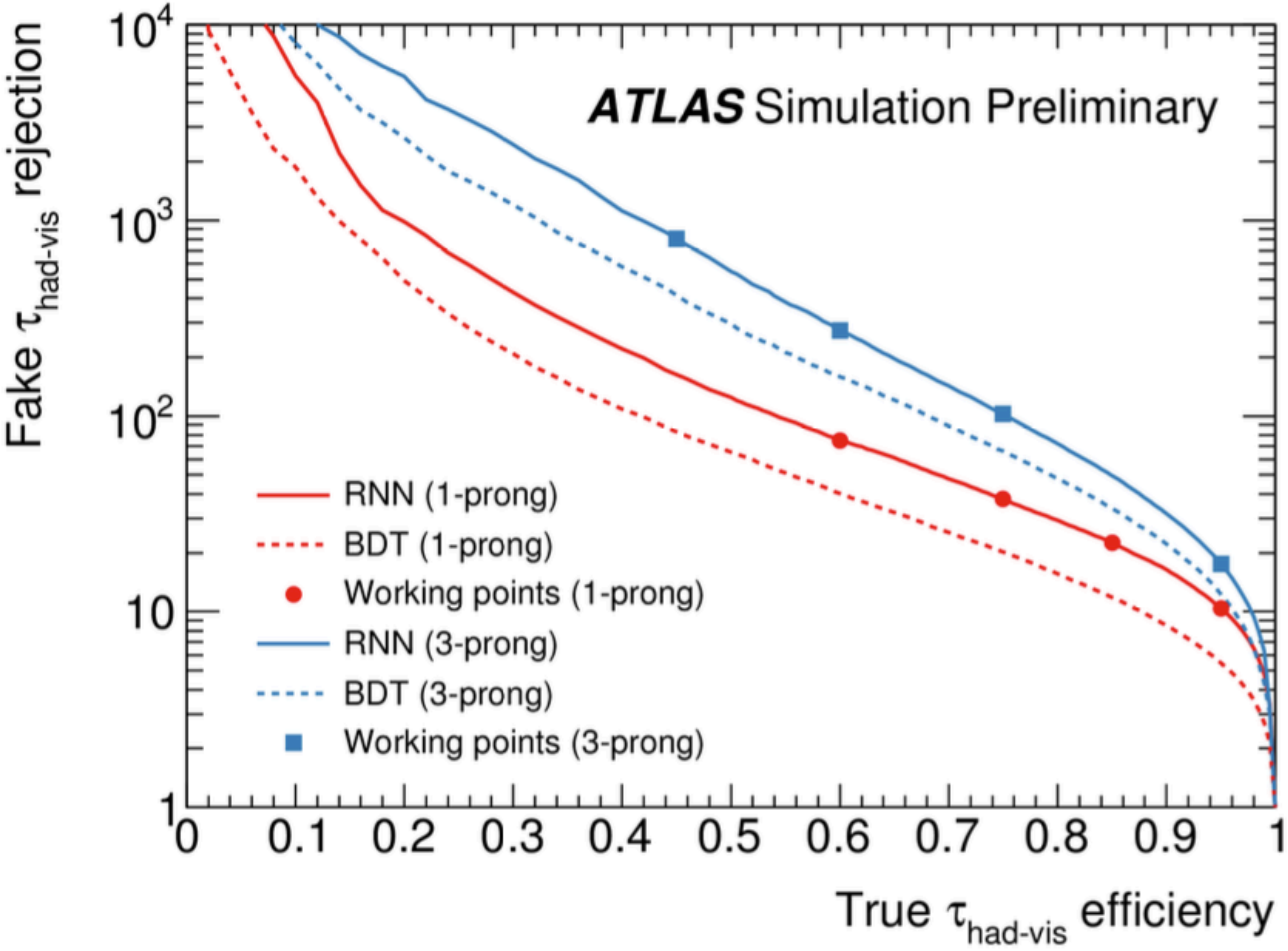

Run-2 Physics Highlights

- SM
- Top
- B physics
- Higgs
- HDBS
- Exotics
- Supersymmetry

Tuesday, 16:40 Standard Model and Top results from ATLAS - Carlos Alberto Gottardo

Tuesday, 17:00 Heavy Flavor results from ATLAS - Markus Cristinziani

Tuesday, 17:20 Search for BSM Physics in ATLAS - Rafael Coelho Lopes de Sá

Standard Model Total Production Cross Section Measurements

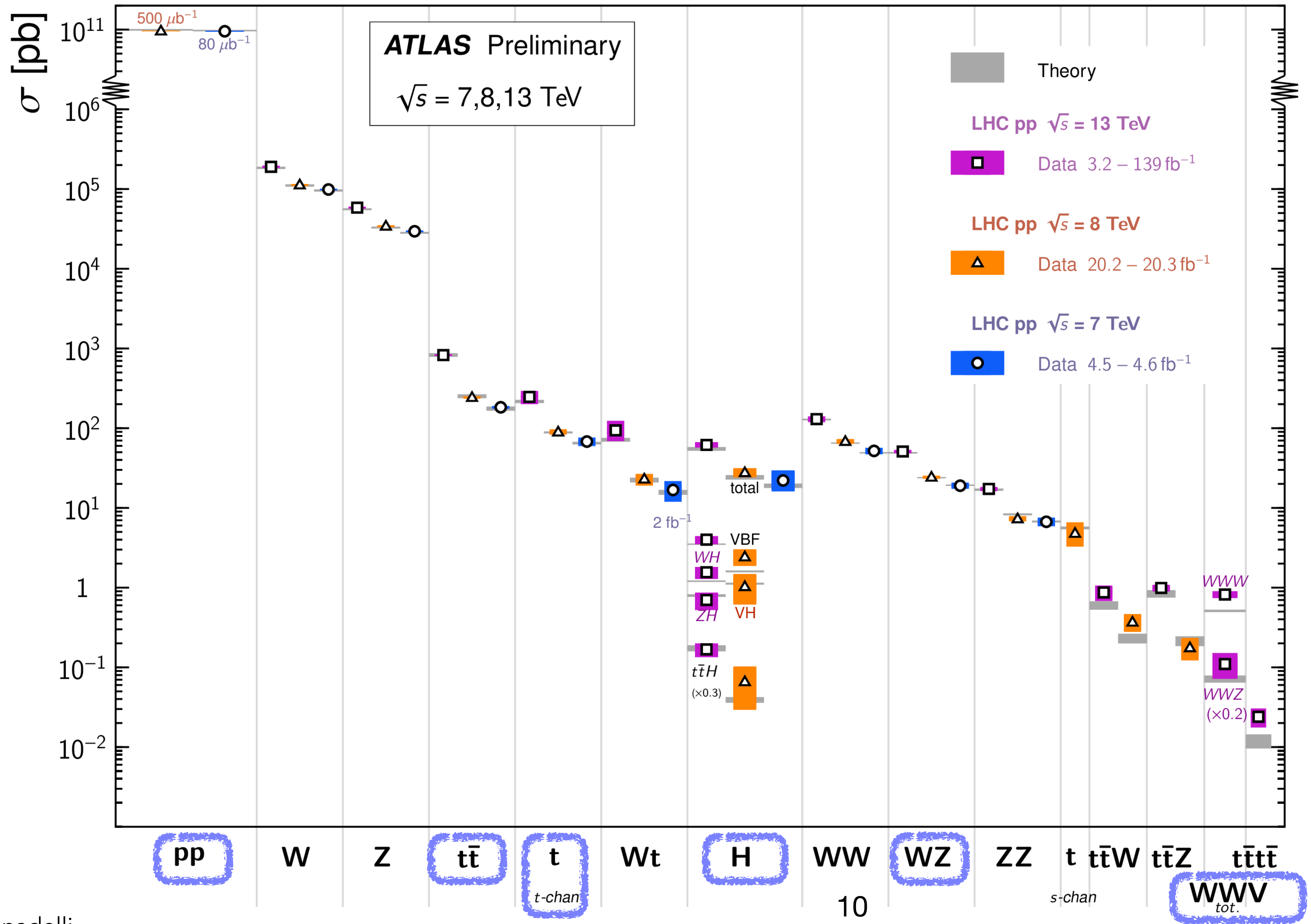

ATL-PHYS-PUB-2022-009

Total pp cross-section

- Differential dσ/dt pp→elastic cross section
  - ALFA subdector : measure scattered protons with detectors located in roman pots ~240 m from IP
  - special run (~340 μb^{-1}) with β* optics = 2.5 km
  - measure Mandelstam ‘t' distribution
  - luminosity calibration from vdM scans
- From precise dσ/dt:
  - ρ (real/imaginary part of elastic-scattering amplitude for t→0)

ρ = 0.098 ± 0.011

σ_{total}= 104.7 ± 1.1 mb
(from optical theorem)

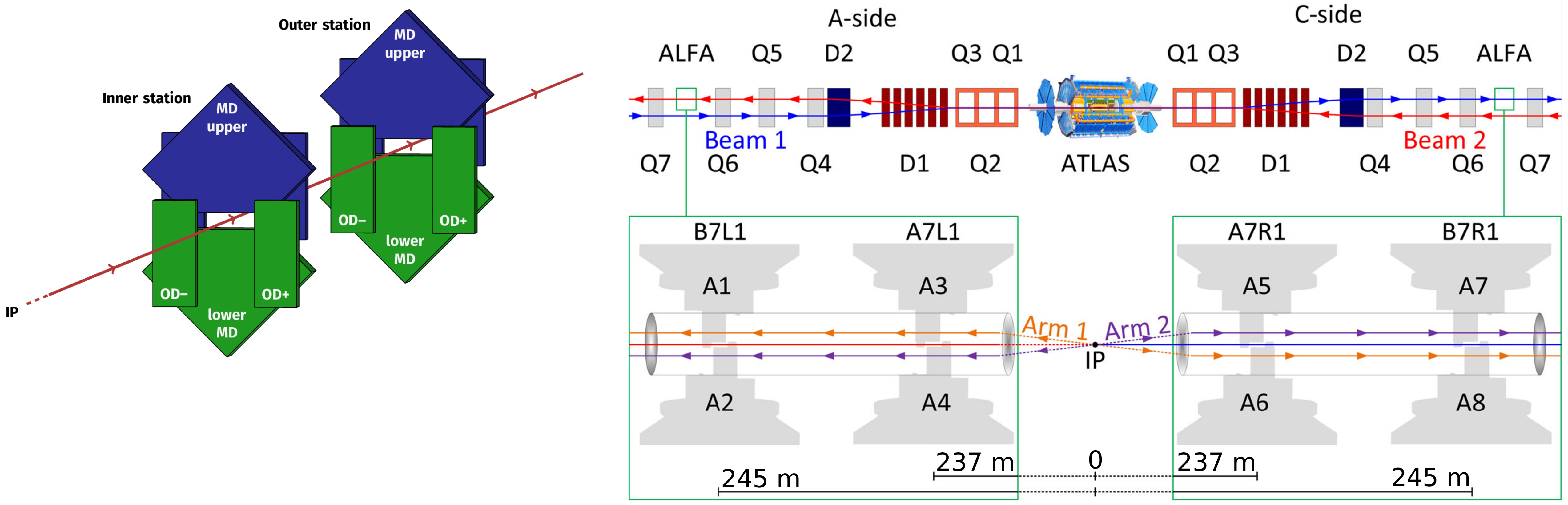

arXiv:2207.12246 (Submitted to: EPJC)

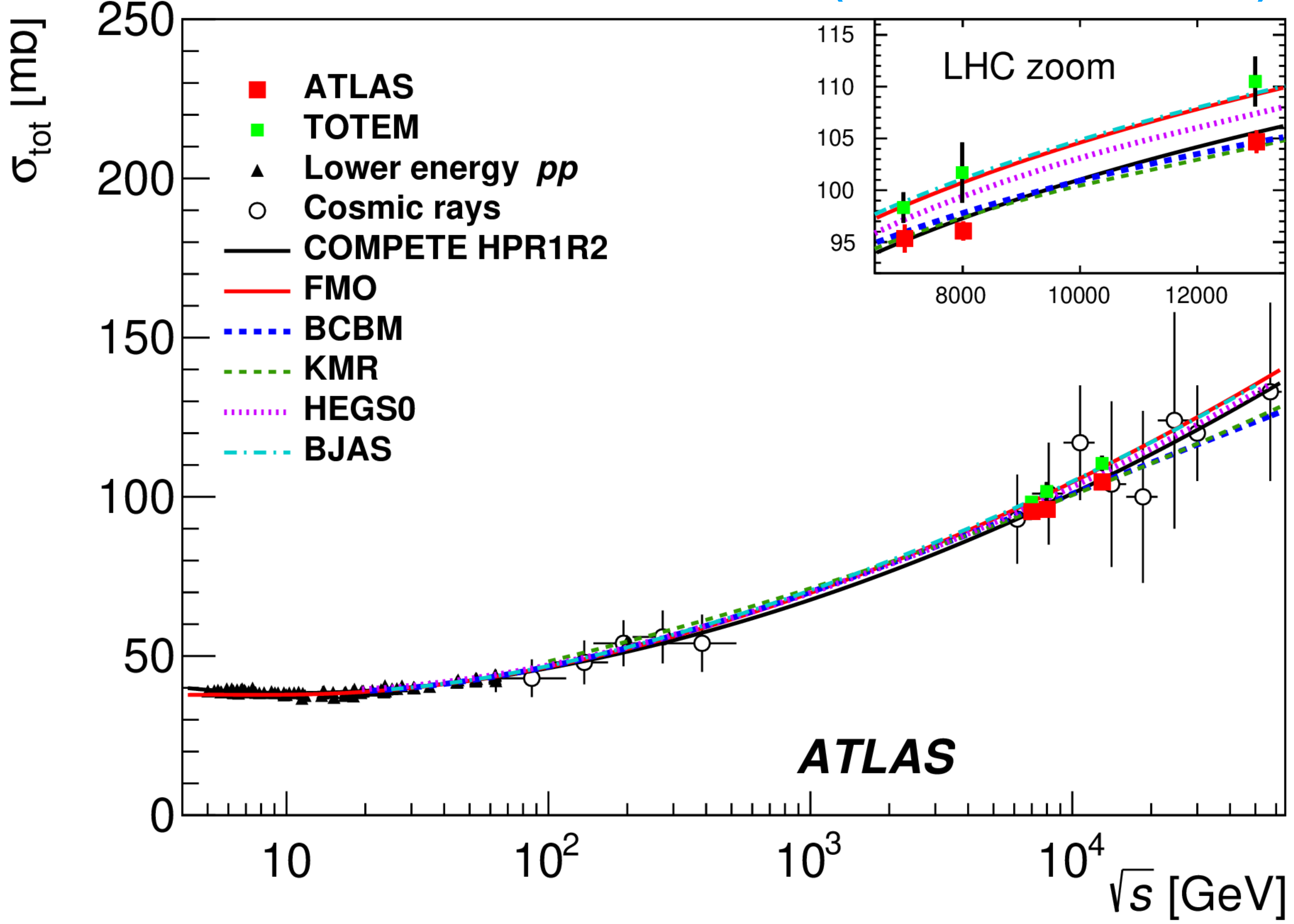

Observation of WWW production

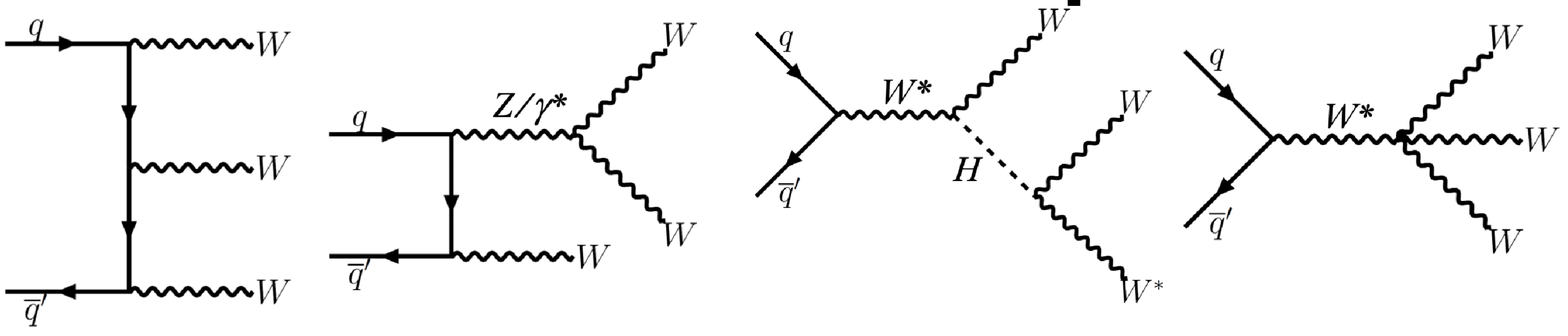

- two channels: WWW→ 3l3v and WWW→ 2l2vjj
- dedicated CR for background modelling, MVA analysis to enhance signal

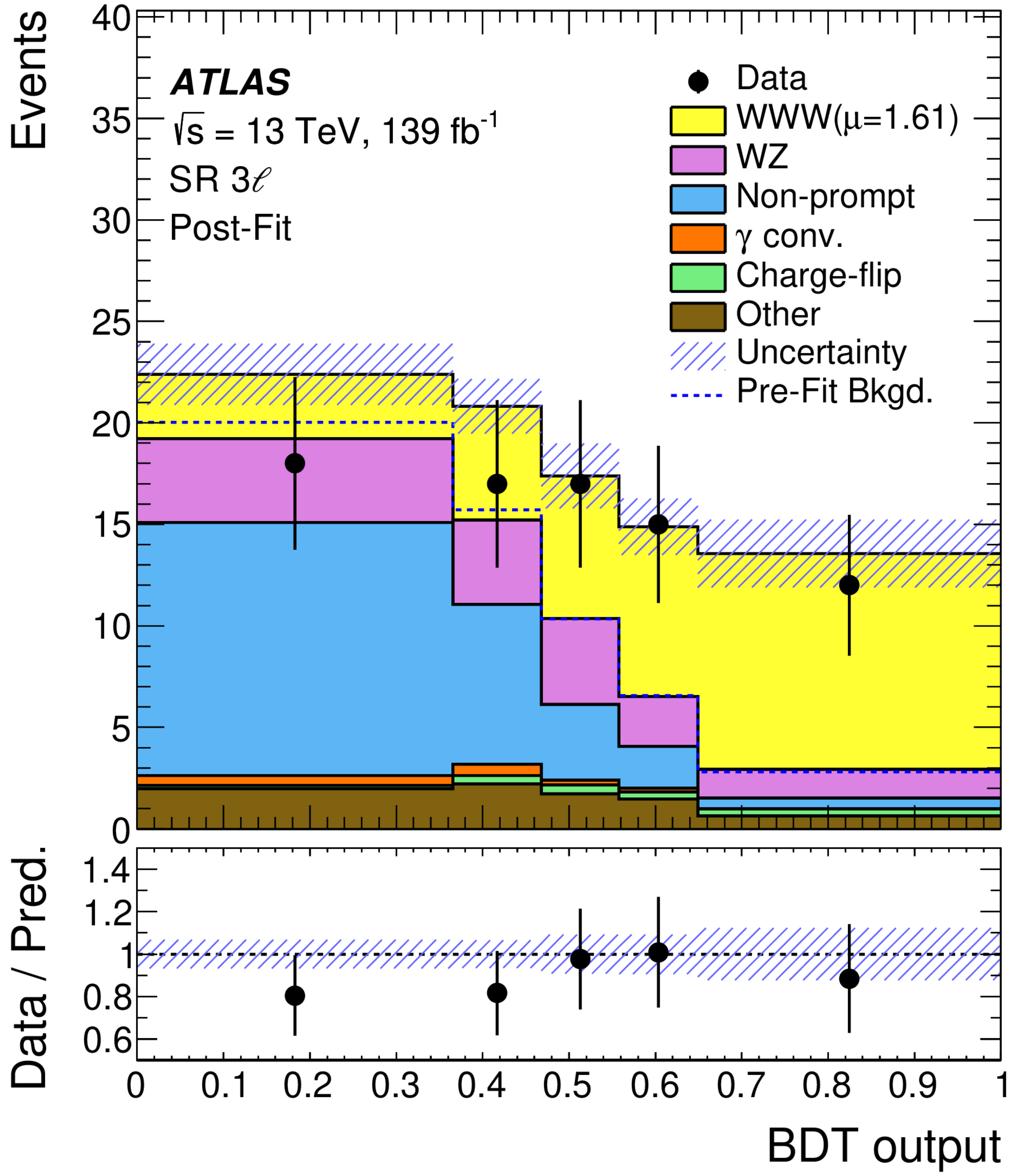

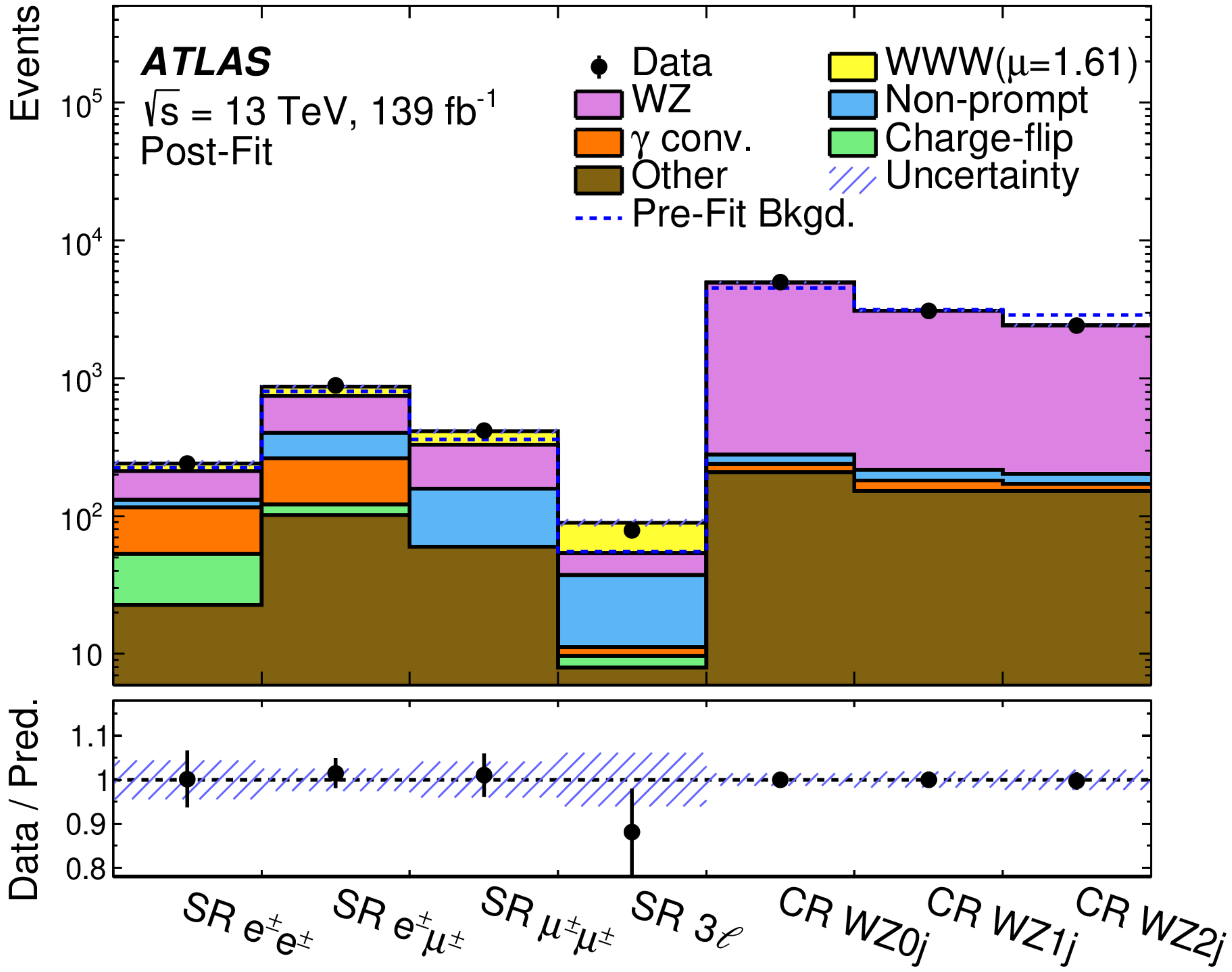

[Phys. Rev. Lett. 129 (2022) 061803]

obs. (exp.) significance: 8.0 σ (5.4 σ)

inclusive cross-section:

820 ±100 (stat) ± 80 (syst) fb

Observation of polarisation in WZ production

arXiv:2211.09435 (Submitted to Phys. Lett. B)

- 3l+ν decay mode
- derive DNN sensitive to 00 - 0T/T0 - TT in 4 categories of |cos θ*$_{lW}$| , |cos θ*$_{lZ}$|

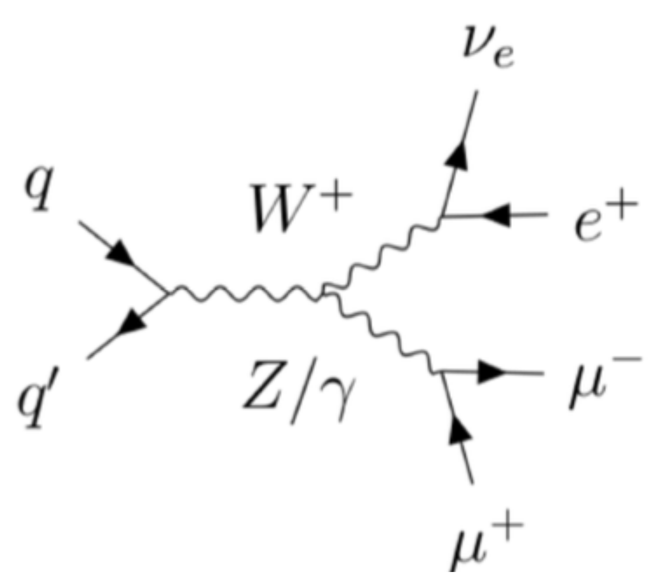

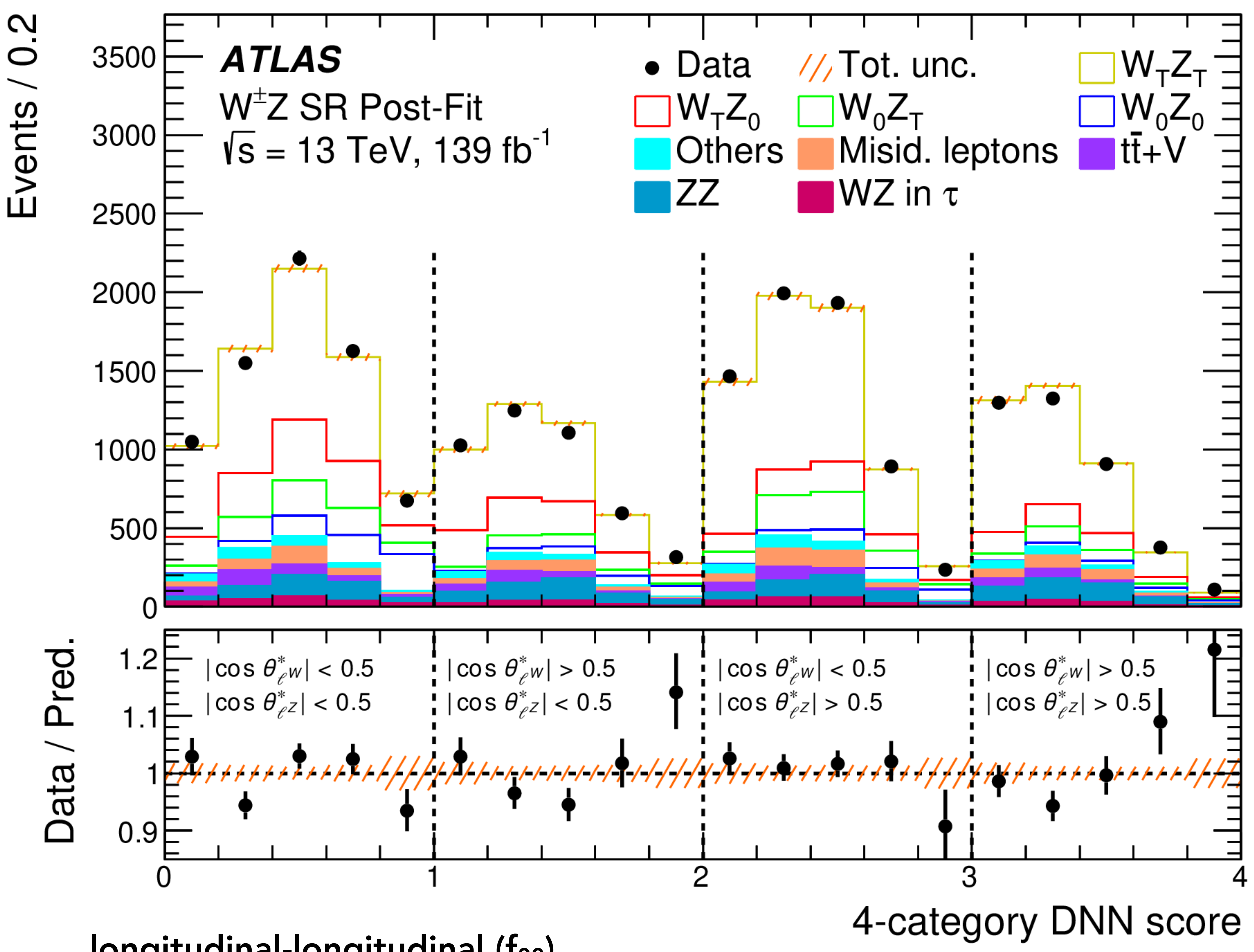

longitudinal-longitudinal (f_{00})

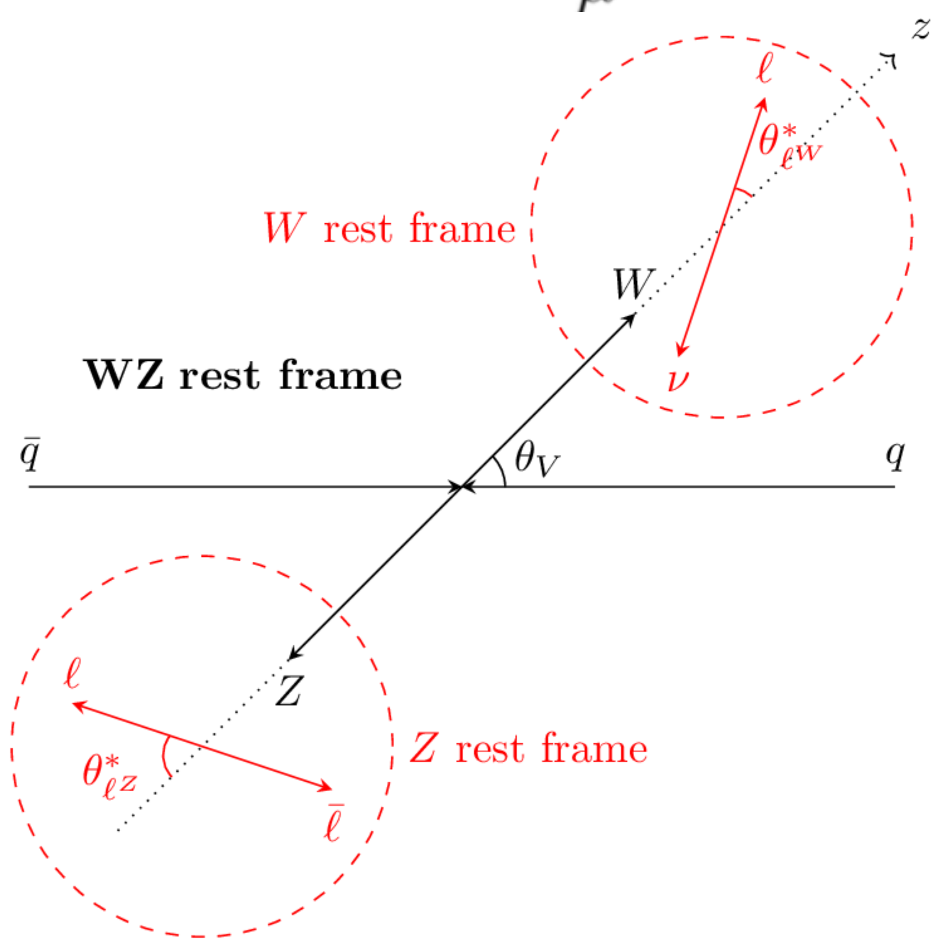

joint helicity fractions in agreement with NLO SM

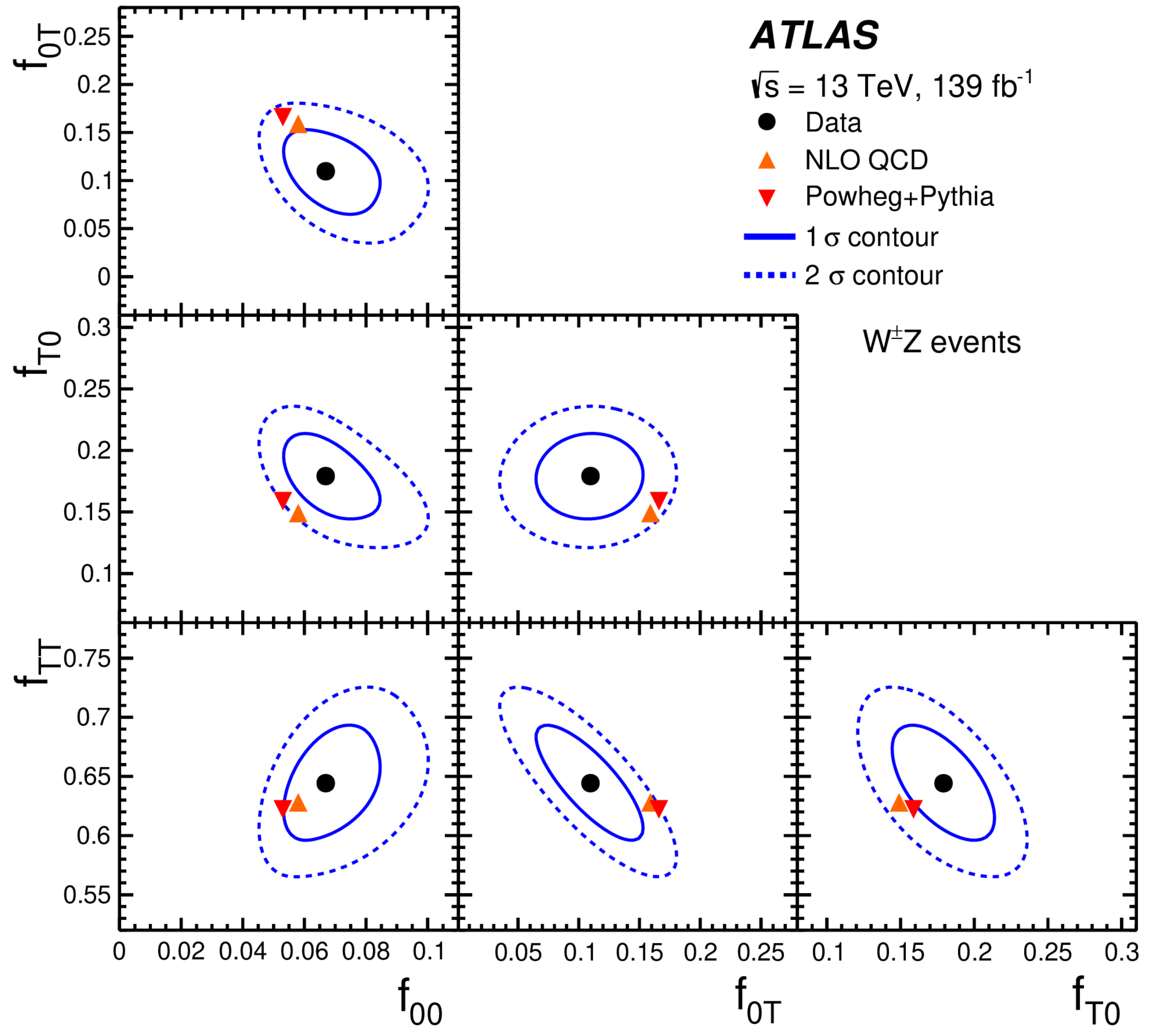

f_{00} = 0.067 ± 0.010
f_{0T} = 0.110 ± 0.029
f_{T0} = 0.179 ± 0.023
f_{TT} = 0.644 ± 0.032

First observation of simultaneous production of longitudinally polarised W and Z bosons with 7.1 σ

Top pair production cross section at 5.02 TeV

arXiv:2207.01353 (Submitted to JHEP)

- 260 pb^{-1} dataset recorded
- done in dilepton and single-lepton final states + combination
- BDT used in single-lepton channel

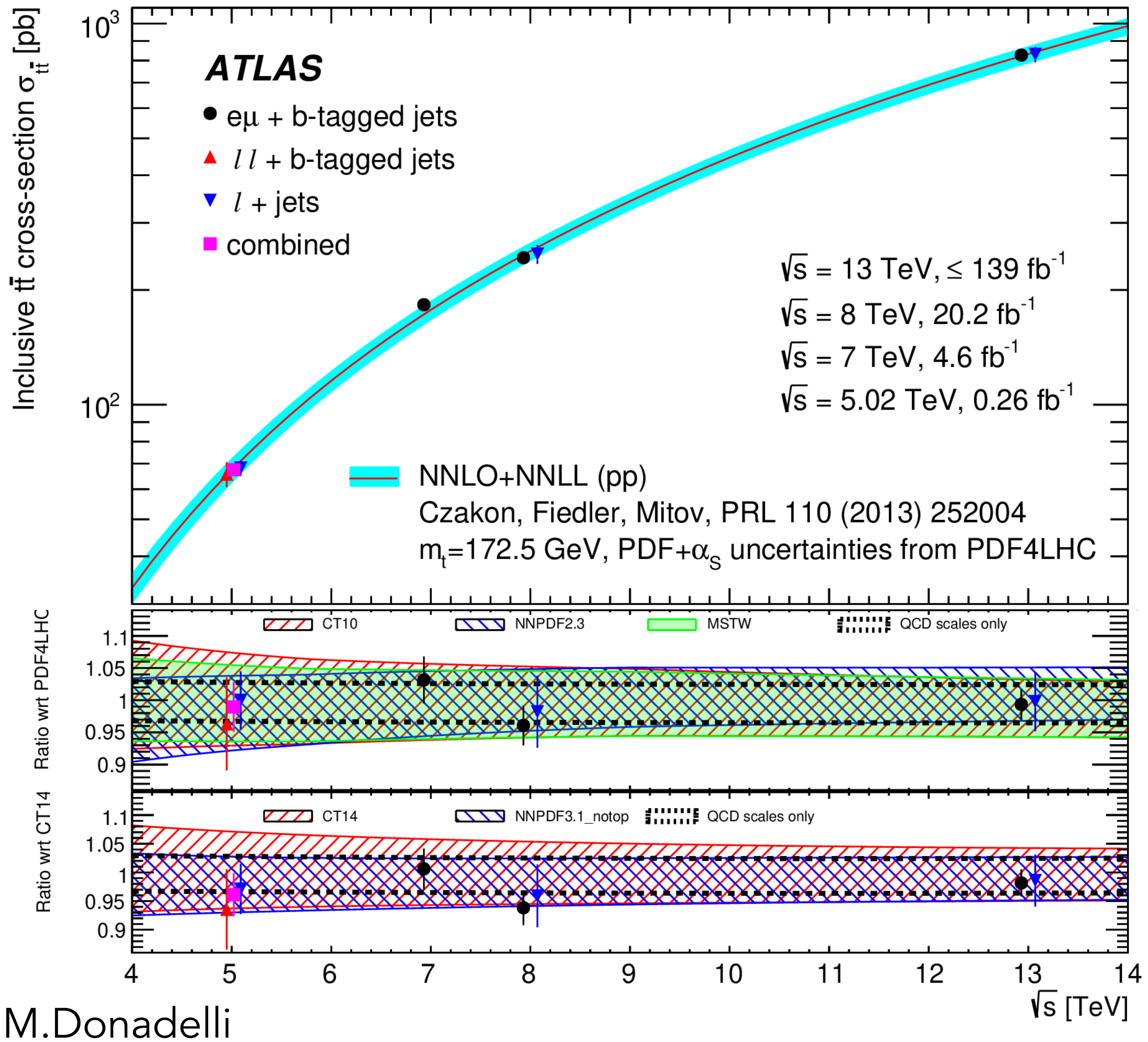

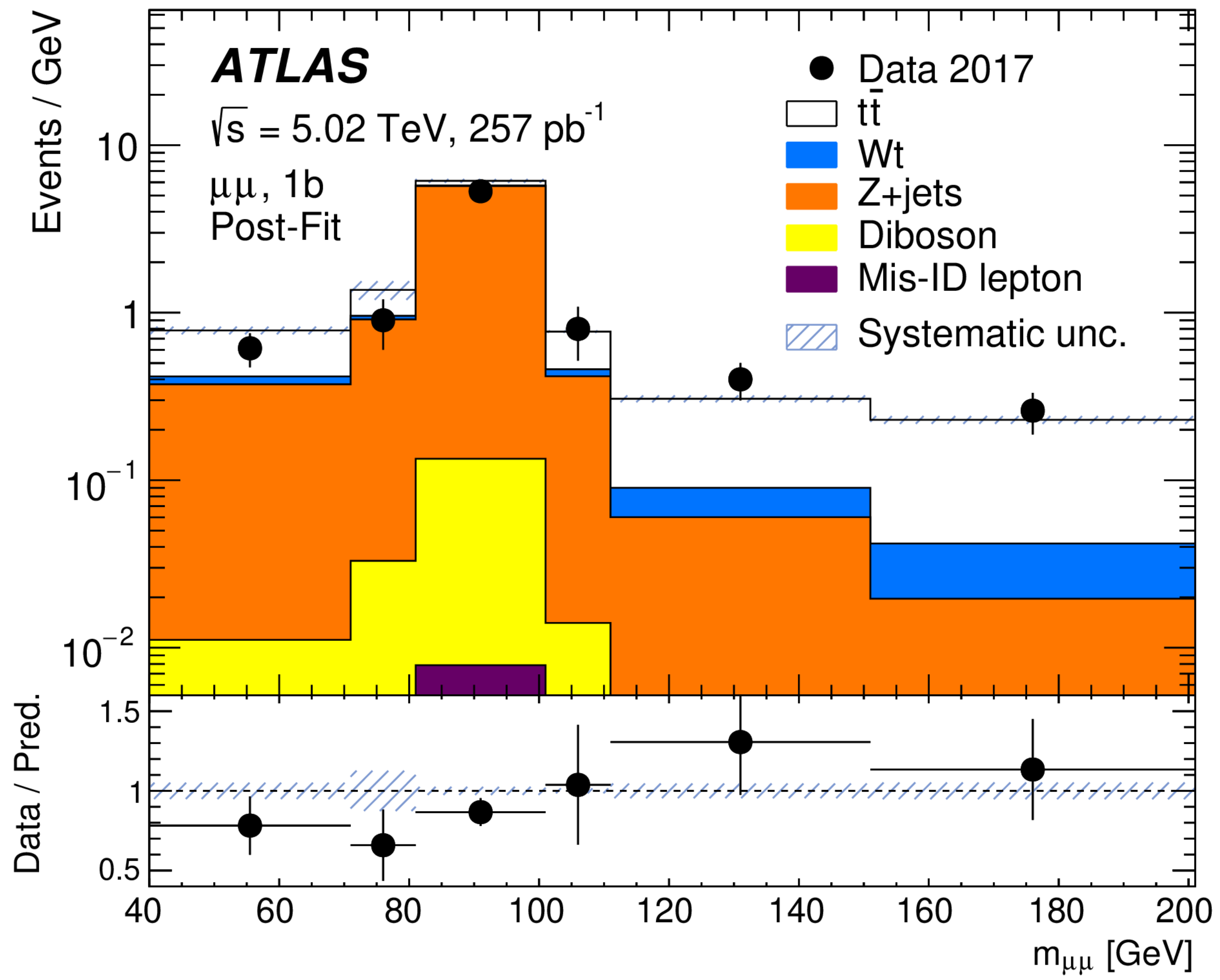

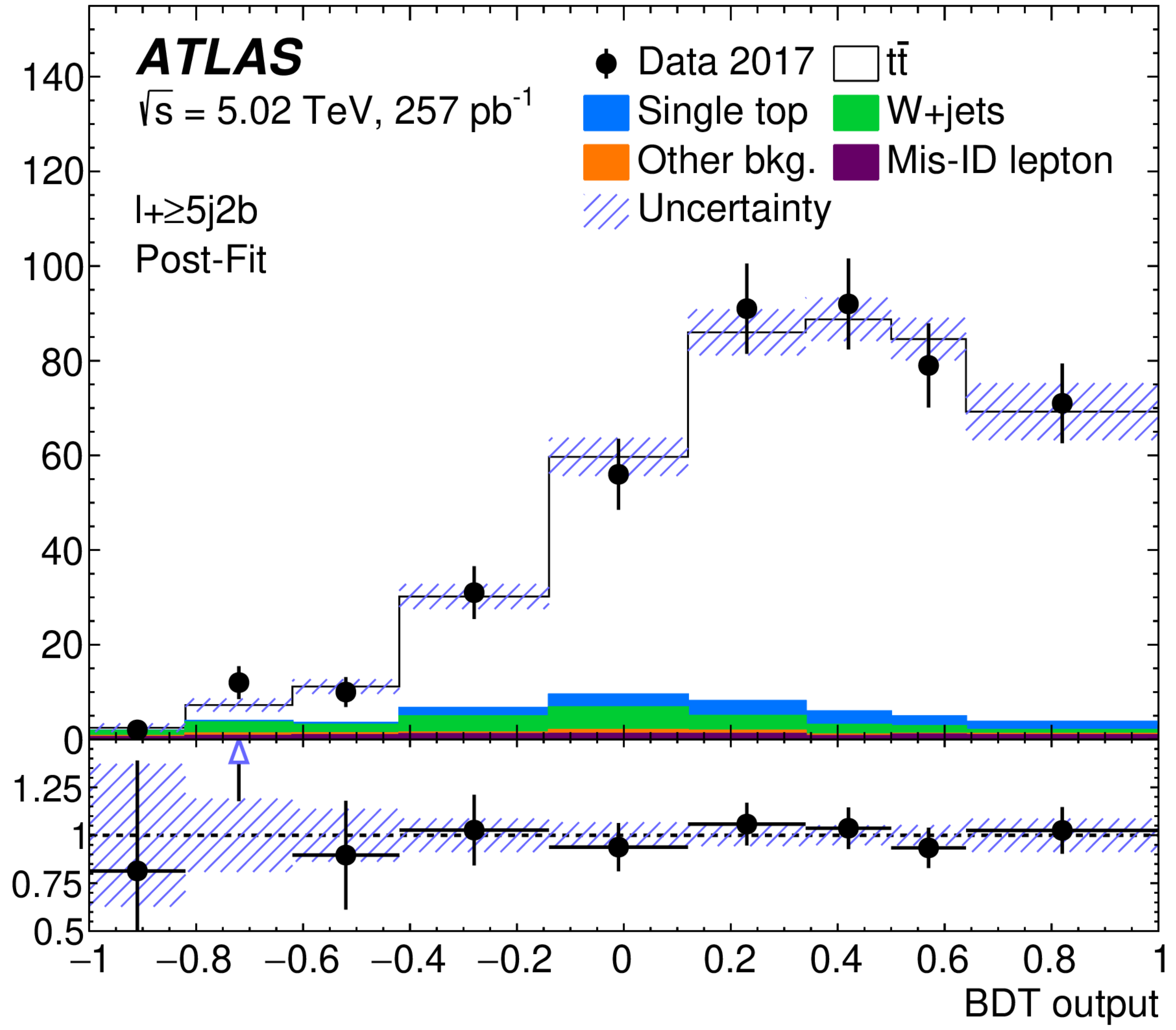

- good agreement with expectations to 4% precision
- measurement helps constrain PDFs

$\sigma_{tt(measured)}$ = **67.5 ± 0.9 (stat.) ± 2.3 (syst.) ± 1.1 (lumi) ± 0.2 (beam) pb**

$\sigma_{tt(predicted)}$ = **68.2 ± 4.8 (PDF + α_S) $^{+1.9}_{-2.3}$ (scale) pb**

Tuesday, 16:40 Standard Model and Top results from ATLAS - Carlos Alberto Gottardo

Single top+photon observation arXiv:2302.01283 (Submitted to Phys. Rev. Lett.)

- t-chan (signature:presence of forward jet)

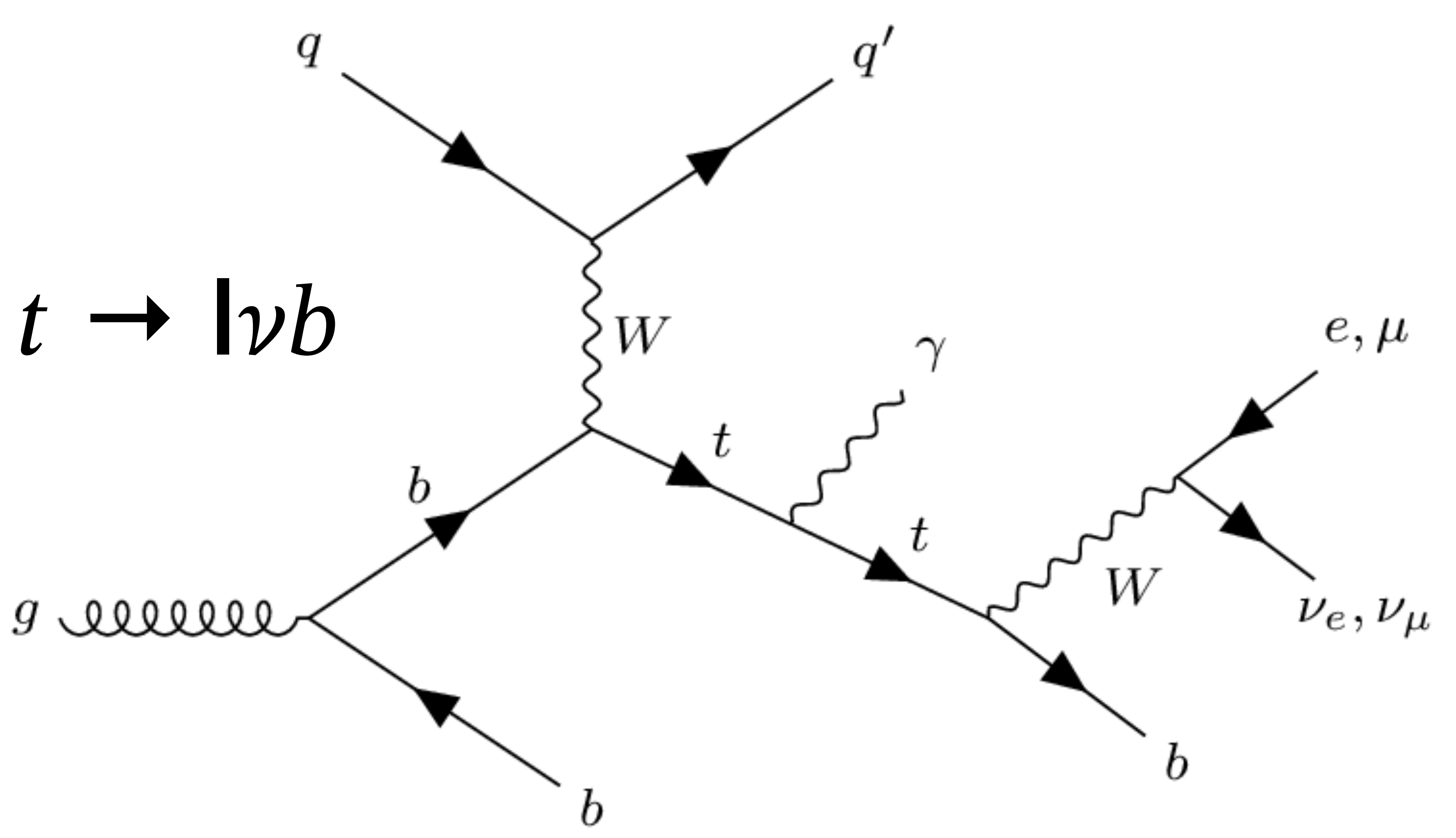

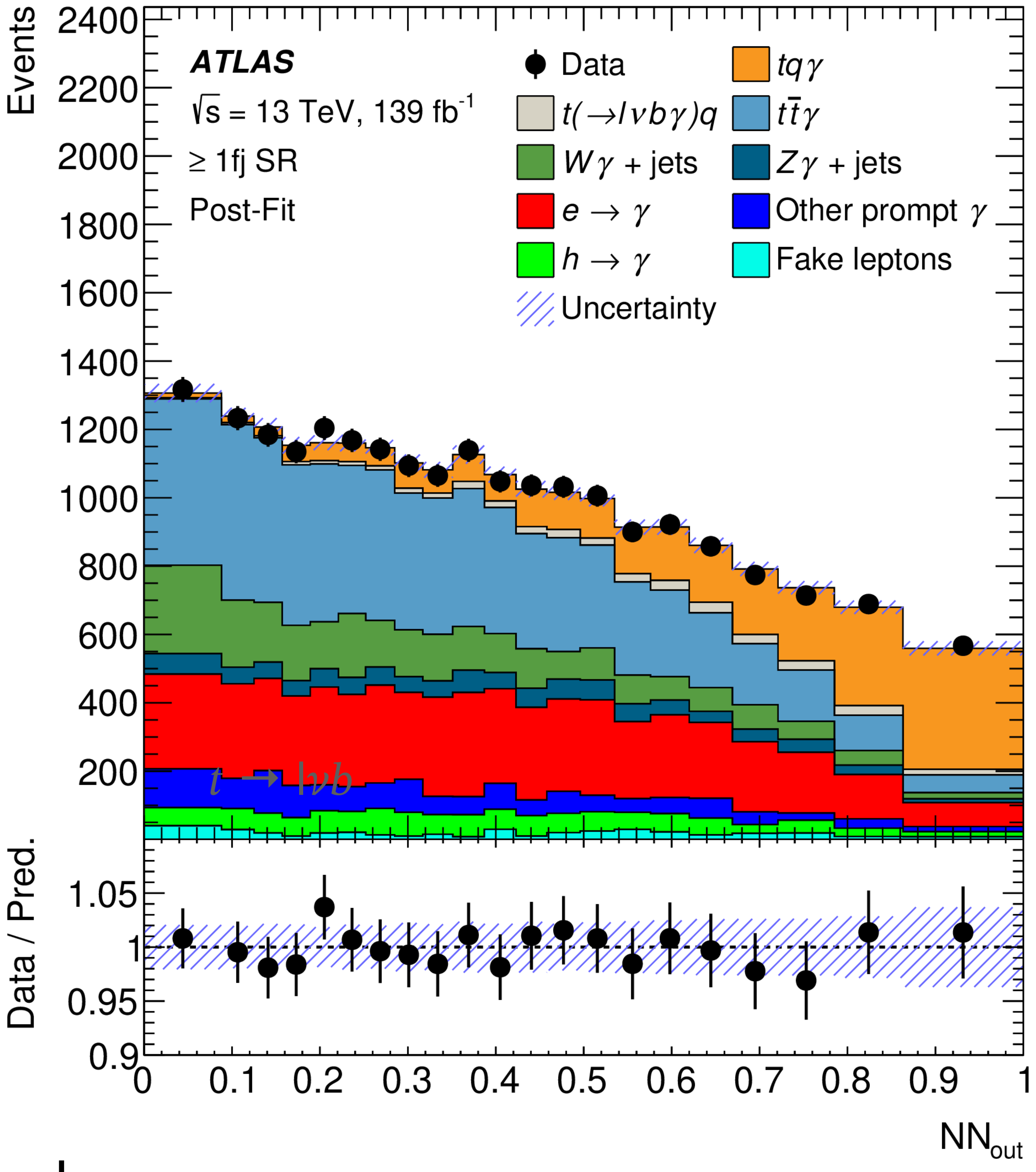

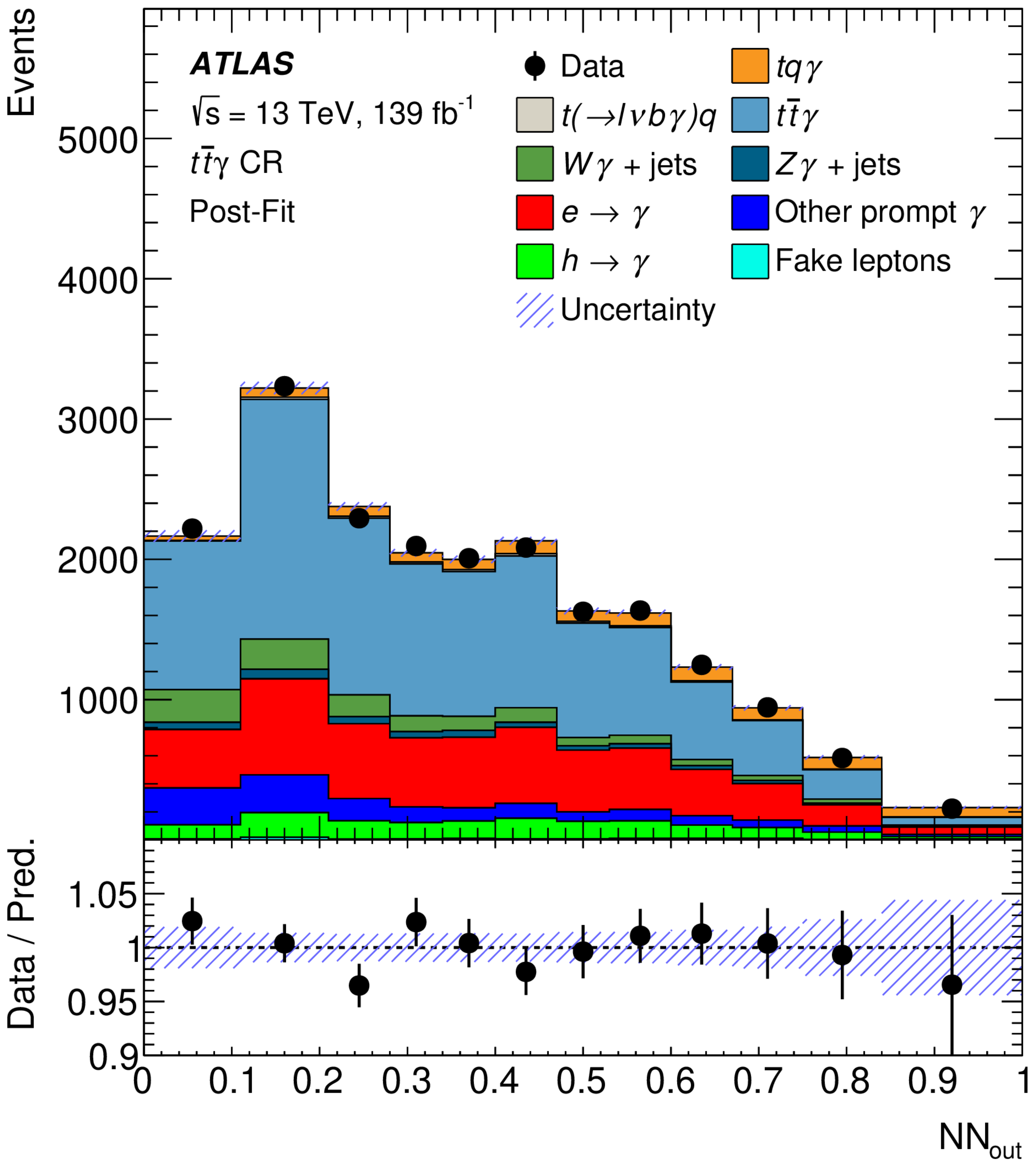

- 2SRs and 2CRs
- NN used to separate signal and background
- profile likelihood fit used to extract cross-section with free floating parameters for background

σ_{tyq} = 580 ± 19 (stat) ± 63 (syst) fb

$\sigma_{tyq\ (prediction)}$ = 406 $^{+25}_{-32}$ fb

Observed (expected) significance: 9.1σ (6.7σ)

Tuesday, 16:40 Standard Model and Top results from ATLAS - Carlos Alberto Gottardo

Observation of di-charmonium in 4μ states

- motivated by tetraquarks, in two channels → $T_{cc\bar{c}\bar{c}} \to J/\psi\, J/\psi \to 4\mu$
  $T_{cc\bar{c}\bar{c}} \to J/\psi\, \psi(2S) \to 4\mu$
- find prompt 4μ events with p_T > 3,3,4,4 GeV
- ΔR < 0.25 between charmonia
- background from single parton and double parton scattering

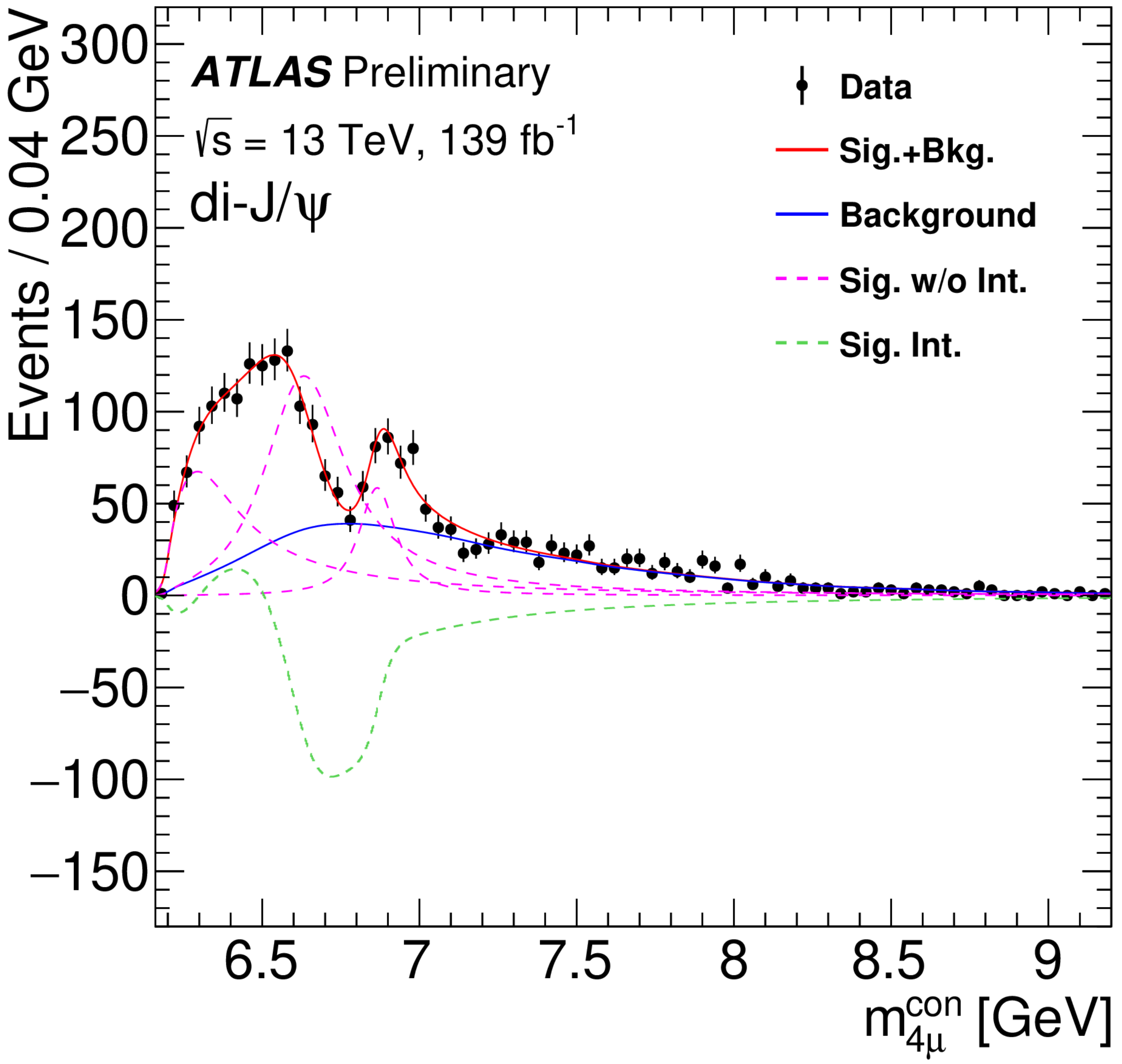

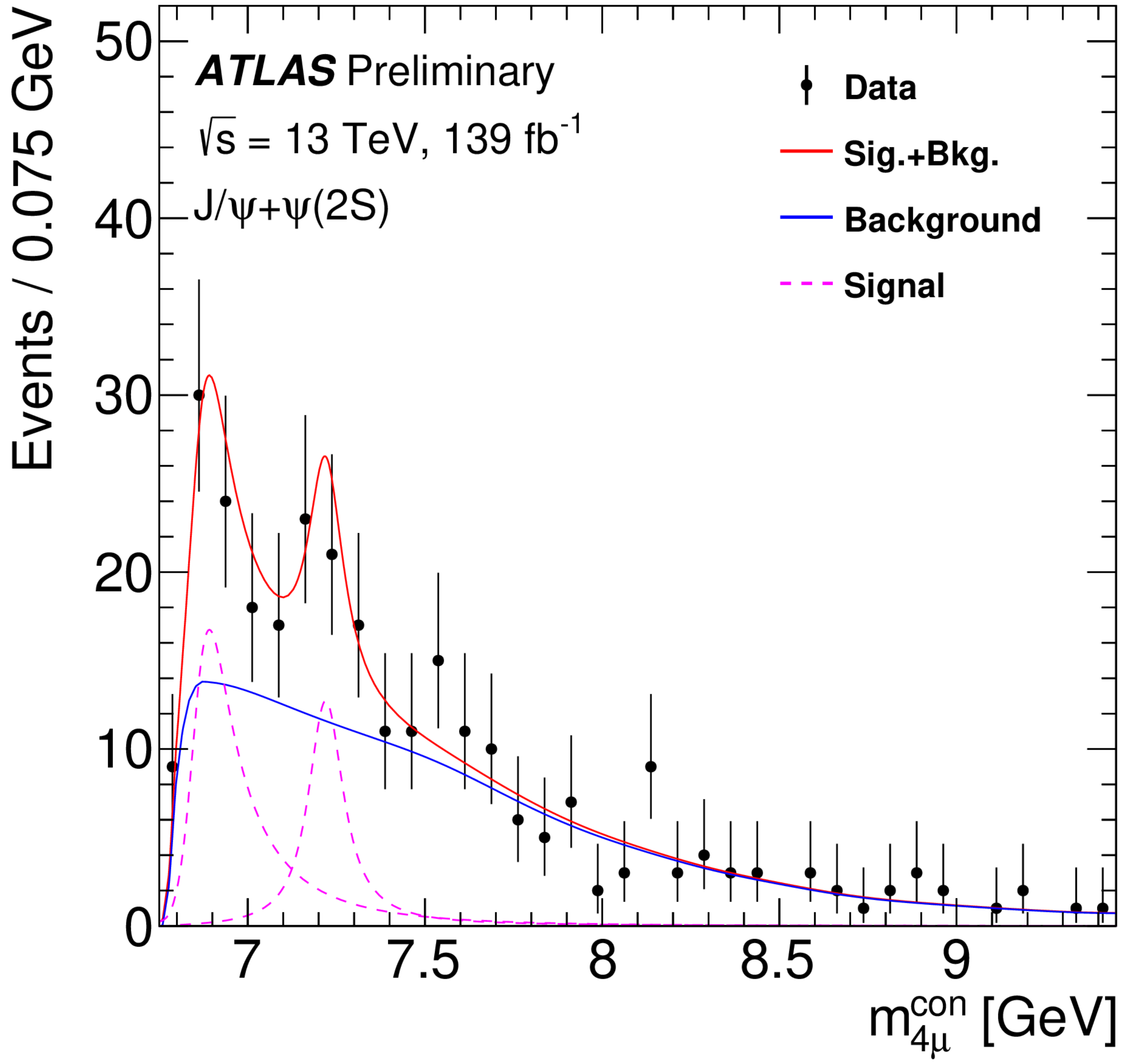

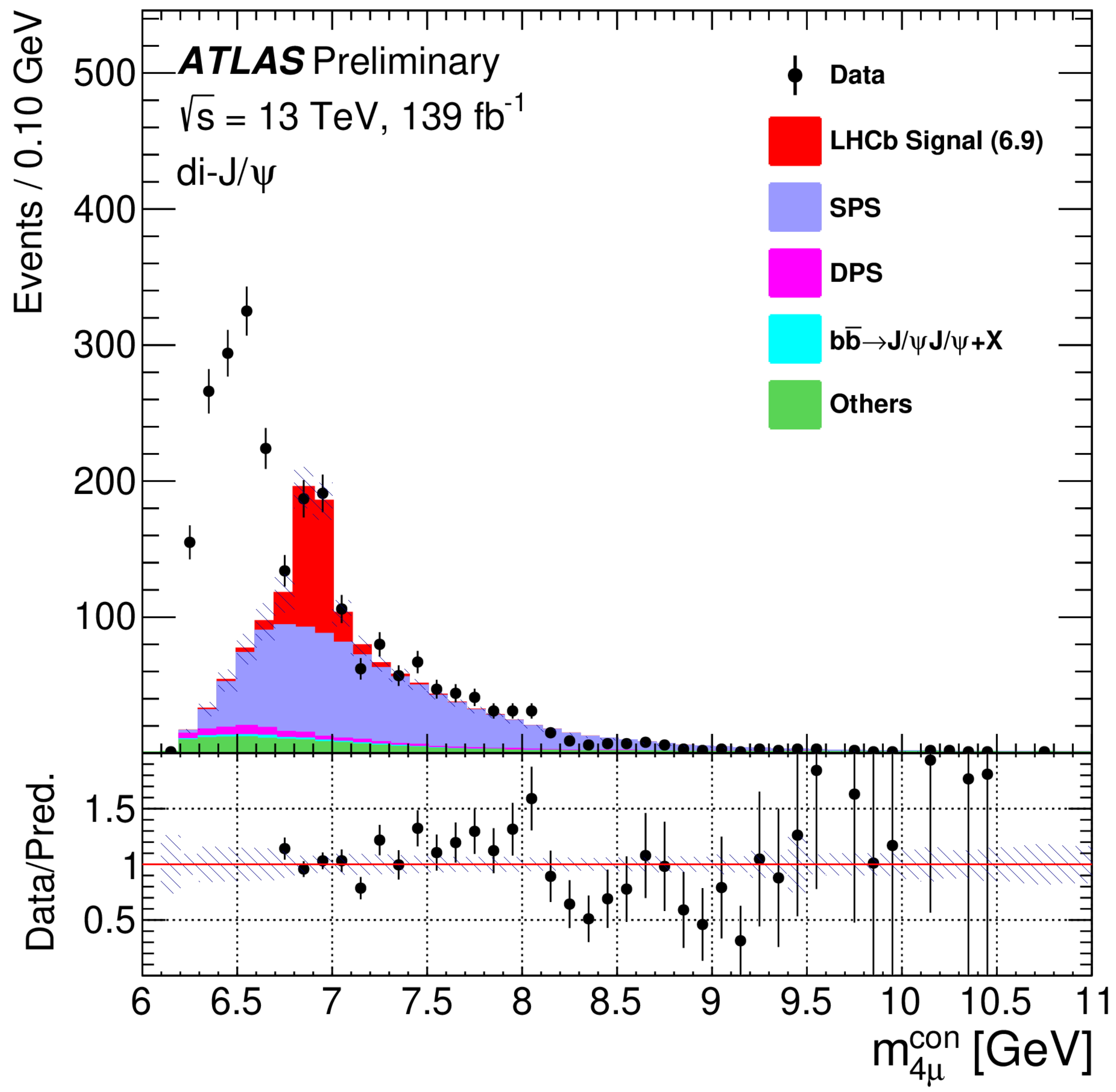

ATLAS-CONF-2022-040

- analogous to LHCb, broad structure at lower mass and a resonance around 6.9 GeV are observed

Tuesday, 17:00 Heavy Flavor results from ATLAS - Markus Cristinziani

H→4l: precise mass measurement

- improved momentum-scale calibration for muons
- event-by-event invariant-mass resolution of 4l system
- DNN used to discriminate signal

arXiv:2207.00320 (Submitted to: Physics Letters B)

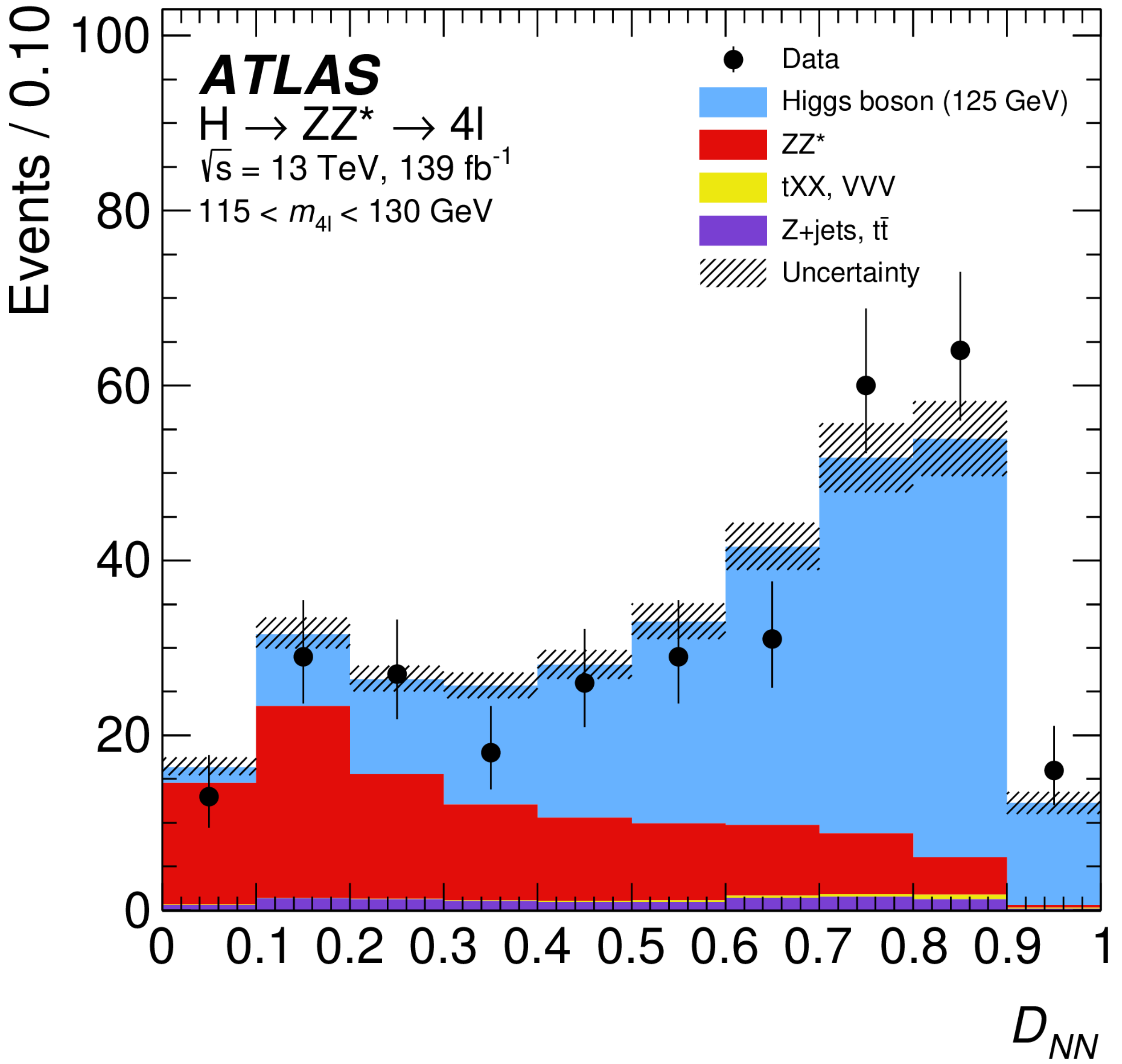

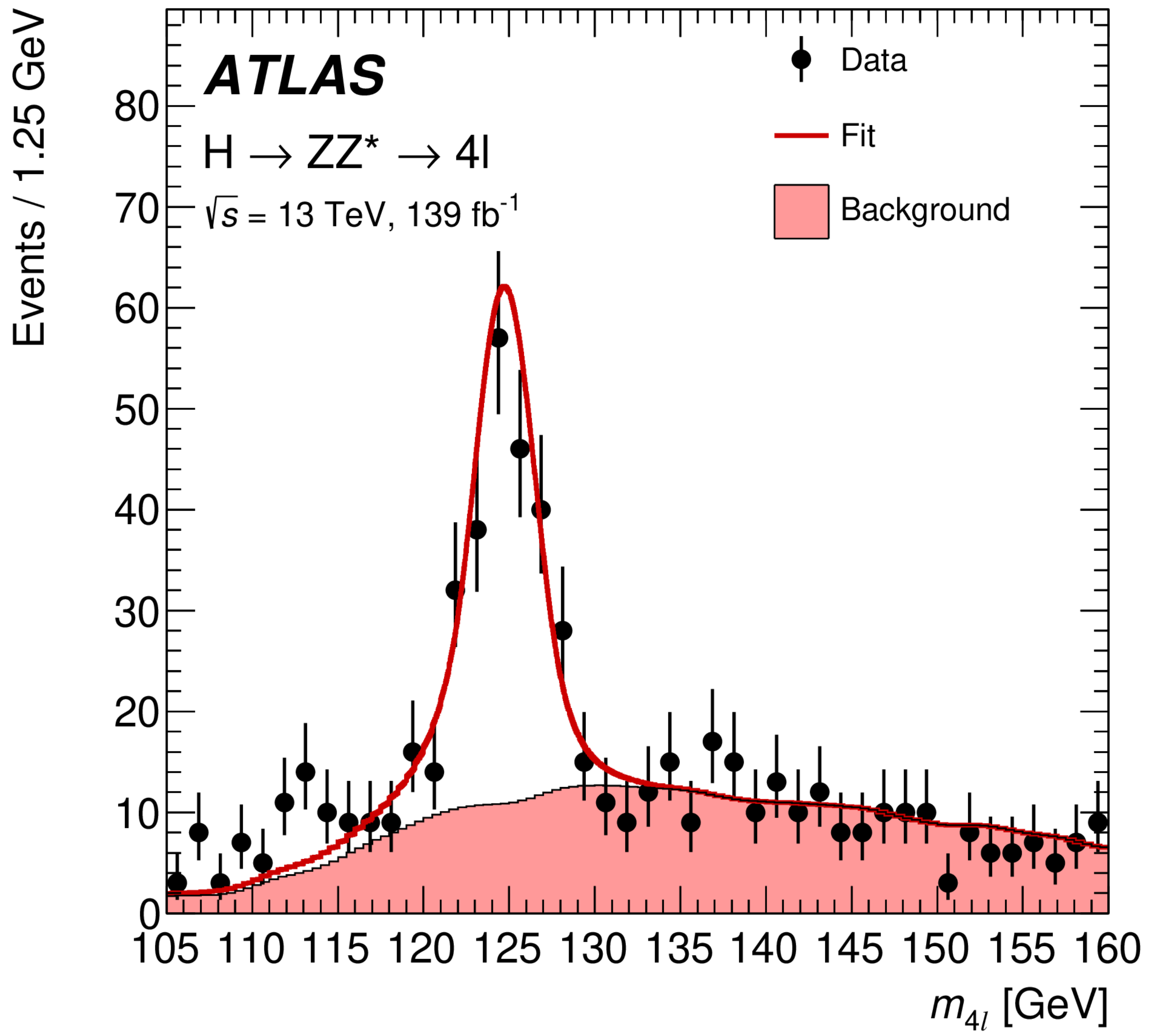

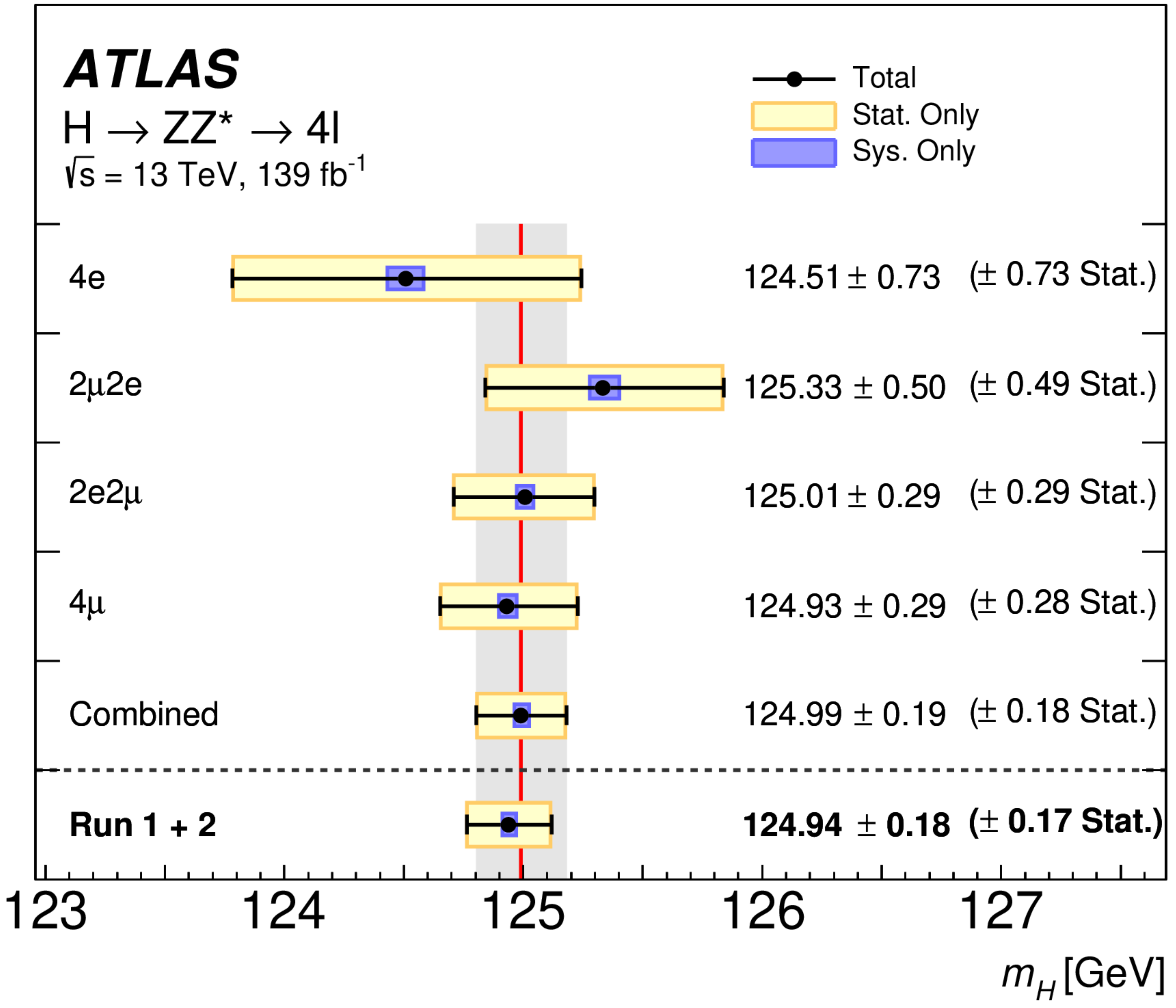

Table 2: Largest contributions to the systematic uncertainty of m_H.

Systematic Uncertainty	Contribution [MeV]
Muon momentum scale	±28
Electron energy scale	±19
Signal-process theory	±14

Combination with 7 and 8 TeV result

m_H = 124.94 ± 0.17 (stat.) ± 0.03 (syst.) GeV

Evidence of off-shell Higgs

ATLAS-CONF-2022-068

- predicted Higgs width of 4.1 MeV much smaller than the detector resolution
- measure the Higgs boson total width by exploiting the ratio between on-shell and off-shell productions

$$\sigma^{\text{off-shell}}_{gg\to H\to VV} \sim \frac{g^2_{ggH} g^2_{HZZ}}{m^2_{ZZ}} \qquad \sigma^{\text{on-shell}}_{gg\to H\to VV} \sim \frac{g^2_{ggH} g^2_{HZZ}}{m_H \Gamma_H}$$

- combination of ZZ →2l 2v and ZZ → 4l offers highest sensitivity, exploiting the independence of off-shell cross section on Γ_H

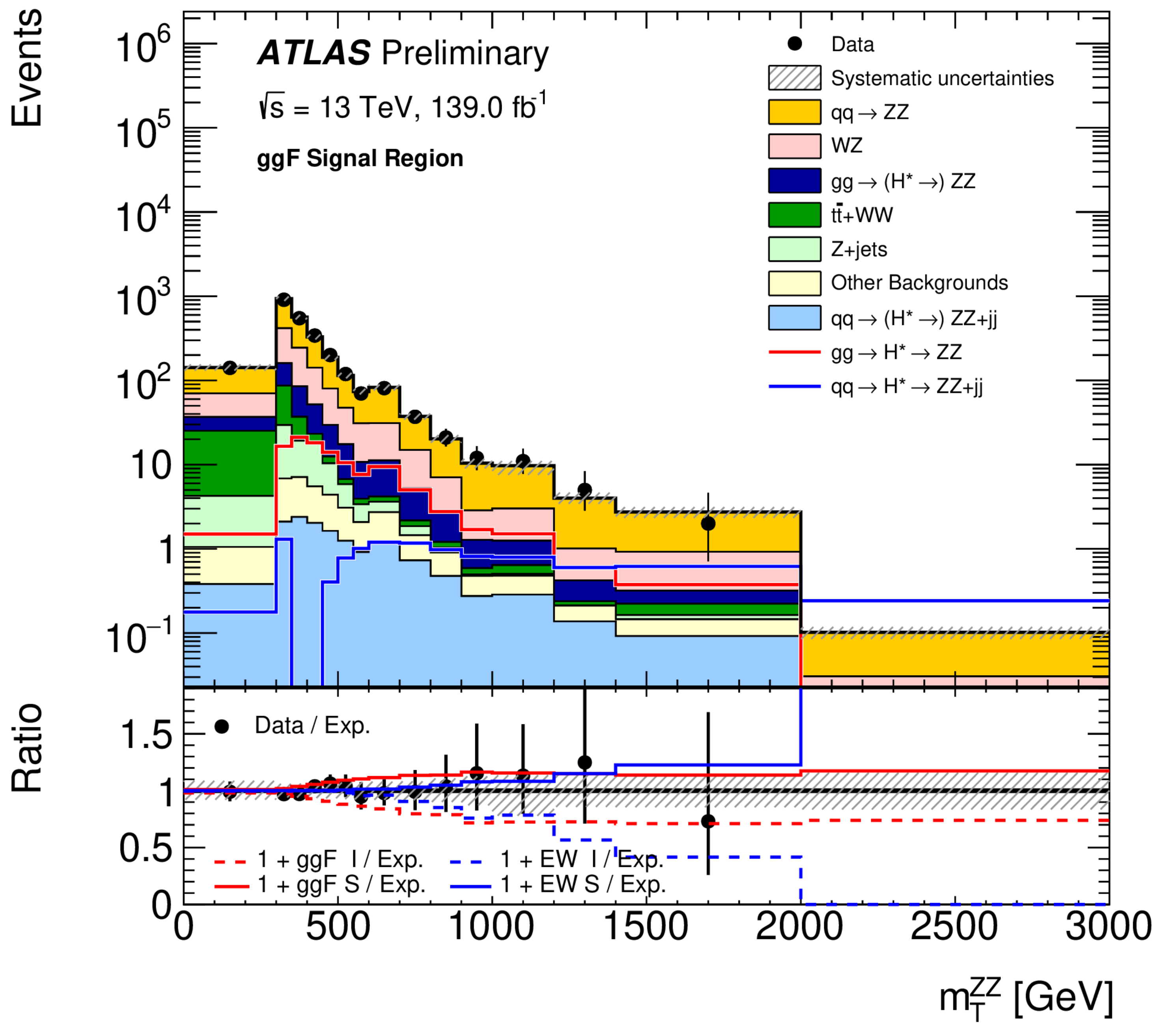

$$m_T^{ZZ} \equiv \sqrt{\left[\sqrt{m_Z^2 + (p_T^{\ell\ell})^2} + \sqrt{m_Z^2 + (E_T^{\text{miss}})^2}\right]^2 - \left|\vec{p}_T^{\,\ell\ell} + \vec{E}_T^{\text{miss}}\right|^2}$$

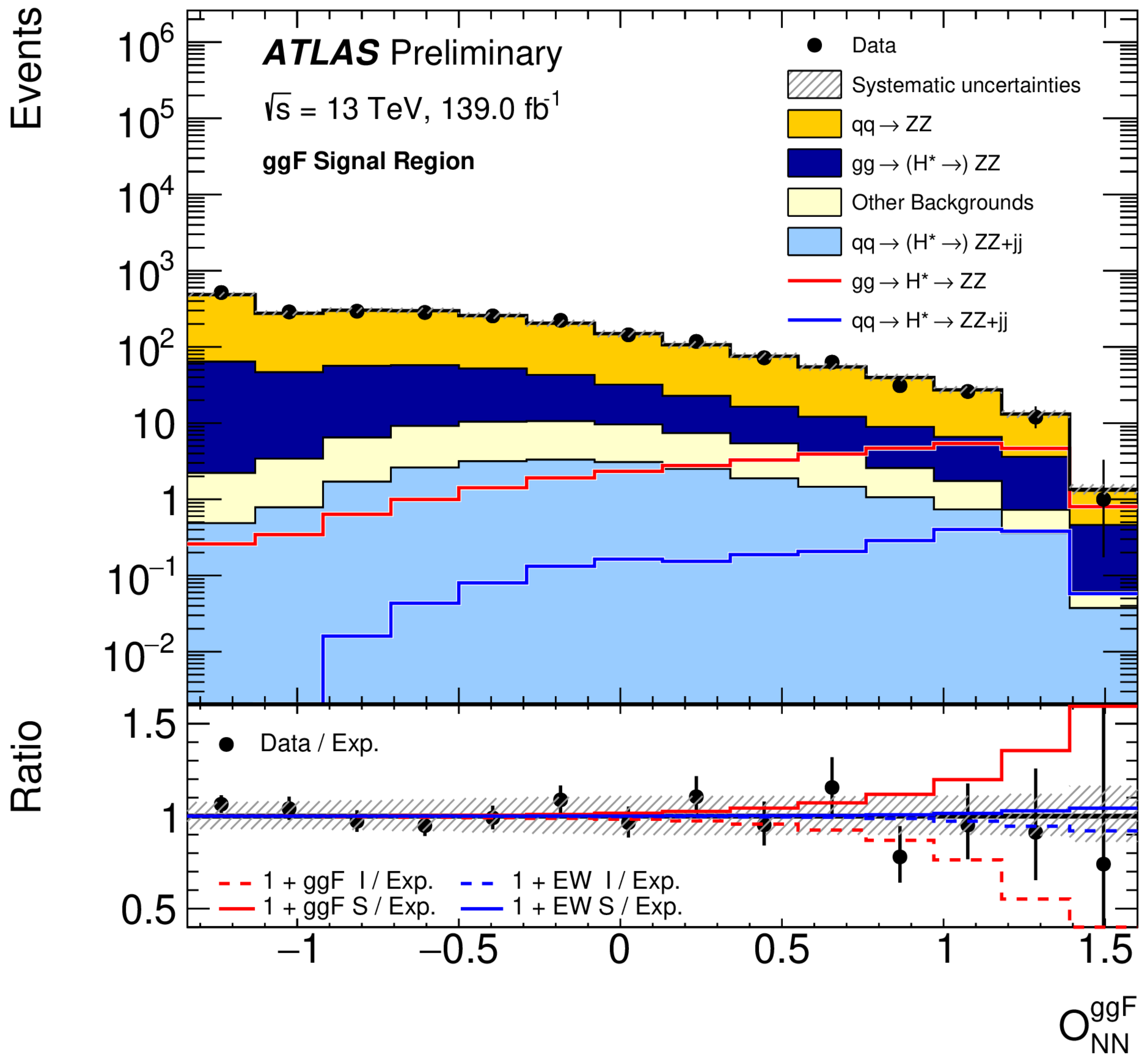

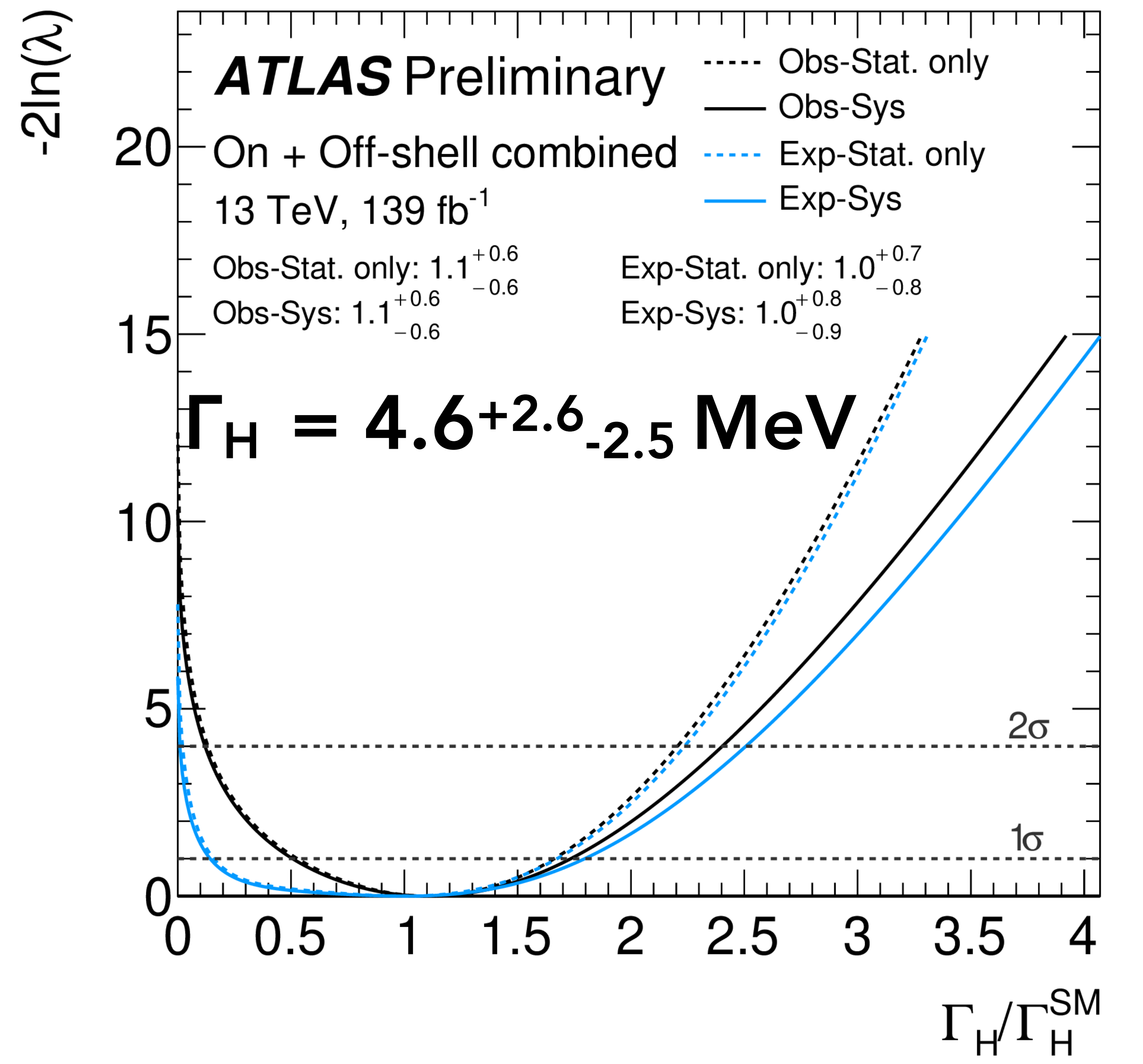

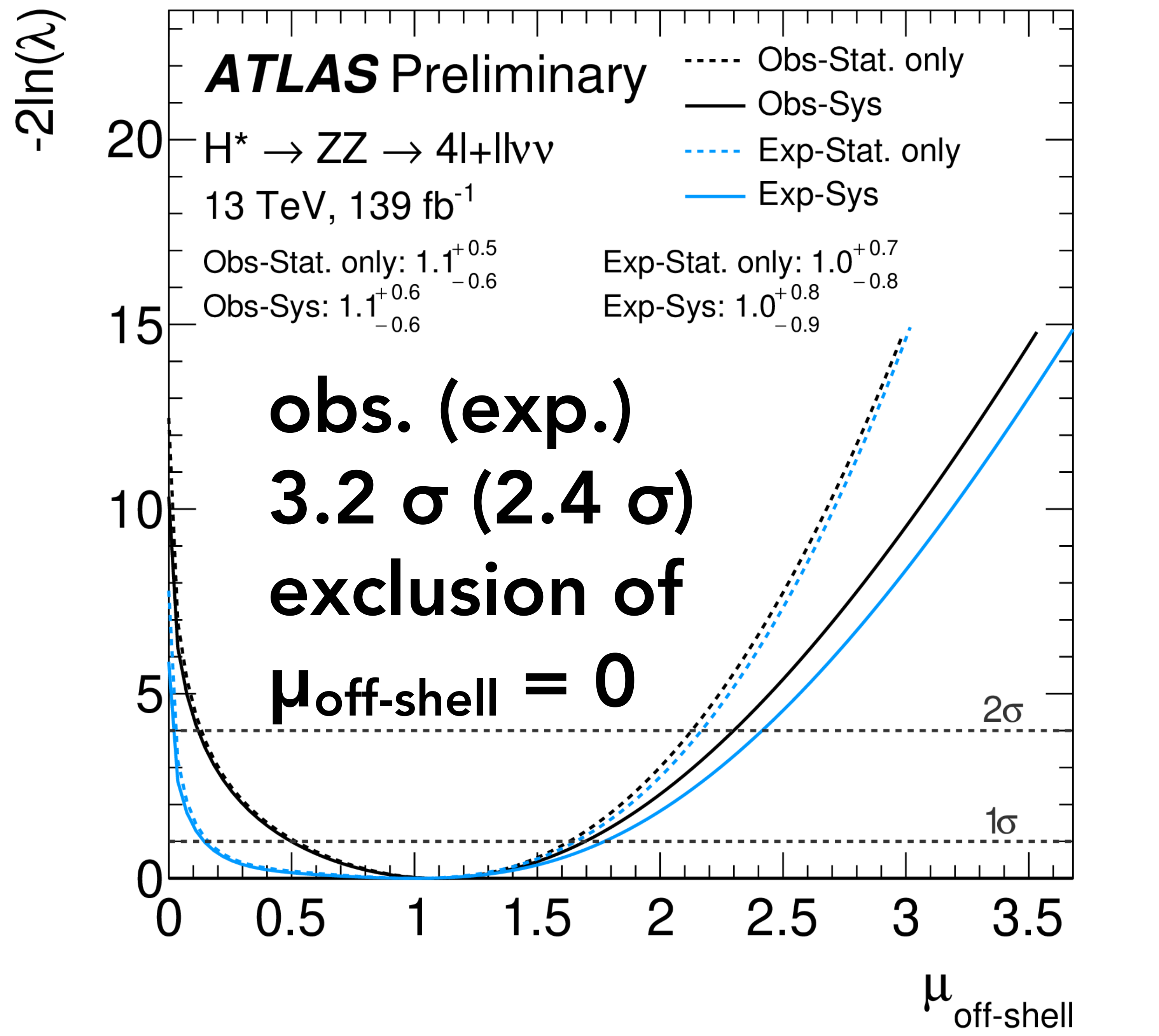

CP properties with H→ττ

arXiv:2212.05833 (Submitted to: EPJC)

- φ^*_{CP} angle is directly related to CP-mixing angle (ϕ_τ) in the $H \to \tau\tau$ differential decay rate

$$d\Gamma_{H\to\tau^+\tau^-} \approx 1 - b(E_+)b(E_-)\frac{\pi^2}{16}\cos(\varphi^*_{CP} - 2\phi_\tau)$$

- 4 different methods to construct φ^*_{CP} observable
- measurement performed in 24 SRs and 10 CRs

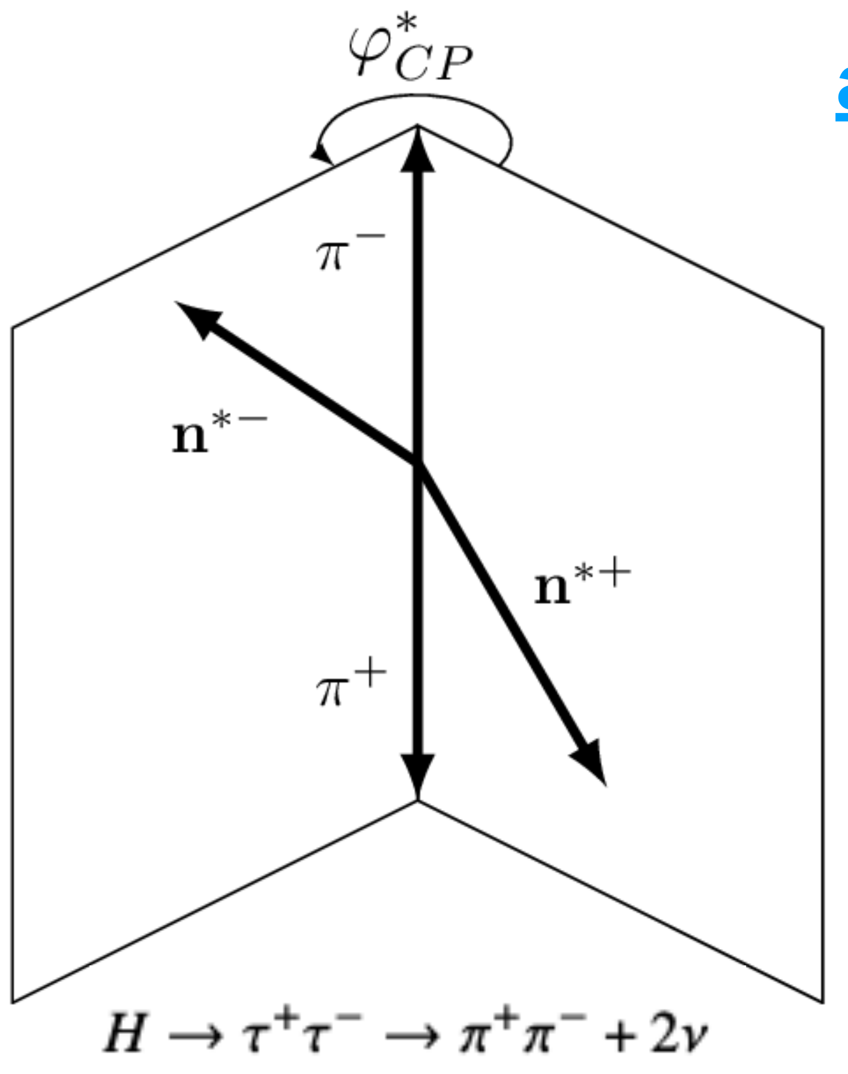

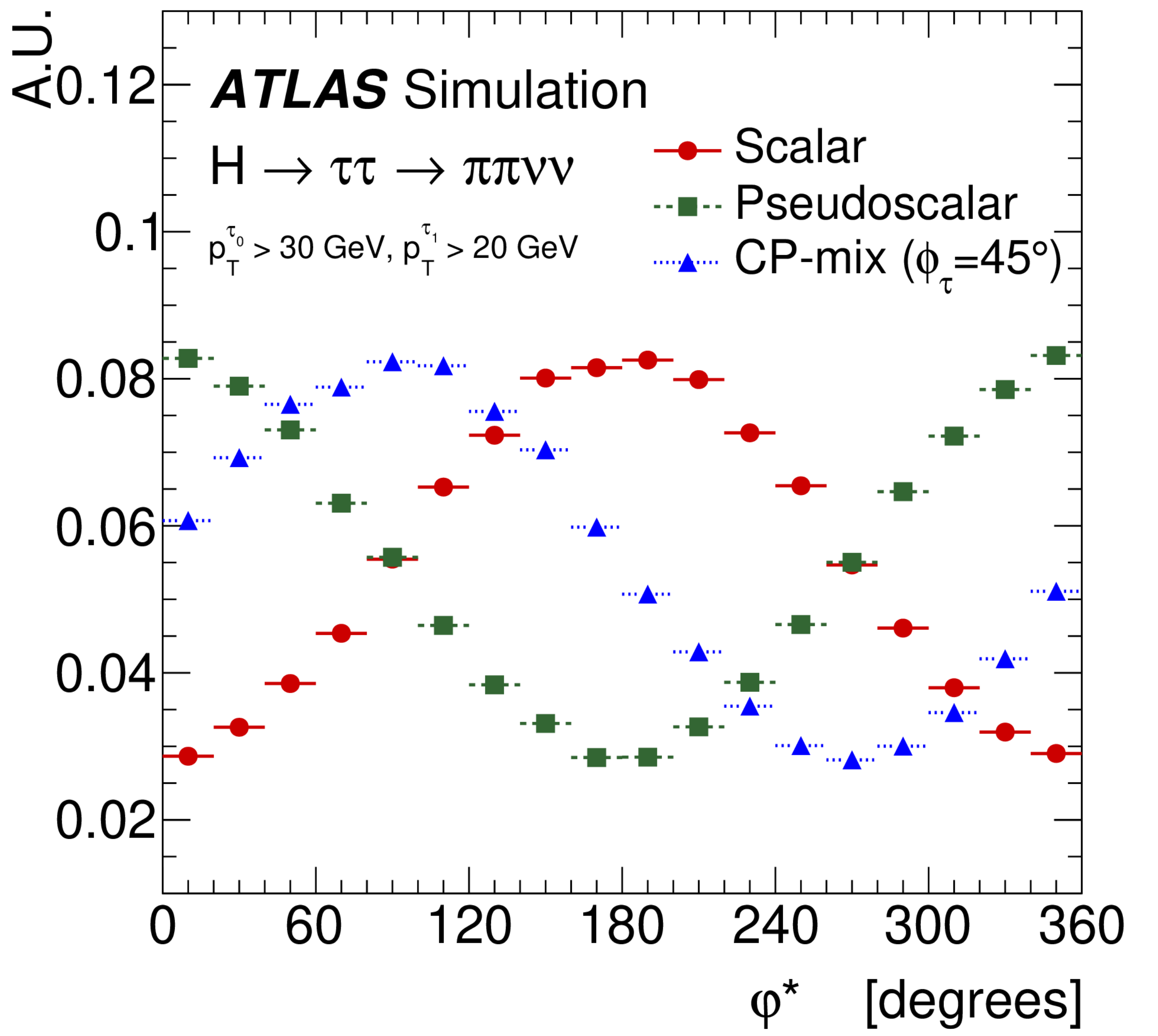

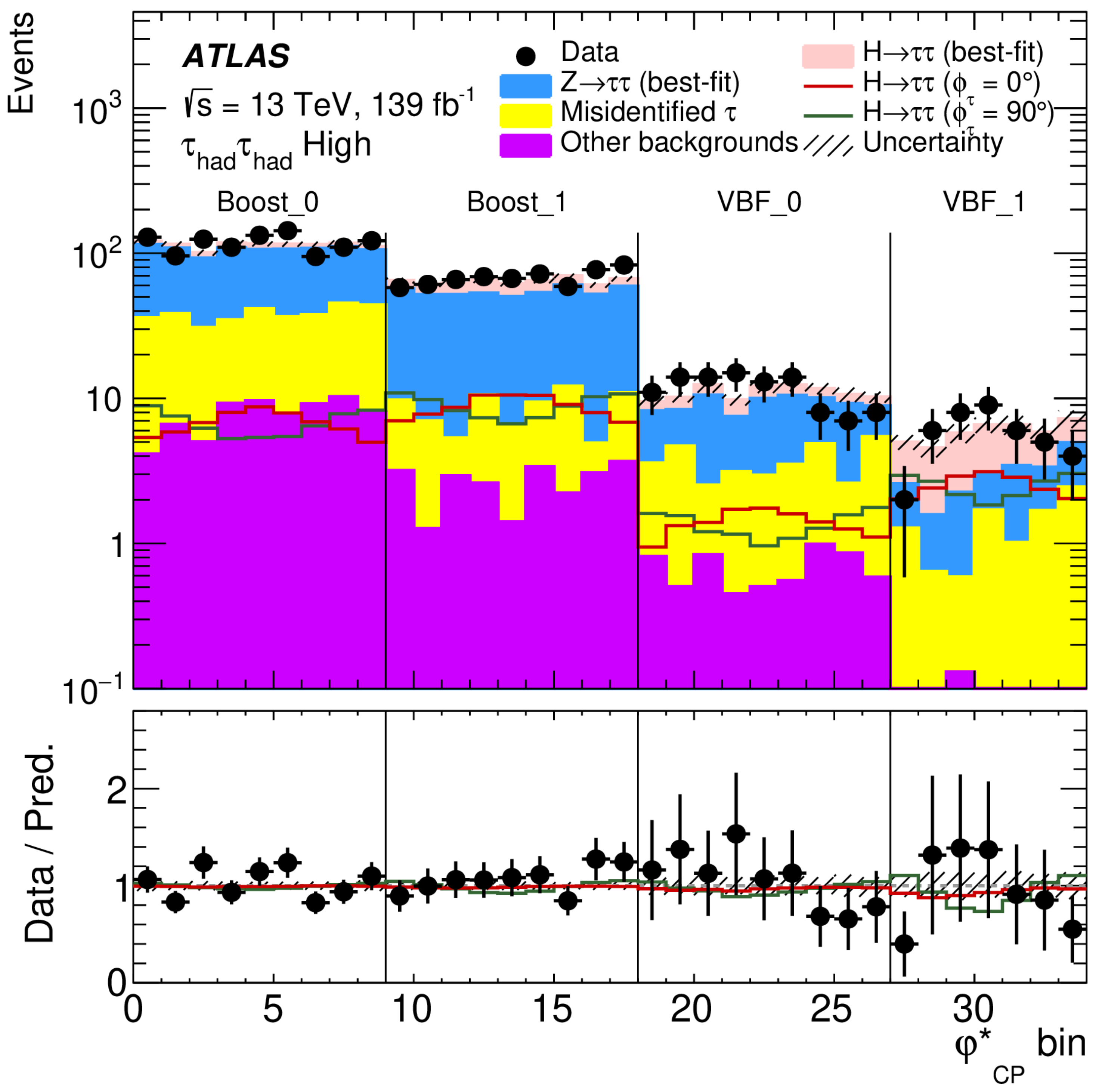

- CP mixing angle extracted from simultaneous fit to all regions

obs. (exp.) ϕ_τ = 9°±16° (0°±28°)

pure CP-odd (ϕ=90°) excluded at 3.4 σ

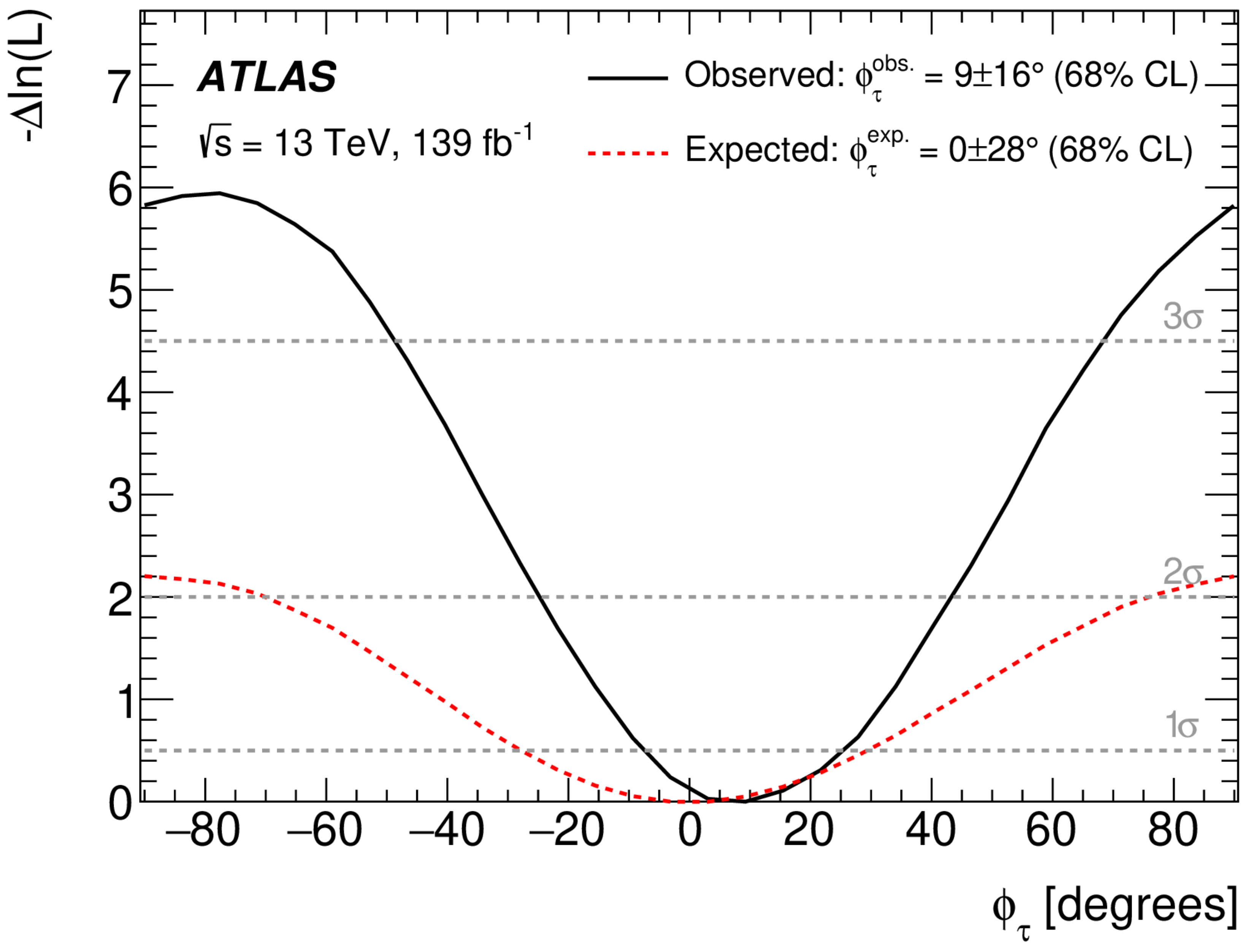

STXS H→γγ [arXiv:2207.00348 (Submitted to: JHEP)]

- cross-section measurements in 28 phase-space regions defined within the Simplified Template Cross-Sections framework (partitioned by production process as well as by kinematic and event properties)

- selected events classified into 101 analysis categories based on multi-class BDT

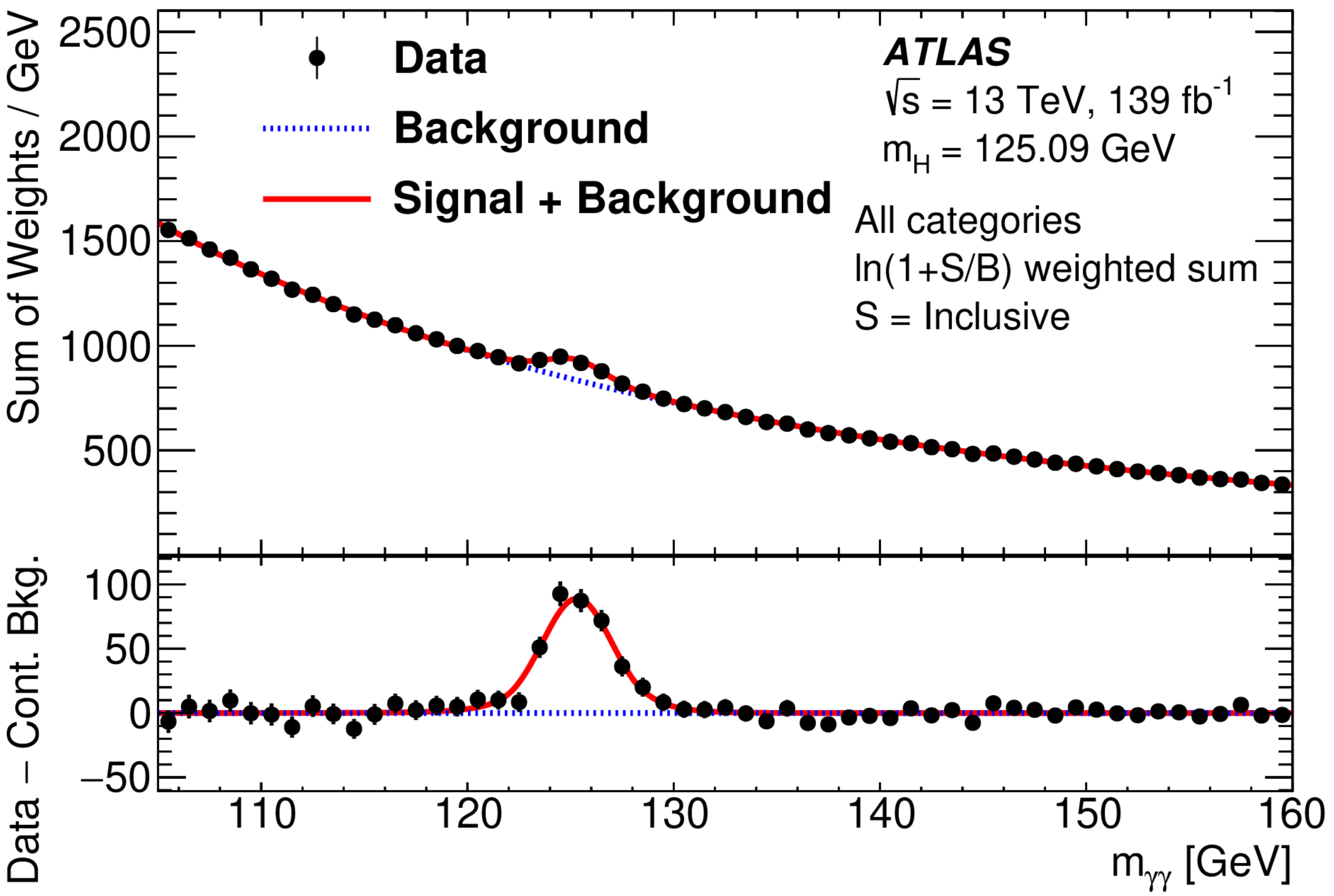

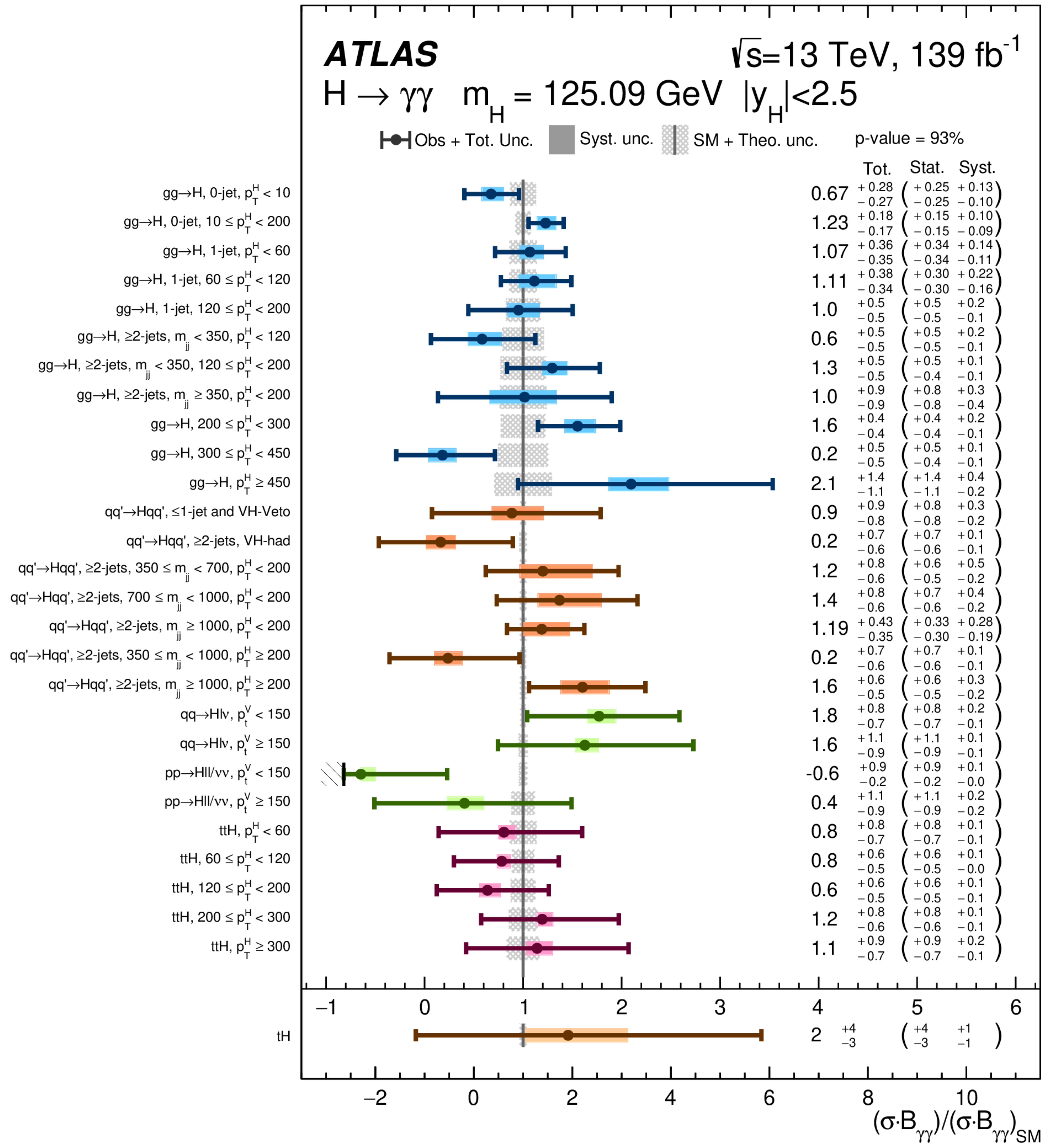

$\mu = 1.04\ ^{+0.10}_{-0.09} = 1.04\ \pm 0.06\ \text{(stat.)}\ ^{+0.06}_{-0.05}\ \text{(theory syst.)}\ ^{+0.05}_{-0.04}\ \text{(exp. syst.)}$

H→γγ (EFT)

arXiv:2207.00348 (Submitted to: JHEP)

- 34 Wilson coefficients considered (out of 60)
  - dimmension-6 operators with significant impact on at least one STXS region
- coefficients measured individually while setting all the others to 0

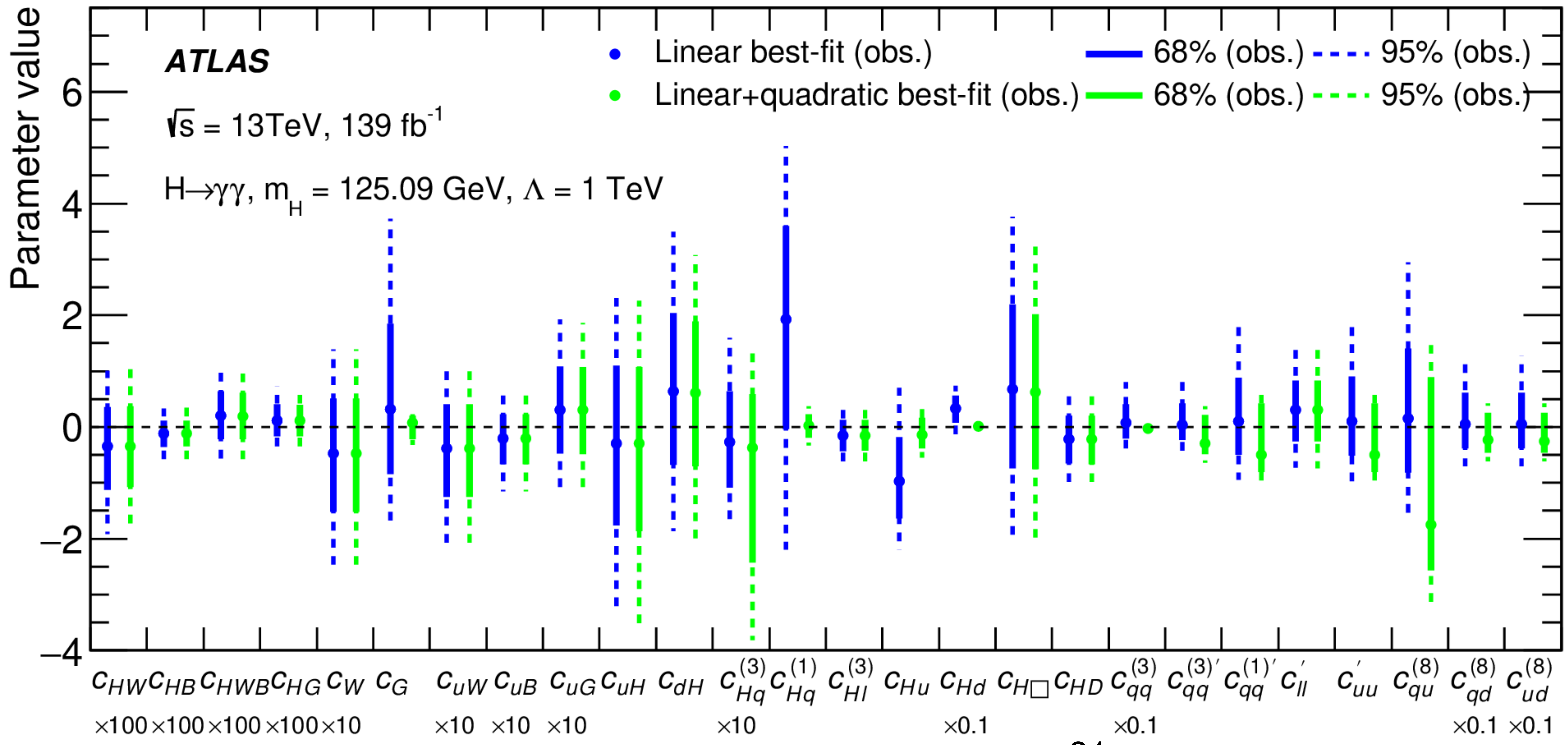

all coefficients compatible with 0 (SM)

Search for H→cc

[Eur. Phys. J. C 82 (2022) 717]

- targeting VH(→cc) with 3 channels: ZH→ννcc, WH→lνcc, ZH→llcc
- analysis strategy validated by simultaneous measurement of diboson processes (VZ→cc, ZW→cq, q is down-quark)
- flavour-tagging: identification of c-jets and orthogonality with VH(bb)
  - c-tagging + b-veto with efficiency WPs ($DL1_c$,MV2)
- simultaneous fit of SRs+CRs using m_{cc} for signal extraction + diboson analysis as cross-check
- uncertainty dominated by V+jets modelling and data statistics

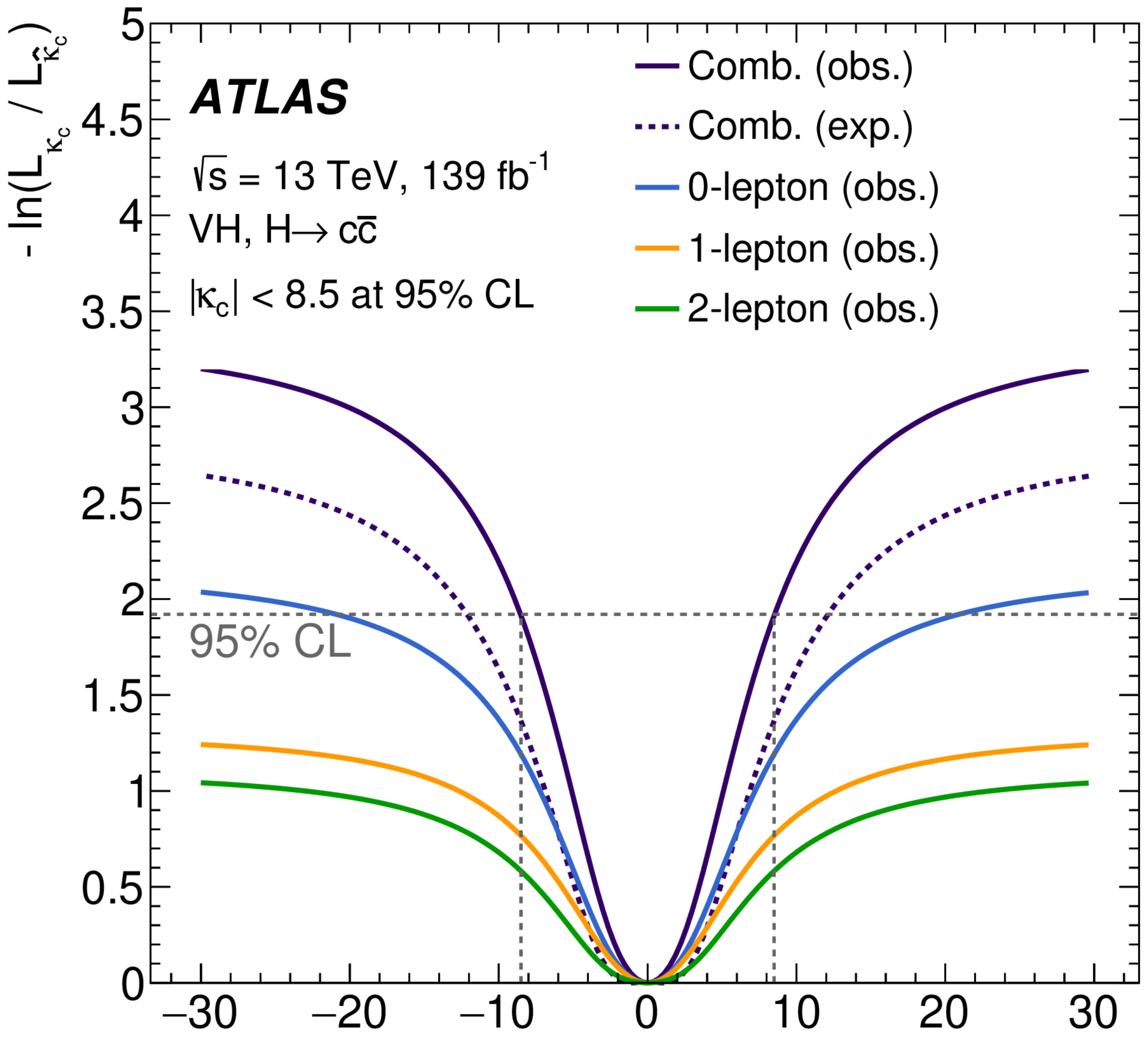

obs. $|\kappa_c|$ < 8.5 @ 95%CL

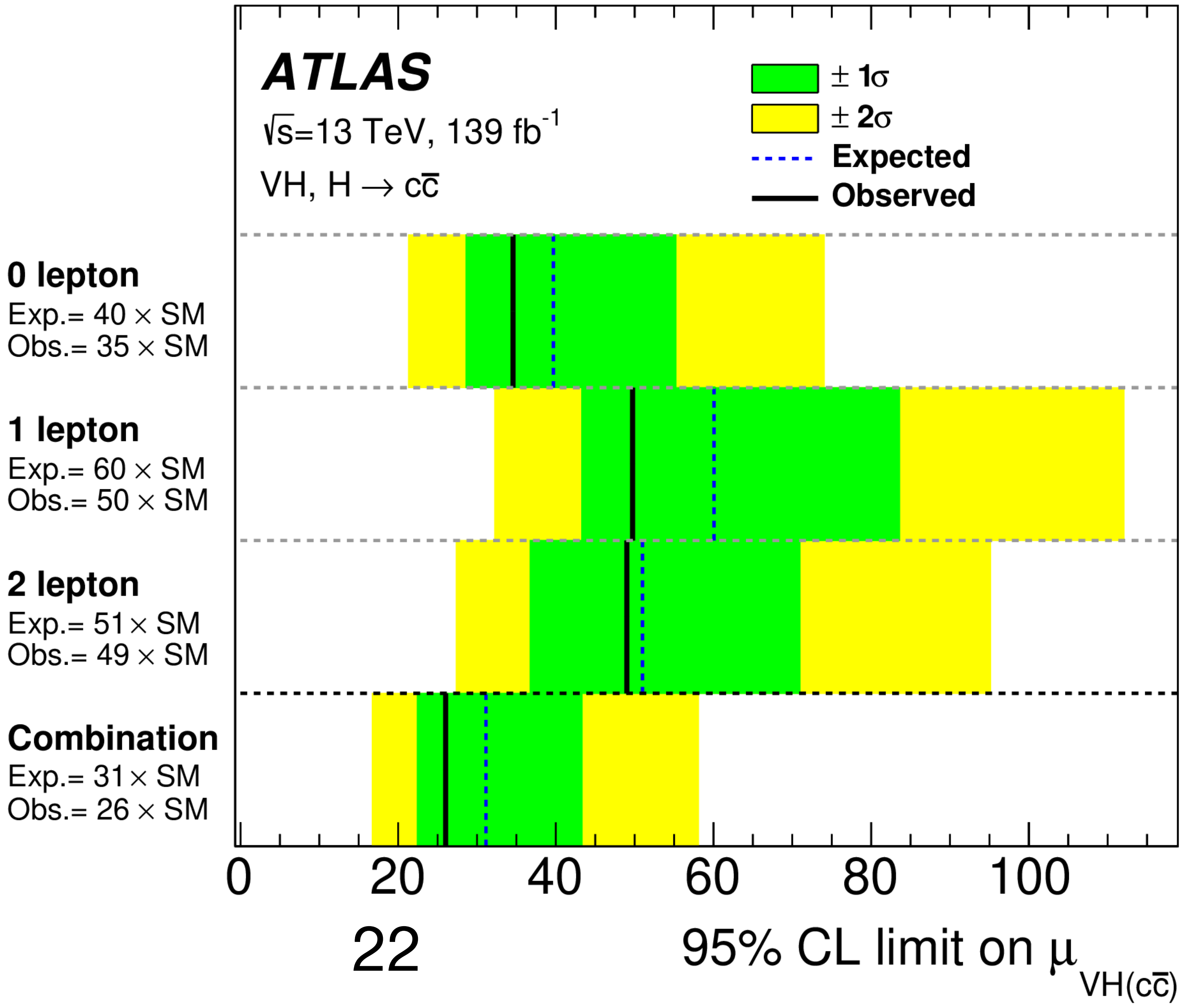

- probing b/c universality: experimentally showing for the first time that H→cc is weaker than H→bb coupling (m_b/m_c= 4.578 ± 0.008)

obs. ratio $|\kappa_c/\kappa_b|$ < 4.5 @ 95%CL

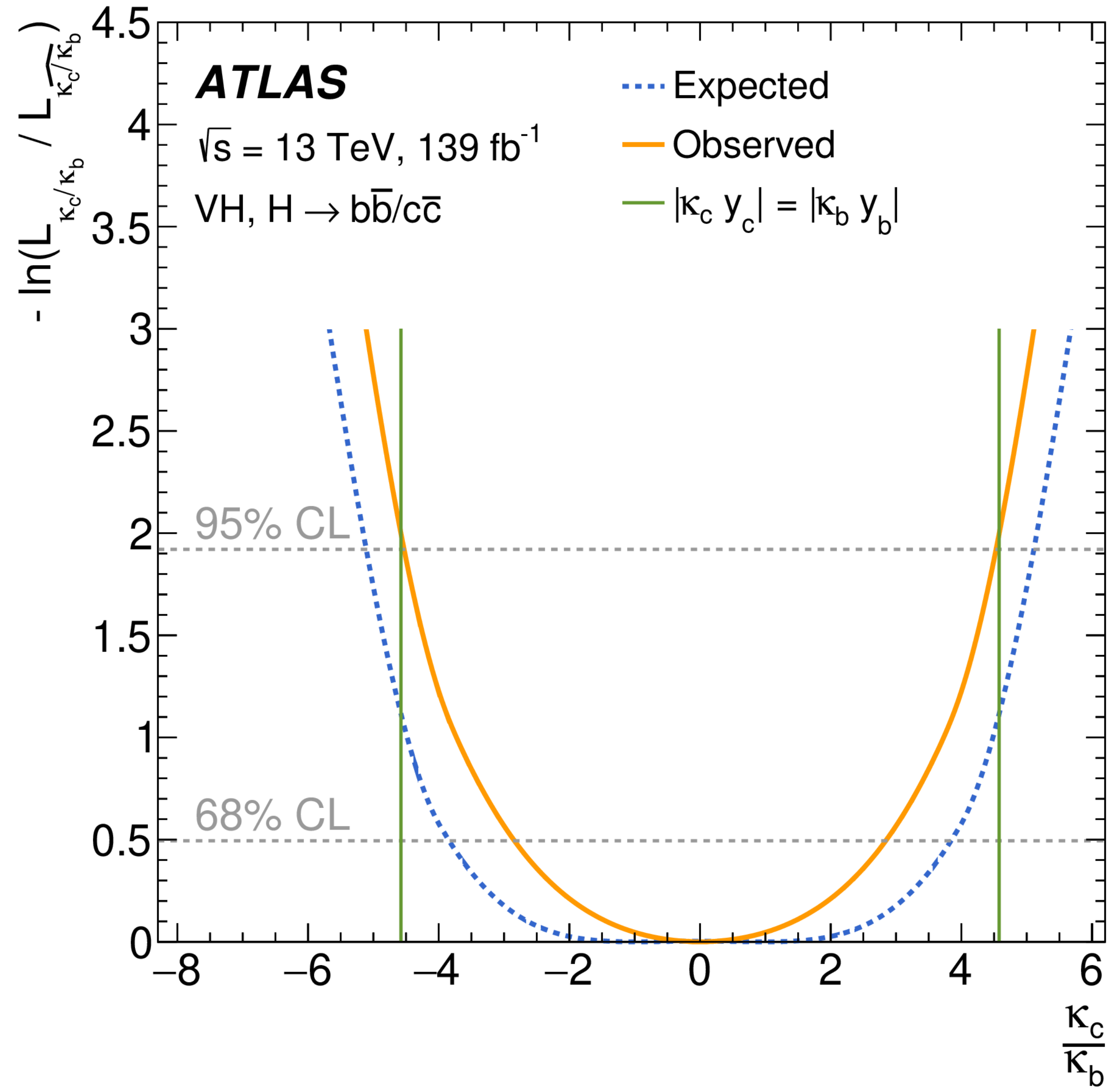

obs. (exp.)

(W/Z)Z→cc 2.6 σ (2.2 σ)

(W/Z)W→cq 3.8 σ (4.6 σ)

(W/Z)H→cc 26 X SM (31 X SM)

Measurement of the VH (H→WW*) cross-section

- WH and ZH production through H→WW*→lνlν and H→WW*→lνjj decays
- 4 channels

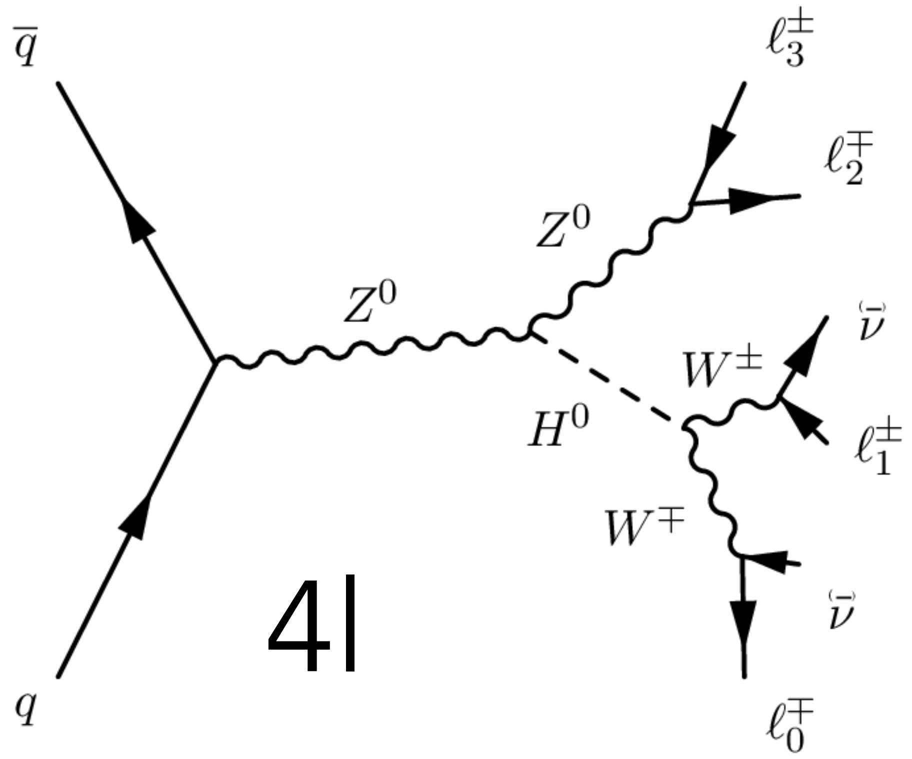

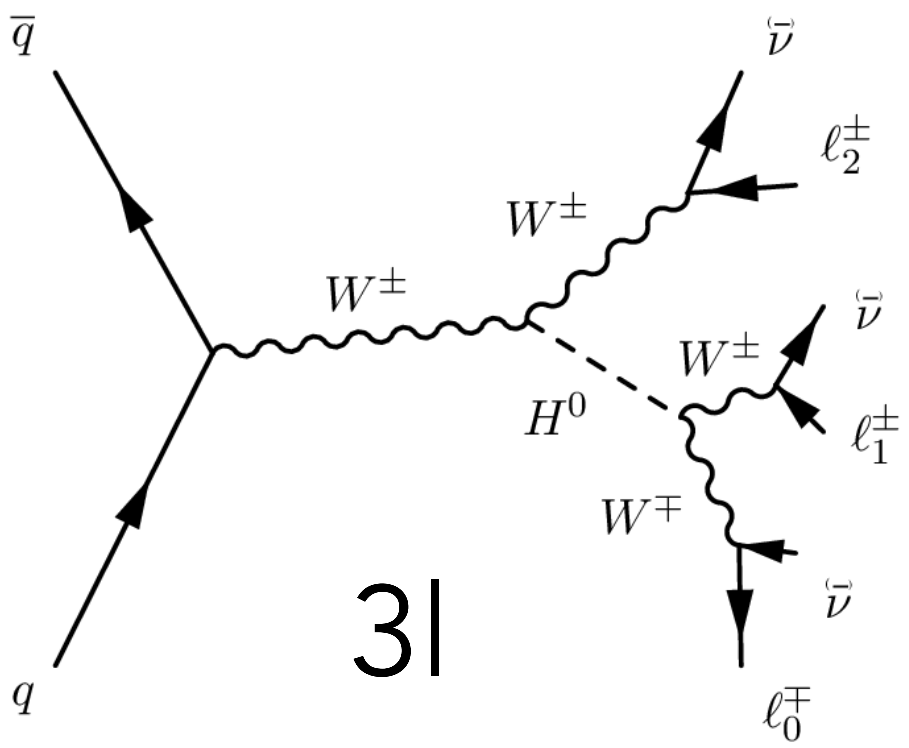

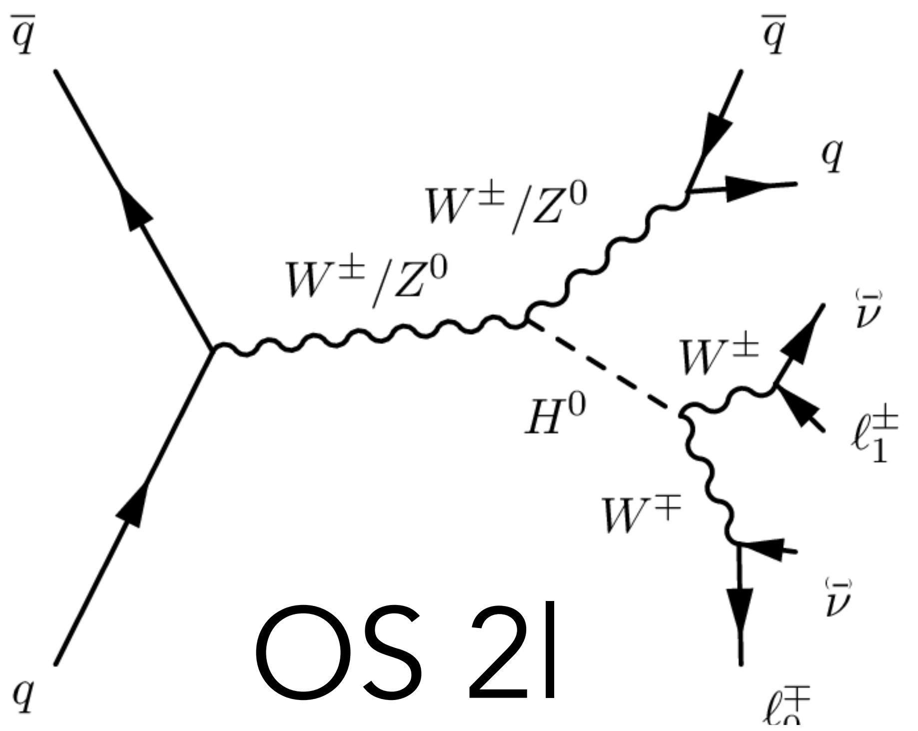

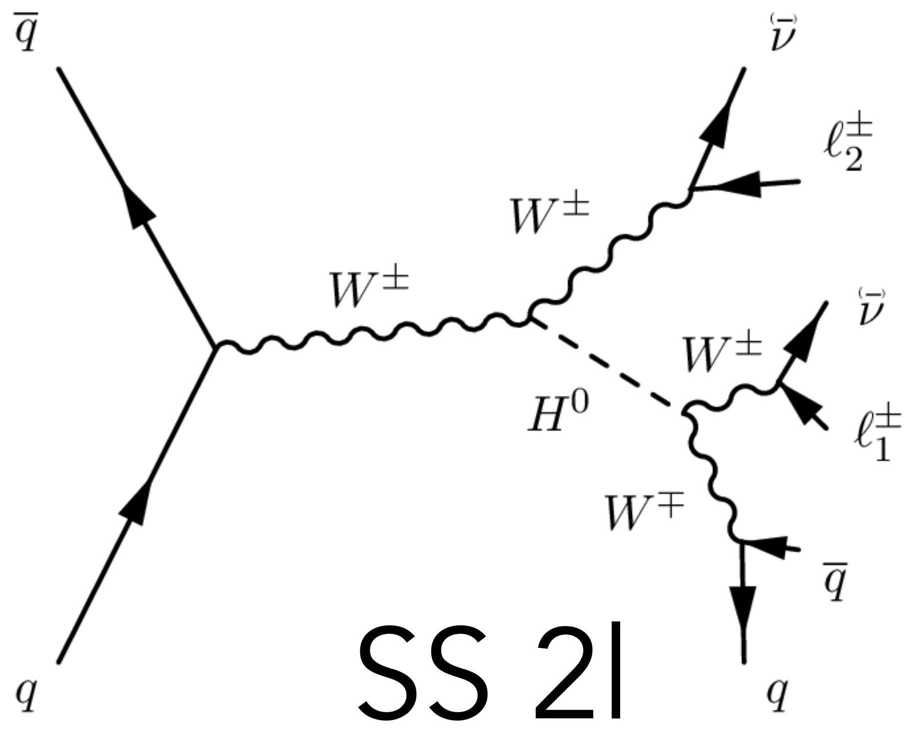

$\sigma_{WH} \times BR_{H\to WW^*} = 0.13^{+0.8}_{-0.7}$ (stat.) $^{+0.05}_{-0.04}$ (syst.) pb

$\sigma_{ZH} \times BR_{H\to WW^*} = 0.31^{+0.09}_{-0.08}$ (stat.) ± 0.03 (syst.) pb

[ATLAS-CONF-2022-067]

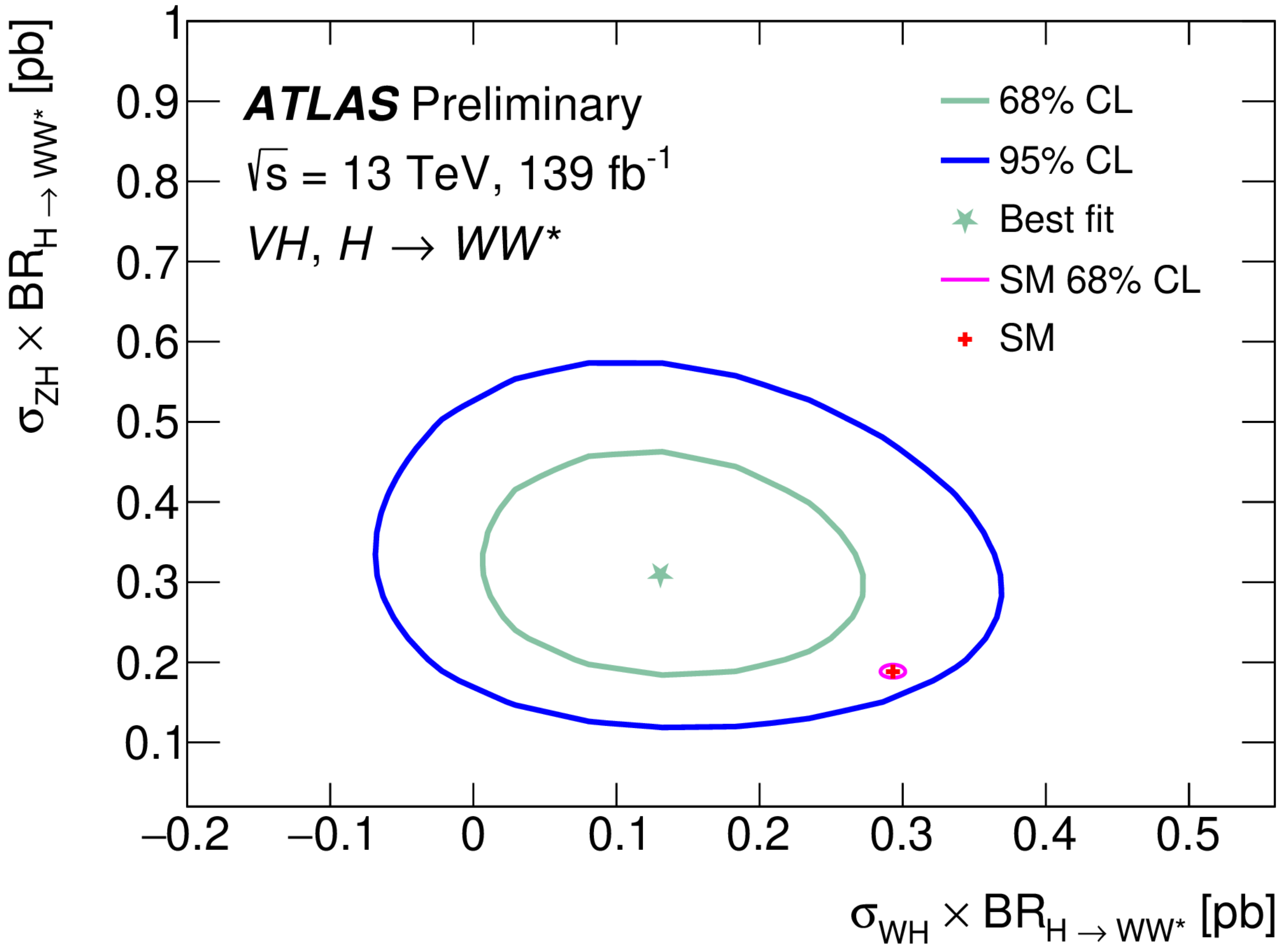

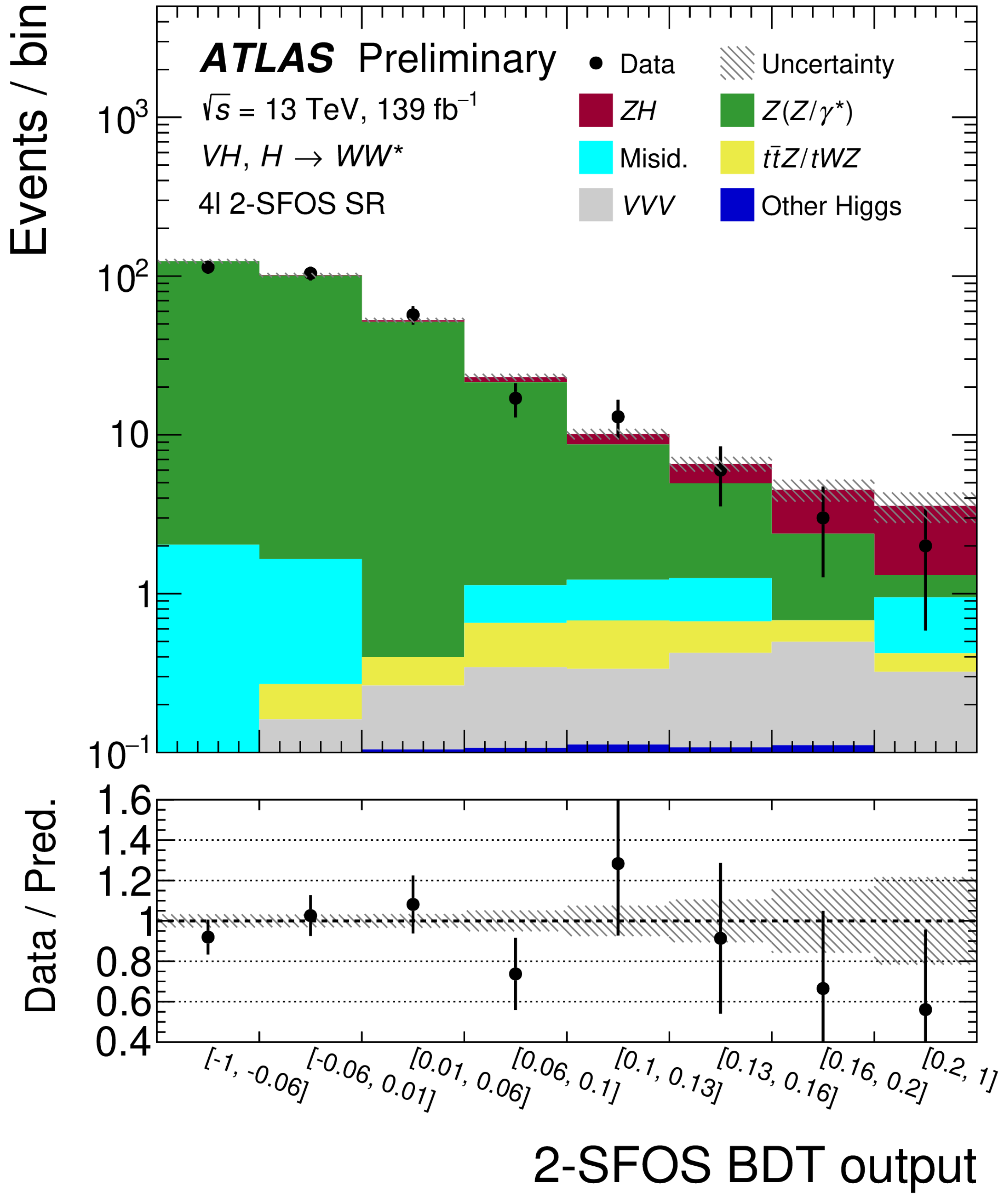

Higgs highlights: 10 years after discovery

- a large number of Higgs production and decay modes have been established
    - ttH with many channels (discovery in 2018), also closing on tH (H→γγ)
- excellent agreement with theory predictions

[Nature 607, pages 52-59 (2022)](#)

$$\kappa_i^2 = \frac{\sigma_i}{\sigma_i^{SM}} \quad \text{and} \quad \kappa_f^2 = \frac{\Gamma_f}{\Gamma_f^{SM}}$$

$$\sigma \cdot \mathcal{B}\,(i \to H \to f) = \kappa_i^2 \cdot \kappa_f^2 \cdot \sigma_i^{SM} \cdot \frac{\Gamma_f^{SM}}{\Gamma_H(\kappa_i^2, \kappa_f^2)}$$

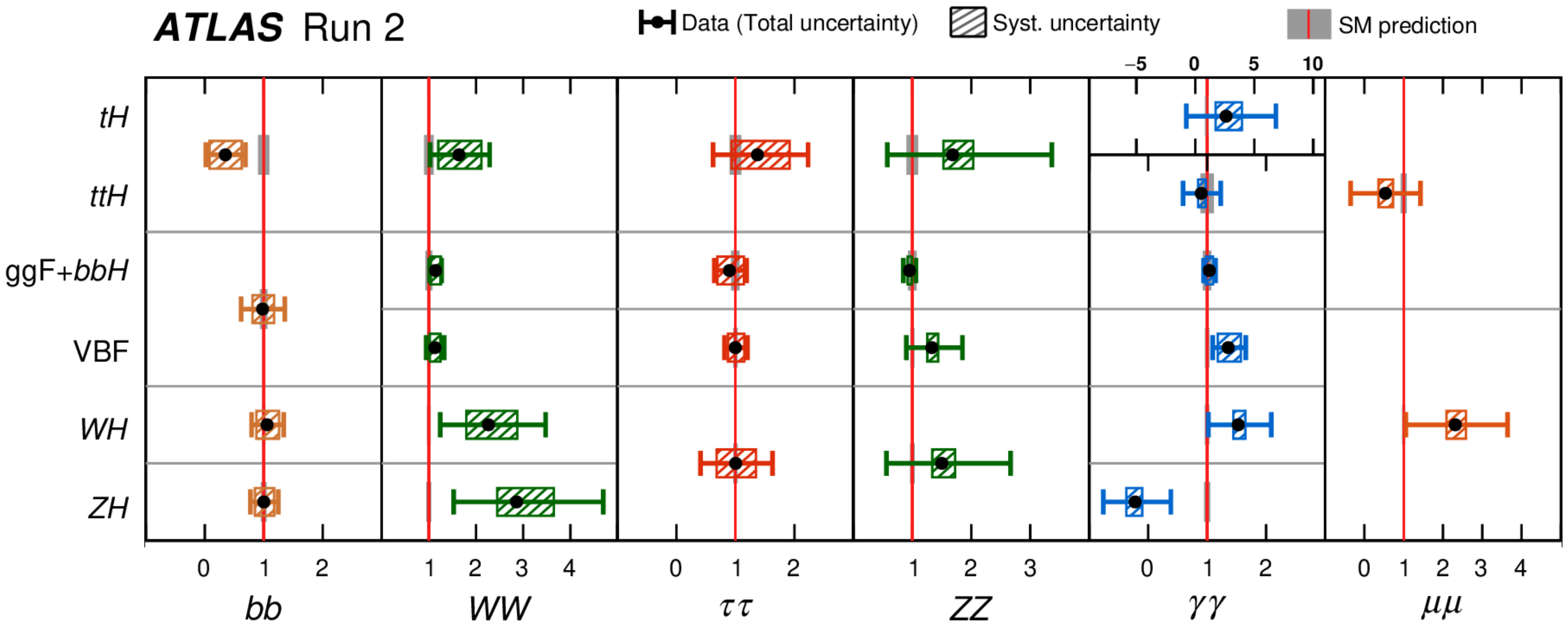

σ × B normalized to SM prediction

μ = 1.05 ± 0.06

= 1.05 ± 0.03 (stat.) ± 0.03 (exp.) ± 0.04 (sig.th.) ± 0.04 (bkg.th.)

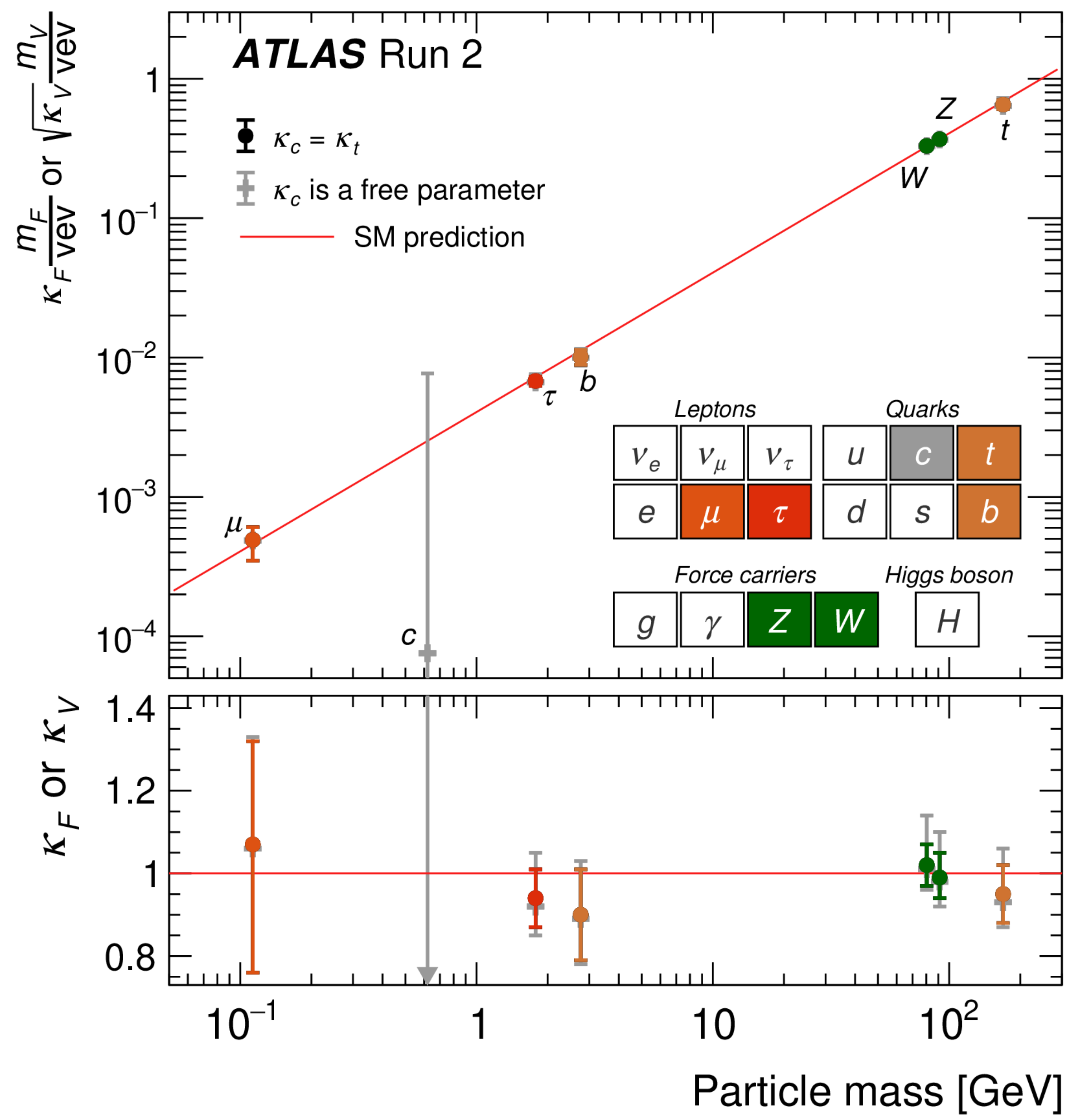

- ATLAS Run 2 results comparable to [2014 HL-LHC projections](#)!

[Search for H→μμ](#)

ATLAS searches

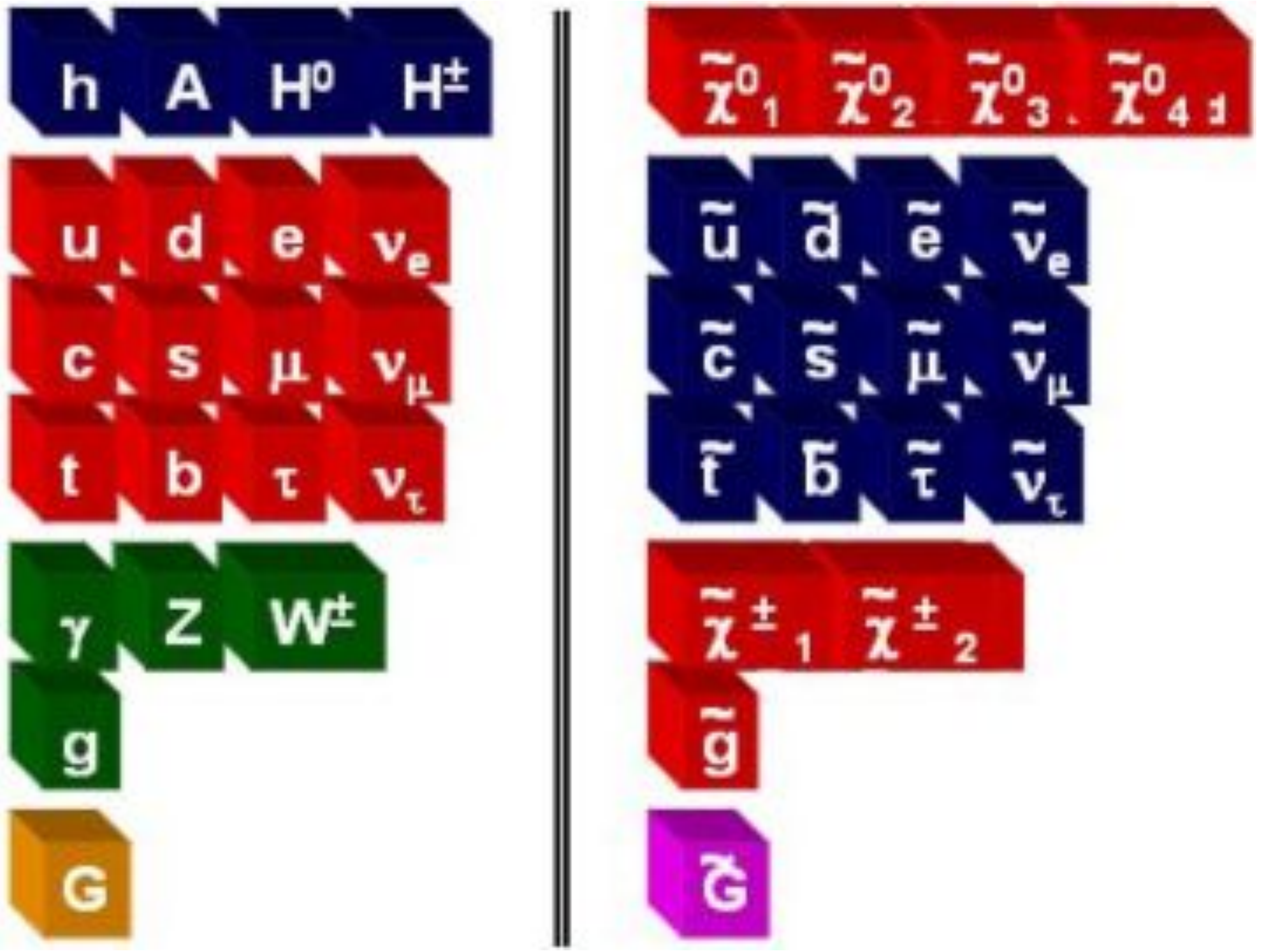

HDBS

ATLAS EXOTICS GROUP

Search for Higgs boson pair production

$$V(\phi^\dagger\phi) = -\mu^2\phi^\dagger\phi + \lambda(\phi^\dagger\phi)^2$$

$$\supset \underbrace{\mu^2}_{\frac{1}{2}m_H^2} H^2 + \sqrt{\frac{\lambda}{2}}\mu H^3 + \frac{\lambda}{4}H^4$$

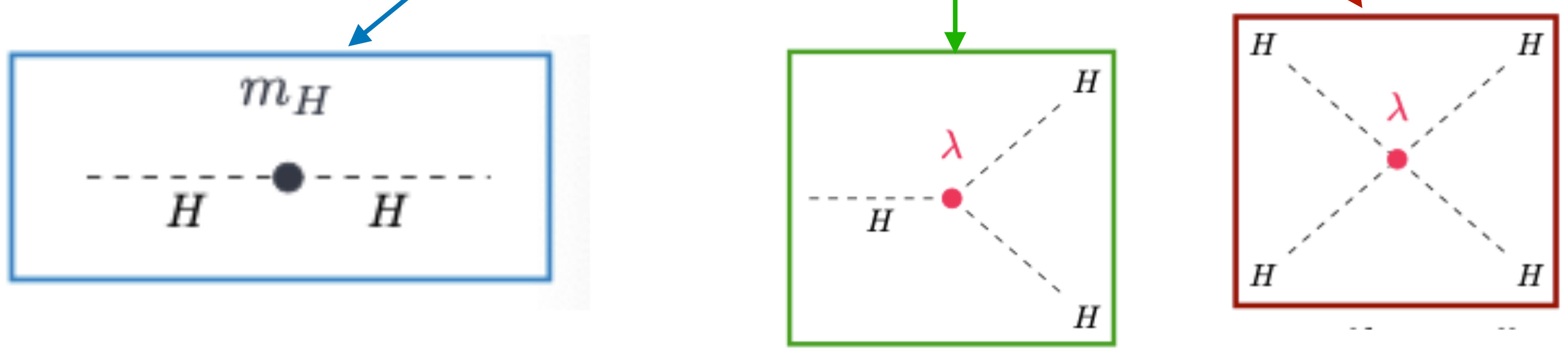

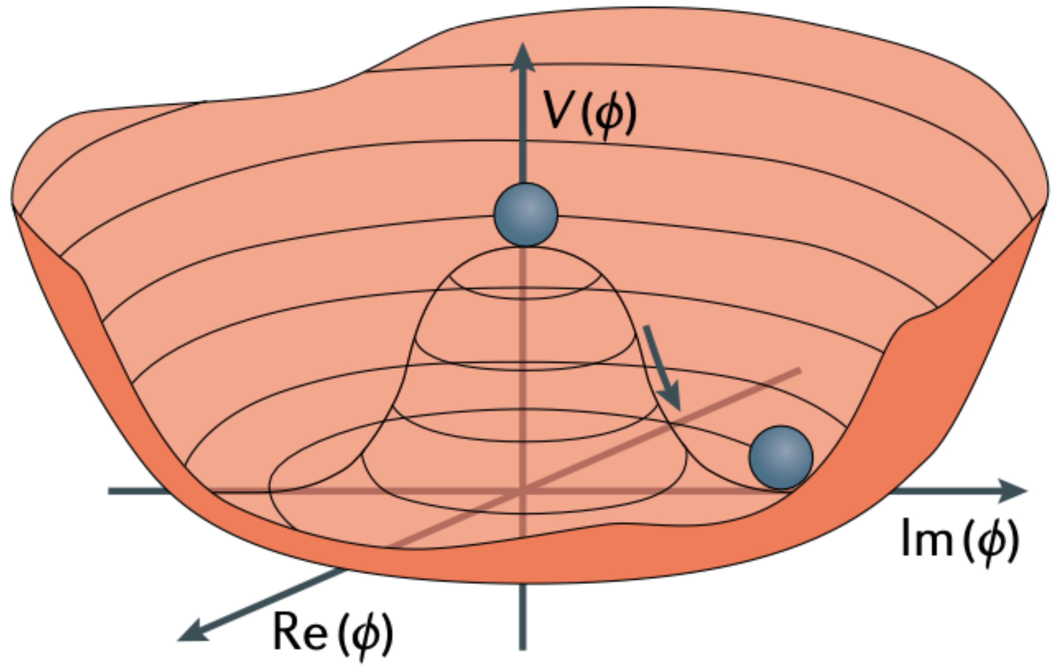

- probe Higgs self-interaction (λ_{HHH}) and Higgs potential

$\kappa_\lambda \equiv \lambda_{HHH}/\lambda^{SM}_{HHH}$

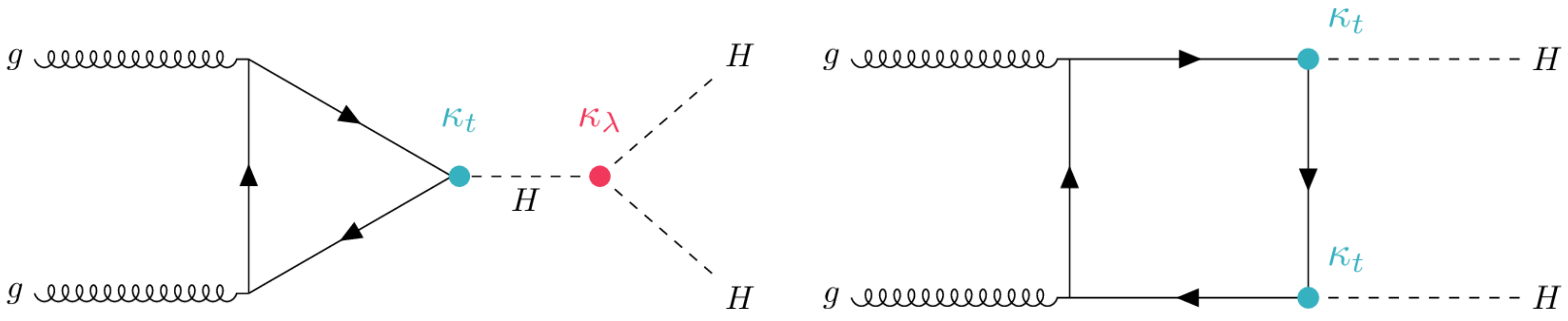

- negative interference between main contributions: very small production cross-section σ_{ggF} **SM = 31.05 fb** (~1000 times smaller than that of single H)

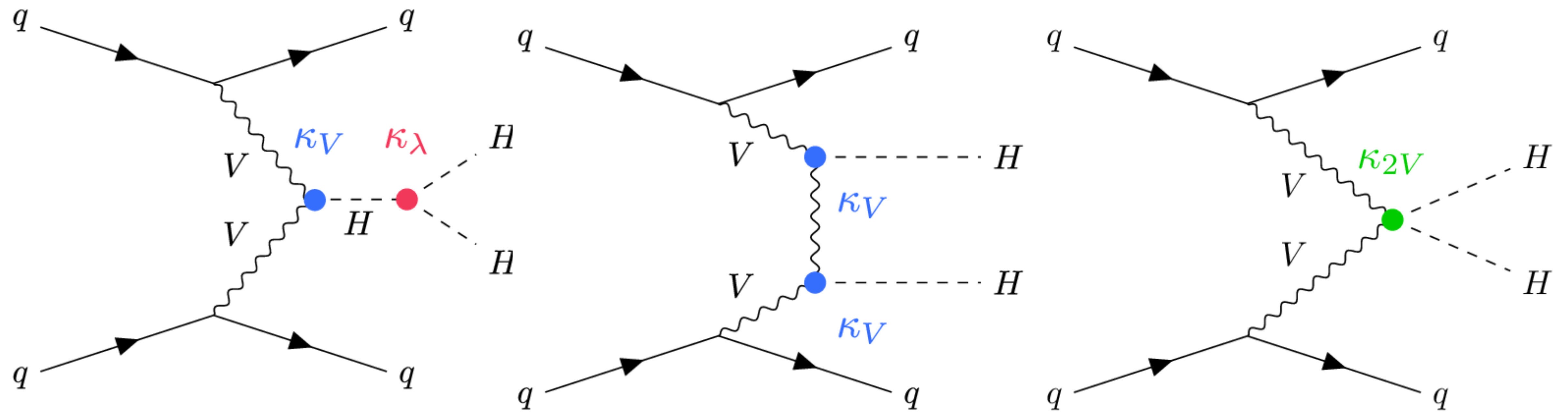

- second leading production mode σ_{VBF} **SM = 1.73 fb**

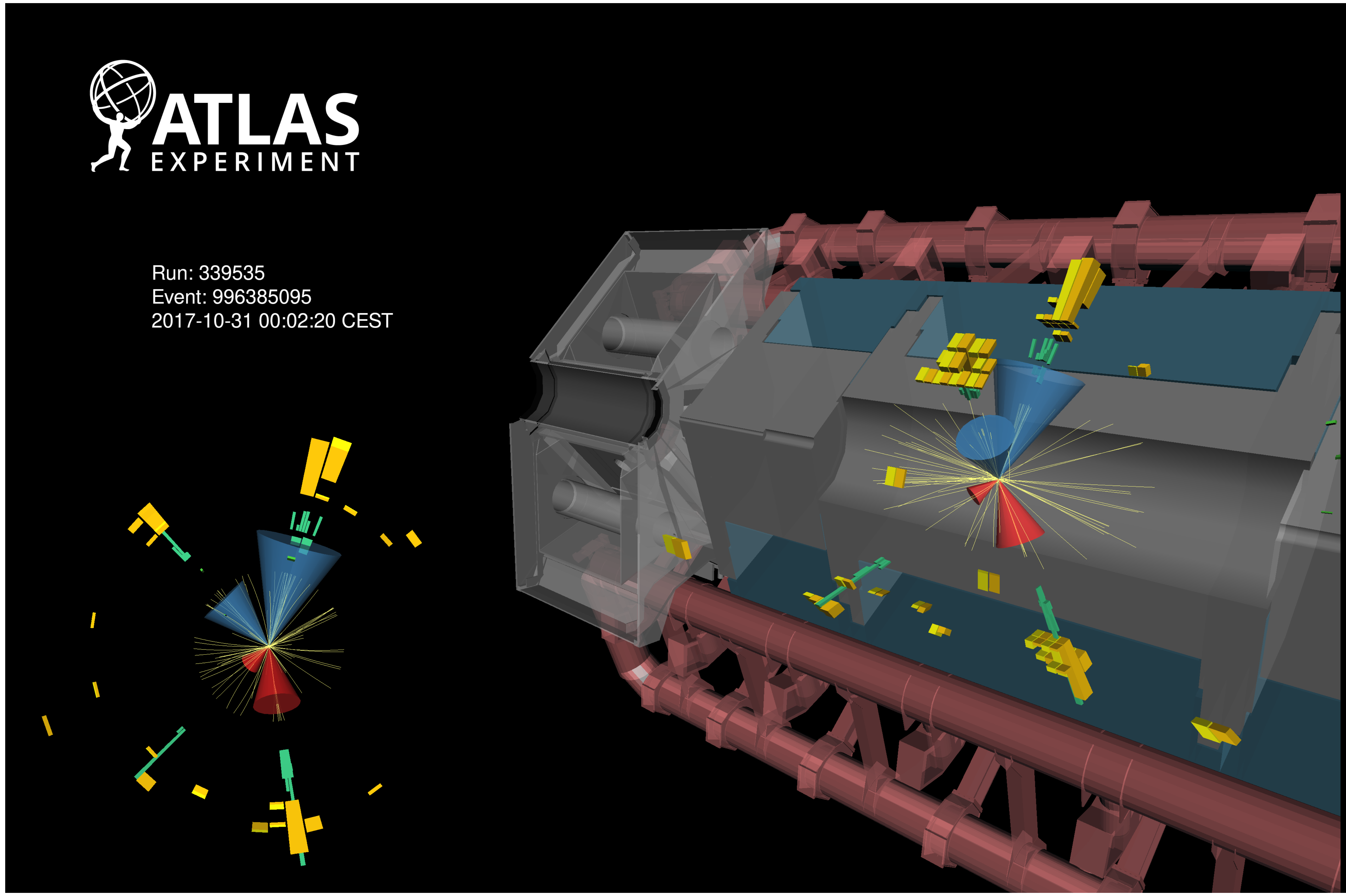

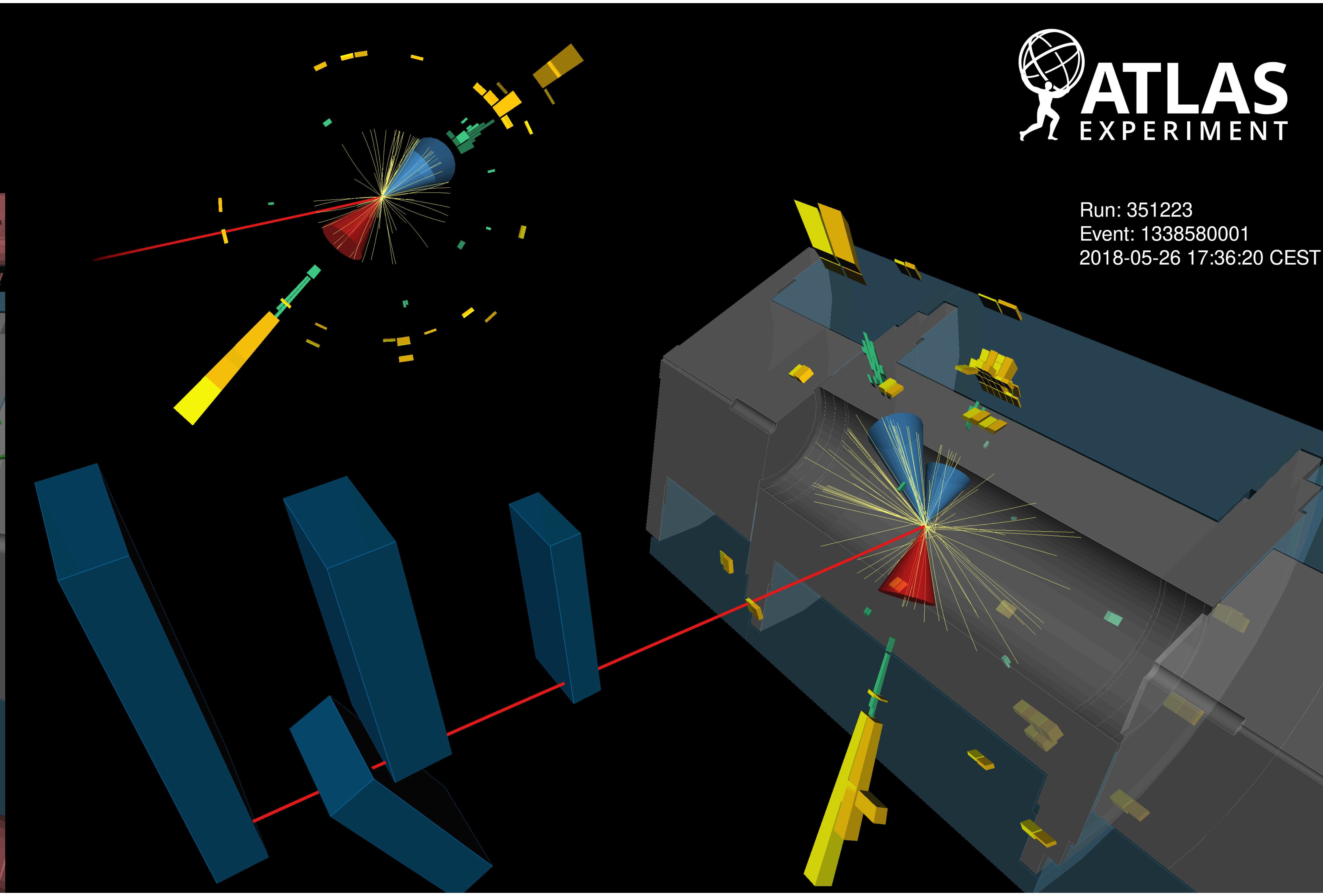

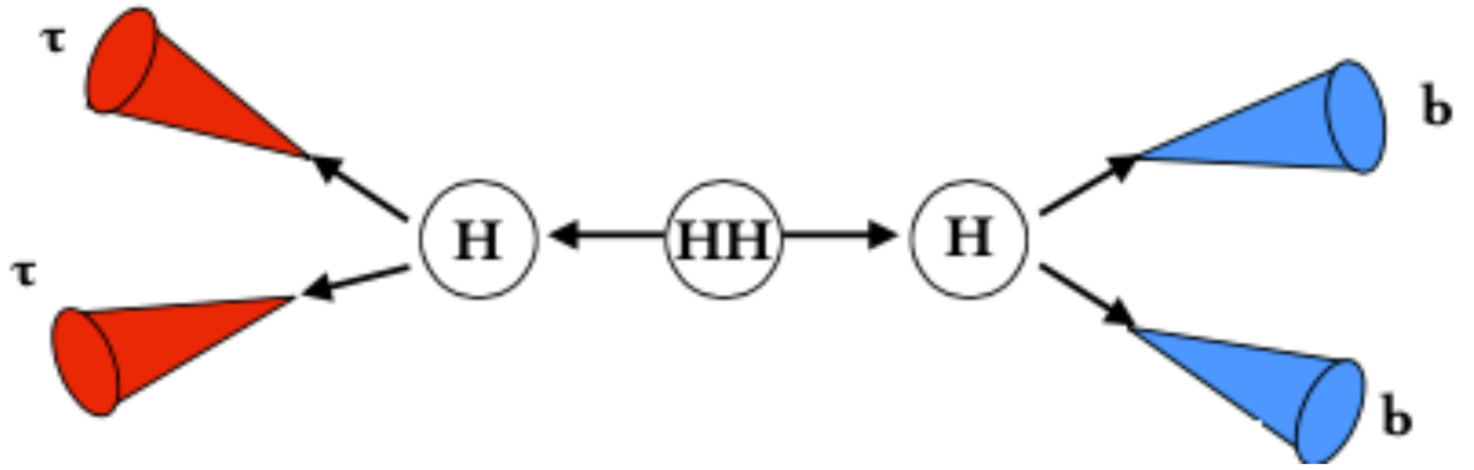

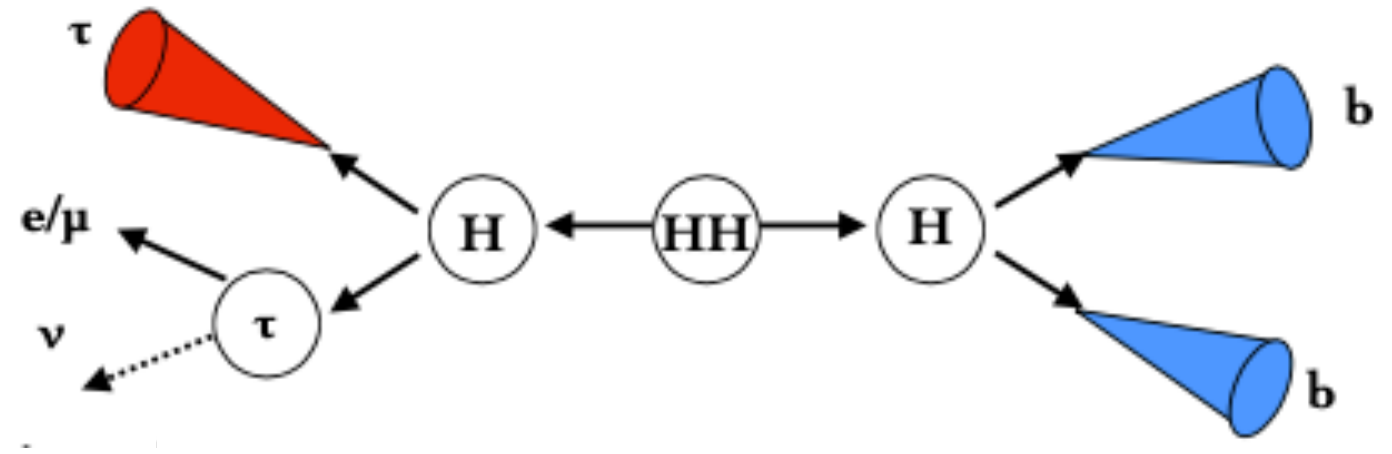

$HH \rightarrow bb\tau_{had}\tau_{had}$

$HH \rightarrow bb\tau_{lep}\tau_{had}$

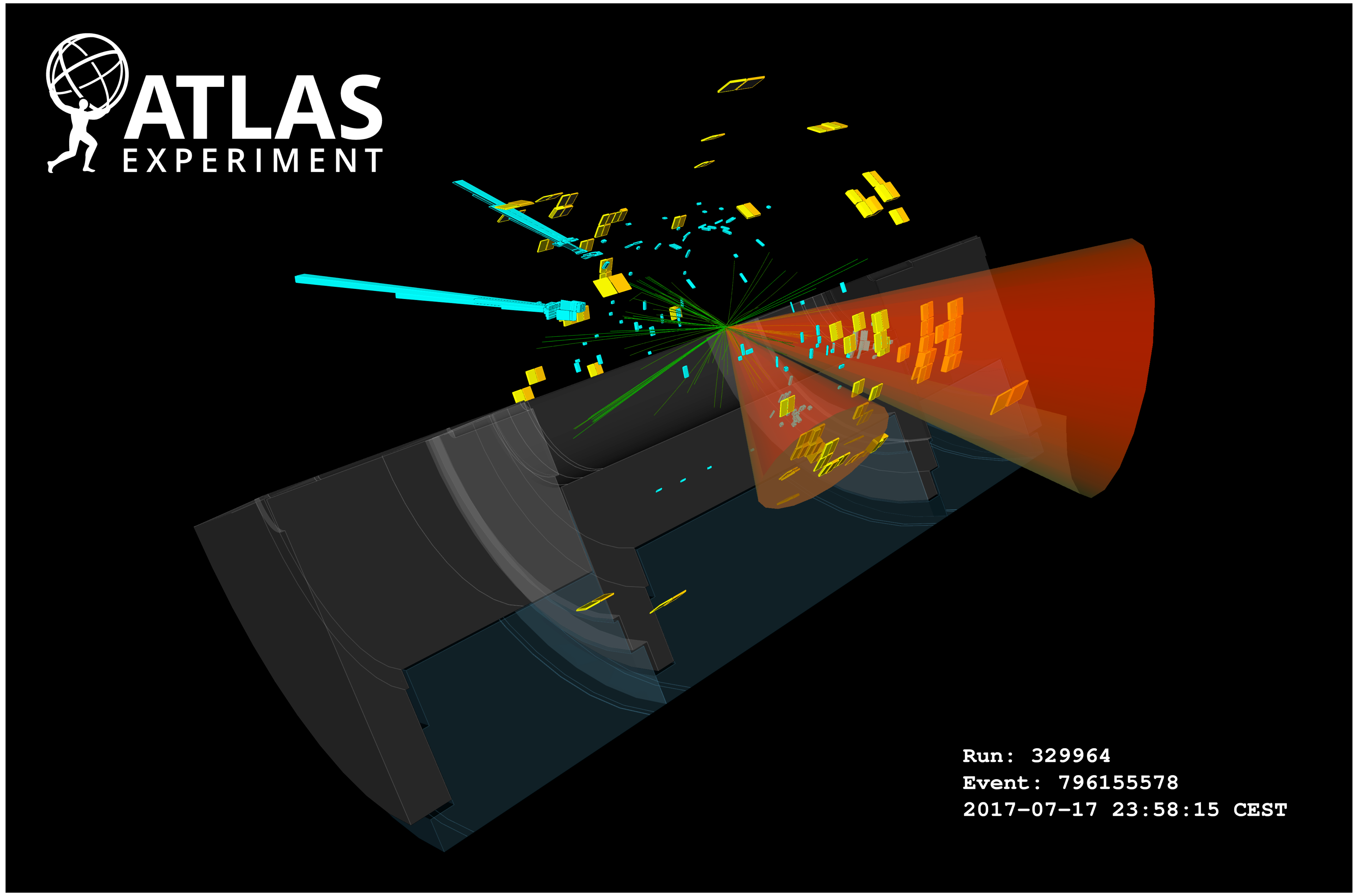

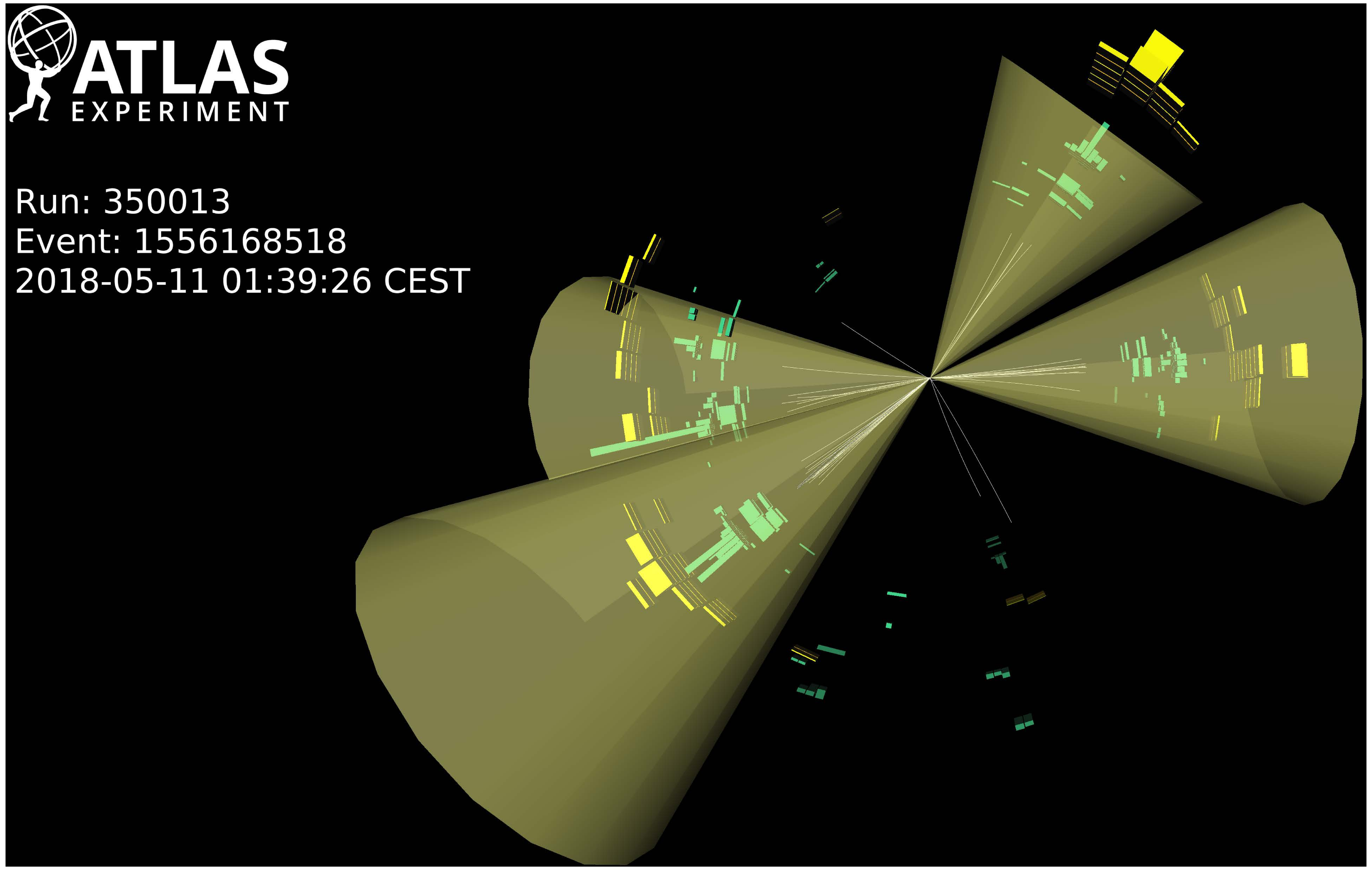

HH → bbγγ

HH → bbbb

HH combination

[arXiv:2211.0121 (Submitted to: Phys. Lett. B.)]

	bb	WW	ττ	ZZ	γγ
bb	34%				
WW	25%	4.6%			
ττ	7.3%	2.7%	0.39%		
ZZ	3.1%	1.1%	0.33%	0.069%	
γγ	0.26%	0.10%	0.028%	0.012%	0.0005%

- multiple search channels, trade-offs between BR vs final state
- results for the combination of the three most sensitive channels: bbbb, bbττ and bbγγ

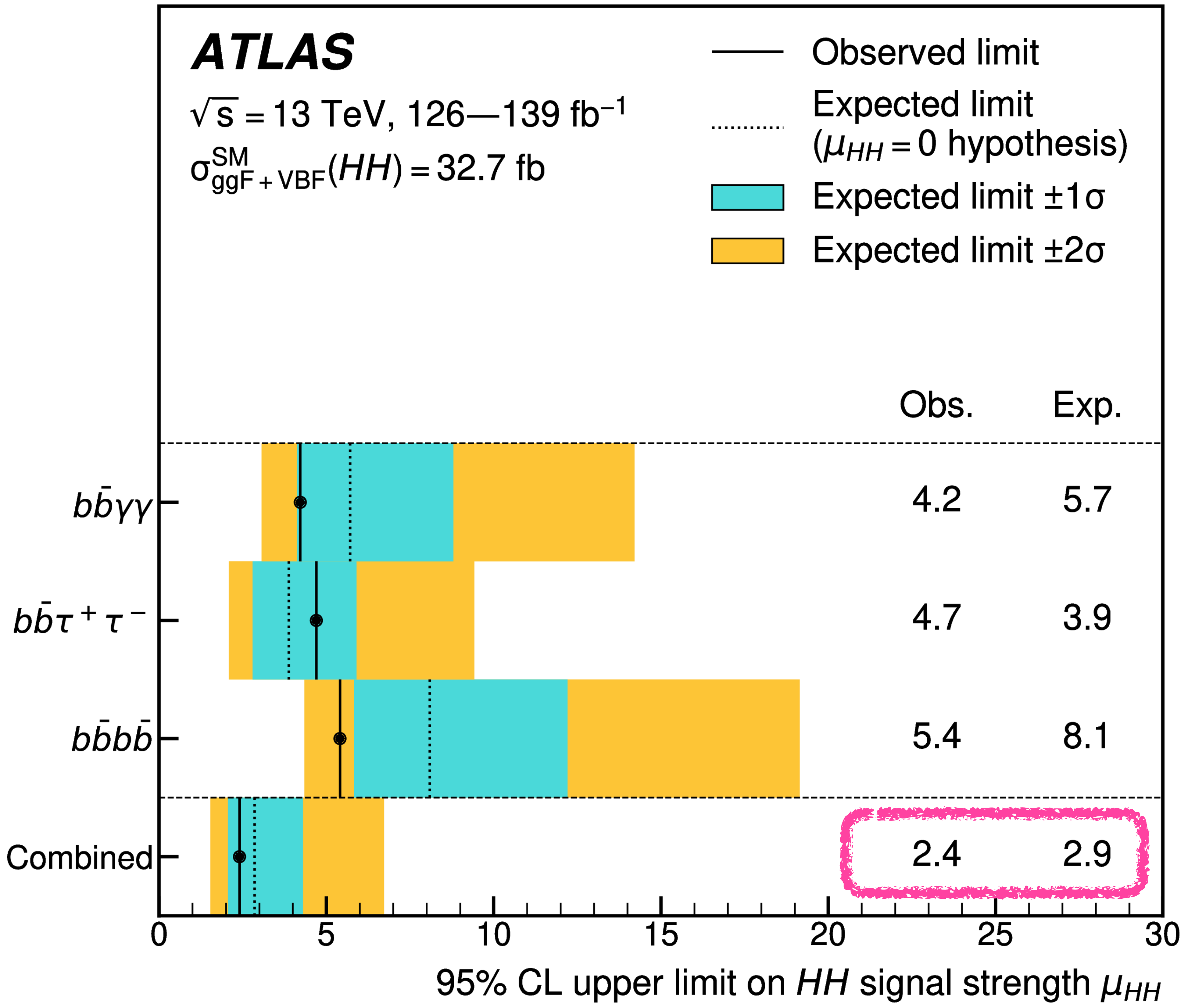

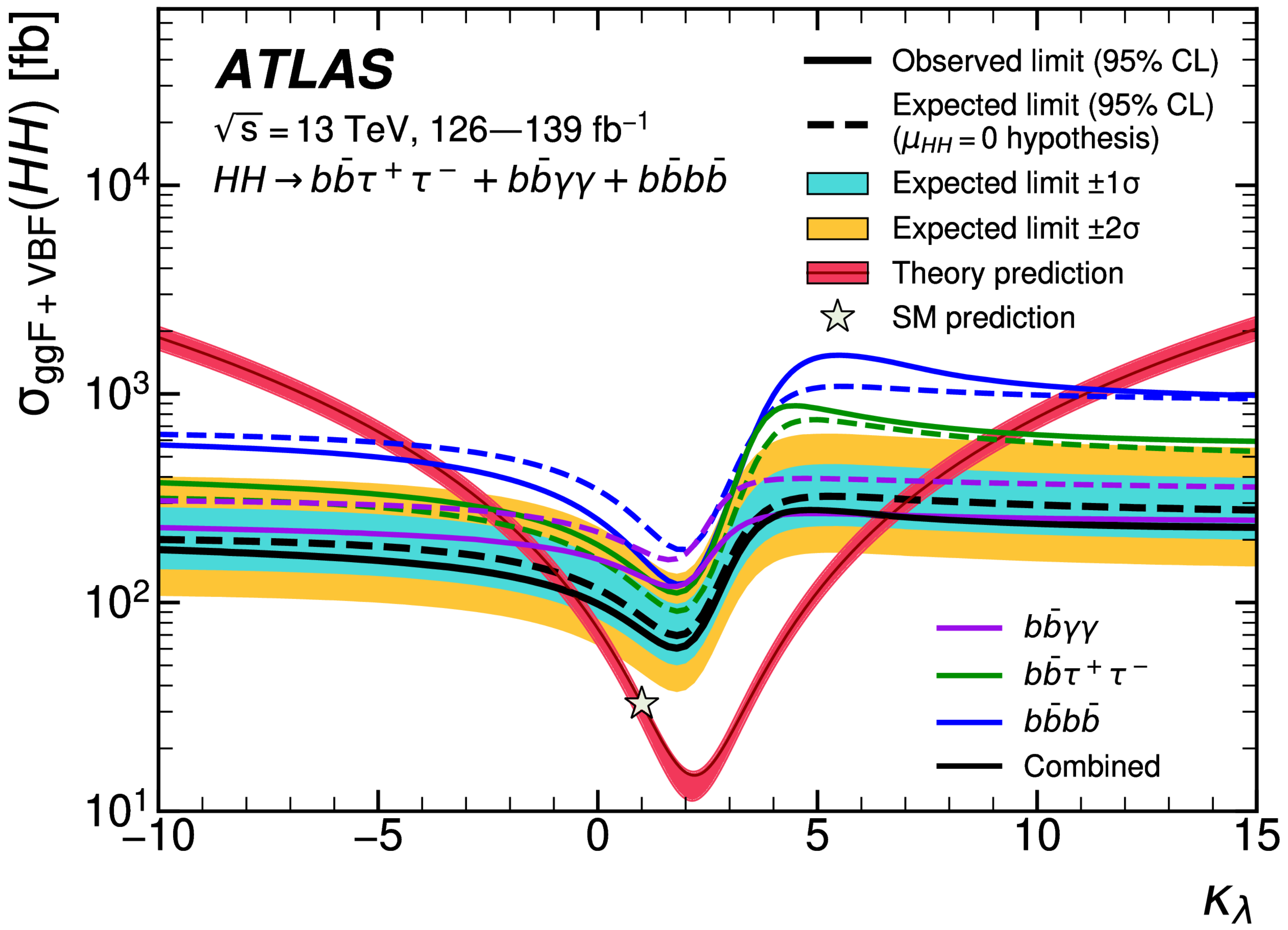

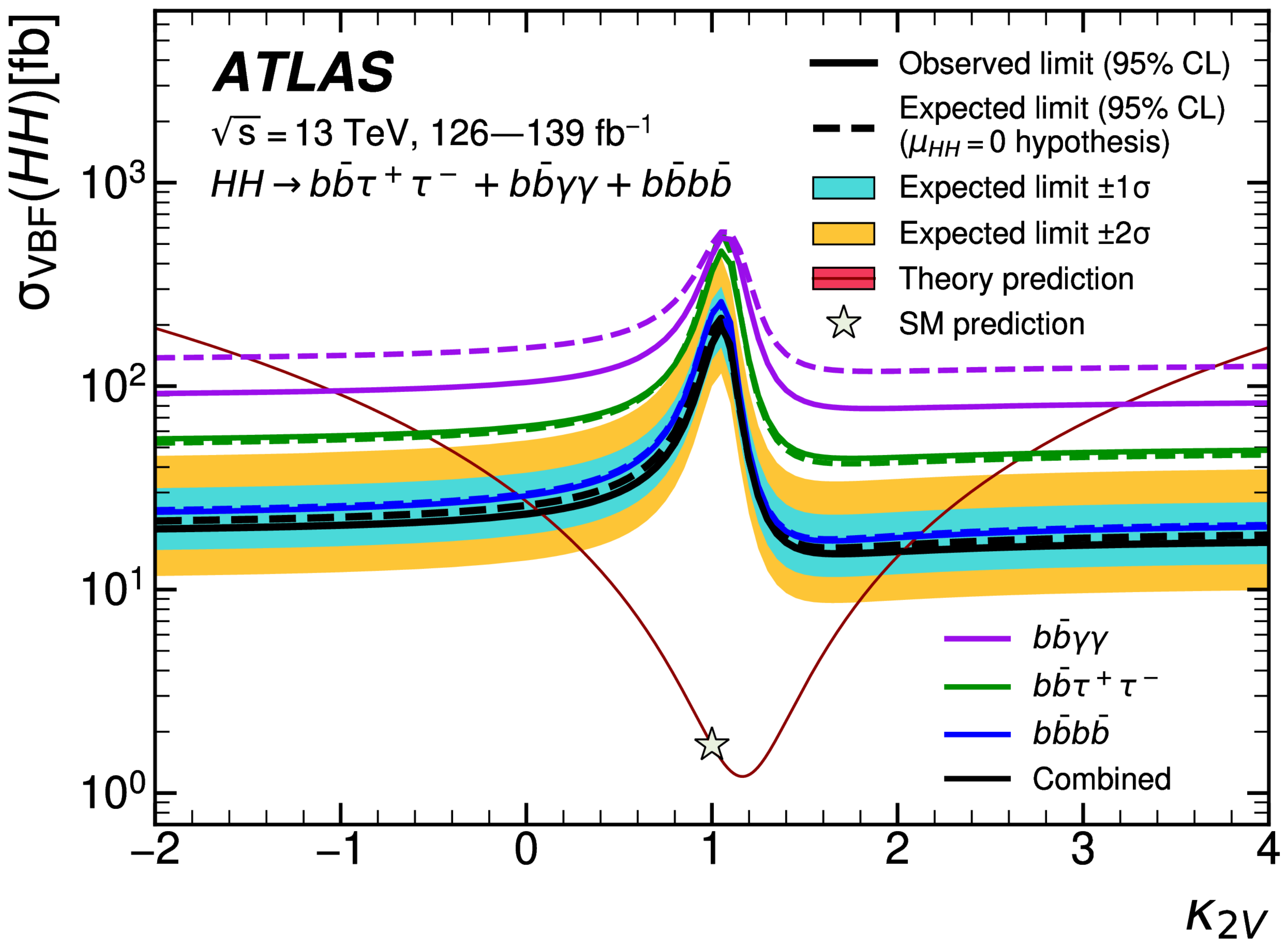

- **most stringent upper limit on HH production to date**

- bbγγ most sensitive for large variations of κ_λ
- bbττ most sensitive for κ_λ values close to the SM
- bbbb most sensitive to VBF production and variations of κ_{2V}

HH + H combination

[arXiv:2211.0121 (Submitted to: Phys. Lett. B.)]

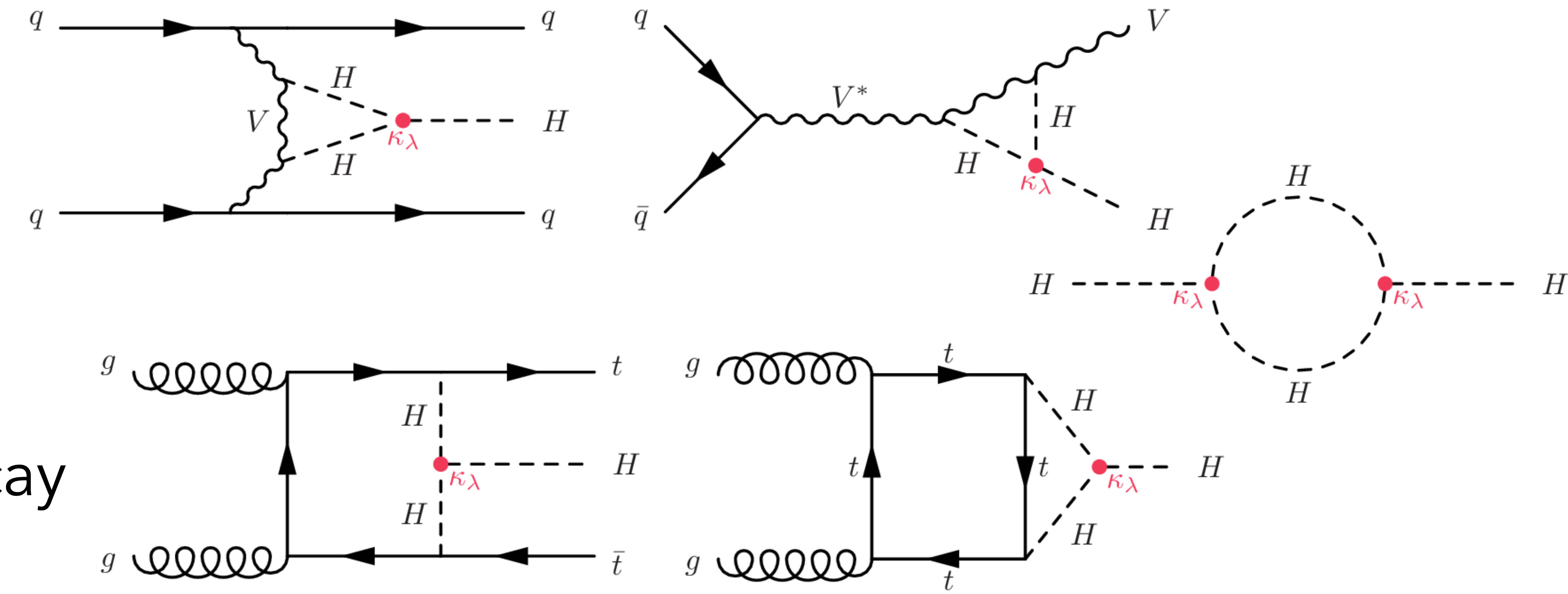

- exploits direct sensitivity to κ_λ of HH and indirect sensitivity to κ_λ of single H through NLO EW corrections affecting single H production and decay

Channel
$HH \to b\bar{b}\gamma\gamma$
$HH \to b\bar{b}\tau^+\tau^-$
$HH \to b\bar{b}b\bar{b}$
$H \to \gamma\gamma$
$H \to ZZ^* \to 4\ell$
$H \to \tau^+\tau^-$
$H \to WW^* \to e\nu\mu\nu$ (ggF,VBF)
$H \to b\bar{b}$ (VH)
$H \to b\bar{b}$ (VBF)
$H \to b\bar{b}$ $(t\bar{t}H)$

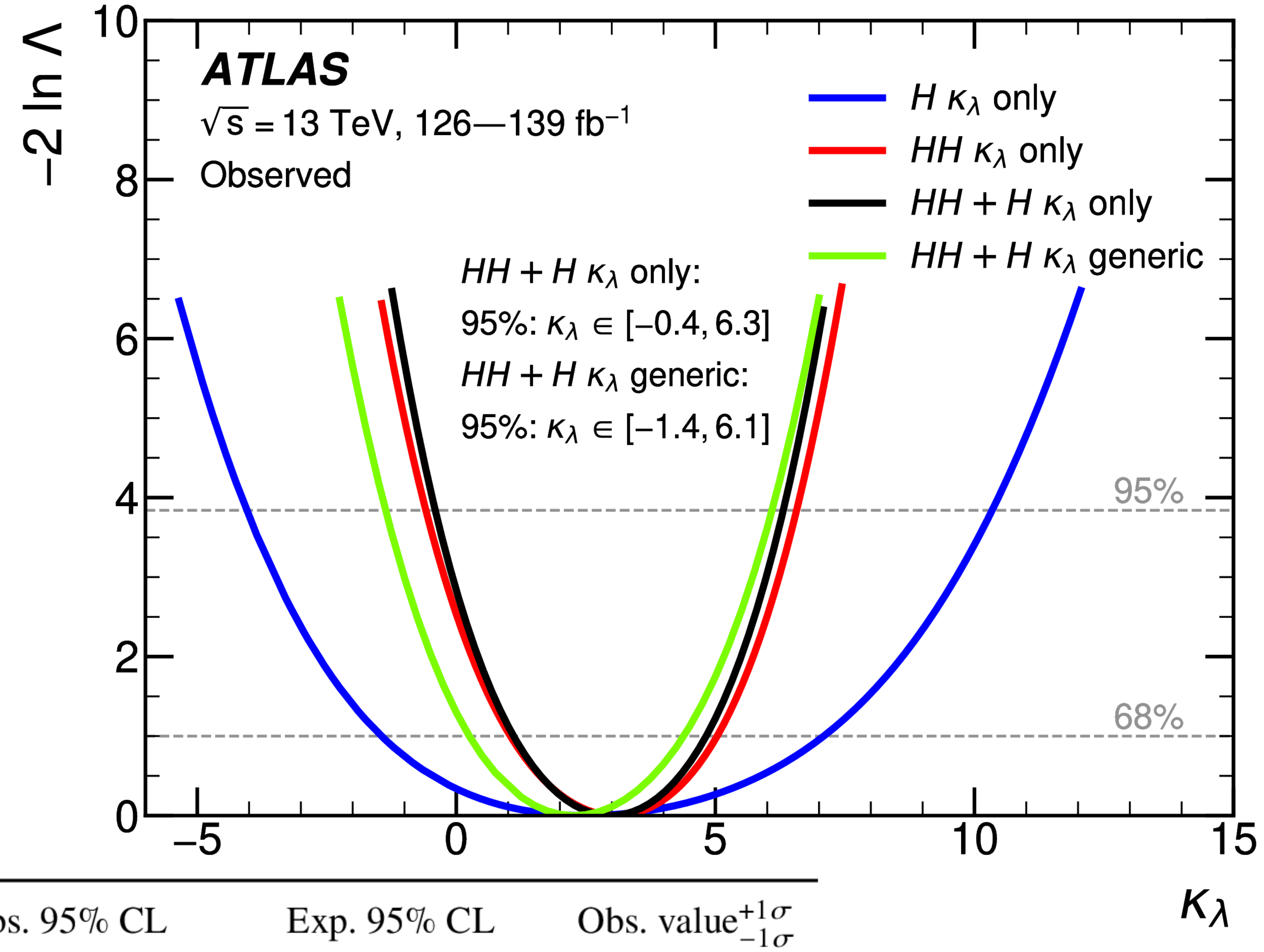

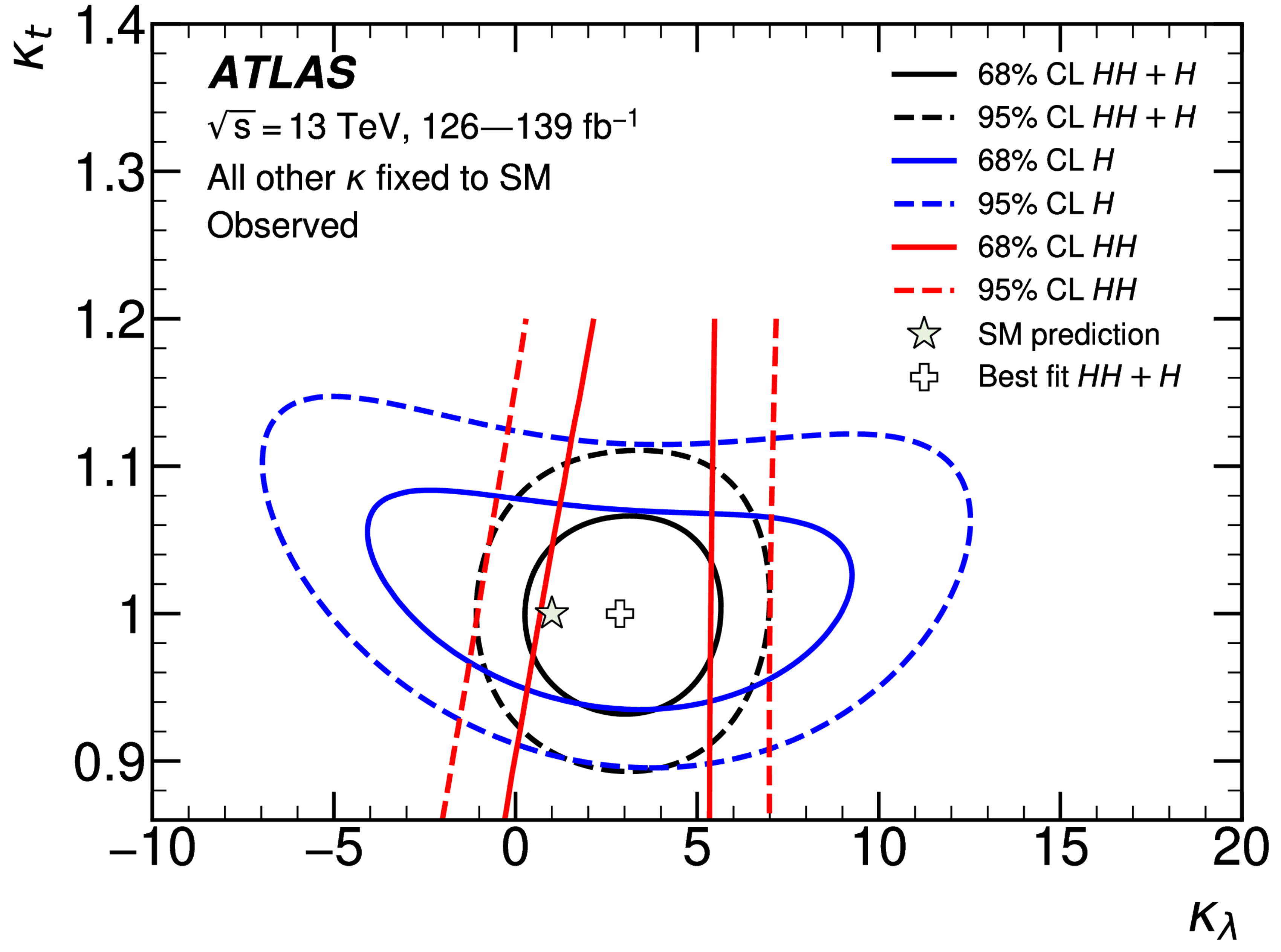

Combination assumption	Obs. 95% CL	Exp. 95% CL	Obs. value$^{+1\sigma}_{-1\sigma}$
HH combination	$-0.6 < \kappa_\lambda < 6.6$	$-2.1 < \kappa_\lambda < 7.8$	$\kappa_\lambda = 3.1^{+1.9}_{-2.0}$
Single-H combination	$-4.0 < \kappa_\lambda < 10.3$	$-5.2 < \kappa_\lambda < 11.5$	$\kappa_\lambda = 2.5^{+4.6}_{-3.9}$
HH+H combination	$-0.4 < \kappa_\lambda < 6.3$	$-1.9 < \kappa_\lambda < 7.6$	$\kappa_\lambda = 3.0^{+1.8}_{-1.9}$
HH+H combination, κ_t floating	$-0.4 < \kappa_\lambda < 6.3$	$-1.9 < \kappa_\lambda < 7.6$	$\kappa_\lambda = 3.0^{+1.8}_{-1.9}$
HH+H combination, κ_t, κ_V, κ_b, κ_τ floating	$-1.4 < \kappa_\lambda < 6.1$	$-2.2 < \kappa_\lambda < 7.7$	$\kappa_\lambda = 2.3^{+2.1}_{-2.0}$

- study provides the **most stringent constraints on κ_λ** to date
- κ_λ interval less constrained in a more generic model

Exclusive H and Z decays into vector quarkonium + γ

- alternative way to probe quark-Yukawa couplings distinct experimental signature (radiative decays)
- exclusive background: μμγ events through DY, MC modelling
- inclusive background: dominant, mostly multi-jet and γ+jets, data-driven modelling

arXiv:2208.03122 (Submitted to: EPJC)

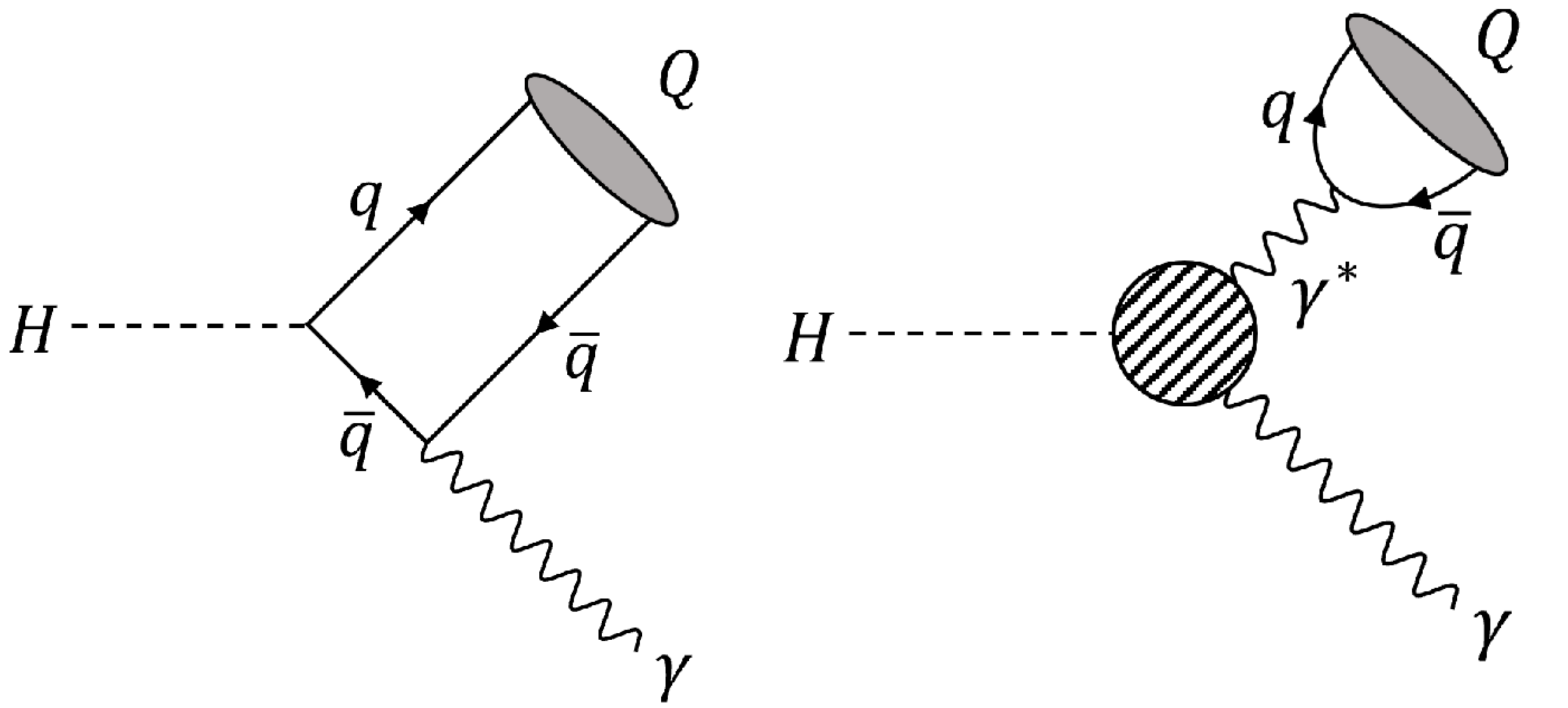

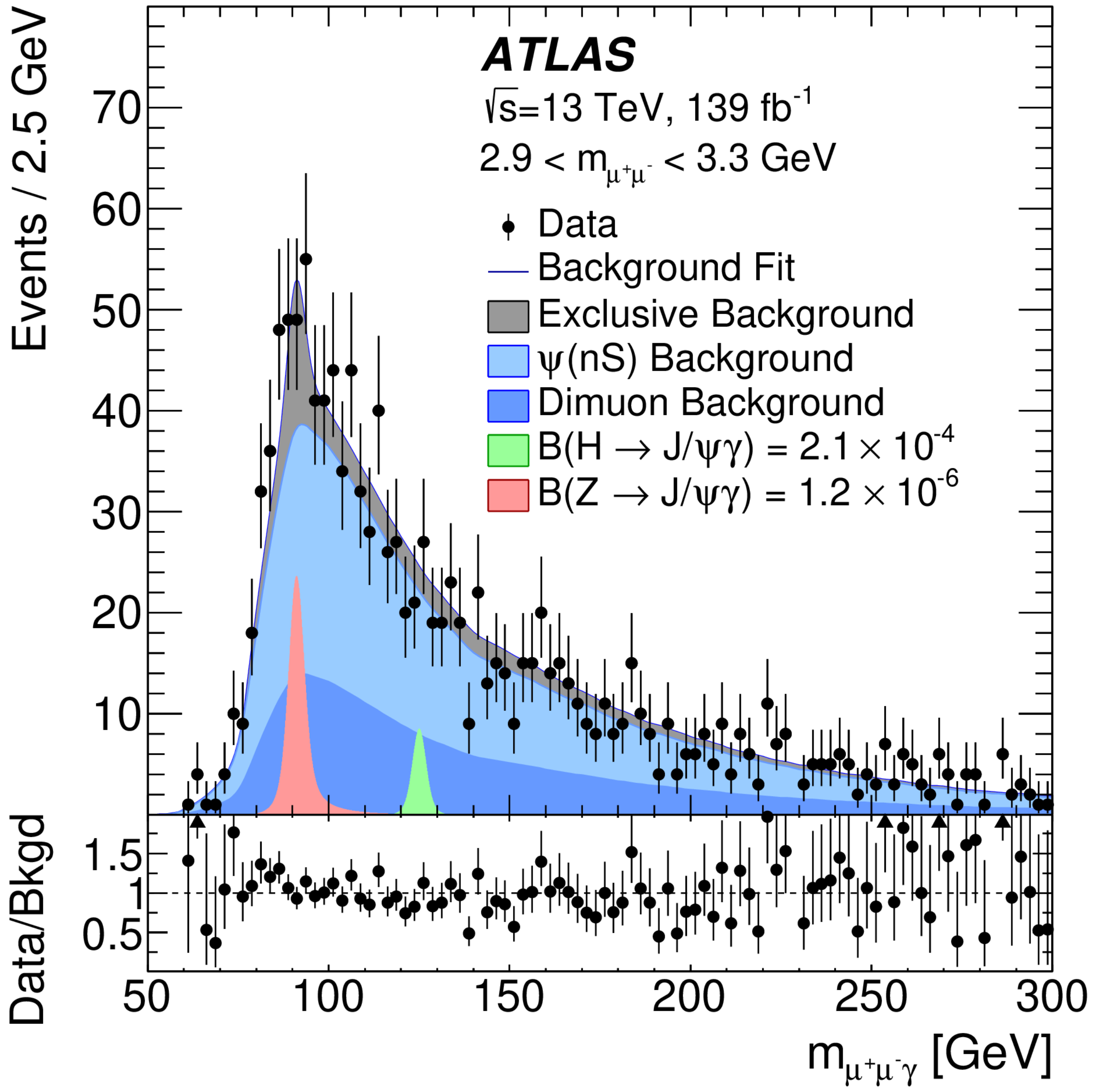

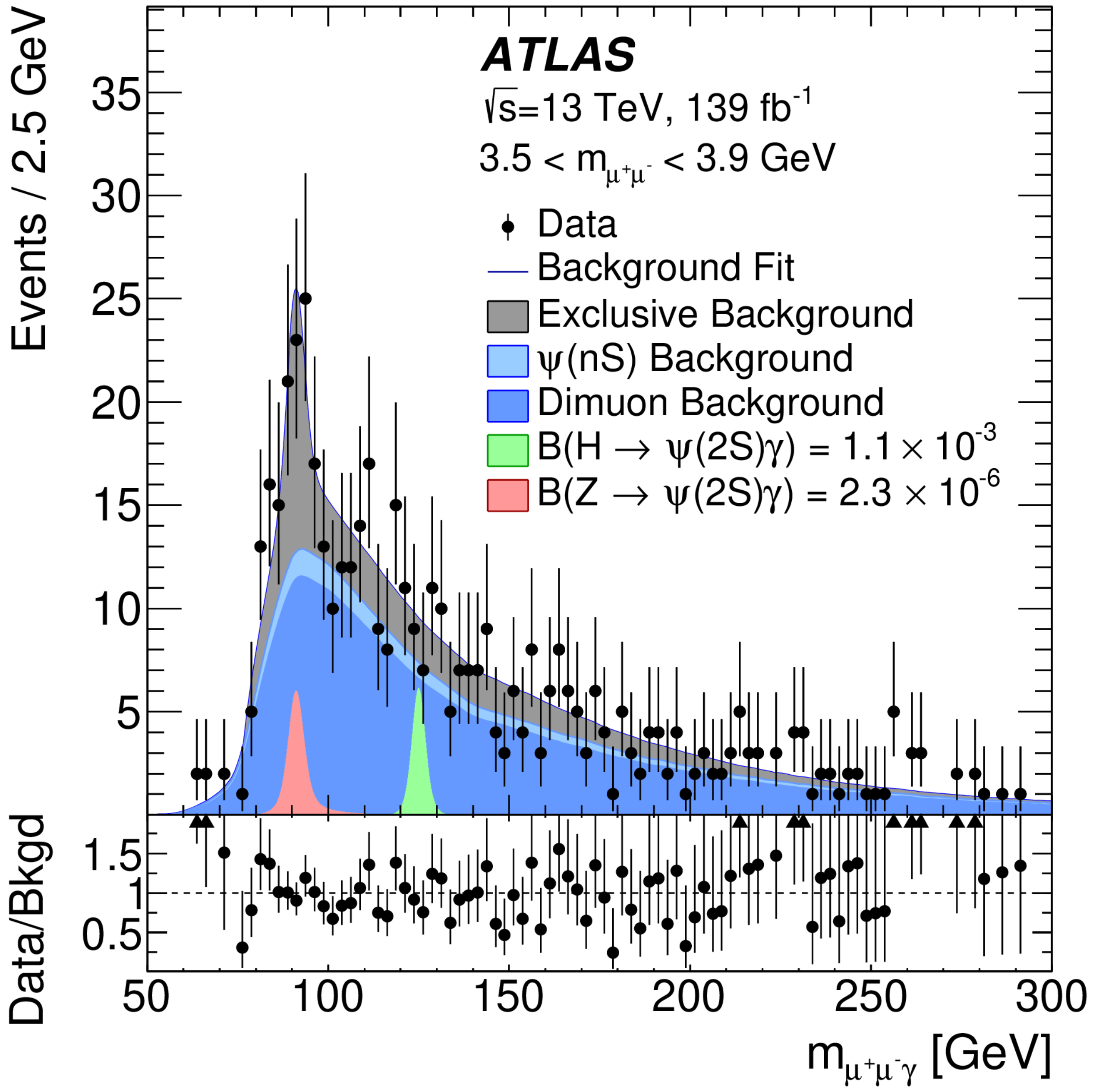

	95% CL upper limits					
	Branching fraction				$\sigma \times \mathcal{B}$	
Decay	Higgs boson [10^{-4}]		Z boson [10^{-6}]		Higgs boson [fb]	Z boson [fb]
channel	Expected	Observed	Expected	Observed	Observed	Observed
$J/\psi\,\gamma$	$1.9^{+0.8}_{-0.5}$	2.1	$0.6^{+0.3}_{-0.2}$	1.2	12	71
$\psi(2S)\,\gamma$	$8.5^{+3.8}_{-2.4}$	10.9	$2.9^{+1.3}_{-0.8}$	2.3	61	135
$\Upsilon(1S)\,\gamma$	$2.8^{+1.3}_{-0.8}$	2.6	$1.5^{+0.6}_{-0.4}$	1.0	14	59
$\Upsilon(2S)\,\gamma$	$3.5^{+1.6}_{-1.0}$	4.4	$2.0^{+0.8}_{-0.6}$	1.2	24	71
$\Upsilon(3S)\,\gamma$	$3.1^{+1.4}_{-0.9}$	3.5	$1.9^{+0.8}_{-0.5}$	2.3	19	135

- search also for H and Z → ω/K* + γ

arXiv:2301.09938 (Submitted to: Phys. Lett. B.)

Tuesday, 17:20 Search for BSM Physics in ATLAS - Rafael Coelho Lopes de Sá

Searches for extended scalar sector

ATL-PHYS-PUB-2022-043

- motivated in many BSM models
- benchmarks: hMSSM and type-I 2HDM

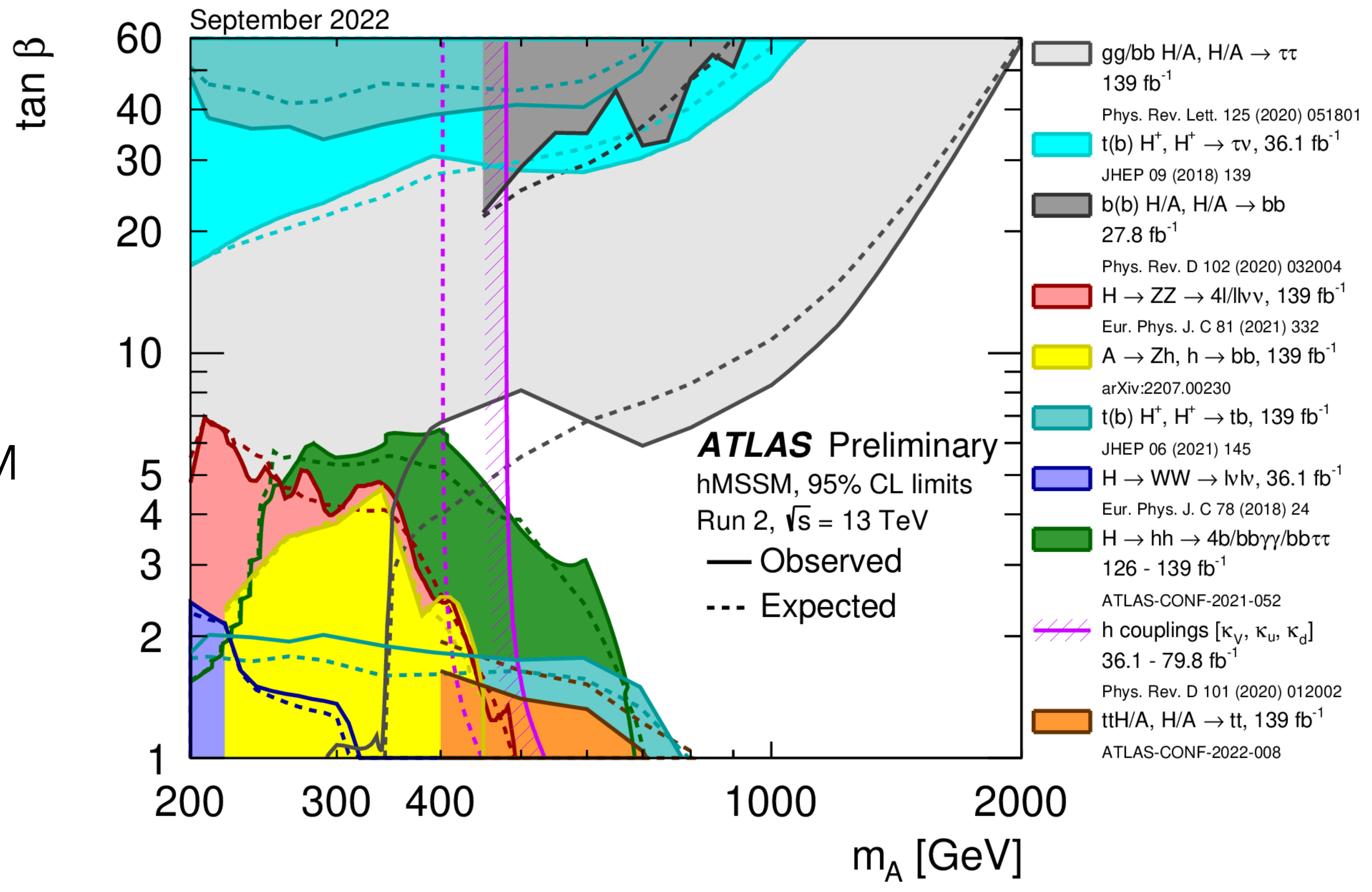

Generic 2HDM

ATLAS-CONF-2022-039

- search for new heavy scalars with flavour-violating decays
- couplings involving top quarks **ρ_{tt}, ρ_{tc}, ρ_{tu}**
- events categorised by lepton multiplicity, total lepton charge and decay topology

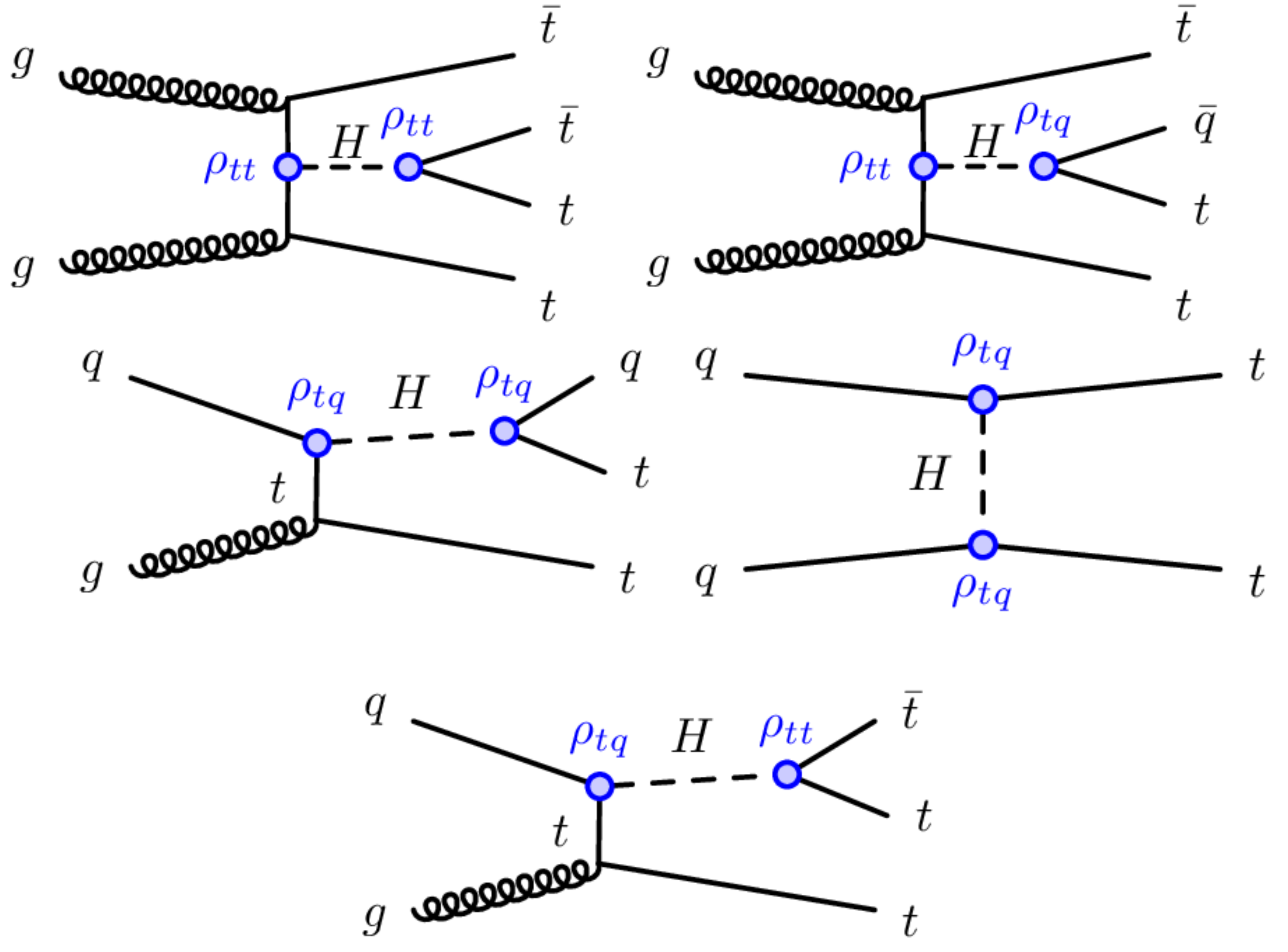

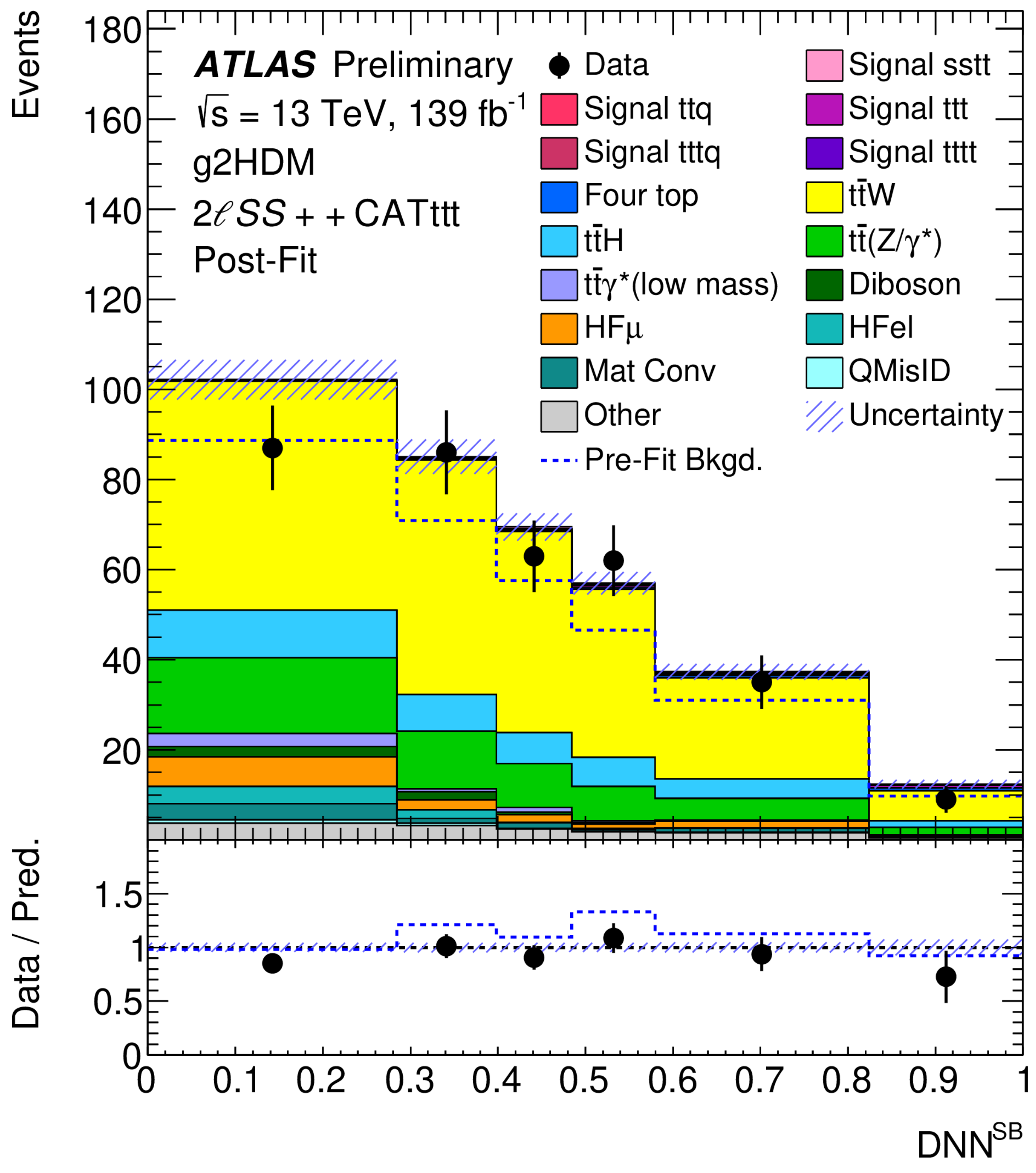

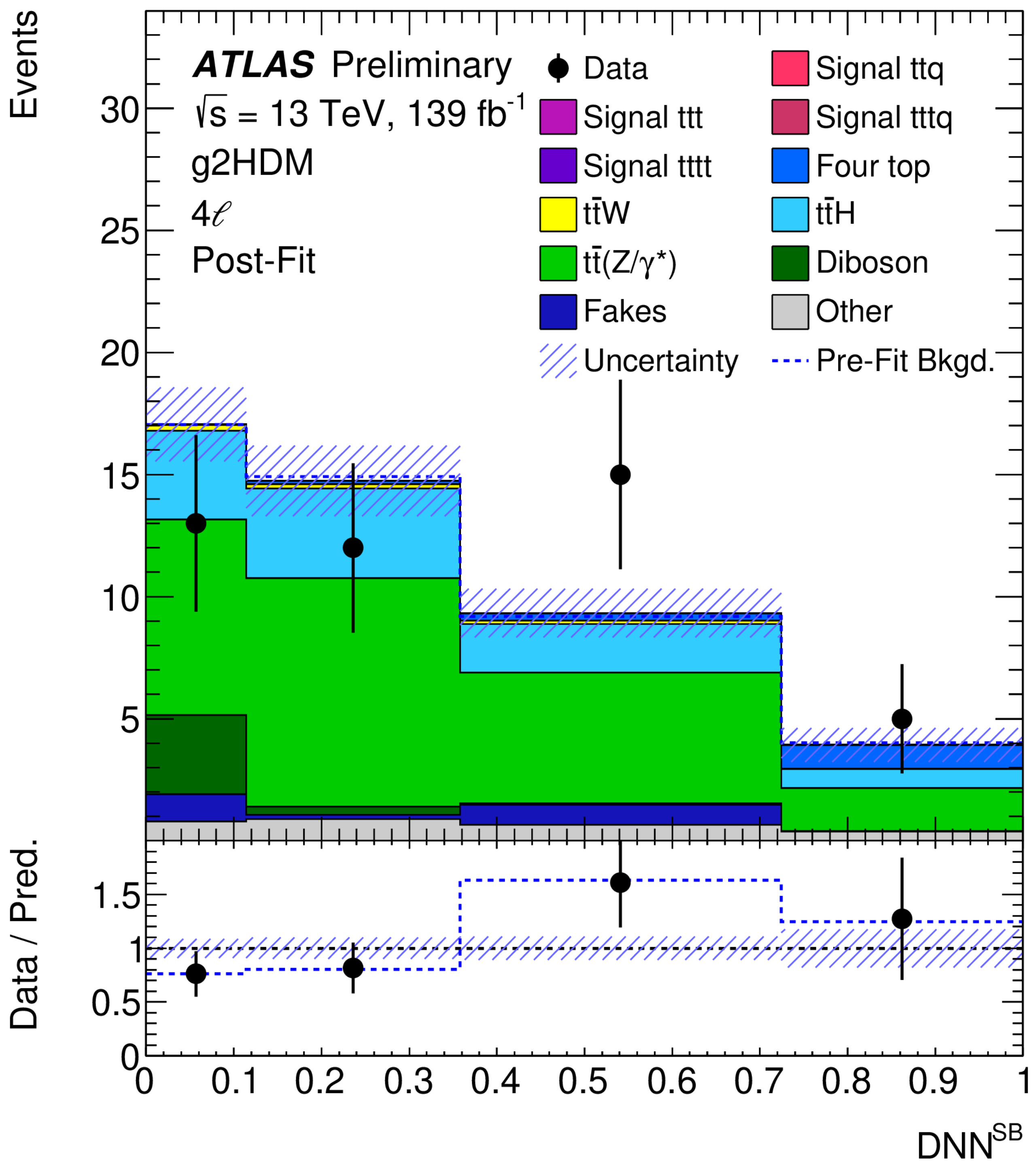

- couplings scans for heavy Higgs masses 200 GeV < m_H < 1000 GeV

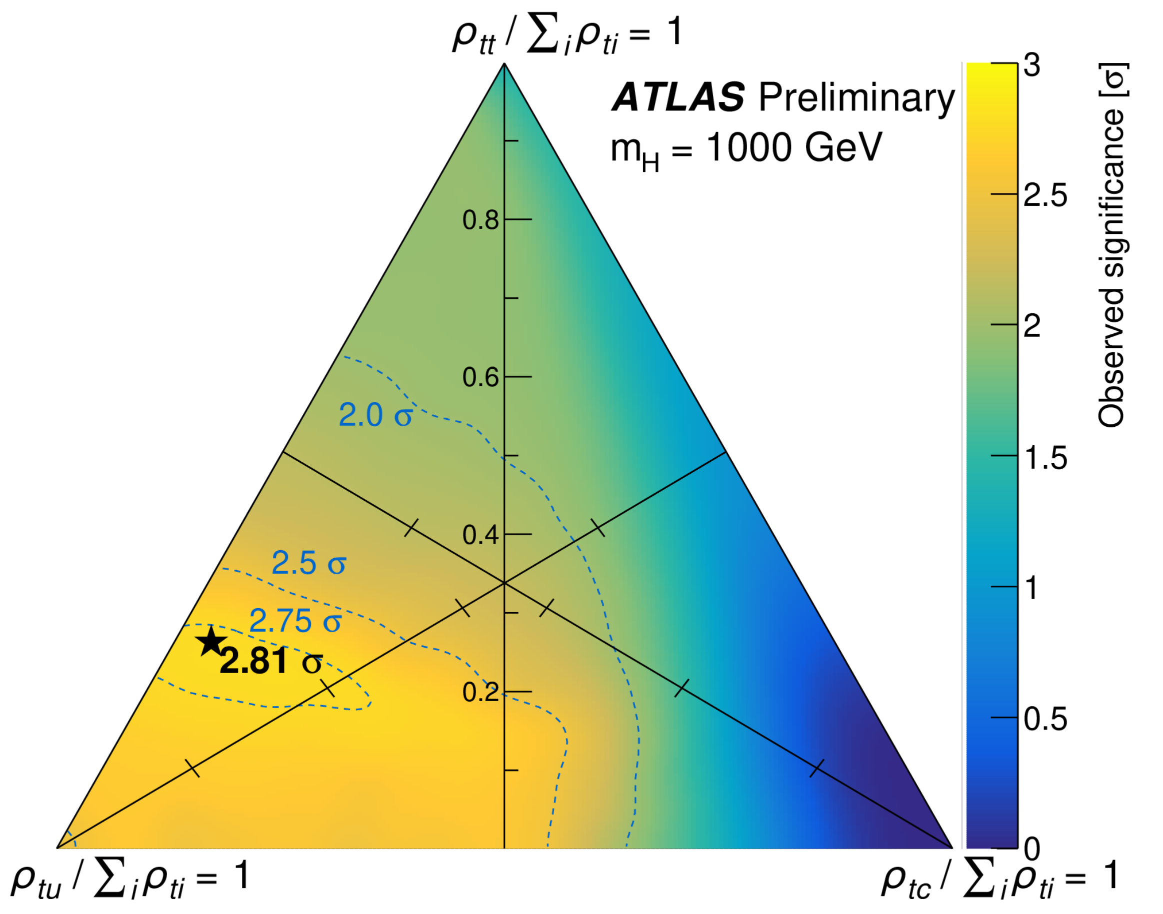

- largest deviation 2.8σ local for m_H = 1000 GeV: **ρ_{tt}**= 0.32, **ρ_{tc}**= 0.05, **ρ_{tu}** = 0.85

Heavy particles searches

ATL-PHYS-PUB-2022-034

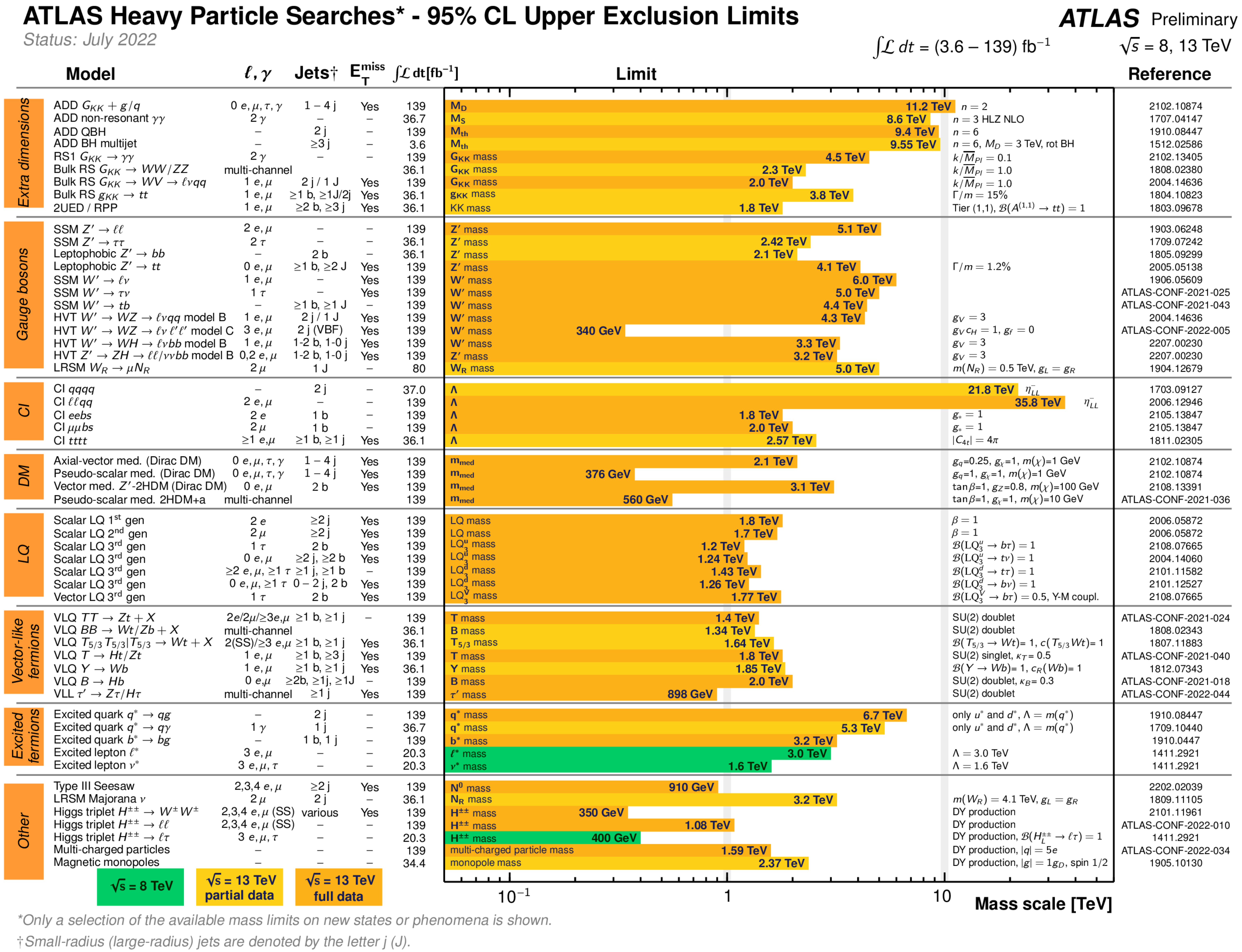

Tuesday, 17:20 Search for BSM Physics in ATLAS - Rafael Coelho Lopes de Sá

Search for neutral heavy resonances in $W^+W^- \to e\nu\mu\nu$

ATLAS-CONF-2022-066

Model	Resonance spin	Production mode		
		ggF	qqA	VBF
NWA	Spin-0	x		x
GM				x
Radion		x		x
HVT	Spin-1		x	x
RS G^*_{KK}	Spin-2	x		x

- search in wide mass range: 200 GeV < m_R < 6 TeV
- Higgs-like narrow width, Georgi-Machacek, radion in the bulk Randall-Sundrum model, spin-1 have vector triplet, spin-2 graviton
- m_T used for statistical analysis
- no significant excess over SM expectations

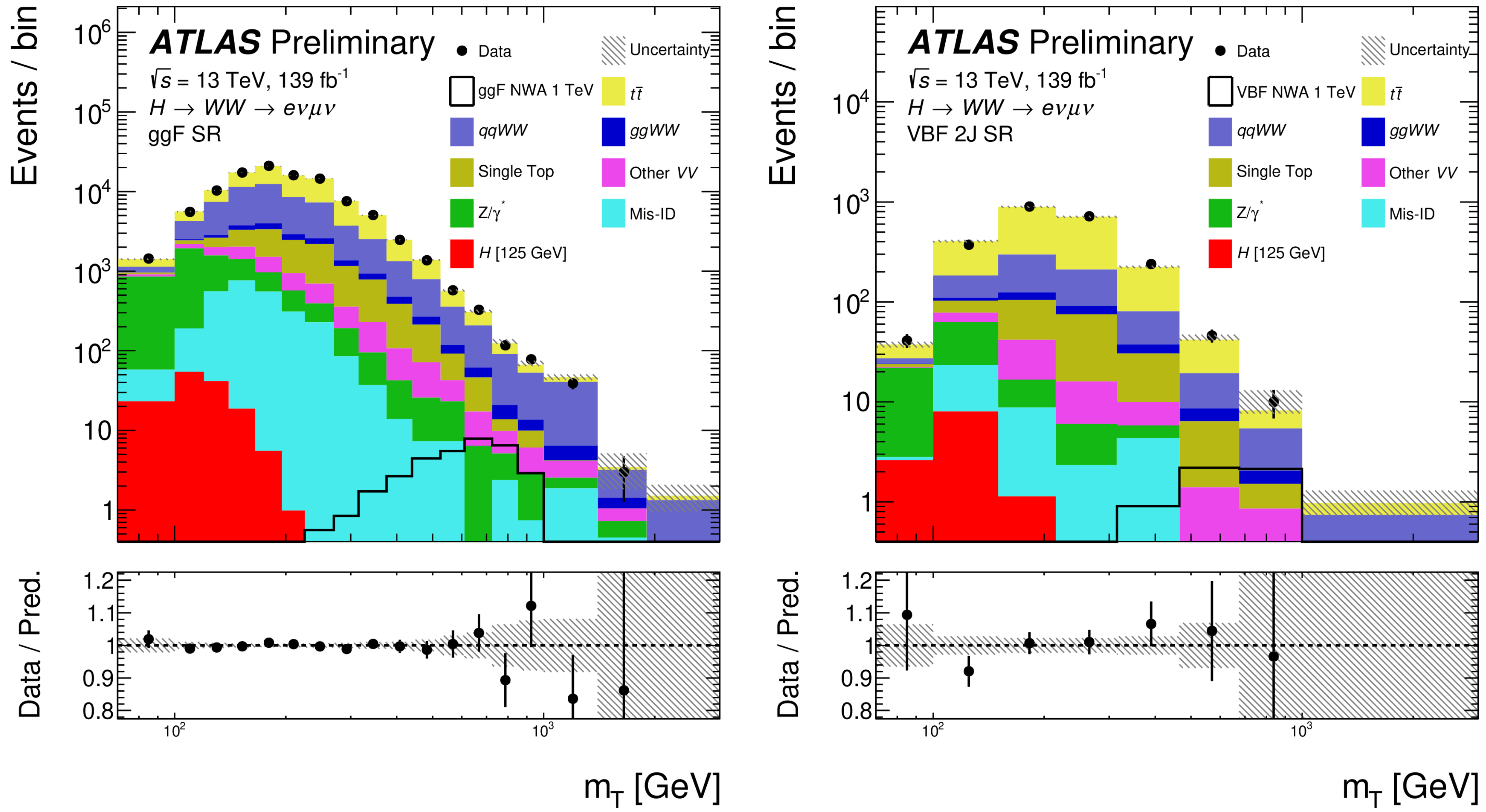

Model	Obs. limit [GeV]	Exp. limit [GeV]
Radion, ggF	1090	1190
Kaluza-Klein graviton, ggF	1340	1340
Kaluza-Klein graviton, VBF	500	500
HVT scenario A, qqA	2100	1890
HVT scenario B, qqA	2350	2130

$$m_T = \sqrt{(E_T^{\ell\ell} + E_T^{\text{miss}})^2 - |\vec{p}_T^{\,\ell\ell} + \vec{E}_T^{\text{miss}}|^2},$$

$$E_T^{\ell\ell} = \sqrt{|\vec{p}_T^{\,\ell\ell}|^2 + m_{\ell\ell}^2},$$

Search for pair production of third-generation leptoquarks

arXiv:2303.01924 (Submitted to: EPJC)

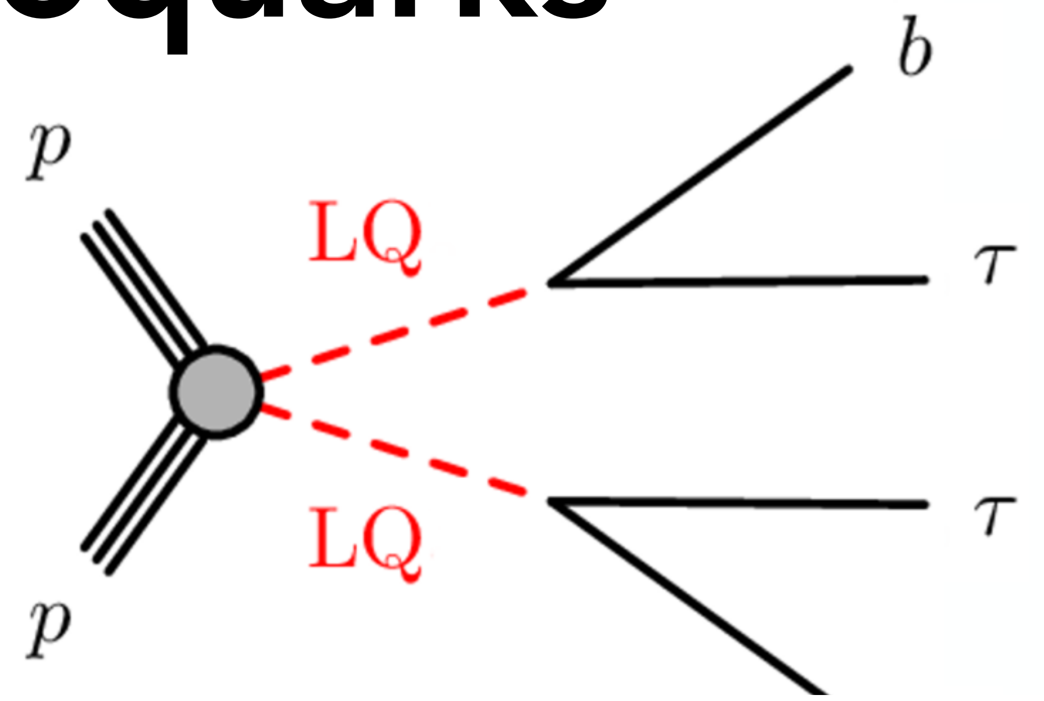

- final state 2b and 2τ, with analysis subdivided into $\tau_{lep}\tau_{had}$, $\tau_{had}\tau_{had}$

- analysis strategy: MVA (PNN)→fit on PNN scores

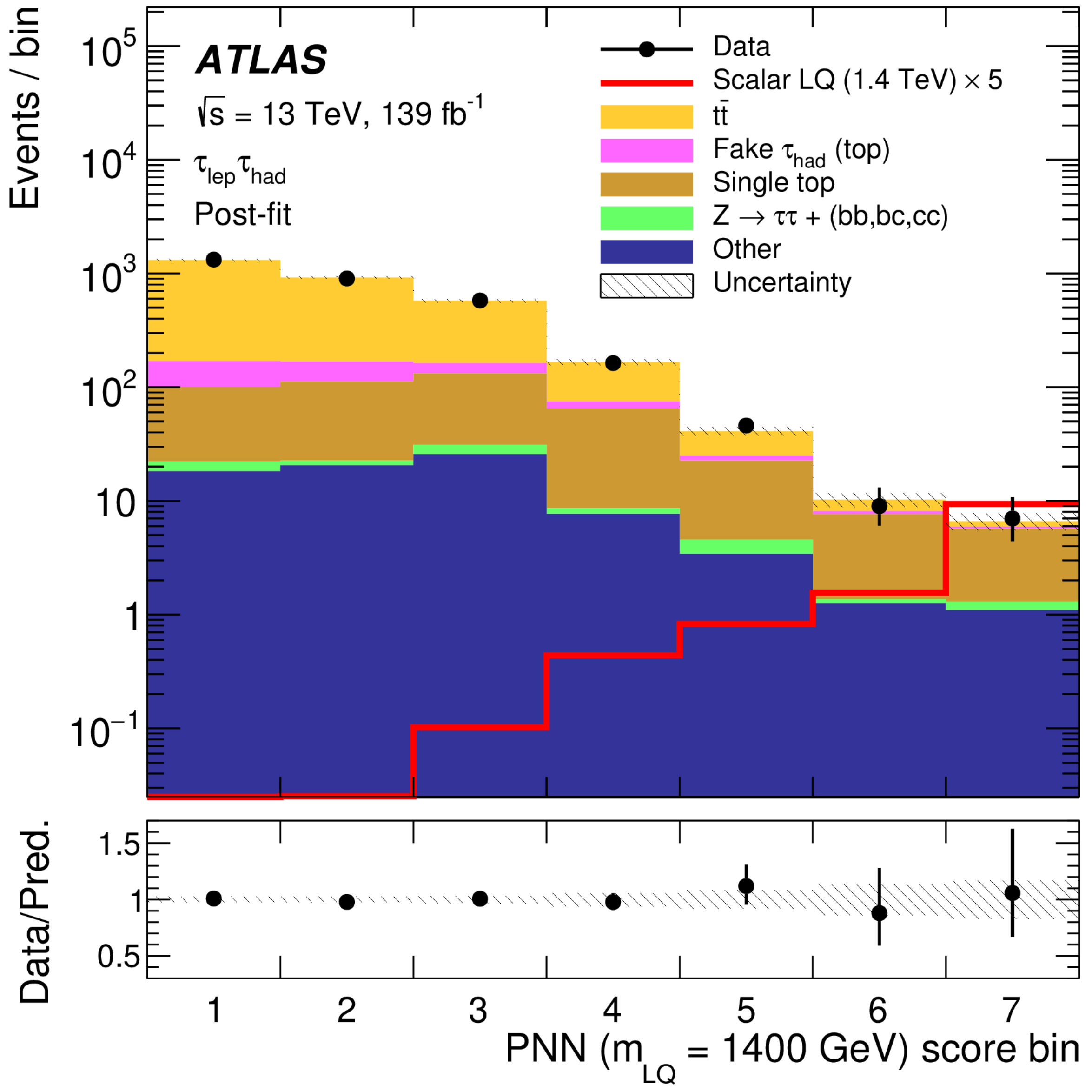

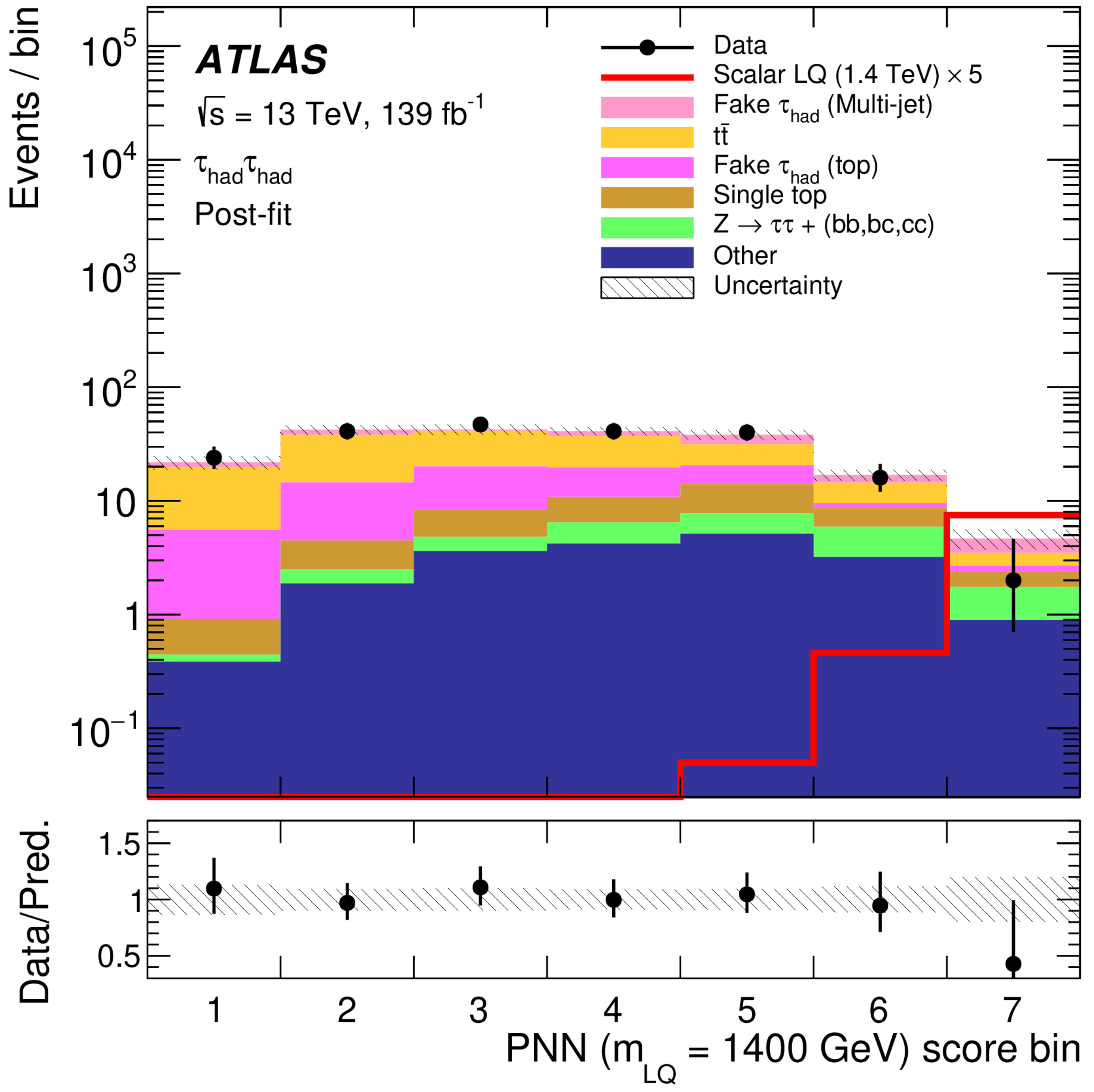

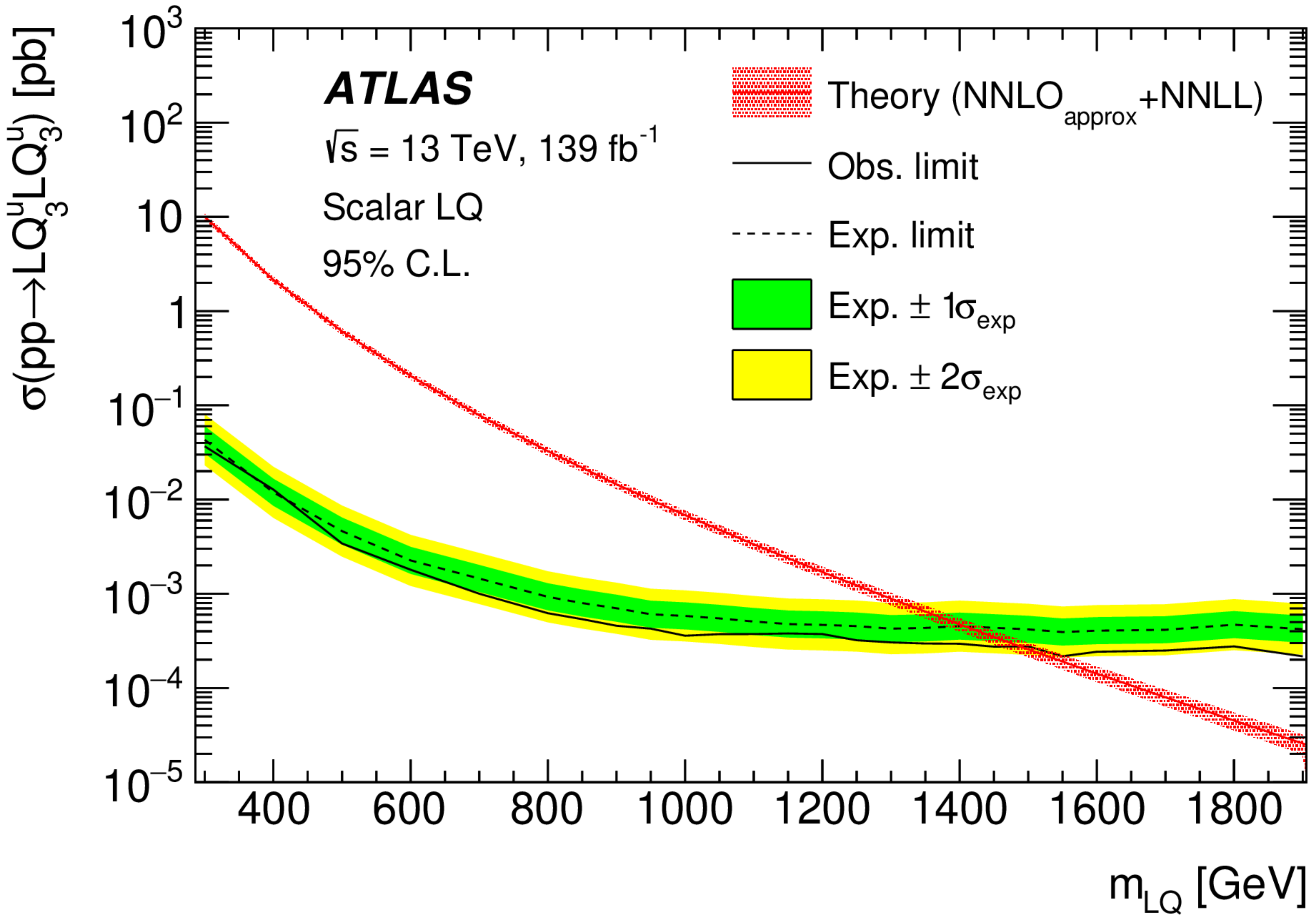

	Obs. limit [GeV]	Exp. limit [GeV]
Scalar LQ	1490	1410
Vector LQ (minimal-coupling)	1690	1600
Vector LQ (Yang–Mills)	1960	1840

- previous ATLAS search in this final state **surpassed by** more than **450 GeV for scalar LQs**

- improved τ_{had} and **b-jet** reconstruction and identification techniques, and a number of analysis-level improvements

Search for H→invisible

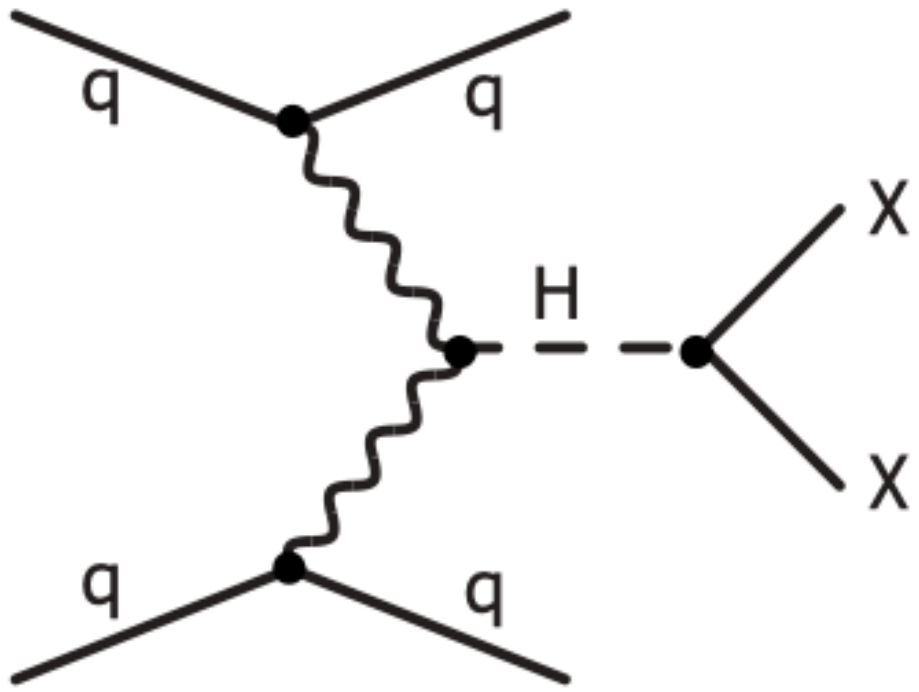

VBF + MET

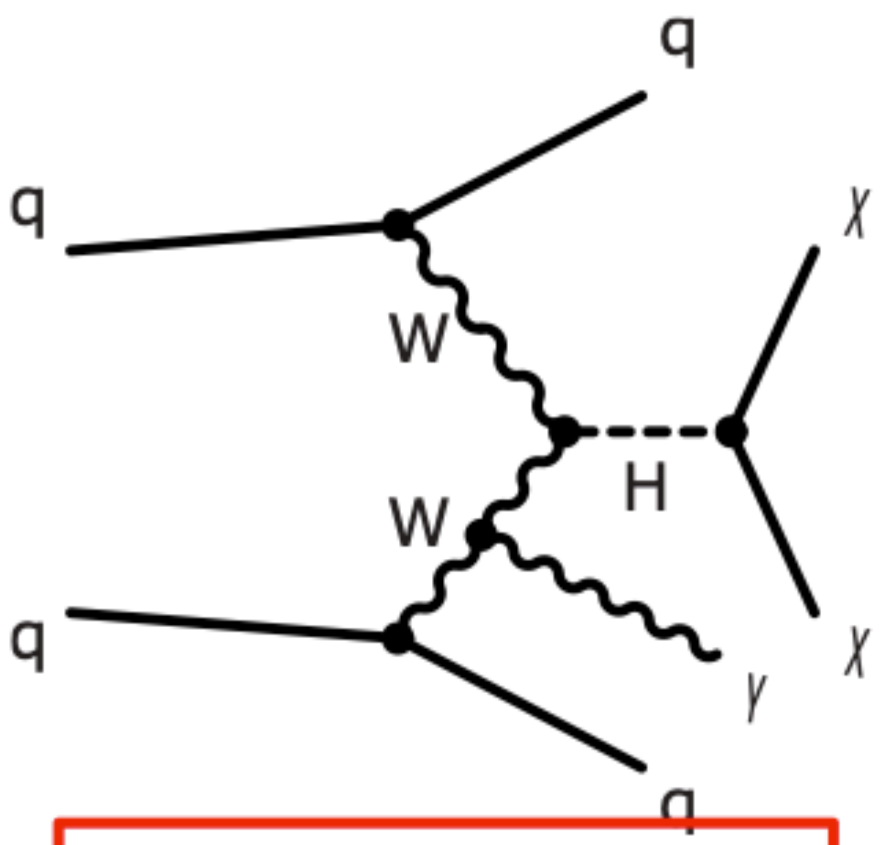

VBF + γ + MET

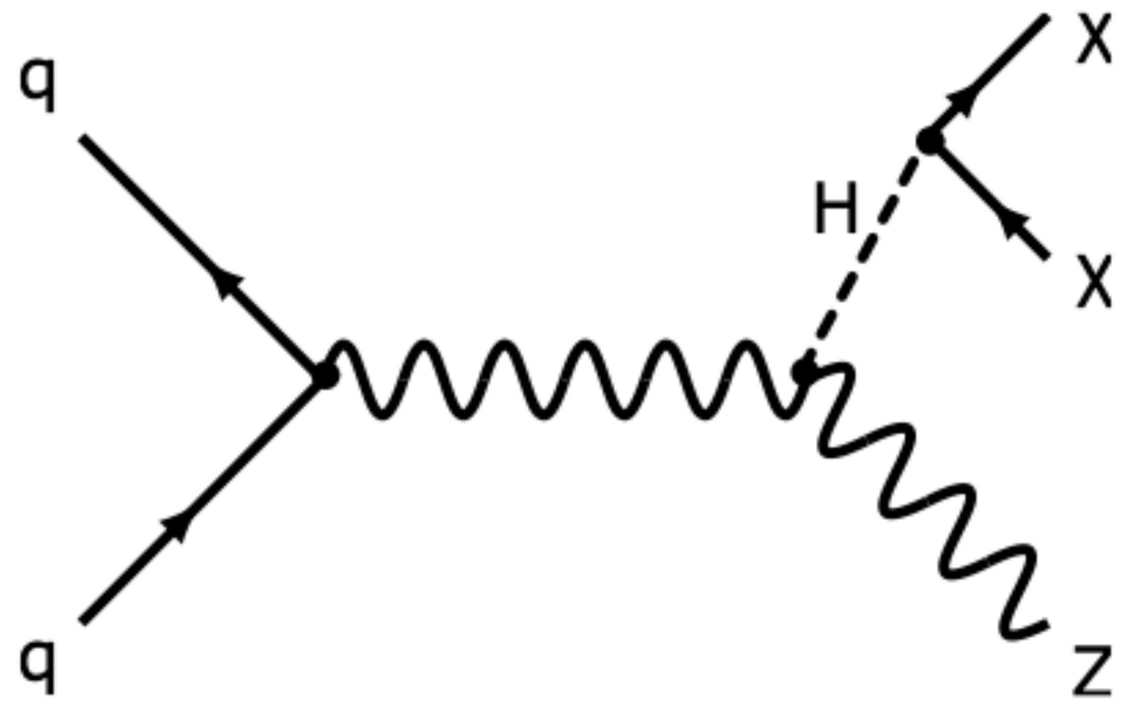

Z + MET

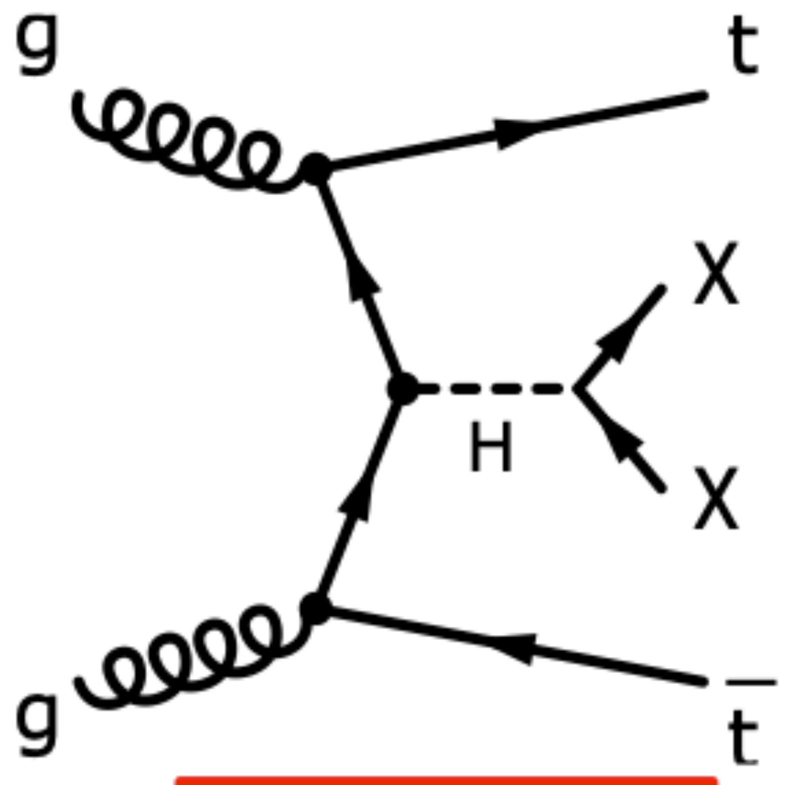

tt + MET

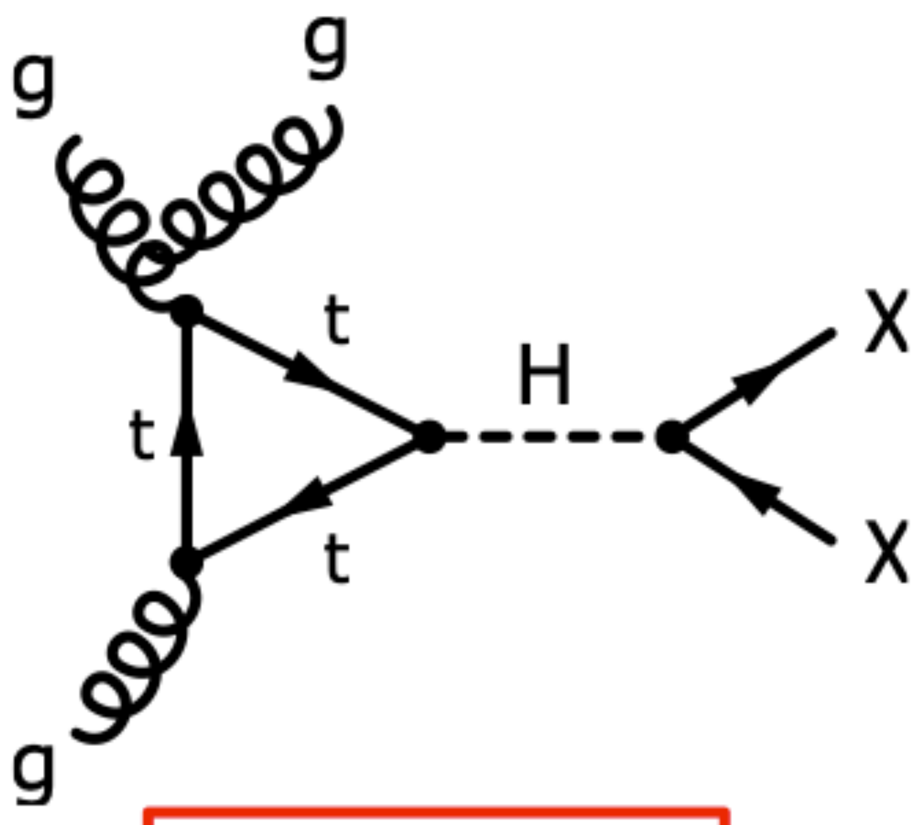

jets + MET

H→invisible in VBF+MET

JHEP 08 (2022) 104

- most sensitive channel among the five searches
- large $E_T^{miss} > 160$ GeV
- 2 VBF jets not back-to-back in ϕ ($\Delta\phi_{jj} < 2$, to suppress multi-jet)
- veto events with e, μ,γ
- VBF topology for 2 leading jets
  - $\eta^{j1} \cdot \eta^{j2} < 0$, $\Delta\eta_{jj} > 3.8$, $m_{jj} > 0.8$ TeV
- background estimation: V+jets from lepton CR
- 16 signal region bins defined in n_{jet}, E_T^{miss}, m_{jj}, $\Delta\phi_{jj}$

$\mathfrak{B}_{inv} < 0.15$ (0.10 exp.) @ 95% CL

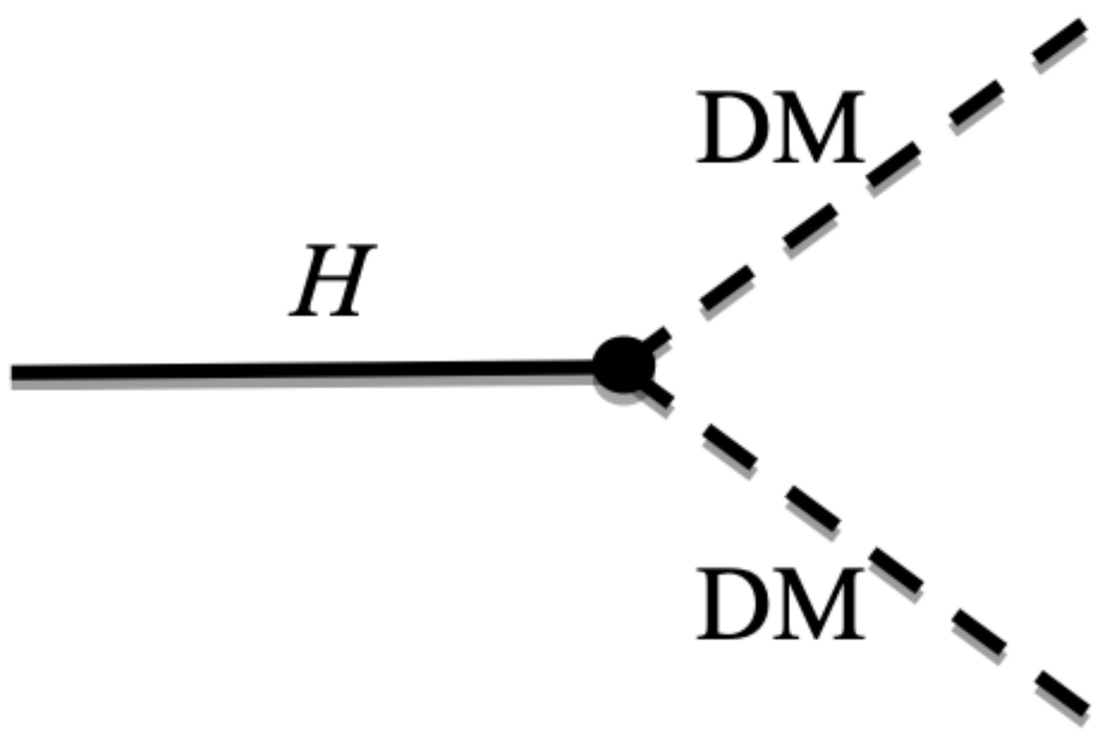

- In SM, branching ratio for Higgs invisible decay (H→ZZ→4ν) ~0.1%
- If DM exists and in the right mass range, we may observe larger BR(H→inv) than SM prediction

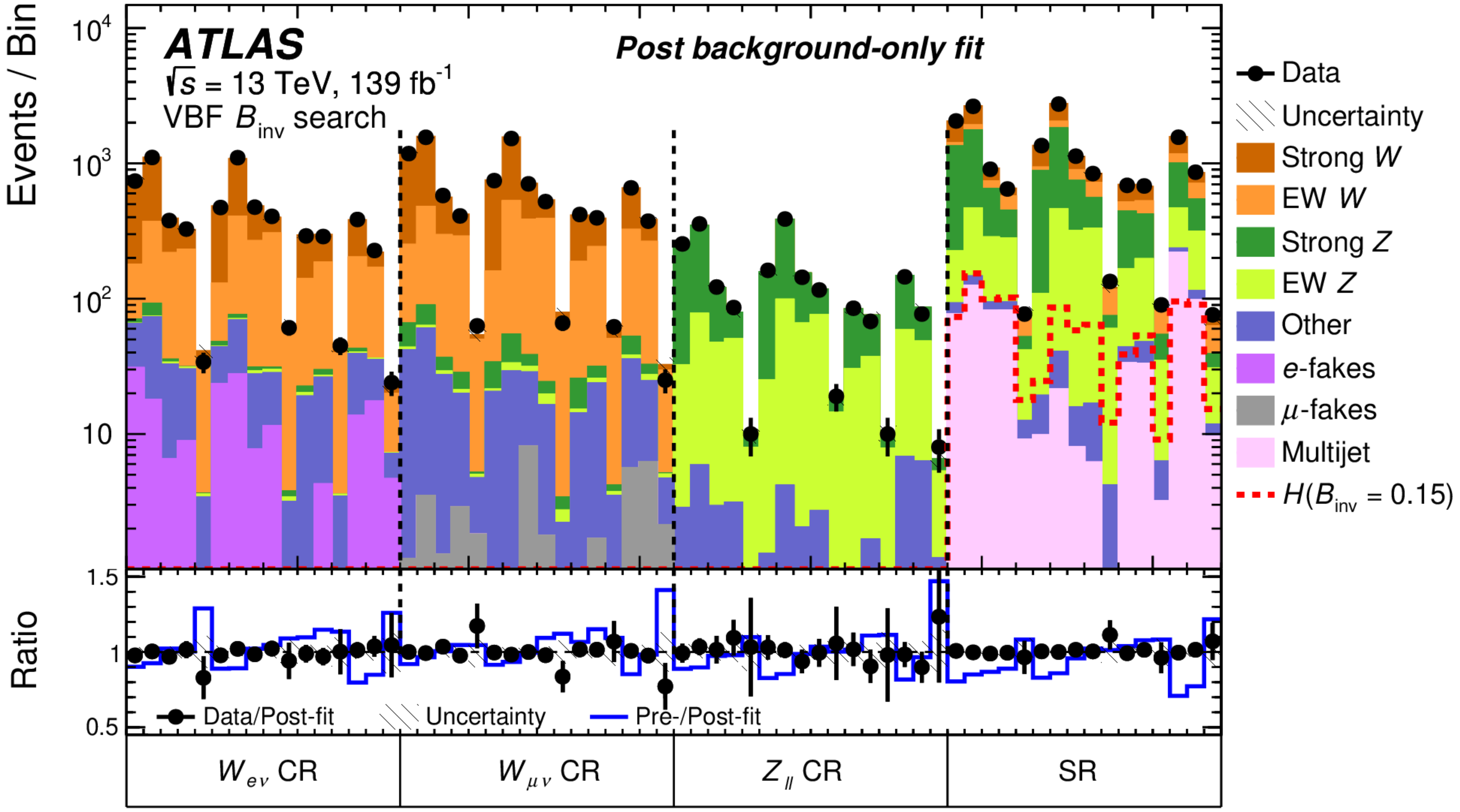

H→invisible search combination

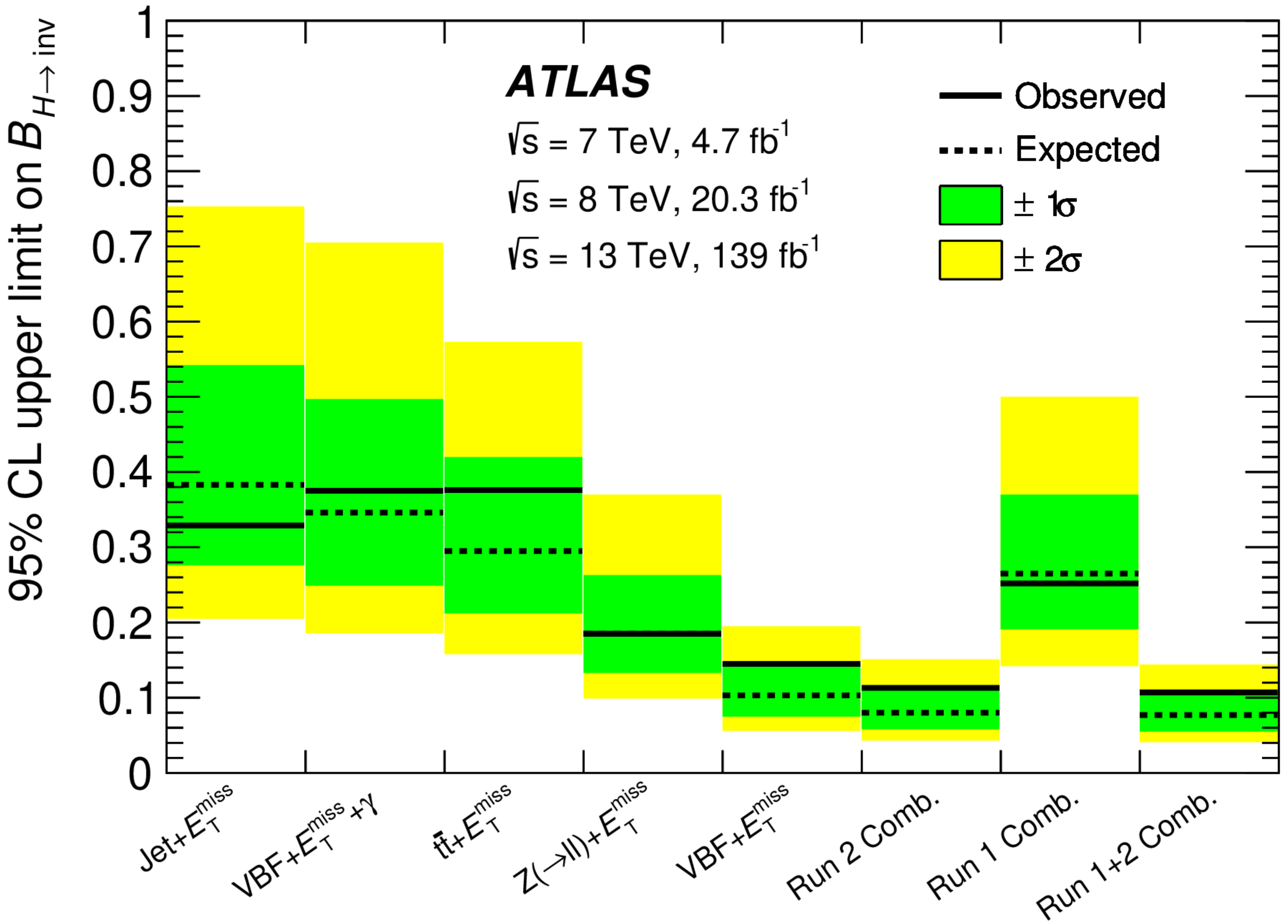

[arXiv:2301.10731 (Submitted to: Phys. Lett. B.)](https://arxiv.org/abs/2301.10731)

𝔅 (H→inv) < 0.107 (0.077) @ 95% CL obs (exp)

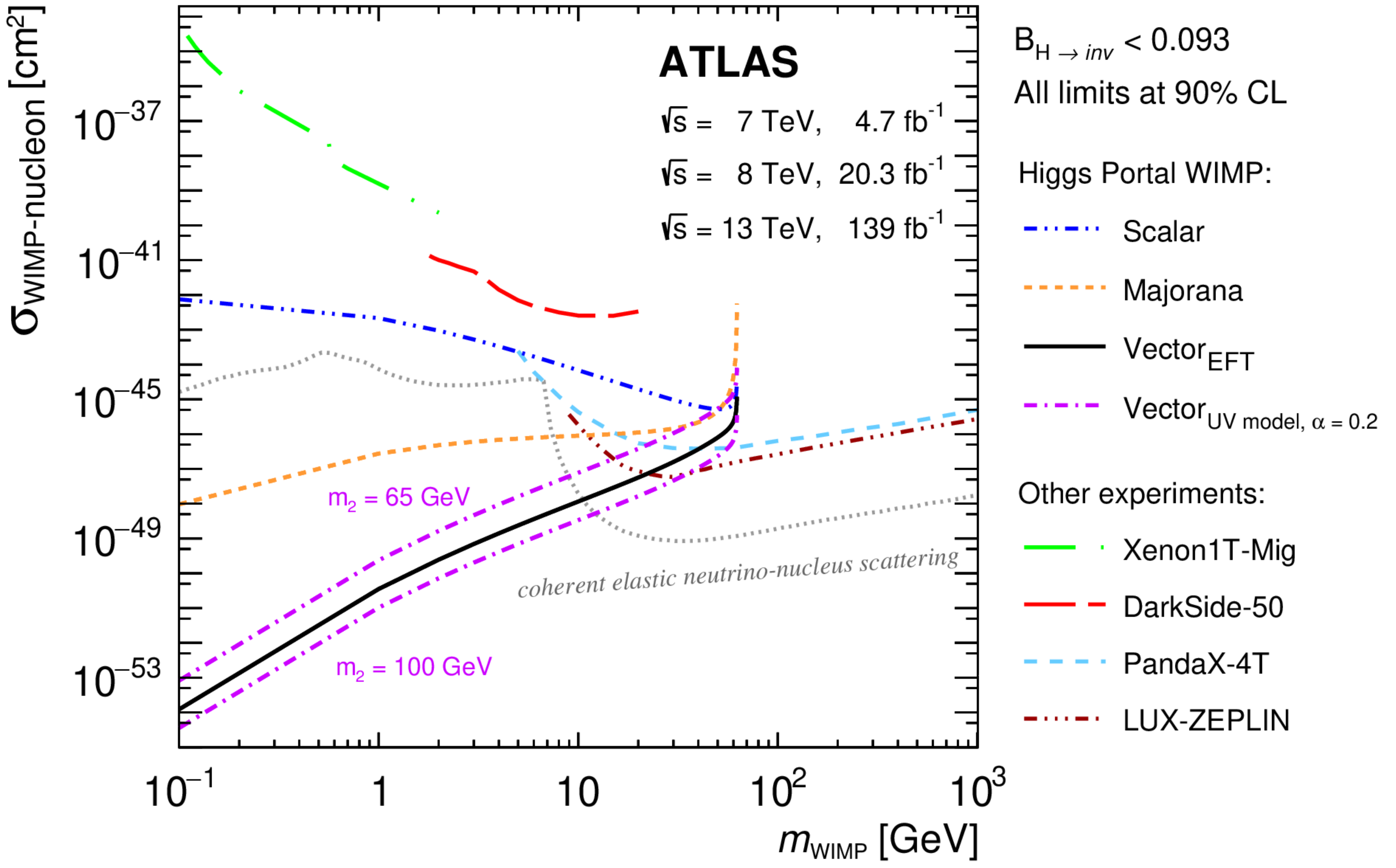

Analysis	Best fit $\mathcal{B}_{H\to inv}$	Observed 95% U.L.	Expected 95% U.L.
Jet +	$-0.09^{+0.19}_{-0.20}$	0.329	$0.383^{+0.157}_{-0.107}$
VBF + + γ	$0.04^{+0.17}_{-0.15}$	0.375	$0.346^{+0.151}_{-0.097}$
$t\bar{t}$ +	0.08 ± 0.15	0.376	$0.295^{+0.125}_{-0.083}$
$Z(\to \ell\ell)$ +	0.00 ± 0.09	0.185	$0.185^{+0.078}_{-0.052}$
VBF +	0.05 ± 0.05	0.145	$0.103^{+0.041}_{-0.028}$
Run 2 Comb.	0.04 ± 0.04	0.113	$0.080^{+0.031}_{-0.022}$
Run 1 Comb.	$-0.02^{+0.14}_{-0.13}$	0.252	$0.265^{+0.105}_{-0.074}$
Run 1+2 Comb.	0.04 ± 0.04	0.107	$0.077^{+0.030}_{-0.022}$

Long-lived particles searches

ATL-PHYS-PUB-2022-034

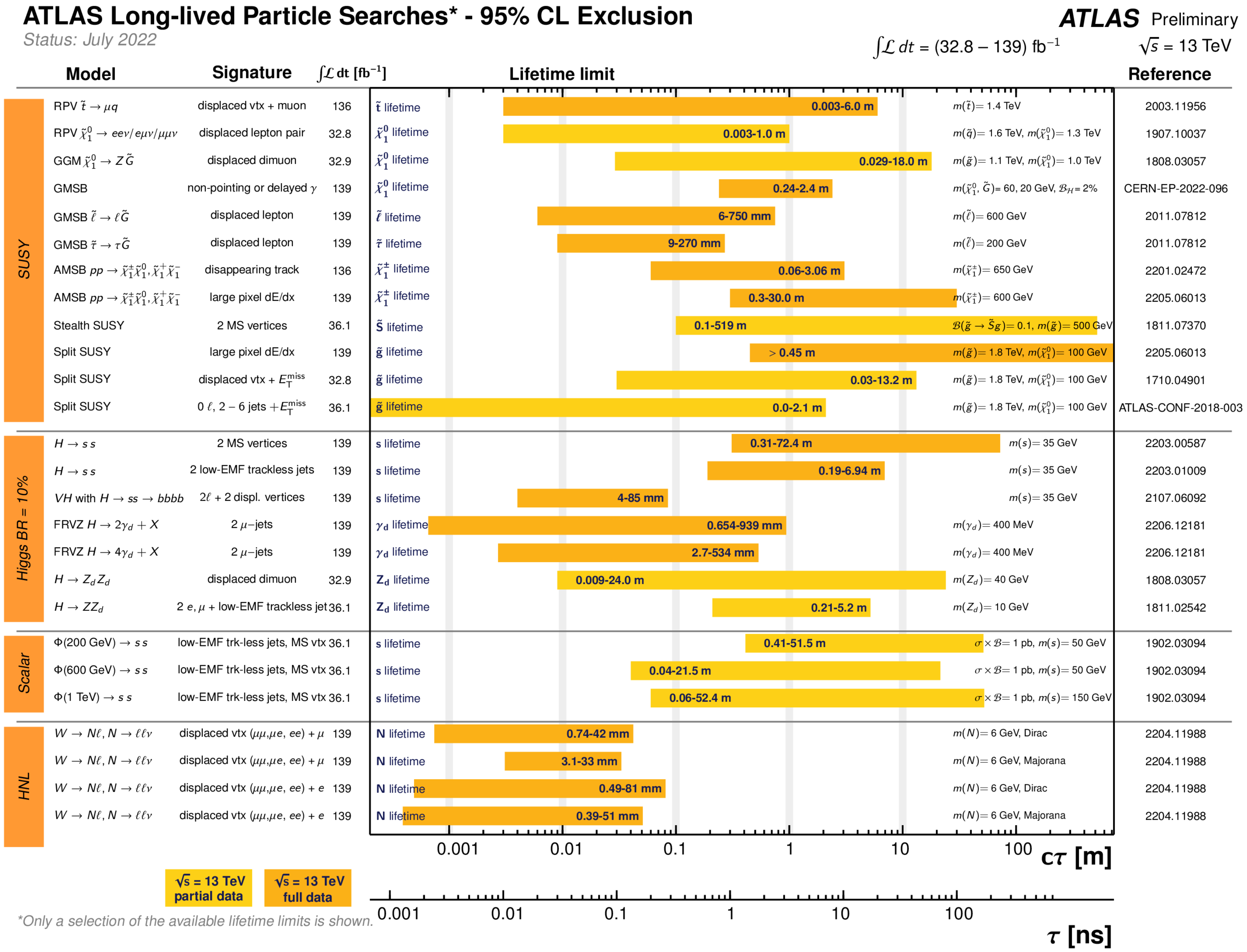

Tuesday, 17:20 Search for BSM Physics in ATLAS - Rafael Coelho Lopes de Sá

Search for long-lived charginos: disappearing track

[Eur. Phys. J. C 82 (2022) 606]

- a chargino directly interacts with the detector material: **a track**
- decays in the middle leaving a LSP and a non-reconstructable soft pion: **disappearing**
- addition of the inner-most IBL layer (2014): **pixel-only-track,** pushing the sensitivity towards short lifetime
- requires a high p_T ISR jet + recoiling E_T^{miss} to trigger events

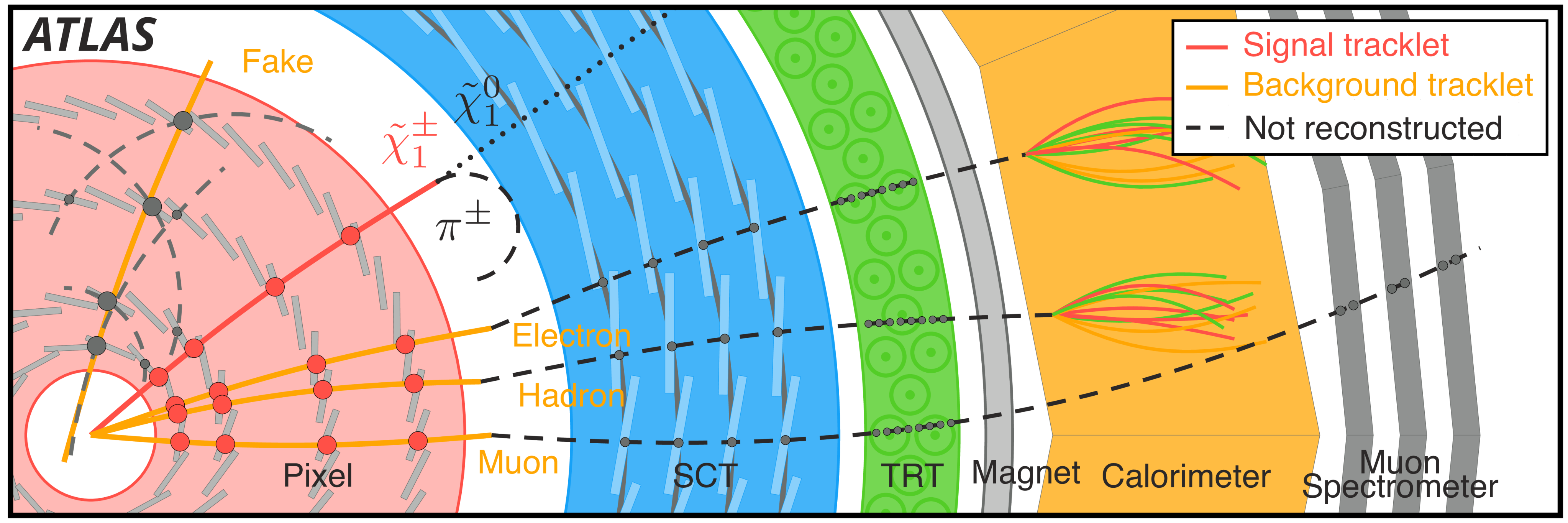

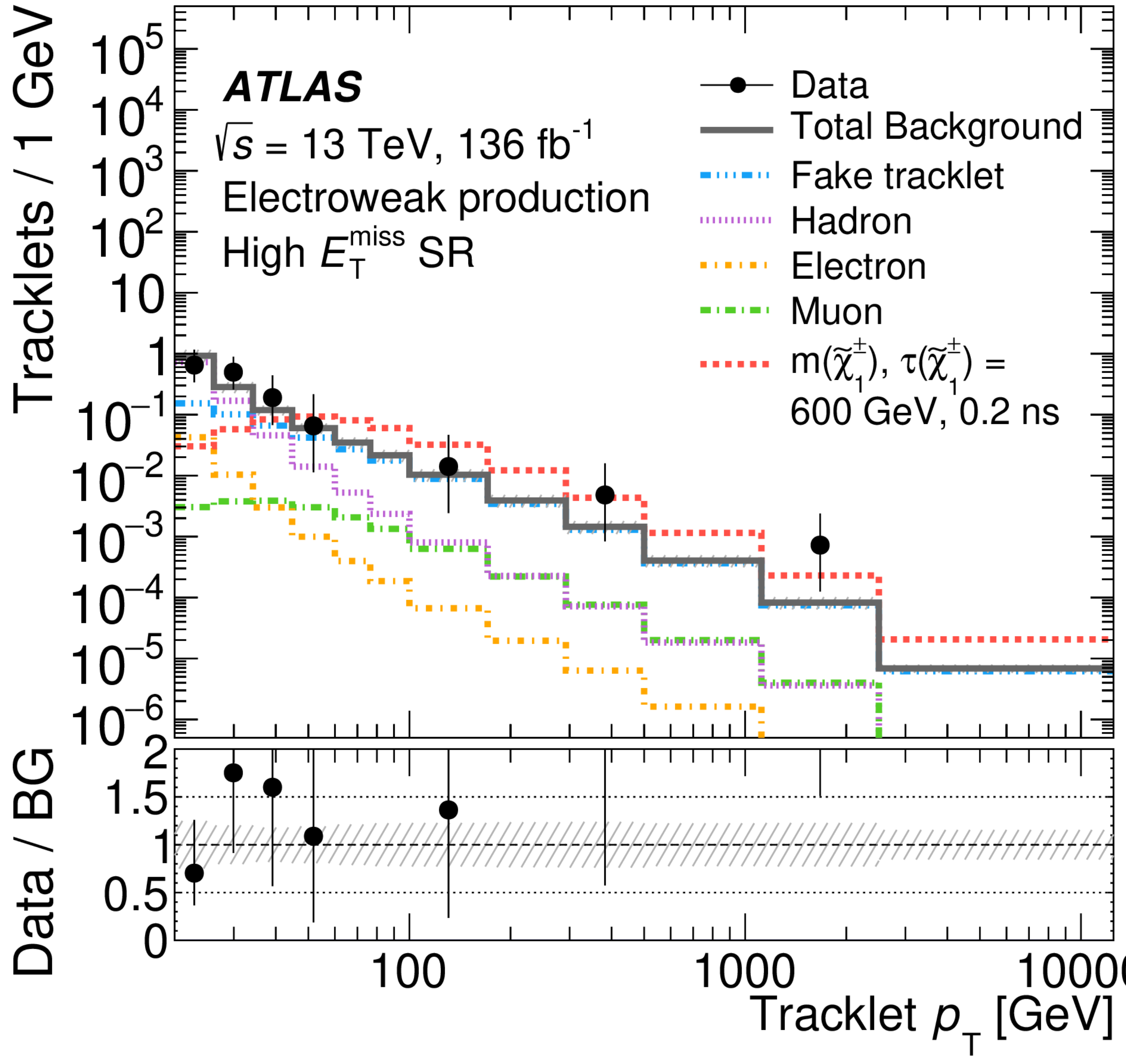

- bkg dominated by combinatorial "fake tracklets", fully data-driven estimation
- thanks to the closer proximity of the innermost pixel layer to beam: ATLAS offers best sensitivity to shorter life-time signals

obs limit excludes chargino masses up to 660 GeV

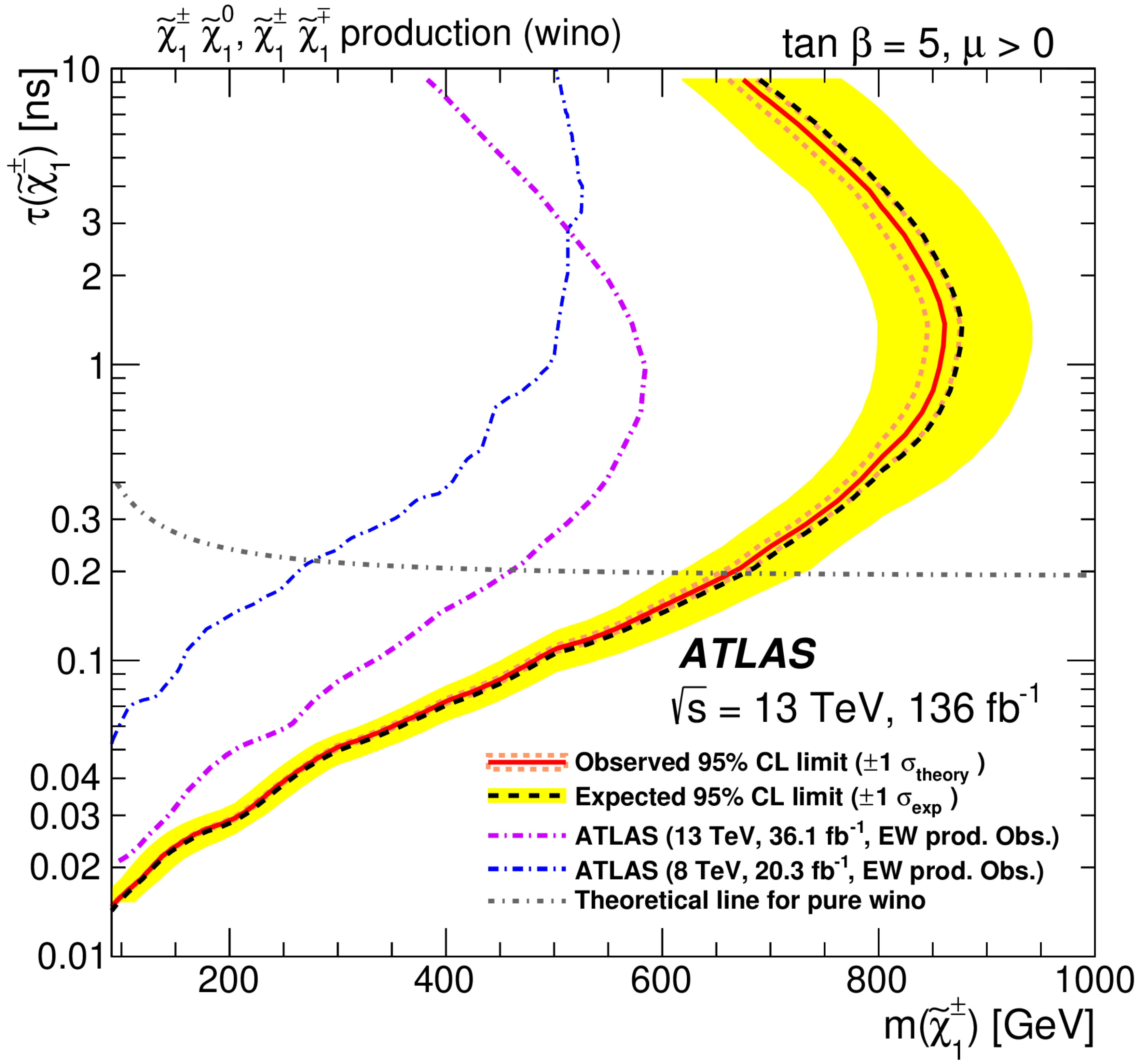

arXiv:2211.08028 (Submitted to: Eur. Phys. J. C)

Search for gluinos in multi-b final states

- ≥ 3 b-jets + 0/1lepton + E_T^{miss}
- DNN in event selection:
  - input: 4 vectors of jets and leptons, E_T^{miss}
  - $m(\tilde{g})$ and $m(\tilde{\chi}_1^0)$ added as parameters
- Interpretation also for 3 mixed decay modes
  - $\tilde{g} \rightarrow tt\tilde{\chi}_1^0, bb\tilde{\chi}_1^0$, or $tb\tilde{\chi}_1^{\pm}$

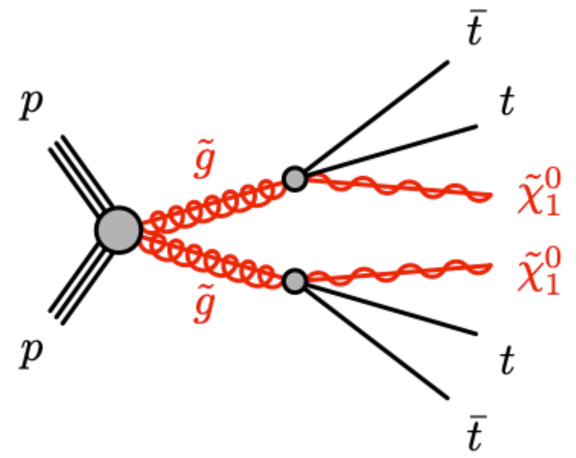

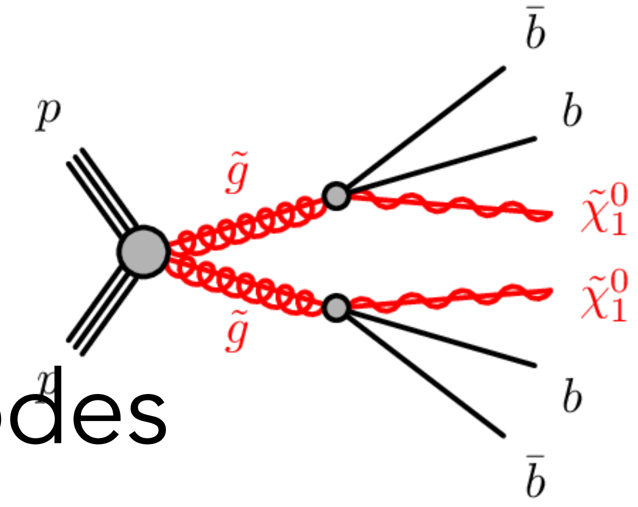

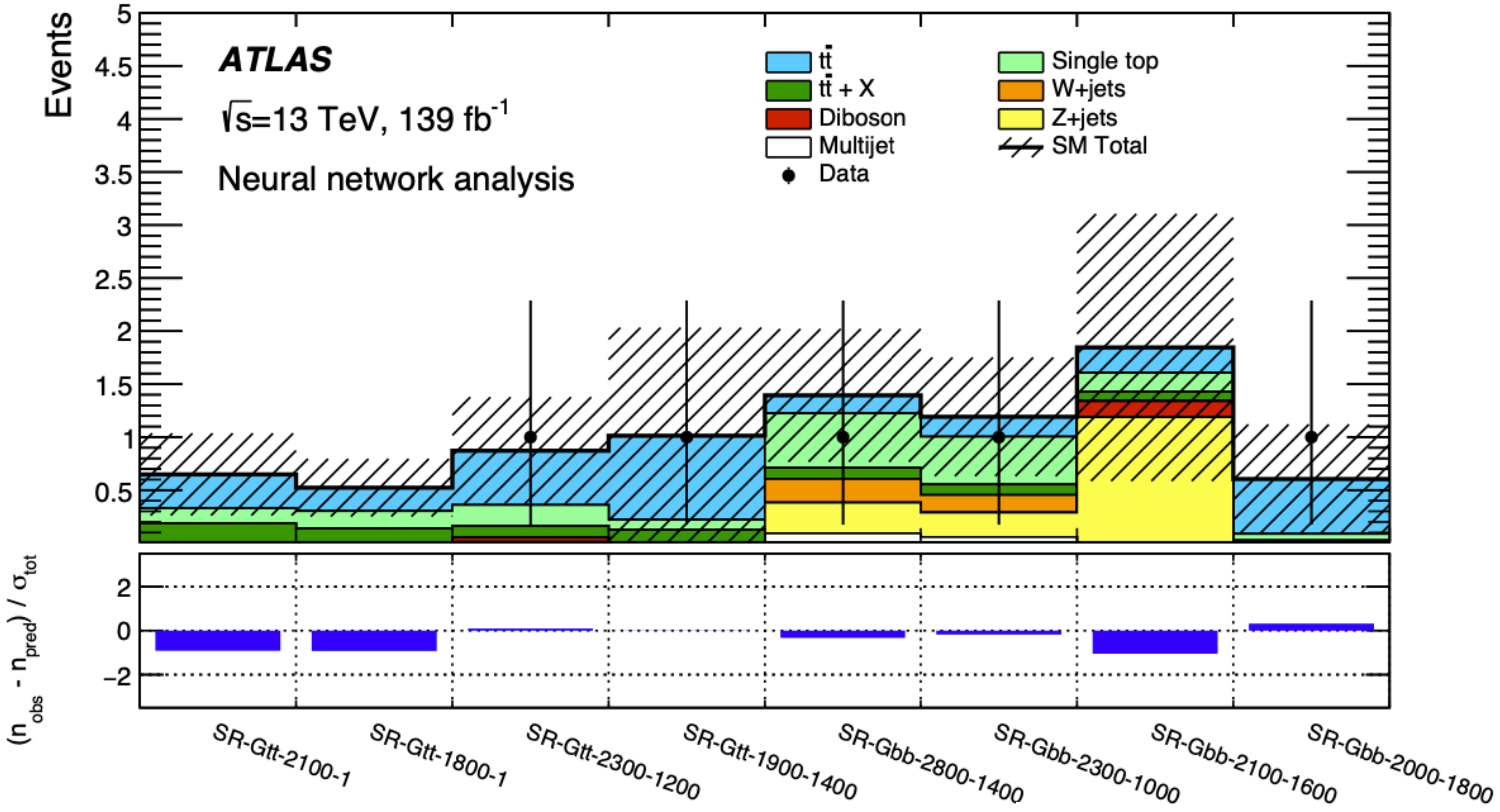

SUSY Summary Plots

gluino masses < 2.44 (2.35) TeV excluded @ 95%CL

Gtt

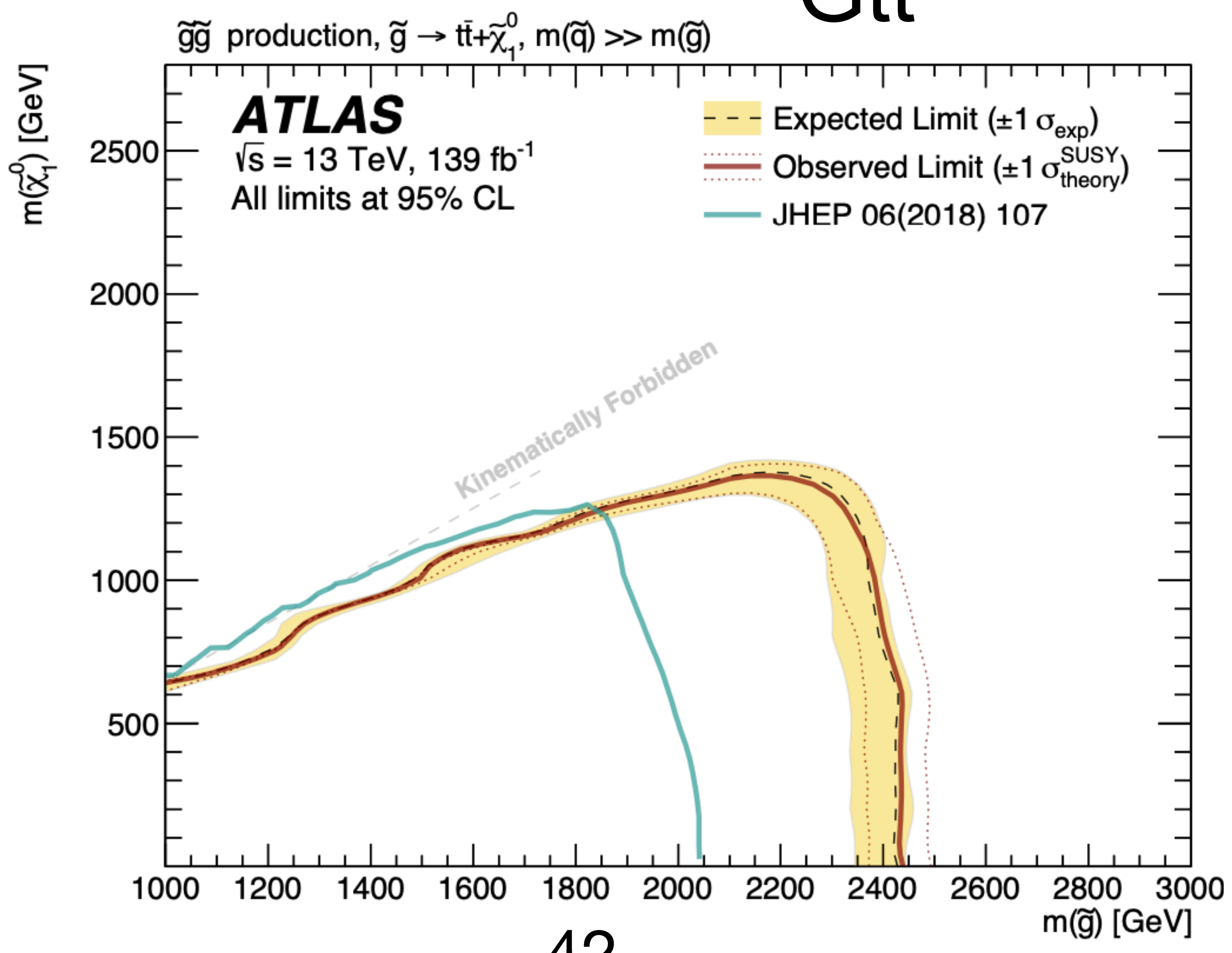

Gbb

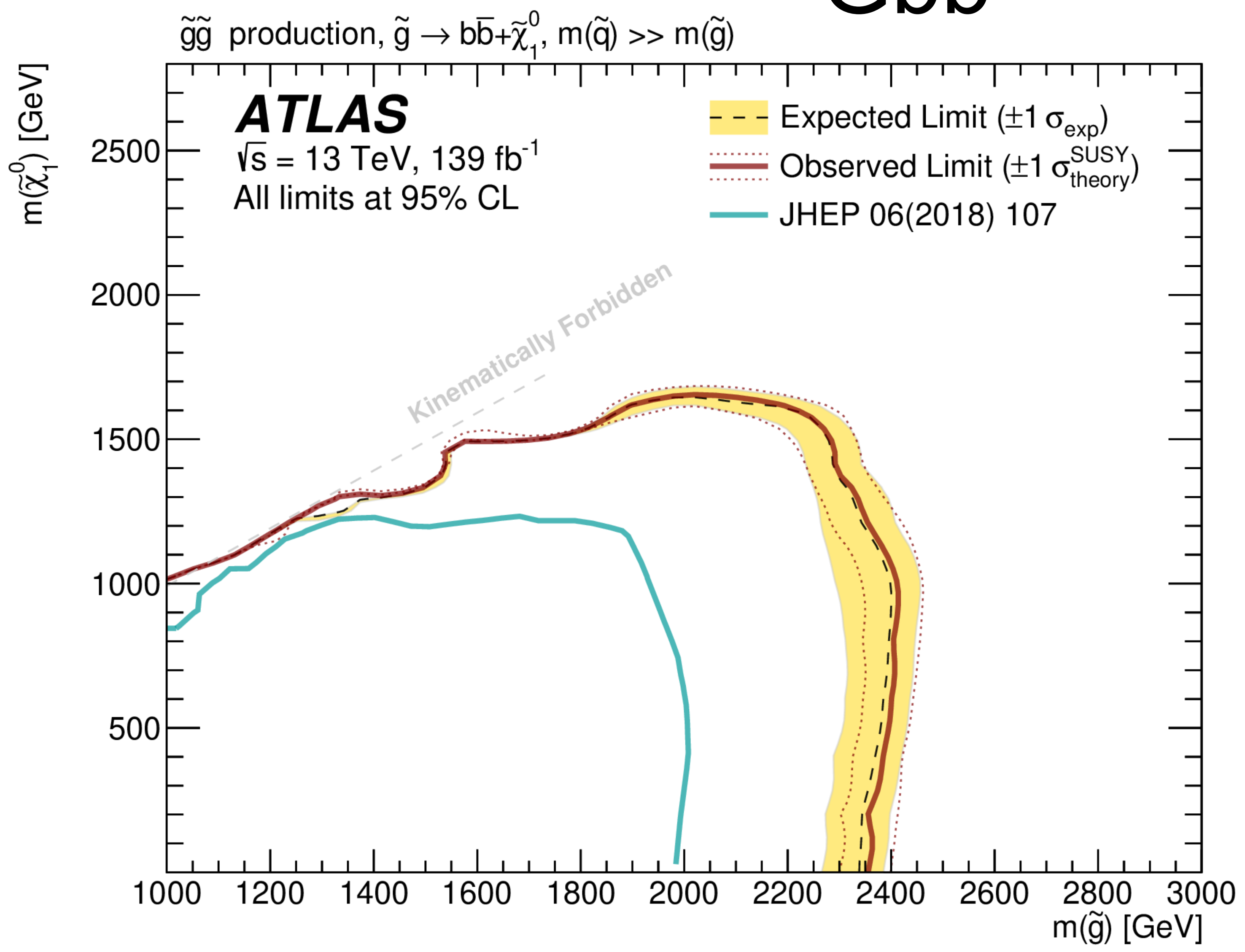

Run-3 Highlights

Phase-I Upgrade

- all Phase-I systems have been integrated in data-taking
- recently with HLT chains seeded by Phase-I items

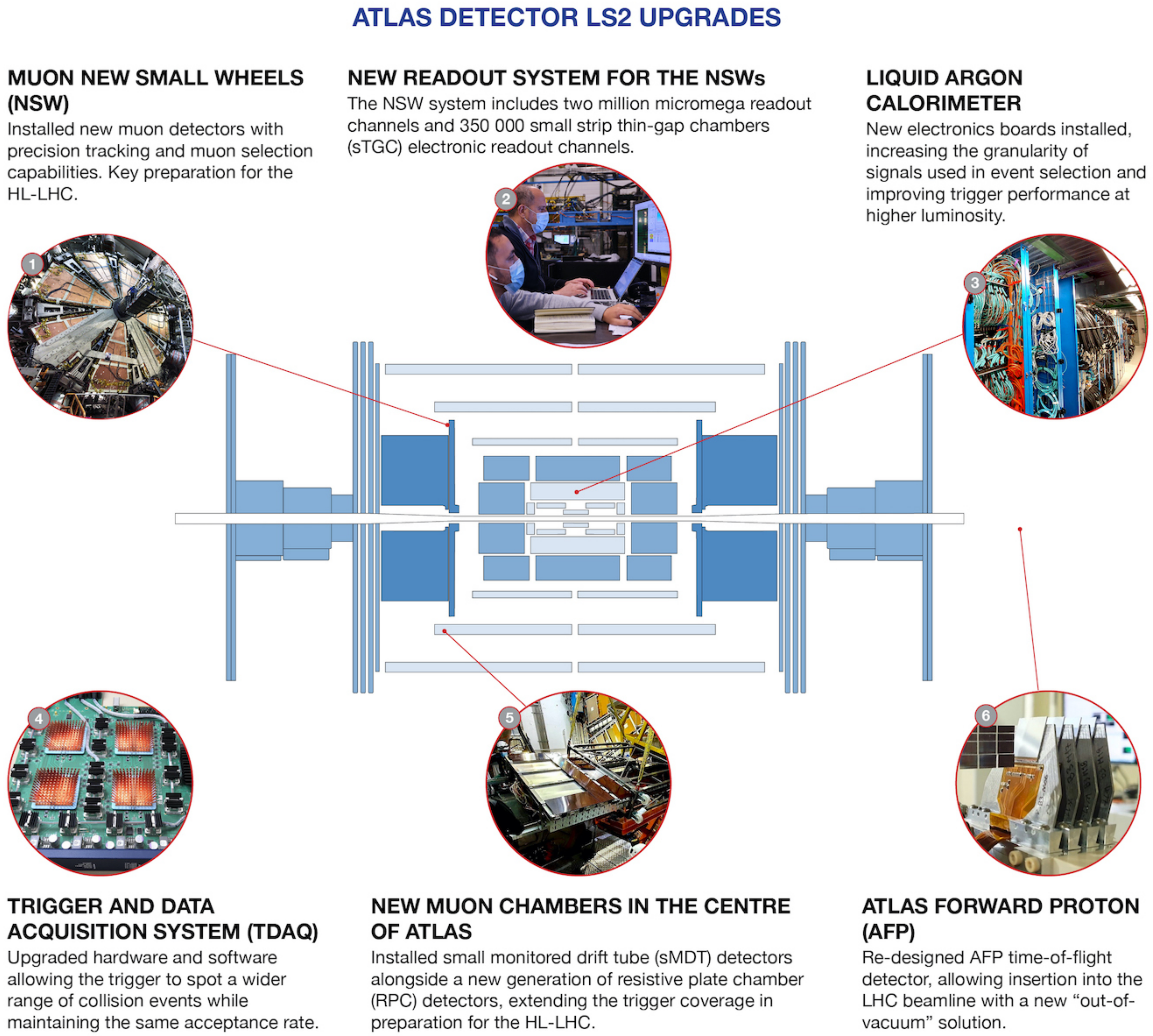

Performance results with early 13.6 TeV data

EGAM-2022-04

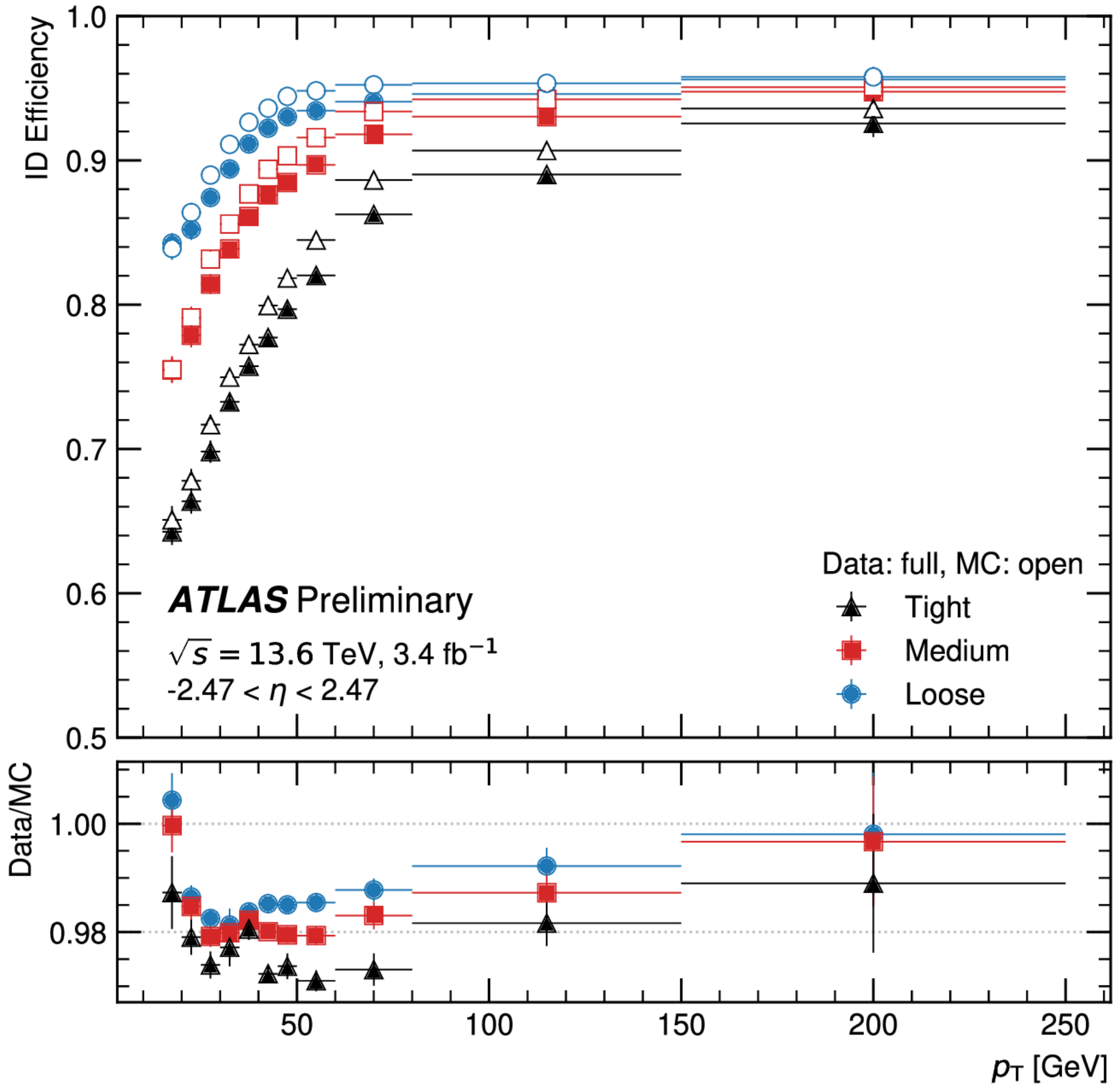

electron ID efficiencies in Z→ee events

MUON-2022-02

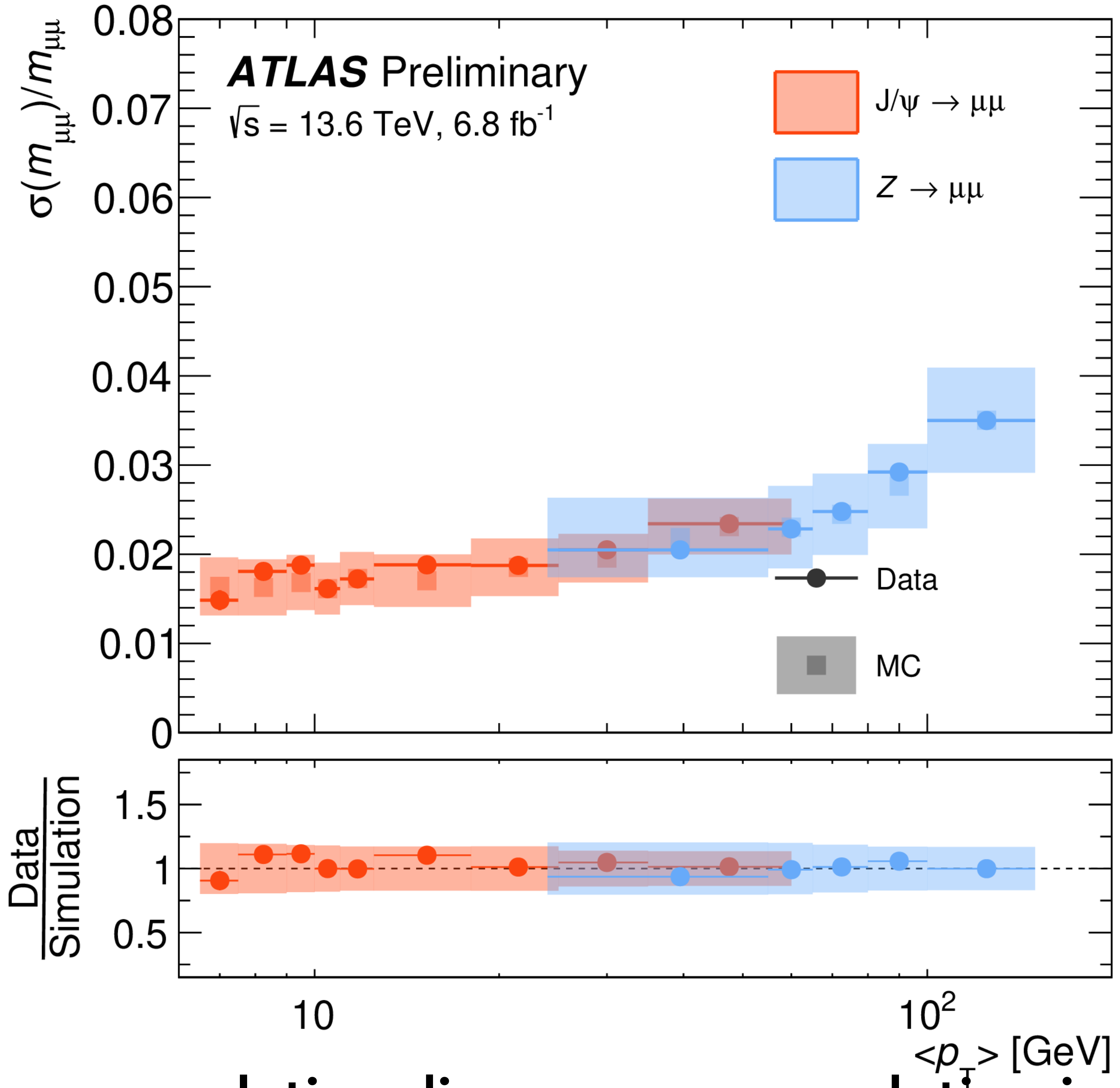

relative dimuon mass resolution in J/ψ and Z→μμ events

BPHYS-2022-001

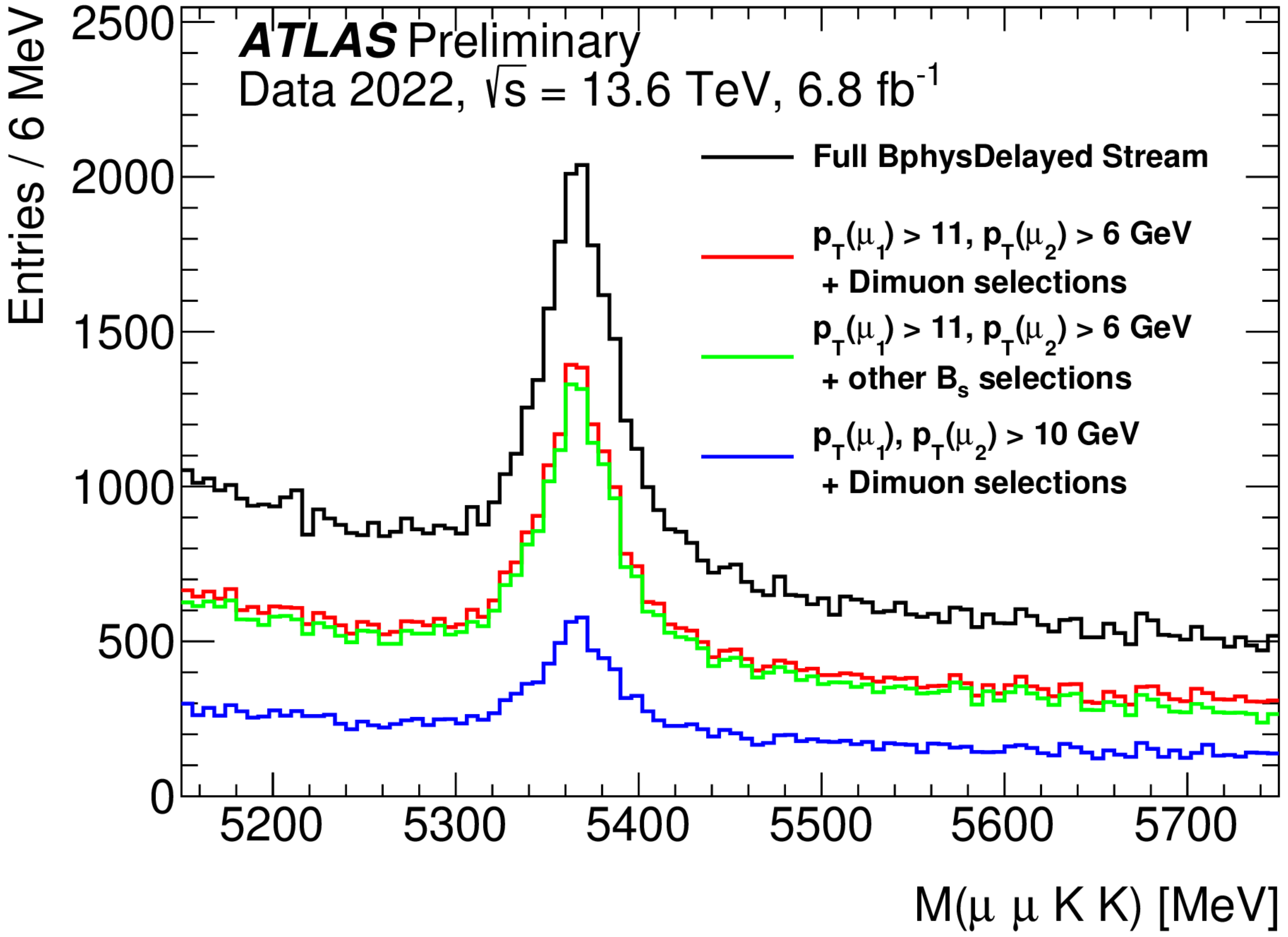

invariant mass spectrum of Bs→J/ψϕ candidates, muons are constrained to J/ψ mass and kaon candidates must satisfy 1008 < m_{KK} < 1030 MeV

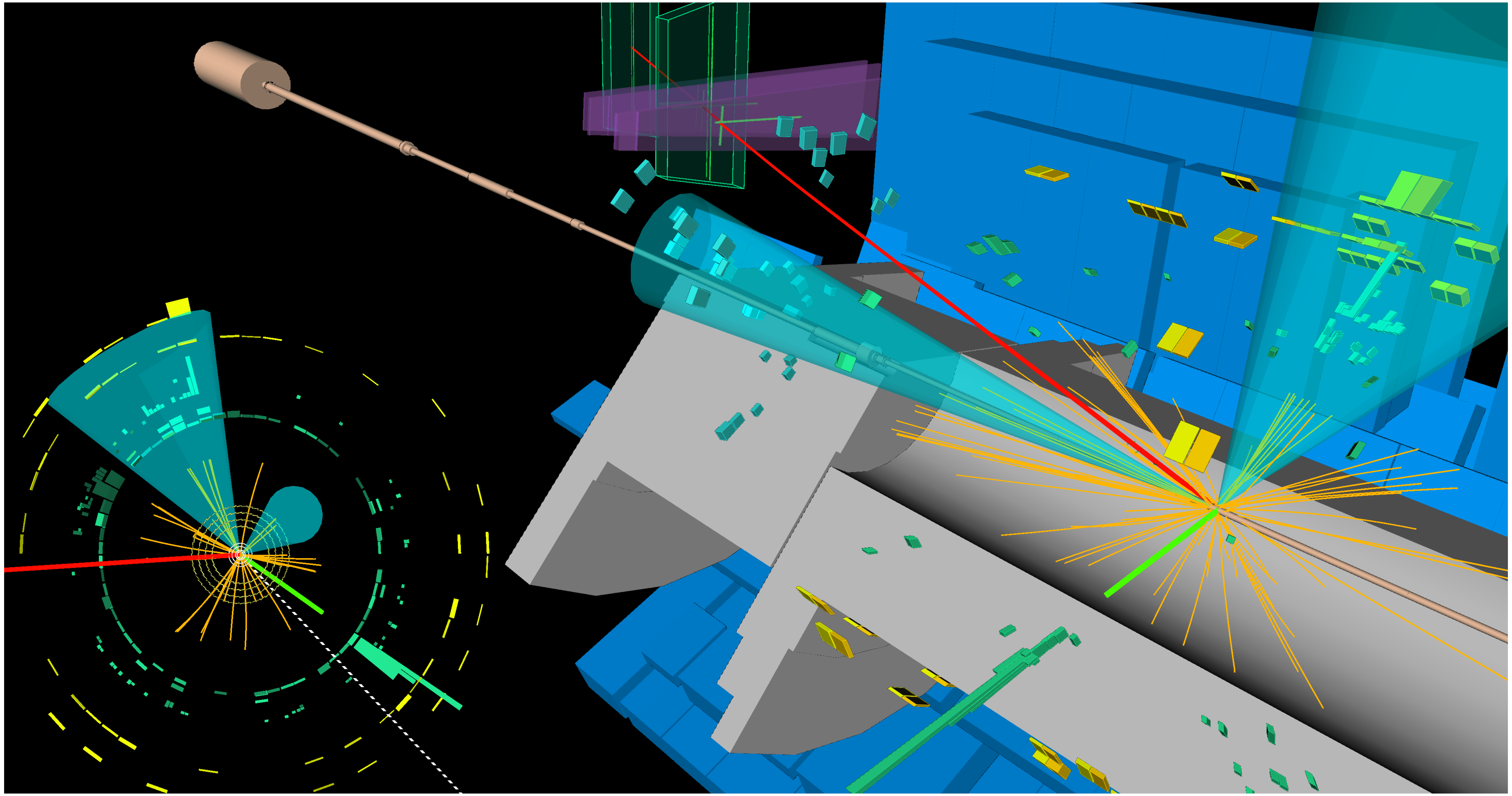

Candidate Run 3 event display of a pair of top quarks decaying the ATLAS detector. This event was **recorded on 18 July 2022 when stable beams of protons at the energy of 6.8 TeV per beam were delivered by the LHC**. The display shows charged particle tracks reconstructed in the inner detector (orange lines), an electron track (green line), a muon track (red line) as well as the energy deposits in the LAr (green and cyan blocks) and Tile (yellow/orange blocks) calorimeters. The event contains two jets that have passed b-tagging requirements and these are delineated with cyan cones. The lower-left-hand view shows the same event in the transverse plane, highlighting the direction of the missing transverse momentum (dashed white line). (Image: ATLAS Collaboration/CERN)

Measurement of tt/Z cross-section ratio at 13.6 TeV

ATLAS-CONF-2022-070

- 1.2 fb^{-1} of data (Aug 2022)
- eμ channel split into 1 or 2 b-tagged jets
- post-fit event counts in signal and bkg regions

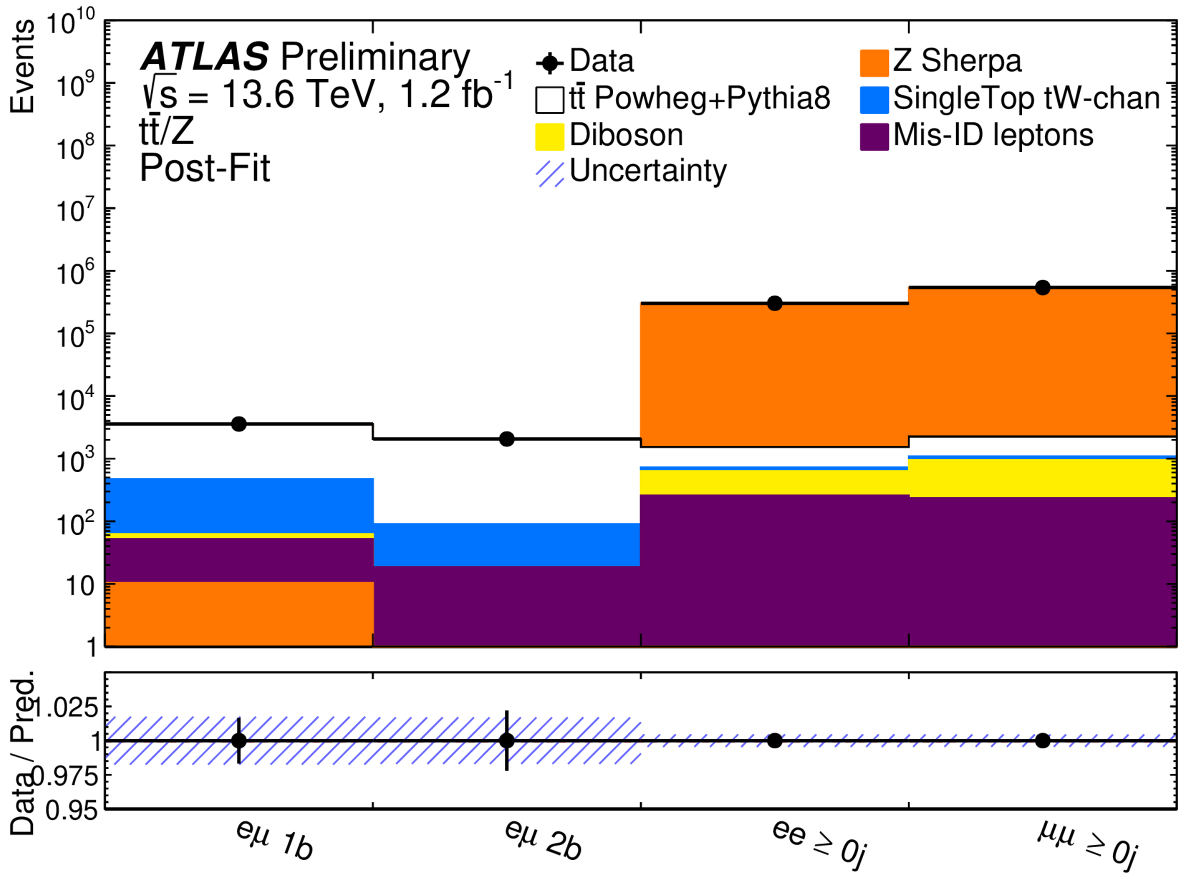

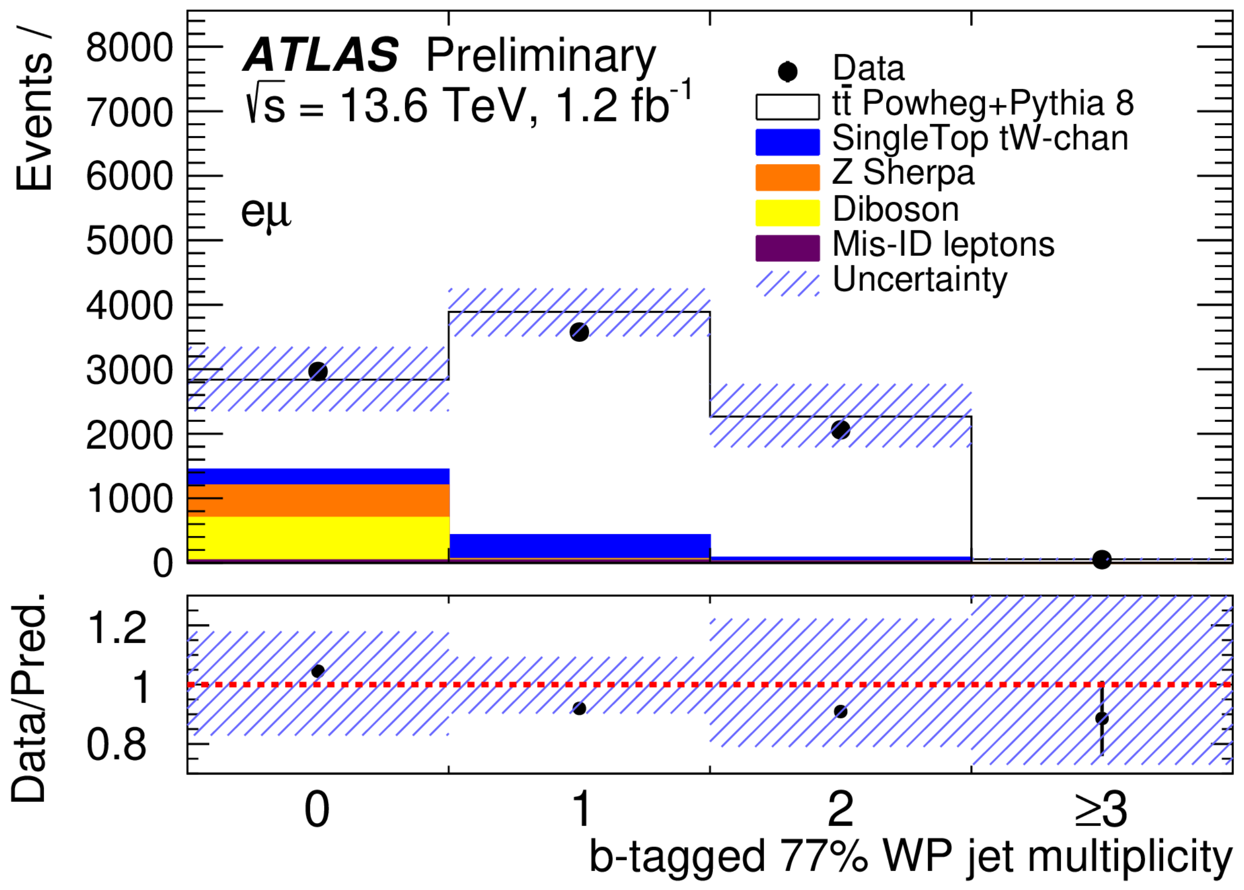

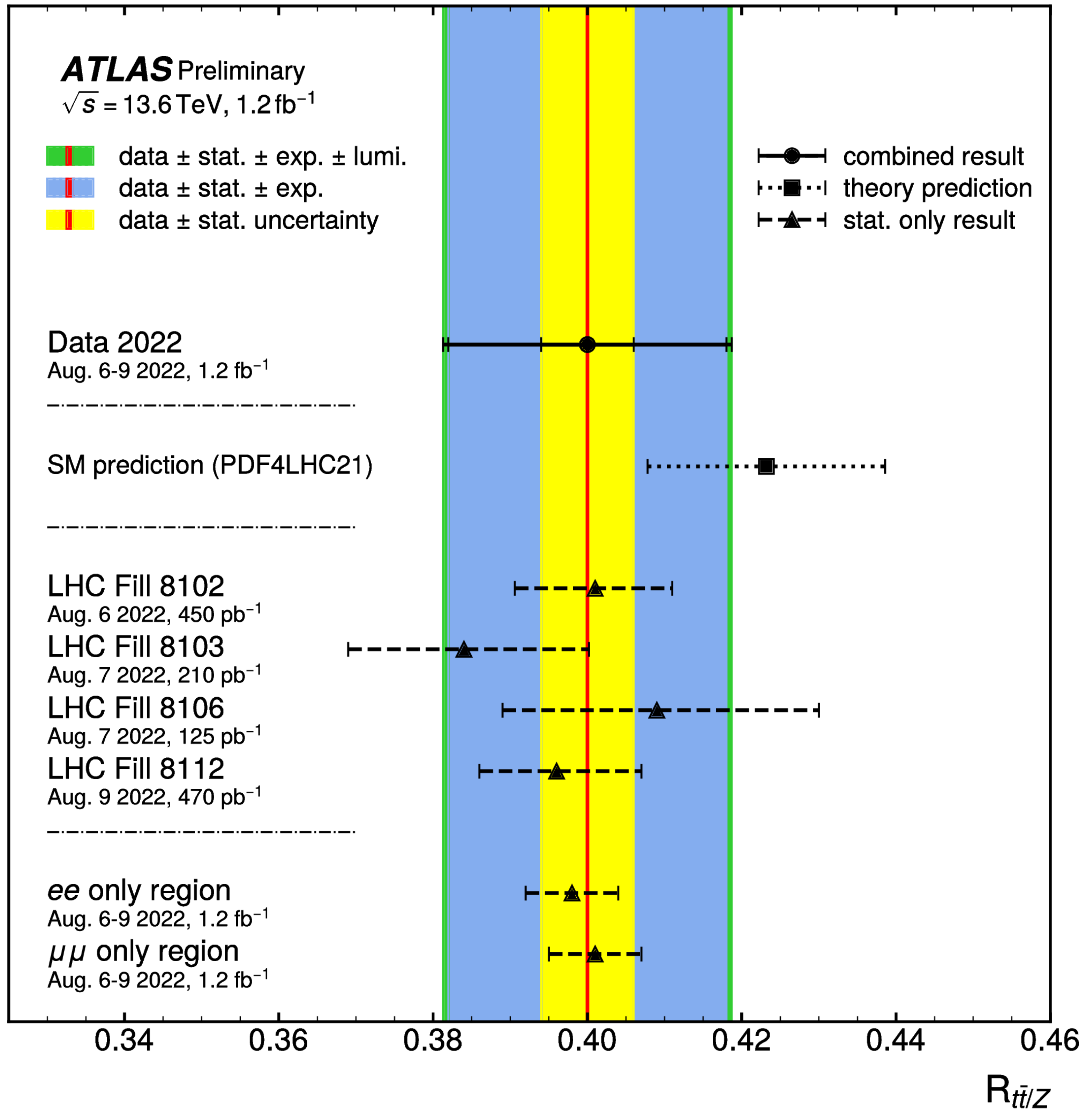

- absolute cross-section limited by large uncertainties on the preliminary luminosity estimate
- 4.7% precision for the ratio of the cross-sections
- measured values consistent with SM PDF4LHC21 PDF set

$\sigma_{tt(measured)}$ = 830 ± 12 (stat.) ± 27 (syst.) ± 86 (lumi) pb

$\sigma_{Z\rightarrow ll}$ = 2075 ± 2 (stat.) ± 98 (syst.) ± 199 (lumi) pb, for m_{ll} > 40 GeV

$R_{tt/Z}$ = 0.400 ± 0.006 (stat.) ± 0.017 (syst.) ± 0.005 (lumi)

Phase-II Upgrade for HL-LHC

The future

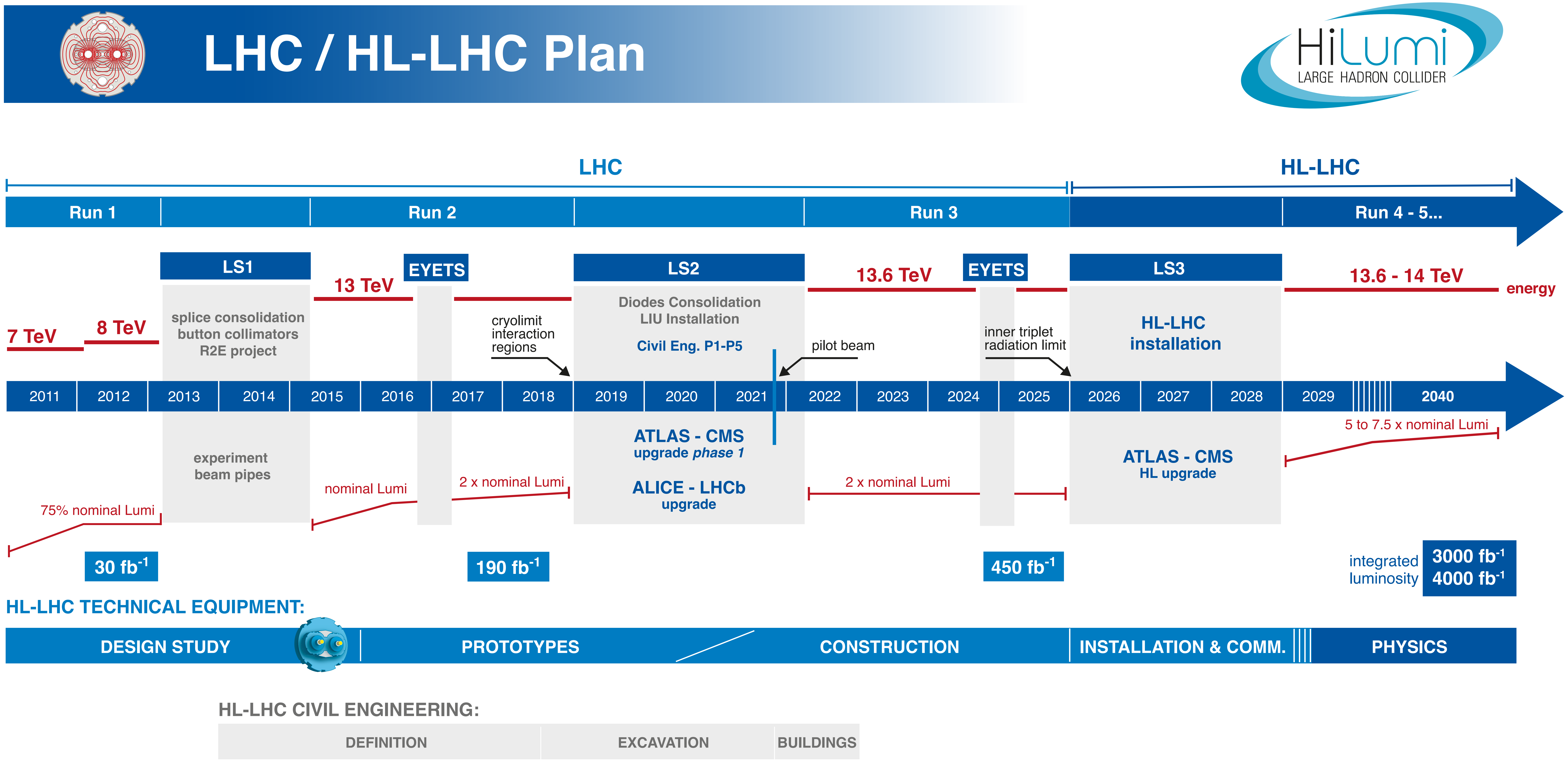

-

- Run 2 brought 140 fb^{-1} @ 13 TeV
- Run 3 may bring 300 fb^{-1} @ 13.6 TeV
- HL-LHC will bring an order of magnitude more!

and the challenge …

HL-LHC $t\bar{t}$ <μ>=200 with 88 reconstructed vertices

ATLAS Phase-II Upgrade

ITk	ITk Silicon Pixel TDR
ITk	ITk Silicon Strip TDR
LAr	LAr Calorimeter TDR
HGTD	High-Granularity Timing Detector TDR
Tile	Tile Calorimeter TDR
Muon	Muon Spectrometer TDR
TDAQ	TDAQ System TDR
SW&C	Computing CDR

New Muon Chambers

Inner barrel region with new RPC and sMDT detectors

High Granularity Timing Detector (HGTD)

Forward region (2.4 < |η| < 4.0)

Low-Gain Avalanche Detectors (LGAD)

with 30 ps track resolution

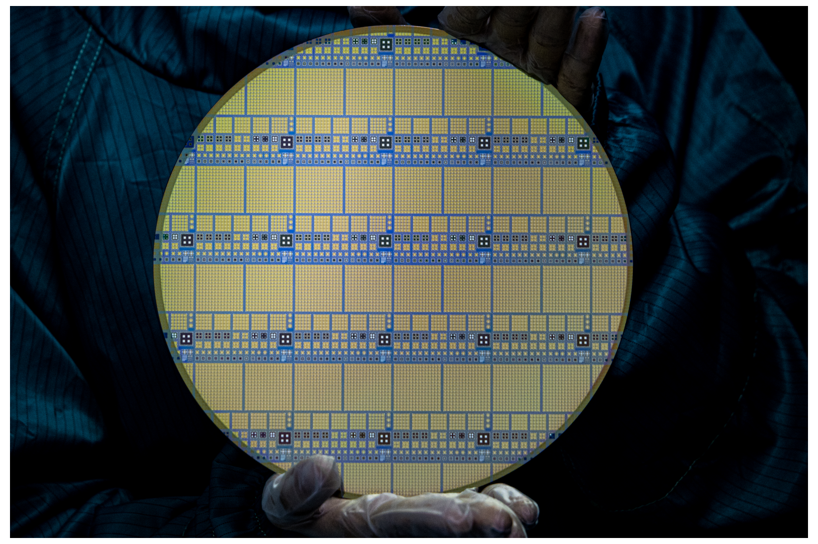

HGTD sensors | ATLAS Phase-2 Upgrade

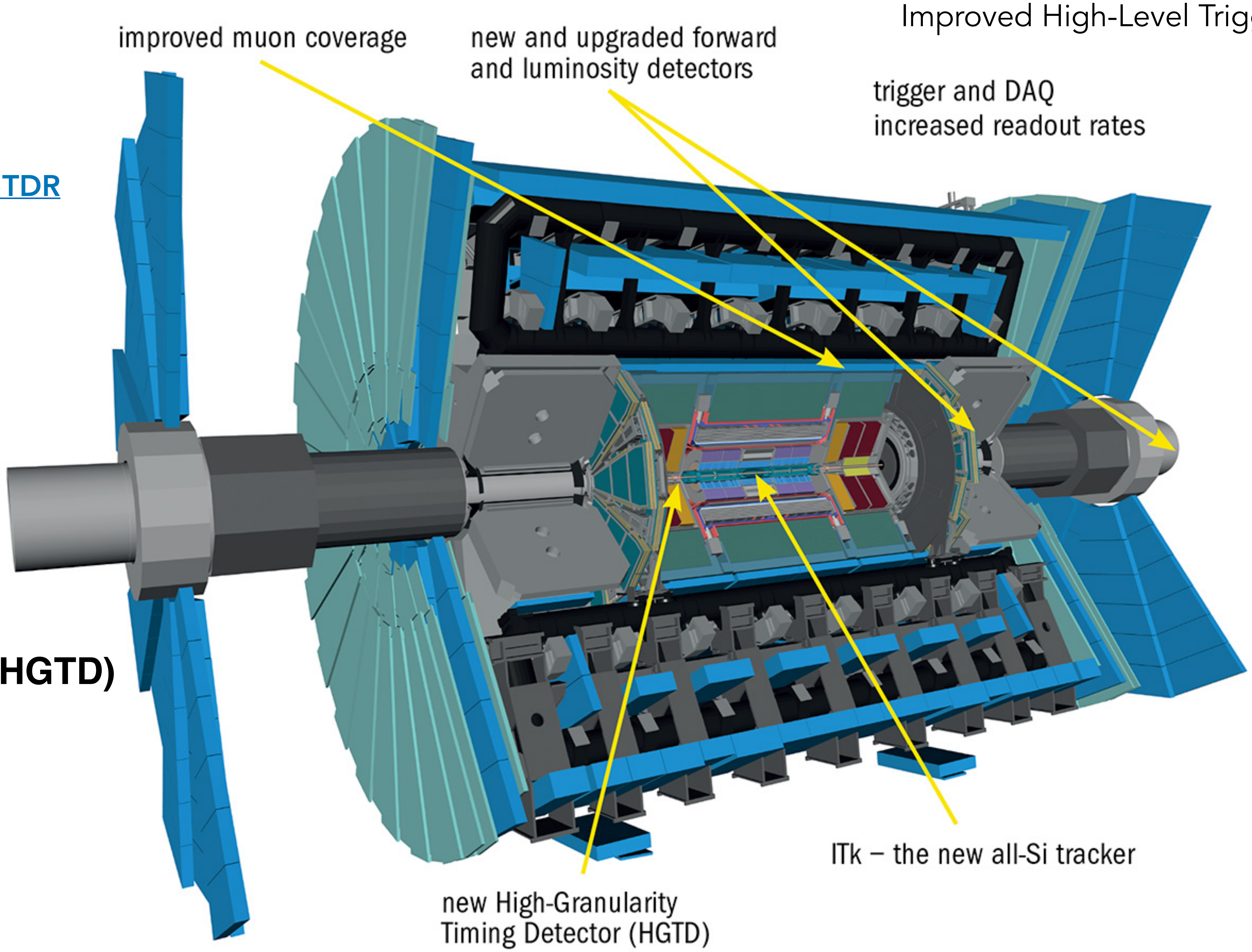

Upgraded Trigger and Data Acquisition system

Level-0 Trigger at 1 MHz

Improved High-Level Trigger (150 kHz full-scan tracking)

Additional small upgrades

Luminosity detectors

(1% precision goal) HL-ZDC

Electronics Upgrades

LAr Calorimeter

Tile Calorimeter

Muon system

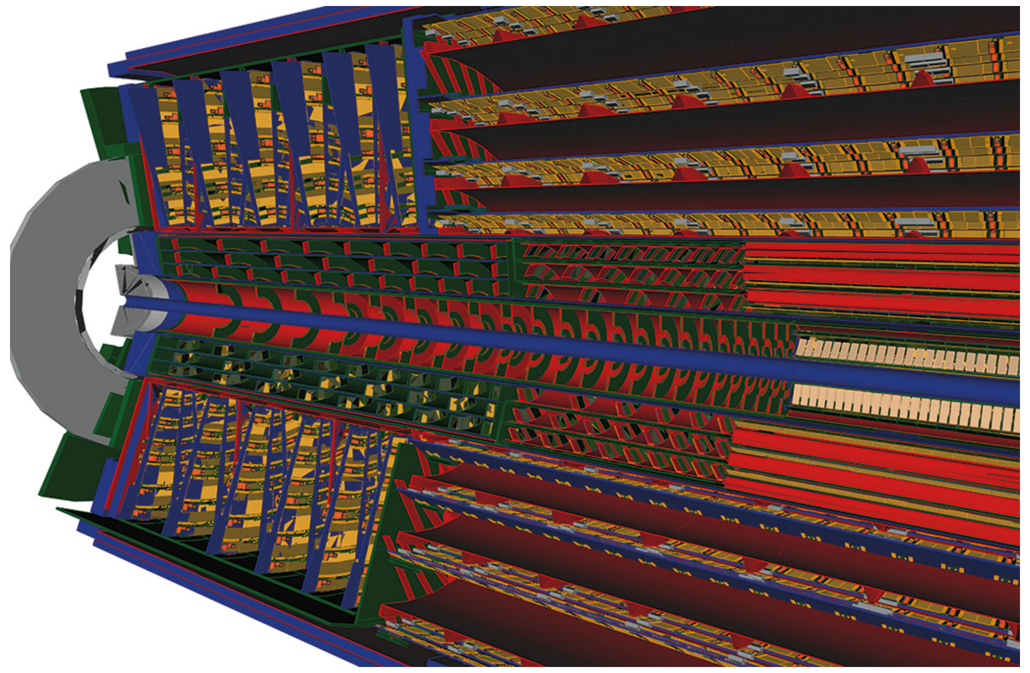

New Inner Tracking Detector (ITk)

All silicon, up to |η| = 4

Example HL-LHC expectations exceeded

ATL-PHYS-PUB-2015-046

- HH->bbττ projections in 2015:

…" *we can project an exclusion at 95% Confidence Level of BSM HH production with* $\boldsymbol{\lambda_{HHH}/\lambda_{SM} \leq -4}$ *and* $\boldsymbol{\lambda_{HHH}/\lambda_{SM} \geq 12}$ "

- HH->bbττ Run 2 results achieved later with 5% of that dataset, already exceed that

- improved τ_{had} and **b-jet** reconstruction and identification techniques, new triggers and a number of analysis-level improvements

ATLAS-CONF-2021-052

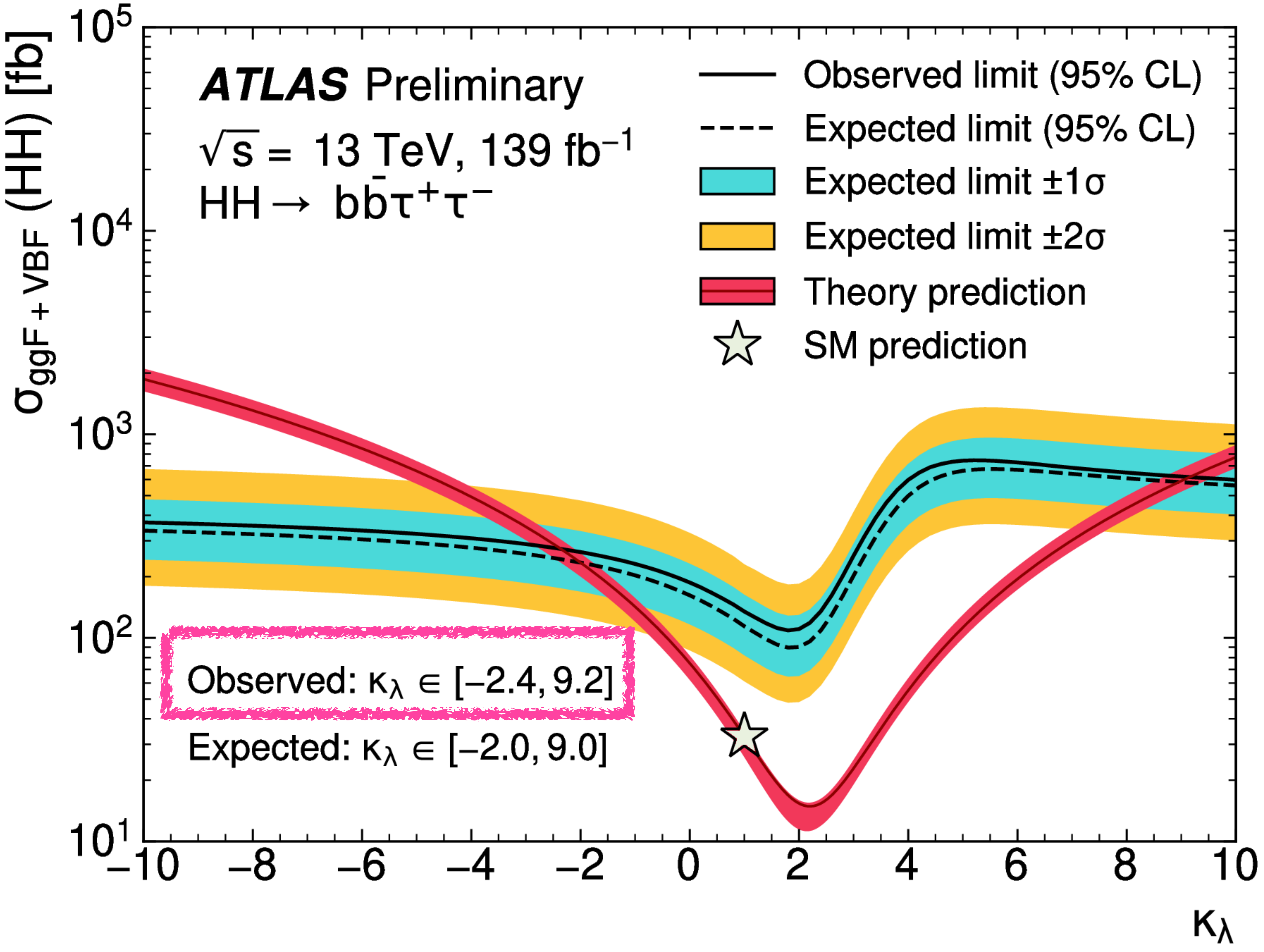

Concluding remarks

- ATLAS performed exceptionally well during Run-2
  - SM measurements over a wide range of phase space
  - reaching 5-10% constraints on main Higgs boson couplings
  - di-Higgs sensitivity approaching fast
  - wide program for BSM searches
  - analysis techniques have undergone a tremendous evolution
    - use of ML on physics objects and analyses design, improvements in signal and background modelling
- Many papers yet to come with the Run-2 dataset, with Run-3 data already on us
- And… preparation towards HL-LHC!!!

Thank you for your attention!

Additional slides

Run 2 flavour tagging

[arXiv:2211.16345 (Submitted to: EPJC)](arXiv:2211.16345)

RNNIP neural network architecture

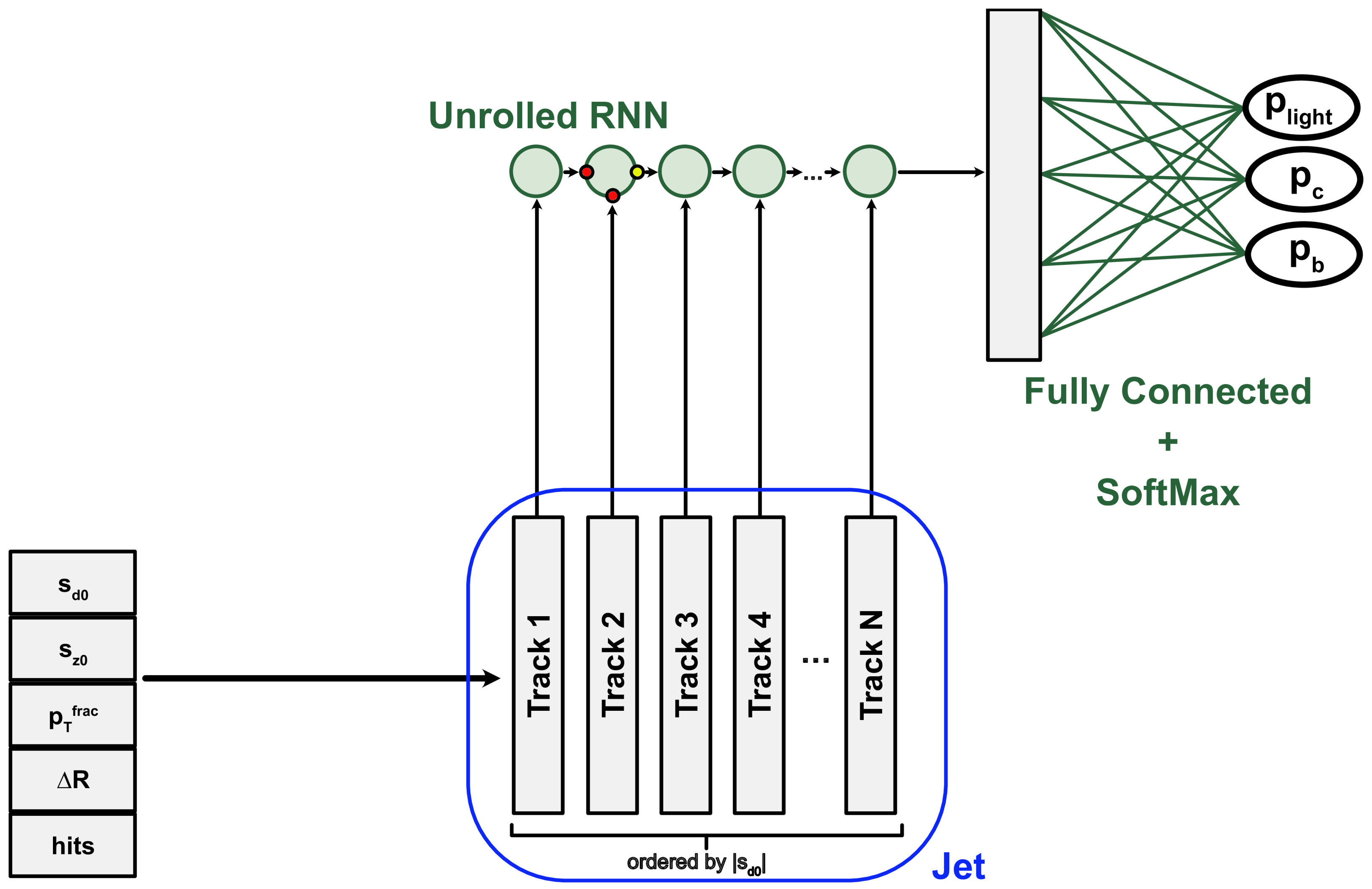

Input	Variable	Description	SVKine	JFKine	DL1	DL1r
Kinematics	p_T	Jet p_T	✓	✓	✓	✓
	η	Jet $\|\eta\|$	✓	✓	✓	✓
IP2D, IP3D	$\log(P_b/P_{light})$	Likelihood ratio of the b-jet to light-flavour jet hypotheses			✓	✓
	$\log(P_b/P_c)$	Likelihood ratio of the b-jet to c-jet hypotheses			✓	✓
	$\log(P_c/P_{light})$	Likelihood ratio of the c-jet to light-flavour jet hypotheses			✓	✓
RNNIP	P_b	b-jet probability				✓
	P_c	c-jet probability				✓
	P_{light}	light-flavour jet probability				✓
SV1	$m(SV)$	Invariant mass of tracks at the secondary vertex assuming pion mass	✓		✓	✓
	$f_E(SV)$	Jet energy fraction of the tracks associated with the secondary vertex	✓		✓	✓
	$N_{TrkAtVtx}(SV)$	Number of tracks used in the secondary vertex	✓		✓	✓
	$N_{2TrkVtx}(SV)$	Number of two-track vertex candidates	✓		✓	✓
	$L_{xy}(SV)$	Transverse distance between the primary and secondary vertices	✓		✓	✓
	$L_{xyz}(SV)$	Distance between the primary and secondary vertices	✓		✓	✓
	$S_{xyz}(SV)$	Distance between the primary and secondary vertices divided by its uncertainty	✓		✓	✓
	$\Delta R(\vec{p}_{jet}, \vec{p}_{vtx})(SV)$	ΔR between the jet axis and the direction of the secondary vertex relative to the primary vertex.	✓		✓	✓
JetFitter	$m(JF)$	Invariant mass of tracks from displaced vertices		✓	✓	✓
	$f_E(JF)$	Jet energy fraction of the tracks associated with the displaced vertices		✓	✓	✓
	$\Delta R(\vec{p}_{jet}, \vec{p}_{vtx})(JF)$	ΔR between the jet axis and the vectorial sum of momenta of all tracks attached to displaced vertices		✓	✓	✓
	$S_{xyz}(JF)$	Significance of the average distance between PV and displaced vertices		✓	✓	✓
	$N_{TrkAtVtx}(JF)$	Number of tracks from multi-prong displaced vertices		✓	✓	✓
	$N_{2TrkVtx}(JF)$	Number of two-track vertex candidates (prior to decay chain fit)		✓	✓	✓
	$N_{1\text{-trk vertices}}(JF)$	Number of single-prong displaced vertices		✓	✓	✓
	$N_{\geq 2\text{-trk vertices}}(JF)$	Number of multi-prong displaced vertices		✓	✓	✓
	$L_{xyz}(2^{nd})(JF)$	Distance of 2^{nd} vertex from PV		✓	✓	✓
	$L_{xy}(2^{nd})(JF)$	Transverse displacement of the 2^{nd} vertex		✓	✓	✓
	$m_{Trk}(2^{nd})(JF)$	Invariant mass of tracks associated with the 2^{nd} vertex		✓	✓	✓
	$E(2^{nd})(JF)$	Energy of the tracks associated with the 2^{nd} vertex		✓	✓	✓
	$f_E(2^{nd})(JF)$	Jet energy fraction of the tracks associated with the 2^{nd} vertex		✓	✓	✓
	$N_{TrkAtVtx}(2^{nd})(JF)$	Number of tracks associated with the 2^{nd} vertex		✓	✓	✓
	$\eta_{trk}^{min,max,avg}(2^{nd})(JF)$	Min., max. and avg. pseudorapidity of tracks at the 2^{nd} vertex		✓	✓	✓

RNN Tau-id

- Impose **physically motivated ordering** on reconstructed tracks
- similar to **RNN b-tagger** (track treated as sequence), each track is a time stamp
- Classify τ_{had} candidate using tracks and associated variables

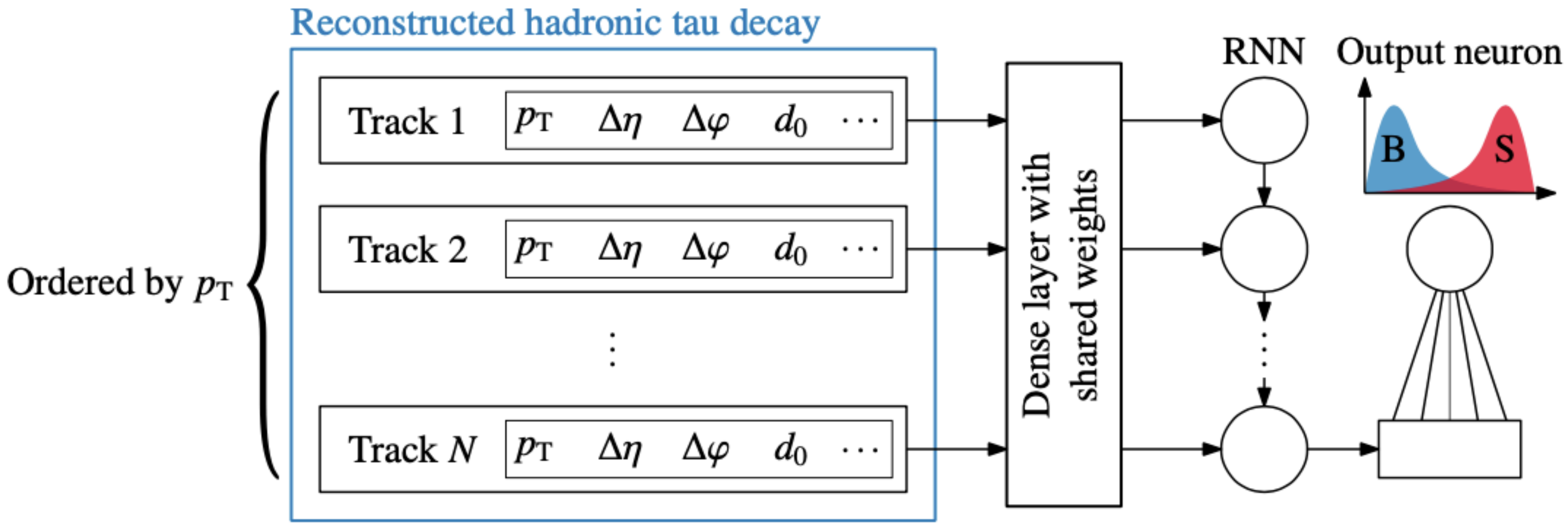

$p_{T,\, track} > 500$ MeV
ΔR(tau axis, track) < 0.4

pp cross-section

- beam optics parameters needed for the reconstruction of the scattering angle θ* at the IP
- in elastic scattering at high energies the four-momentum transfer t is calculated from θ* by:

$$-t = \left(\theta^{\star} \times p\right)^2$$

- p is the nominal LHC beam momentum of 6.5 TeV and θ* is reconstructed from the proton trajectories in ALFA

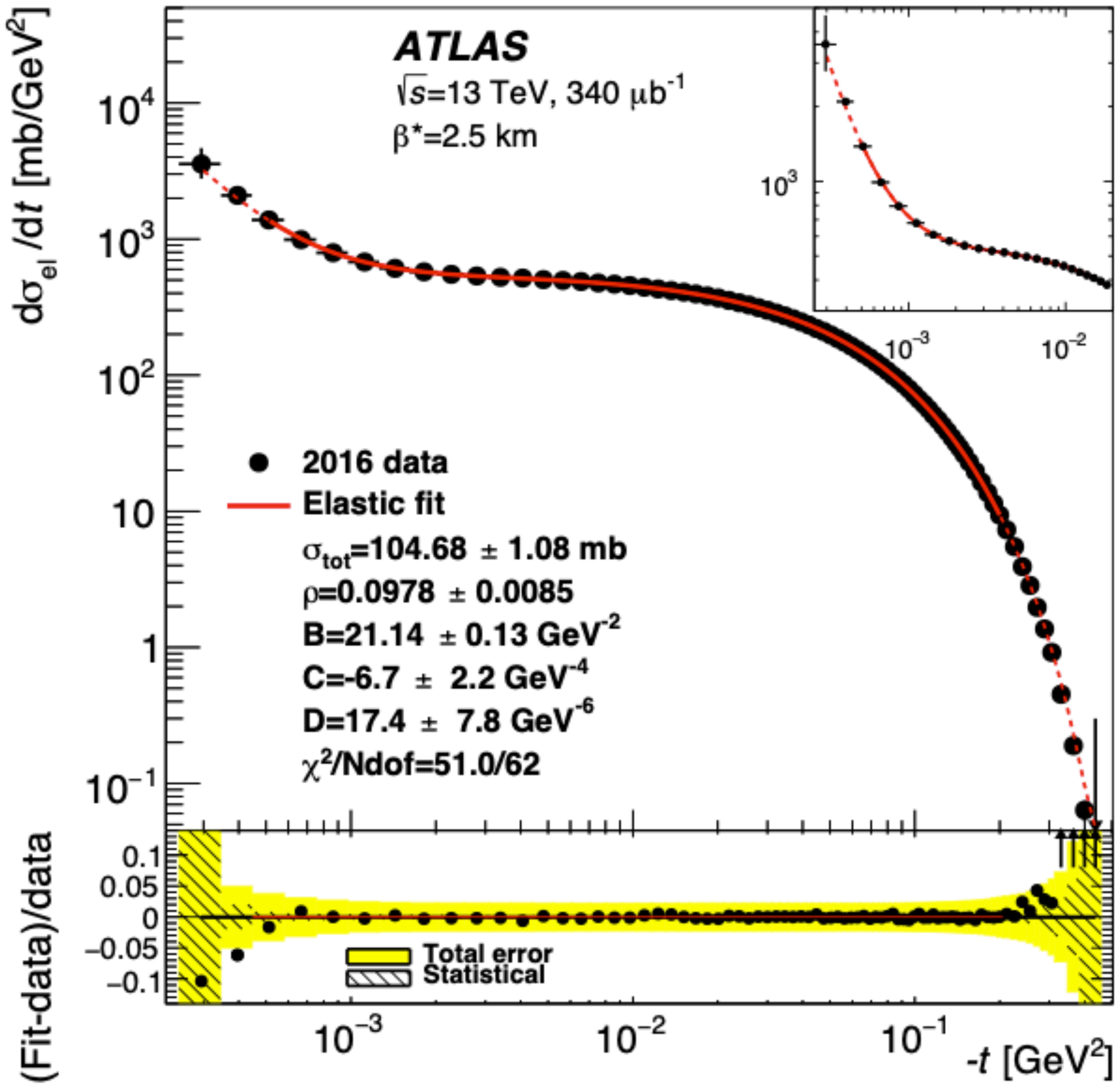

- theoretical form of t-dependence

$$\begin{aligned}\frac{d\sigma}{dt} &= \frac{4\pi\alpha^2(\hbar c)^2}{|t|^2} \times G^4(t) \\ &- \sigma_{\mathrm{tot}} \times \frac{\alpha G^2(t)}{|t|} \left[\sin\left(\alpha\phi(t)\right) + \rho\cos\left(\alpha\phi(t)\right)\right] \times e^{\frac{-B|t| - Ct^2 - D|t|^3}{2}} \\ &+ \sigma_{\mathrm{tot}}^2 \frac{1+\rho^2}{16\pi(\hbar c)^2} \times e^{\left(-B|t| - Ct^2 - D|t|^3\right)},\end{aligned}$$

Observation of WWW production

Phys. Rev. Lett. 129 (2022) 061803

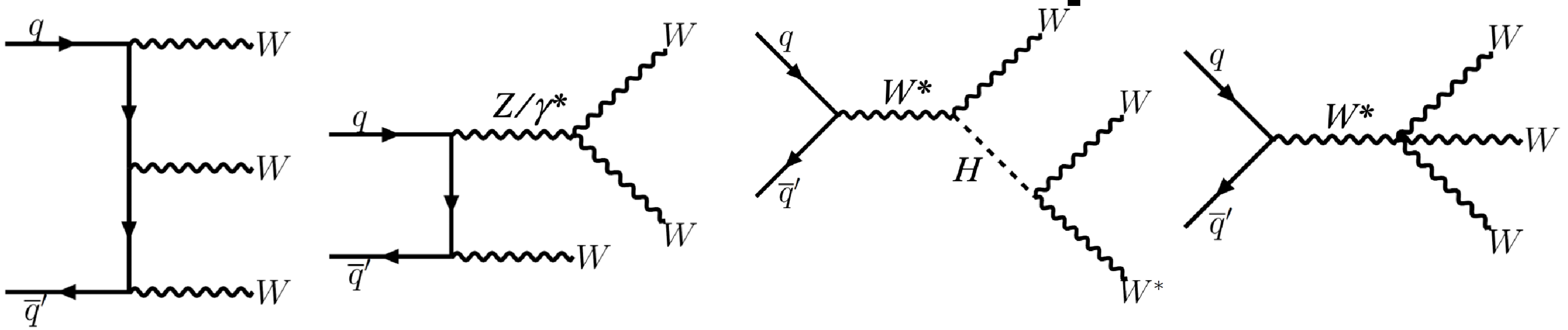

- BDT variables

2ℓ	3ℓ
$\lvert m_{jj} - m_W \rvert$	E_T^{miss} significance $\times 10/E_T^{miss}$
p_T(forward jet)	$p_T(\ell_2)$
E_T^{miss} significance	N(jets)
$p_T(j_2)$	same flavor $m_{\ell\ell}$
minimum $m(\ell, j)$	$m_T(\ell\ell\ell, E_T^{miss})$
$m(\ell_2, j_1)$	$m(\ell_2, \ell_3)$
N(jets)	$\Delta\phi(\ell\ell\ell, E_T^{miss})$
$p_T\ (\ell_2)$	minimum $\Delta R(\ell, \ell)$
$\lvert\eta(\ell_1)\rvert$	$p_T(\ell_3)$
N(leptons in jets)	$m_T(\ell_2, E_T^{miss})$
$m(\ell_1, j_1)$	E_T^{miss} significance

$$\mathcal{S} = \frac{E_T^{miss}}{\sqrt{H_T}} \text{ or } \mathcal{S} = \frac{E_T^{miss}}{\sqrt{\sum E_T}};$$

- post-fit number of events

	$e^\pm e^\pm$	$e^\pm \mu^\pm$	$\mu^\pm \mu^\pm$	3ℓ
WWW signal	28.4 ± 4.3	124 ± 19	82 ± 12	34.8 ± 5.2
WZ	81.1 ± 5.7	346 ± 22	170 ± 10	16.4 ± 1.5
Charge-flip	31.1 ± 7.3	19 ± 5	-	1.7 ± 0.4
γ conversions	60.8 ± 8.5	139 ± 15	-	1.5 ± 0.1
Non-prompt	17.0 ± 4.0	145 ± 23	104 ± 21	26.6 ± 2.9
Other	22.3 ± 2.4	100 ± 10	58 ± 6	8.0 ± 0.9
Total predicted	241 ± 11	873 ± 22	415 ± 17	89.0 ± 5.4
Data	242	885	418	79

$$H_T = \sum p_T^\mu + \sum p_T^e + \sum p_T^\gamma + \sum p_T^\tau + \sum p_T^{jets}$$

Observation of polarisation in WZ production

	Data	Powheg+Pythia	NLO QCD
		$W^{\pm}Z$	
f_{00}	0.067 ± 0.010	0.0590 ± 0.0009	0.058 ± 0.002
f_{0T}	0.110 ± 0.029	0.1515 ± 0.0017	0.159 ± 0.003
f_{T0}	0.179 ± 0.023	0.1465 ± 0.0017	0.149 ± 0.003
f_{TT}	0.644 ± 0.032	0.6431 ± 0.0021	0.628 ± 0.004
		$W^{+}Z$	
f_{00}	0.072 ± 0.016	0.0583 ± 0.0012	0.057 ± 0.002
f_{0T}	0.119 ± 0.034	0.1484 ± 0.0022	0.155 ± 0.003
f_{T0}	0.152 ± 0.033	0.1461 ± 0.0022	0.147 ± 0.003
f_{TT}	0.66 ± 0.04	0.6472 ± 0.0026	0.635 ± 0.004
		$W^{-}Z$	
f_{00}	0.063 ± 0.016	0.0600 ± 0.0014	0.059 ± 0.002
f_{0T}	0.11 ± 0.04	0.1560 ± 0.0027	0.166 ± 0.003
f_{T0}	0.21 ± 0.04	0.1470 ± 0.0027	0.152 ± 0.003
f_{TT}	0.62 ± 0.05	0.6370 ± 0.0033	0.618 ± 0.004

	f_{00}	f_{0T}	f_{T0}	f_{TT}
e energy scale and id. efficiency	0.00018	0.0009	0.0012	0.0019
μ energy scale and id. efficiency	0.0004	0.0004	0.0004	0.0008
E_T^{miss} and jets	0.0017	0.0021	0.0020	0.0023
Pile-up	0.00031	0.00027	0.0007	0.0010
Misidentified lepton background	0.0012	0.0026	0.0013	0.0016
ZZ background	0.0005	0.00028	0.0005	0.0004
Other backgrounds	0.0016	0.0025	0.0021	0.0025
Parton Distribution Function	0.00025	0.0029	0.00014	0.0028
QCD scale	0.00010	0.014	0.0014	0.012
Modelling	0.005	0.007	0.005	0.008
Total systematic uncertainty	0.006	0.017	0.006	0.016
Luminosity	0.00019	0.0004	0.0004	0.00034
Statistical uncertainty	0.007	0.016	0.019	0.019
Total	0.010	0.029	0.023	0.032

Top pair production cross section at 5.02 TeV

	$\ell + 2j \geq 1b$	$\ell + 3j\ 1b$	$\ell + 3j\ 2b$	$\ell + \geq 4j\ 1b$	$\ell + 4j\ 2b$	$\ell + \geq 5j\ 2b$
$t\bar{t}$	194 ± 27	310 ± 33	199 ± 24	690 ± 60	318 ± 32	380 ± 60
Single top	195 ± 22	98 ± 12	38 ± 5	67 ± 9	22 ± 4	15.9 ± 2.7
W+ jets	1700 ± 400	690 ± 210	58 ± 23	350 ± 120	30 ± 14	19 ± 10
Other bkg.	110 ± 40	55 ± 23	7.2 ± 3.0	29 ± 12	3.5 ± 1.5	3.7 ± 1.7
Misidentified leptons	250 ± 130	110 ± 60	10 ± 5	60 ± 30	6 ± 3	8 ± 5
Total	2500 ± 400	1260 ± 210	312 ± 34	1200 ± 160	380 ± 40	430 ± 70
Data	2411	1214	293	1135	375	444

Category	$\delta\sigma_{t\bar{t}}$ [%] Dilepton	Single lepton	Combination
$t\bar{t}$ generator†	1.2	1.0	0.8
$t\bar{t}$ parton-shower/hadronisation*,†	0.3	0.9	0.7
$t\bar{t}$ h_{damp} and scale variations†	1.0	1.1	0.8
$t\bar{t}$ parton distribution functions†	0.2	0.2	0.2
Single-top background	1.1	0.8	0.6
W/Z + jets background*	0.8	2.4	1.8
Diboson background	0.3	0.1	< 0.1
Misidentified leptons*	0.7	0.3	0.3
Electron identification/isolation	0.8	1.2	0.8
Electron energy scale/resolution	0.1	0.1	< 0.1
Muon identification/isolation	0.6	0.2	0.3
Muon momentum scale/resolution	0.1	0.1	0.1
Lepton-trigger efficiency	0.2	0.9	0.7
Jet-energy scale/resolution	0.1	1.1	0.8
$\sqrt{s}$ = 5.02 TeV JES correction	0.1	0.6	0.5
Jet-vertex tagging	< 0.1	0.2	0.2
Flavour tagging	0.1	1.1	0.8
$E_{\mathrm{T}}^{\mathrm{miss}}$	0.1	0.4	0.3
Simulation statistical uncertainty*	0.2	0.6	0.5
Data statistical uncertainty*	6.8	1.3	1.3
Total systematic uncertainty	3.1	4.2	3.7
Integrated luminosity	1.8	1.6	1.6
Beam energy	0.3	0.3	0.3
Total uncertainty	7.5	4.5	3.9

arXiv:2207.01353 (Submitted to JHEP)

Single top+photon observation

arXiv:2302.01283 (Submitted to Phys. Rev. Lett.)

Uncertainty	$\Delta\sigma/\sigma$
$t\bar{t}\gamma$ modeling	±5.5%
Background MC statistics	±3.6%
$t\,(\rightarrow \ell\nu b\gamma)\,q$ modeling	±3.3%
$tq\gamma$ MC statistics	±3.0%
$t\bar{t}$ modeling	±2.3%
$tq\gamma$ modeling	±2.3%
Additional background uncertainties	±2.0%
$t\,(\rightarrow \ell\nu b\gamma)\,q$ MC statistics	±0.3%
Lepton fakes	±2.2%
$h\rightarrow\gamma$ photon fakes	±2.1%
$e\rightarrow\gamma$ photon fakes	±0.6%
Luminosity	±2.2%
Pileup	±1.3%
Jets and $E_{\mathrm{T}}^{\mathrm{miss}}$	±3.5%
Photons	±2.5%
Leptons	±0.9%
b-tagging	±0.7%
Total systematic uncertainty	±10.7%

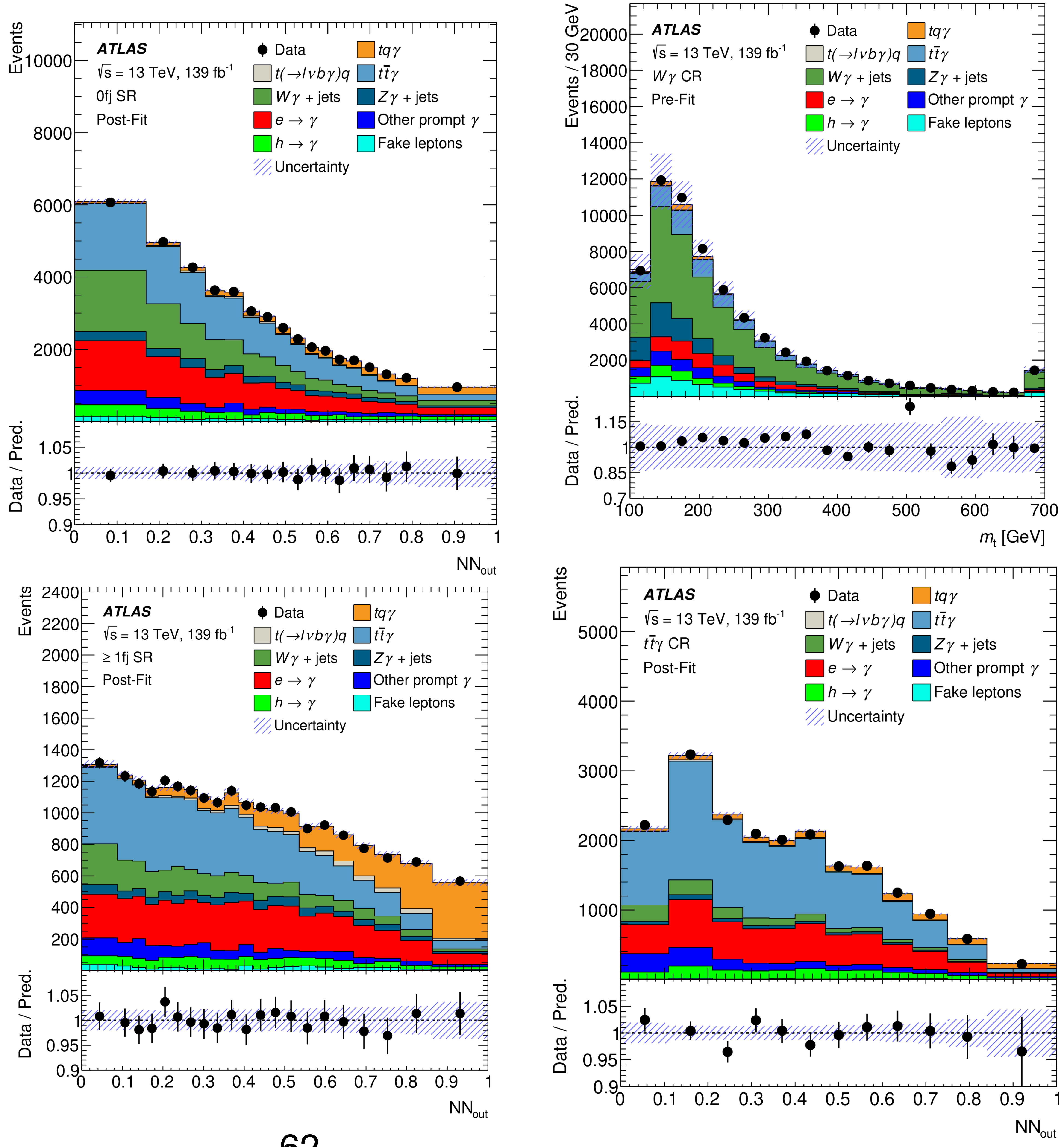

Observation of di-charmonium in 4μ states

- motivated by tetraquarks, in two channels:

$$T_{cc\bar{c}\bar{c}} \to J/\psi\, J/\psi \to 4\mu$$

$$T_{cc\bar{c}\bar{c}} \to J/\psi\, \psi(2S) \to 4\mu$$

<table>
<tr><th>Signal region</th><th>SPS/DPS control region</th><th>non-prompt region</th></tr>
<tr><td colspan="3">Di-muon or tri-muon triggers,
Opposite charged muons from the same J/ψ or ψ(2S) vertex,
Loose muon ID, $p_{\mathrm{T}}^{1,2,3,4} > 4, 4, 3, 3$ GeV and $|\eta_{1,2,3,4}| < 2.5$ for the four muons
$m_{J/\psi} \in \{2.94, 3.25\}$ GeV, or $m_{\psi(2S)} \in \{3.56, 3.80\}$ GeV,
Loose vertex cuts $\chi^2_{4\mu}/N < 40$ and $\chi^2_{\text{di-}\mu}/N < 100$,</td></tr>
<tr><td colspan="2">Vertex $\chi^2_{4\mu}/N < 3$,
$L^{4\mu}_{xy} < 0.2$ mm, $|L^{\text{di-}\mu}_{xy}| < 0.3$ mm,</td><td rowspan="2">Vertex $\chi^2_{4\mu}/N > 6$,
$|L^{\text{di-}\mu}_{xy}| > 0.4$ mm</td></tr>
<tr><td>$m_{4\mu} < 7.5$ GeV,
$\Delta R < 0.25$ between charmonia</td><td>7.5 GeV$< m_{4\mu} < 12.0$ GeV (SPS)
14.0 GeV$< m_{4\mu} < 25.0$ GeV (DPS)</td></tr>
</table>

H→4l: precise mass measurement

arXiv:2207.00320 (Submitted to: Physics Letters B)

Final state	Higgs	ZZ, tXX, VVV	Reducible backgrounds	Expected total yield	Observed yield	S/B
4μ	78 ± 5	38.7 ± 2.2	2.84 ± 0.17	120 ± 5	115	1.89
$2e2\mu$	53.4 ± 3.2	26.7 ± 1.4	3.02 ± 0.19	83.1 ± 3.5	94	1.80
$2\mu 2e$	41.2 ± 3.0	17.9 ± 1.3	3.4 ± 0.5	62.5 ± 3.3	59	1.93
$4e$	36.2 ± 2.7	15.7 ± 1.6	2.83 ± 0.35	54.8 ± 3.2	45	1.95
Total	209 ± 13	99 ± 6	12.2 ± 0.9	321 ± 14	313	1.88

Systematic Uncertainty	Contribution [MeV]
Muon momentum scale	± 28
Electron energy scale	± 19
Signal-process theory	± 14

Evidence of off-shell Higgs

ATLAS-CONF-2022-068

ZZ→ 4ℓ

Process	ggF	Mixed	EW
$gg \to (H^* \to)ZZ$	341 ± 117	42.5 ± 14.9	11.8 ± 4.3
$gg \to H^* \to ZZ$	32.6 ± 9.07	3.68 ± 1.03	1.58 ± 0.47
$gg \to ZZ$	345 ± 119	43.0 ± 15.2	11.9 ± 4.4
$qq \to (H^* \to)ZZ + 2j$	23.2 ± 1.0	2.03 ± 0.16	9.89 ± 0.96
$qqZZ$	1878 ± 151	135 ± 23	22.0 ± 8.3
Other backgrounds	50.6 ± 2.5	1.79 ± 0.16	1.65 ± 0.16
Total expected (SM)	2293 ± 209	181 ± 29	45.3 ± 10.0
Observed	2327	178	50

ZZ→ 2ℓ2ν

Process	ggF	Mixed	EW
$gg \to (H^* \to)ZZ$	210 ± 53	19.7 ± 4.9	4.29 ± 1.10
$gg \to H^* \to ZZ$	111 ± 26	10.9 ± 2.5	3.26 ± 0.82
$gg \to ZZ$	251 ± 66	23.4 ± 6.2	5.31 ± 1.46
$qq \to (H^* \to)ZZ + 2j$	14.0 ± 3.0	1.63 ± 0.17	4.46 ± 0.50
$qqZZ$	1422 ± 112	80.4 ± 11.9	7.74 ± 2.99
WZ	678 ± 54	51.9 ± 6.9	7.89 ± 2.50
Z+jets	62.3 ± 24.3	7.51 ± 6.94	0.62 ± 0.54
Non-resonant-$\ell\ell$	106 ± 39	9.17 ± 2.73	1.55 ± 0.42
Other backgrounds	22.6 ± 5.2	1.62 ± 0.25	1.40 ± 0.10
Total expected (SM)	2515 ± 165	172 ± 17	28.0 ± 4.1
Observed	2496	181	27

ggF Signal region

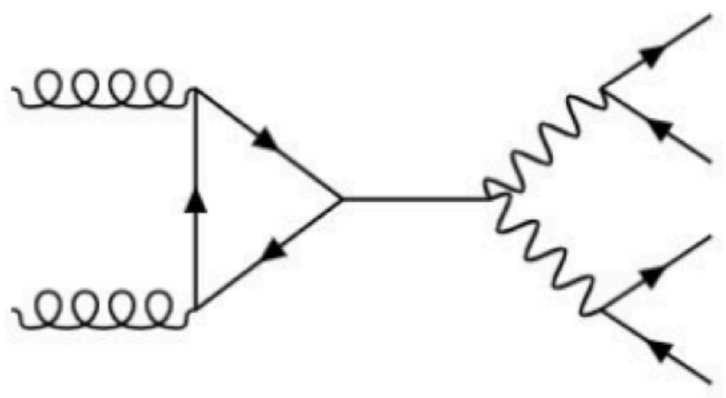

$n_{\text{jets}} = 0$

$n_{\text{jets}} = 1$ and $\eta_j < 2.2$

$n_{\text{jets}} \geq 2$ and $\Delta\eta_{jj} < 4.0$

1 jet mixed signal region

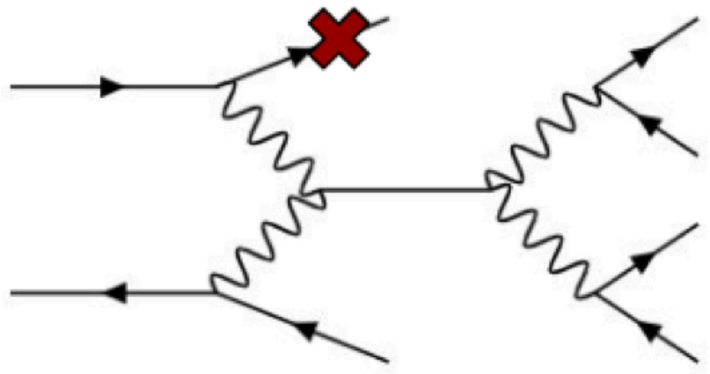

$n_{\text{jets}} = 1$ and $\eta_j \geq 2.2$

EW signal region

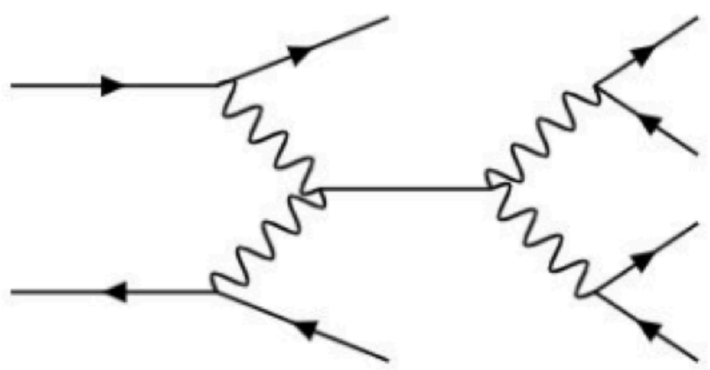

$n_{\text{jets}} \geq 2$ and $\Delta\eta_{jj} \geq 4.0$

EW includes VBF and VH

Search for H→ μμ

Phys. Lett. B 812 (2021) 135980

- 20 categories exploiting topological and kinematic differences between background and different H production modes (ggF, VBF, VH and ttH)
- background dominated inclusively by DY processes

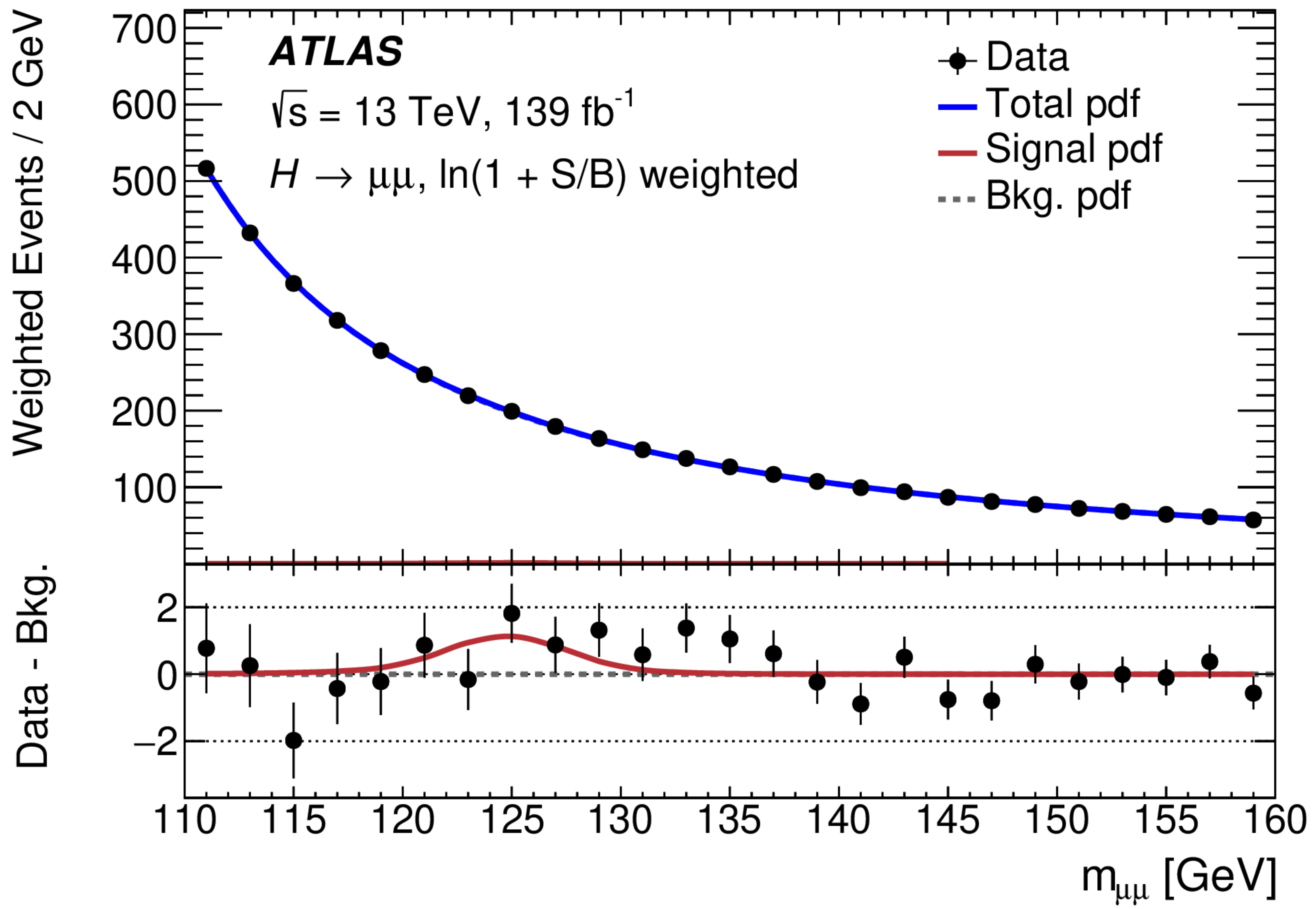

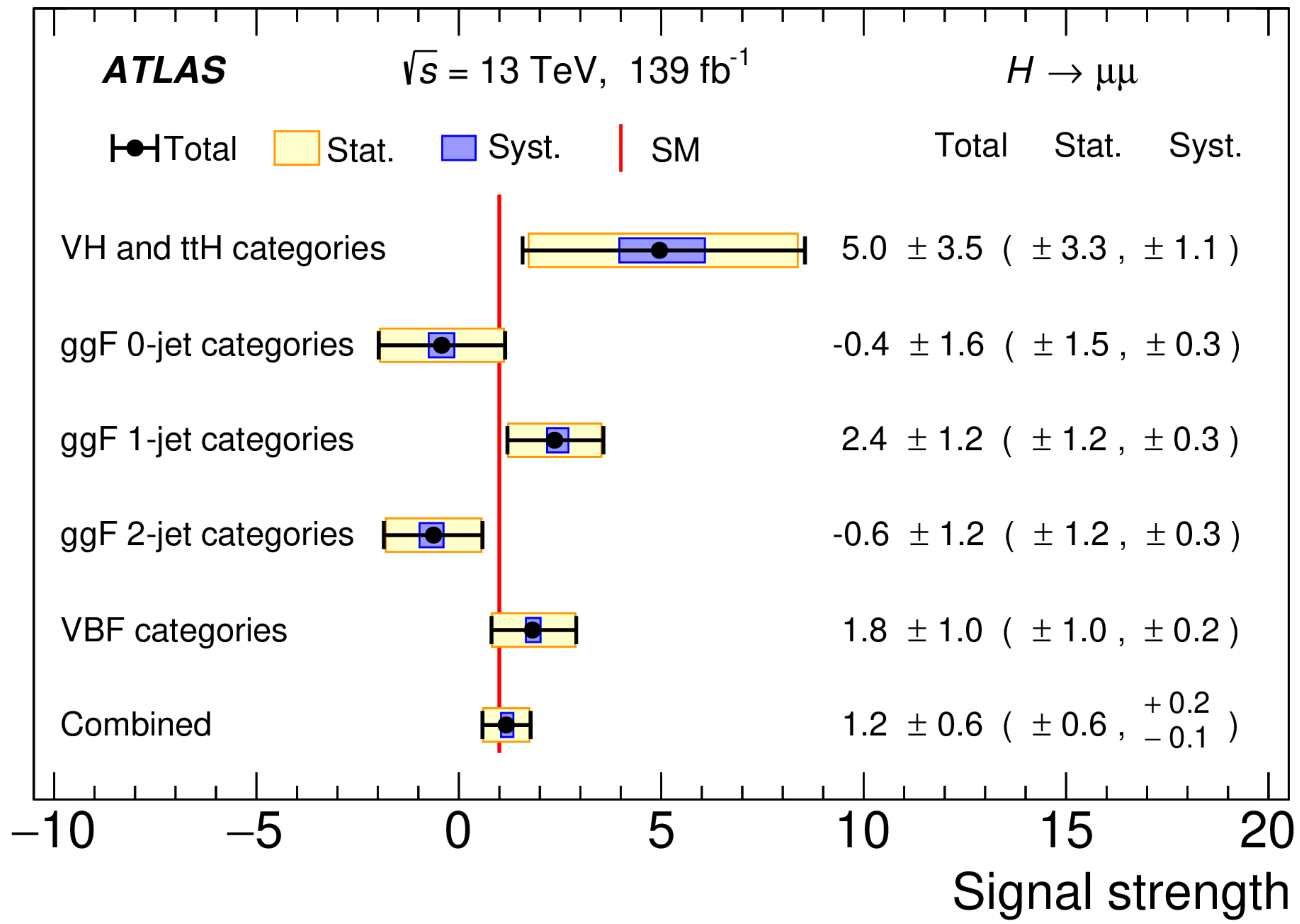

observed (expected) 2.0 σ (1.7 σ)

μ = 1.2 ± 0.6

CP properties with H→ττ

$$d\Gamma_{H\to\tau^+\tau^-} \approx 1 - b(E_+)b(E_-)\frac{\pi^2}{16}\cos(\varphi^*_{CP} - 2\phi_\tau)$$

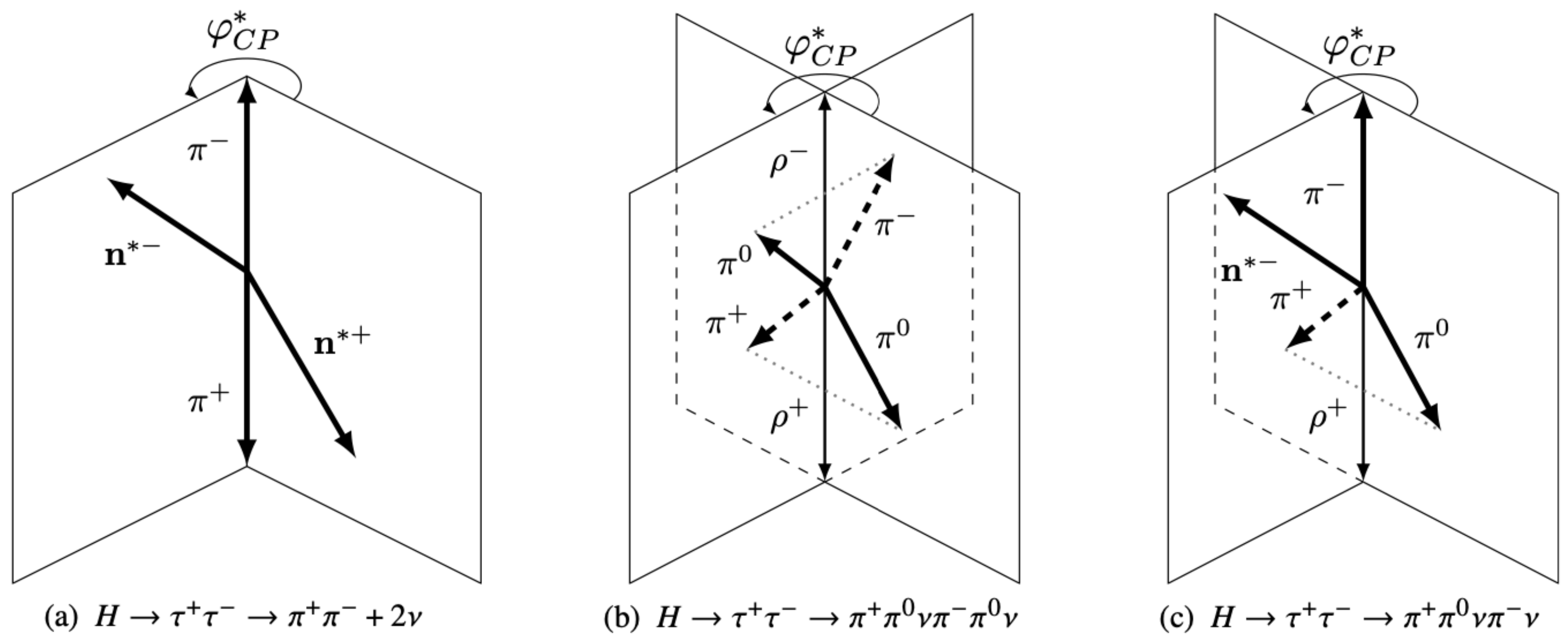

Figure 1: Illustration of the τ-lepton decay planes for constructing the φ^*_{CP} observable in (a) $H \to \tau^+\tau^- \to \pi^+\pi^- + 2\nu$ decay using the impact parameter method, (b) $H \to \tau^+\tau^- \to \pi^+\pi^0\nu\pi^-\pi^0\nu$ using the ρ-decay plane method, and (c) $H \to \tau^+\tau^- \to \pi^+\pi^0\nu\pi^-\nu$ using the combined impact parameter and ρ-decay plane method. The decay planes are spanned by the spatial momentum vector of the charged decay particle of the τ-lepton ($\pi^\pm$) and either its impact parameter $\mathbf{n}^{*\pm}$ or the spatial momentum vector of the neutral decay particle of the τ-lepton (π^0).

Decay channel	Decay mode combination	Method	Fraction in all τ-lepton-pair decays
$\tau_{\text{lep}}\tau_{\text{had}}$	ℓ–1p0n	IP	8.1%
	ℓ–1p1n	IP–ρ	18.3%
	ℓ–1pXn	IP–ρ	7.6%
	ℓ–3p0n	IP–a_1	6.9%
$\tau_{\text{had}}\tau_{\text{had}}$	1p0n–1p0n	IP	1.3%
	1p0n–1p1n	IP–ρ	6.0%
	1p1n–1p1n	ρ	6.7%
	1p0n–1pXn	IP–ρ	2.5%
	1p1n–1pXn	ρ	5.6%
	1p1n–3p0n	ρ–a_1	5.1%

STXS H→γγ

arXiv:2207.00348

- multi-class BDT used to classify events into STXS regions
  - allows the selection of target process events that otherwise would fail a requirement based on detector-level quantities corresponding to the STXS region definition.

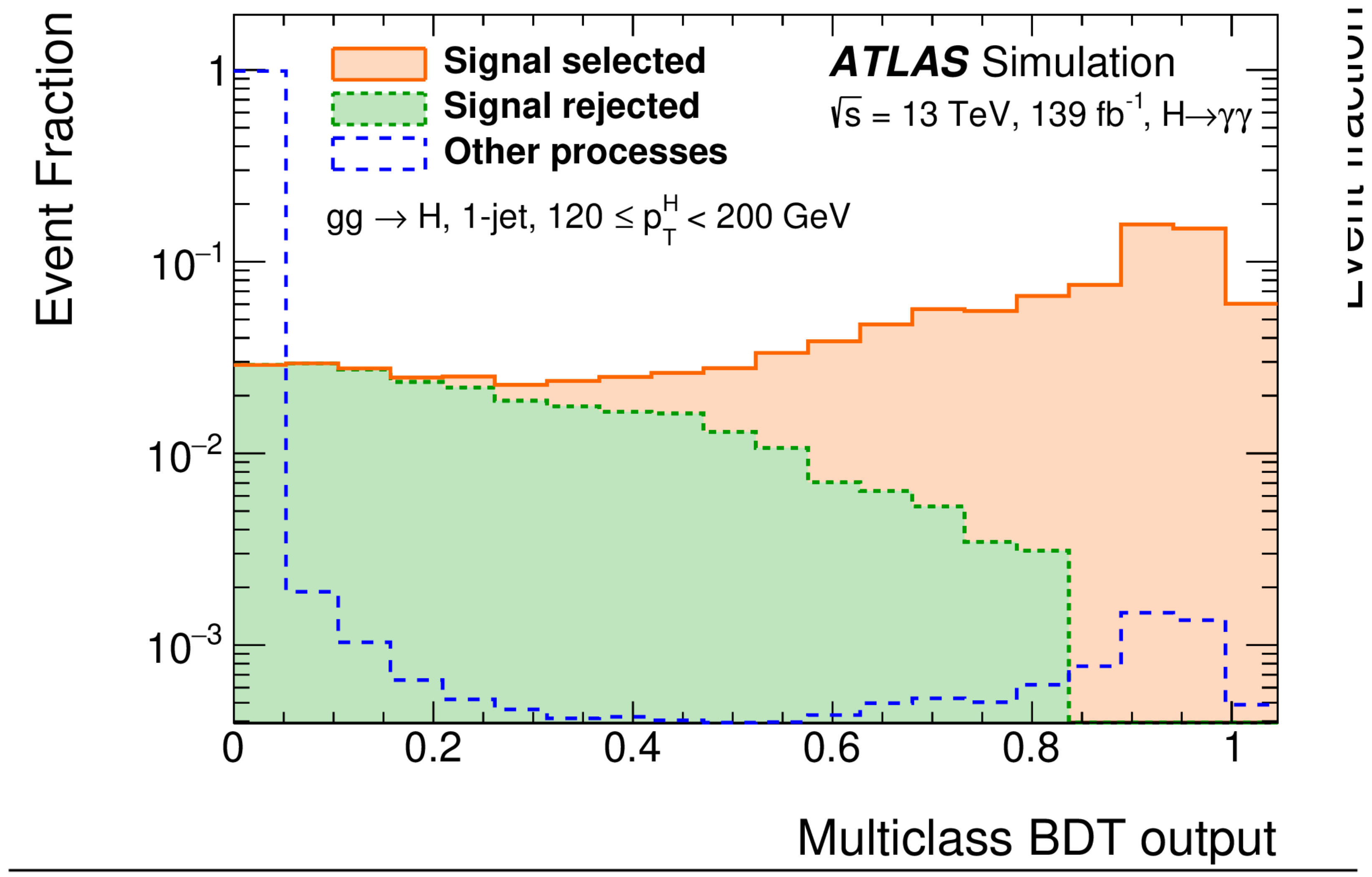

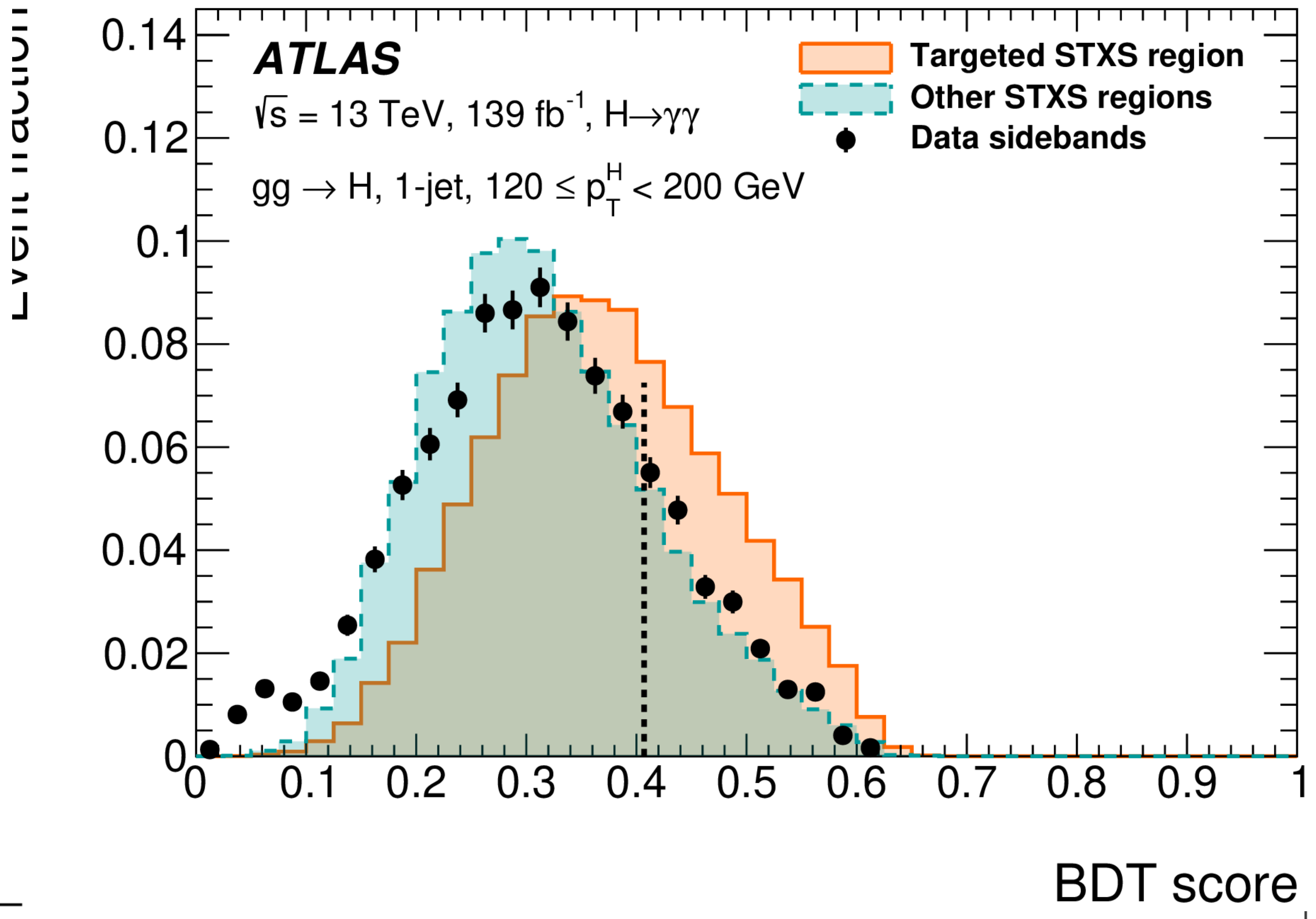

	ggF + $b\bar{b}H$	VBF	WH	ZH	$t\bar{t}H$	tH
Uncertainty source	$\Delta\sigma$[%]	$\Delta\sigma$[%]	$\Delta\sigma$[%]	$\Delta\sigma$[%]	$\Delta\sigma$[%]	$\Delta\sigma$[%]
Theory uncertainties						
Higher-order QCD terms	±1.4	±4.1	±4.1	±12	±2.8	±16
Underlying event and parton shower	±2.5	±16	±2.5	±4.0	±3.6	±48
PDF and α_s	< ±1	±2.0	±1.4	±2.3	< ±1	±5.8
Matrix element	< ±1	±3.2	< ±1	±1.2	±2.5	±8.2
Heavy-flavour jet modelling in non-$t\bar{t}H$ processes	< ±1	< ±1	< ±1	< ±1	< ±1	±13
Experimental uncertainties						
Photon energy resolution	±3.0	±3.0	±3.8	±4.8	±3.0	±12
Photon efficiency	±2.7	±2.7	±3.3	±3.6	±2.9	±9.3
Luminosity	±1.8	±2.0	±2.4	±2.7	±2.2	±6.6
Pile-up	±1.4	±2.2	±2.0	±2.3	±1.4	±7.3
Background modelling	±2.0	±4.6	±3.6	±7.2	±2.5	±63
Photon energy scale	< ±1	< ±1	< ±1	±1.3	< ±1	±5.6
Jet/E_T^{miss}	< ±1	±6.8	< ±1	±2.2	±3.5	±22
Flavour tagging	< ±1	< ±1	< ±1	< ±1	±1.5	±3.4
Leptons	< ±1	< ±1	< ±1	< ±1	< ±1	±1.8
Higgs boson mass	< ±1	< ±1	< ±1	< ±1	< ±1	< ±1

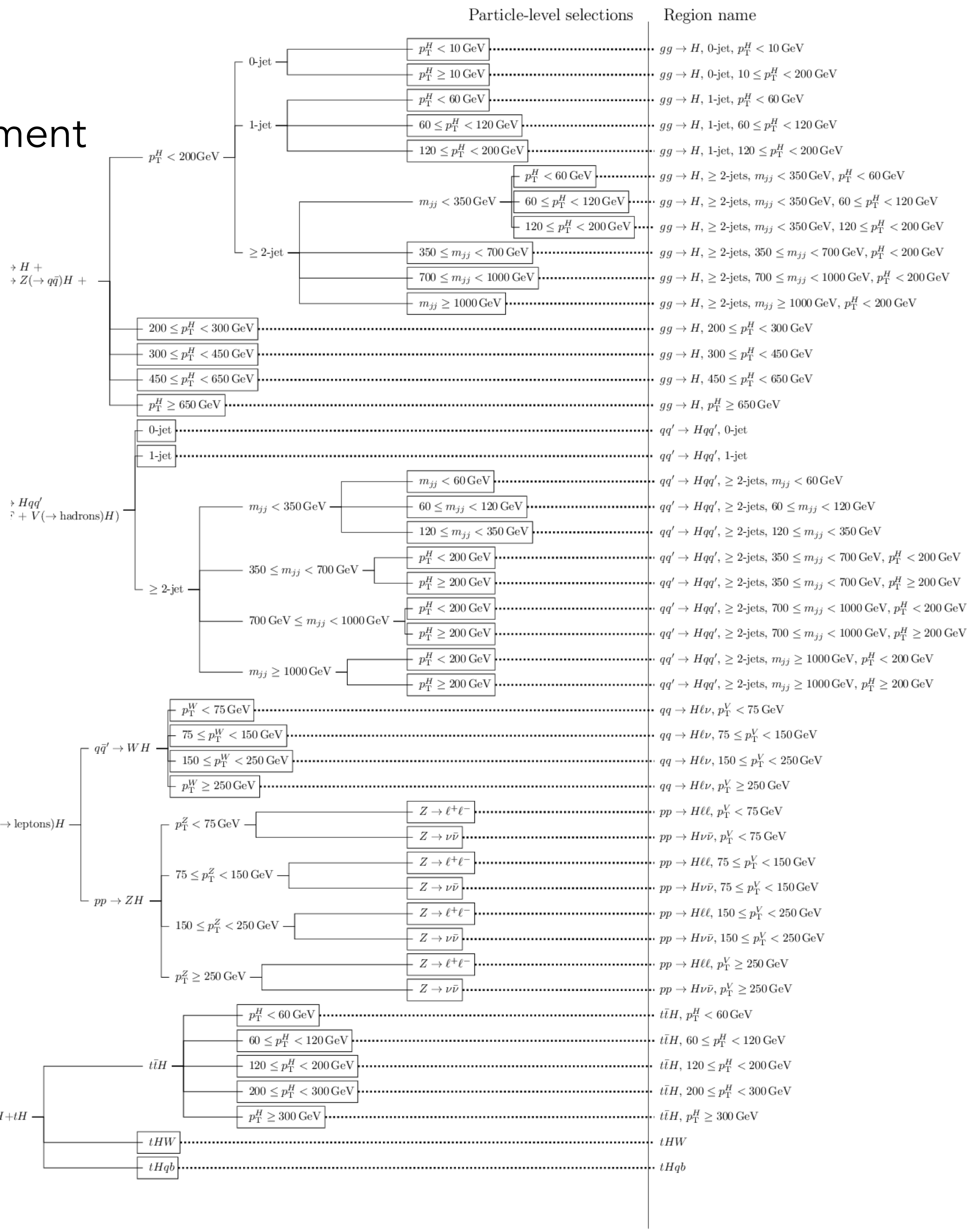

H→γγ (EFT)

Coeff.	Operator	Incl.	Coeff.	Operator	Incl.
c_G	$f^{ABC}G_\mu^{A\nu}G_\nu^{B\rho}G_\rho^{C\mu}$	✓	$c_{qq}^{(3)}$	$(\bar{q}_r\gamma_\mu\tau^I q_r)(\bar{q}_s\gamma^\mu\tau^I q_s)$	✓
c_W	$\epsilon^{IJK}W_\mu^{I\nu}W_\nu^{J\rho}W_\rho^{K\mu}$	✓	$c_{qq}^{(3)\prime}$	$(\bar{q}_r\gamma_\mu\tau^I q_s)(\bar{q}_s\gamma^\mu\tau^I q_r)$	✓
c_H	$(H^\dagger H)^3$		$c_{qq}^{(1)}$	$(\bar{q}_r\gamma_\mu q_r)(\bar{q}_s\gamma^\mu q_s)$	✓
$c_{H\Box}$	$(H^\dagger H)\Box(H^\dagger H)$	✓	$c_{qq}^{(1)\prime}$	$(\bar{q}_r\gamma_\mu q_s)(\bar{q}_s\gamma^\mu q_r)$	✓
c_{HD}	$(H^\dagger D^\mu H)^*(H^\dagger D_\mu H)$	✓	$c_{lq}^{(3)}$	$(\bar{l}_r\gamma_\mu\tau^I l_r)(\bar{q}_s\gamma^\mu\tau^I q_s)$	
c_{HG}	$H^\dagger H\, G^A_{\mu\nu}G^{A\mu\nu}$	✓	$c_{lq}^{(1)}$	$(\bar{l}_r\gamma_\mu l_r)(\bar{q}_s\gamma^\mu q_s)$	
c_{HW}	$H^\dagger H\, W^I_{\mu\nu}W^{I\mu\nu}$	✓	c_{ee}	$(\bar{e}_r\gamma_\mu e_r)(\bar{e}_s\gamma^\mu e_s)$	
c_{HB}	$H^\dagger H\, B_{\mu\nu}B^{\mu\nu}$	✓	c_{eu}	$(\bar{e}_r\gamma_\mu e_r)(\bar{u}_s\gamma^\mu u_s)$	
c_{HWB}	$H^\dagger\tau^I H\, W^I_{\mu\nu}B^{\mu\nu}$	✓	c_{ed}	$(\bar{e}_r\gamma_\mu e_r)(\bar{d}_s\gamma^\mu d_s)$	
c_{eH}	$(H^\dagger H)(\bar{l}_p[Y_e^\dagger]_{pq}e_q H)$	✓	c_{uu}	$(\bar{u}_r\gamma_\mu u_r)(\bar{u}_s\gamma^\mu u_s)$	✓
c_{uH}	$(H^\dagger H)(\bar{q}_p[Y_u^\dagger]_{pq}u_q\widetilde{H})$	✓	c'_{uu}	$(\bar{u}_r\gamma_\mu u_s)(\bar{u}_s\gamma^\mu u_r)$	✓
c_{dH}	$(H^\dagger H)(\bar{q}_p[Y_d^\dagger]_{pq}d_q H)$	✓	c_{dd}	$(\bar{d}_r\gamma_\mu d_r)(\bar{d}_s\gamma^\mu d_s)$	
c_{eW}	$(\bar{l}_p\sigma^{\mu\nu}[Y_e^\dagger]_{pq}e_q)\tau^I H\, W^I_{\mu\nu}$		c'_{dd}	$(\bar{d}_r\gamma_\mu d_s)(\bar{d}_s\gamma^\mu d_r)$	
c_{eB}	$(\bar{l}_p\sigma^{\mu\nu}[Y_e^\dagger]_{pq}e_q)H\, B_{\mu\nu}$		$c_{ud}^{(1)}$	$(\bar{u}_r\gamma_\mu u_r)(\bar{d}_s\gamma^\mu d_s)$	✓
c_{uG}	$(\bar{q}_p\sigma^{\mu\nu}T^A[Y_u^\dagger]_{pq}u_q)\widetilde{H}\, G^A_{\mu\nu}$	✓	$c_{ud}^{(8)}$	$(\bar{u}_r\gamma_\mu T^A u_r)(\bar{d}_s\gamma^\mu T^A d_s)$	✓
c_{uW}	$(\bar{q}_p\sigma^{\mu\nu}[Y_u^\dagger]_{pq}u_q)\tau^I\widetilde{H}\, W^I_{\mu\nu}$	✓	c_{le}	$(\bar{l}_r\gamma_\mu l_r)(\bar{e}_s\gamma^\mu e_s)$	
c_{uB}	$(\bar{q}_p\sigma^{\mu\nu}[Y_u^\dagger]_{pq}u_q)\widetilde{H}\, B_{\mu\nu}$	✓	c_{lu}	$(\bar{l}_r\gamma_\mu l_r)(\bar{u}_s\gamma^\mu u_s)$	
c_{dG}	$(\bar{q}_p\sigma^{\mu\nu}T^A[Y_d^\dagger]_{pq}d_q)H\, G^A_{\mu\nu}$		c_{ld}	$(\bar{l}_r\gamma_\mu l_r)(\bar{d}_s\gamma^\mu d_s)$	
c_{dW}	$(\bar{q}_p\sigma^{\mu\nu}[Y_d^\dagger]_{pq}d_q)\tau^I H\, W^I_{\mu\nu}$		c_{qe}	$(\bar{q}_r\gamma_\mu q_r)(\bar{e}_s\gamma^\mu e_s)$	
c_{dB}	$(\bar{q}_p\sigma^{\mu\nu}[Y_d^\dagger]_{pq}d_q)H\, B_{\mu\nu}$		$c_{qu}^{(1)}$	$(\bar{q}_r\gamma_\mu q_r)(\bar{u}_s\gamma^\mu u_s)$	✓
$c_{Hl}^{(3)}$	$(H^\dagger i\overleftrightarrow{D}^I_\mu H)(\bar{l}_r\tau^I\gamma^\mu l_r)$	✓	$c_{qu}^{(8)}$	$(\bar{q}_r\gamma_\mu T^A q_r)(\bar{u}_s\gamma^\mu T^A u_s)$	✓
$c_{Hl}^{(1)}$	$(H^\dagger i\overleftrightarrow{D}_\mu H)(\bar{l}_r\gamma^\mu l_r)$	✓	$c_{qd}^{(1)}$	$(\bar{q}_r\gamma_\mu q_r)(\bar{d}_s\gamma^\mu d_s)$	✓
c_{He}	$(H^\dagger i\overleftrightarrow{D}_\mu H)(\bar{e}_r\gamma^\mu e_r)$	✓	$c_{qd}^{(8)}$	$(\bar{q}_r\gamma_\mu T^A q_r)(\bar{d}_s\gamma^\mu T^A d_s)$	✓
$c_{Hq}^{(3)}$	$(H^\dagger i\overleftrightarrow{D}^I_\mu H)(\bar{q}_r\tau^I\gamma^\mu q_r)$	✓	c_{ledq}	$(\bar{l}^j_p[Y_l^\dagger]_{pq}e_q)(\bar{d}_r[Y_d]_{rs}q^j_s)$	
$c_{Hq}^{(1)}$	$(H^\dagger i\overleftrightarrow{D}_\mu H)(\bar{q}_r\gamma^\mu q_r)$	✓	$c_{quqd}^{(1)}$	$(\bar{q}^j_p[Y_u^\dagger]_{pq}u_q)\epsilon_{jk}(\bar{q}^k_r[Y_d^\dagger]_{rs}d_s)$	
c_{Hu}	$(H^\dagger i\overleftrightarrow{D}_\mu H)(\bar{u}_r\gamma^\mu u_r)$	✓	$c_{quqd}^{(1)\prime}$	$(\bar{q}^j_p[Y_d^\dagger]_{ps}u_q)\epsilon_{jk}(\bar{q}^k_r[Y_u^\dagger]_{rq}d_s)$	
c_{Hd}	$(H^\dagger i\overleftrightarrow{D}_\mu H)(\bar{d}_r\gamma^\mu d_r)$	✓	$c_{quqd}^{(8)}$	$(\bar{q}^j_p T^A[Y_u^\dagger]_{pq}u_q)\epsilon_{jk}(\bar{q}^k_r T^A[Y_d^\dagger]_{rs}d_s)$	
c_{Hud}	$(H^\dagger iD_\mu H)(\bar{u}_p\gamma^\mu[Y_u Y_d^\dagger]_{pq}d_q)$		$c_{quqd}^{(8)\prime}$	$(\bar{q}^j_p T^A[Y_d^\dagger]_{ps}u_q)\epsilon_{jk}(\bar{q}^k_r T^A[Y_u^\dagger]_{rq}d_s)$	
c_{ll}	$(\bar{l}_r\gamma_\mu l_r)(\bar{l}_s\gamma^\mu l_s)$		$c_{lequ}^{(1)}$	$(\bar{l}^j_p[Y_e^\dagger]_{pq}e_q)\epsilon_{jk}(\bar{q}^k_r[Y_u^\dagger]_{rs}u_s)$	
c'_{ll}	$(\bar{l}_r\gamma_\mu l_s)(\bar{l}_s\gamma^\mu l_r)$	✓	$c_{lequ}^{(3)}$	$(\bar{l}^j_p\sigma^{\mu\nu}[Y_e^\dagger]_{ps}e_q)\epsilon_{jk}(\bar{q}^k_r\sigma_{\mu\nu}[Y_u^\dagger]_{rq}u_s)$	

arXiv:2207.00348

Search for H→ μμ

Phys. Lett. B 812 (2021) 135980

	Selection
Common preselection	Primary vertex Two opposite-charge muons Muons: $\lvert\eta\rvert < 2.7$, $p_T^{lead} > 27$ GeV, $p_T^{sublead} > 15$ GeV (except VH 3-lepton)
Fit Region	$110 < m_{\mu\mu} < 160$ GeV
Jets	$p_T > 25$ GeV and $\lvert\eta\rvert < 2.4$ or with $p_T > 30$ GeV and $2.4 < \lvert\eta\rvert < 4.5$
$t\bar{t}H$ Category	at least one additional e or μ with $p_T > 15$ GeV, at least one b-jet (85% WP)
VH 3-lepton Categories	$p_T^{sublead} > 10$ GeV, one additional e (μ) with $p_T > 15(10)$ GeV, no b-jets (85% WP)
VH 4-lepton Category	at least two additional e or μ with $p_T > 8, 6$ GeV, no b-jets (85% WP)
ggF +VBF Categories	no additional μ, no b-jets (60% WP)

Category	Data	S_{SM}	S	B	$S/\sqrt{B}$	S/B [%]	σ [GeV]
VBF Very High	15	2.81 ± 0.27	3.3 ± 1.7	14.5 ± 2.1	0.86	22.6	3.0
VBF High	39	3.46 ± 0.36	4.0 ± 2.1	32.5 ± 2.9	0.71	12.4	3.0
VBF Medium	112	4.8 ± 0.5	5.6 ± 2.8	85 ± 4	0.61	6.6	2.9
VBF Low	284	7.5 ± 0.9	9 ± 4	273 ± 8	0.53	3.2	3.0
2-jet Very High	1030	17.6 ± 3.3	21 ± 10	1024 ± 22	0.63	2.0	3.1
2-jet High	5433	50 ± 8	58 ± 30	5440 ± 50	0.77	1.0	2.9
2-jet Medium	18 311	79 ± 15	90 ± 50	18 320 ± 90	0.66	0.5	2.9
2-jet Low	36 409	63 ± 17	70 ± 40	36 340 ± 140	0.37	0.2	2.9
1-jet Very High	1097	16.5 ± 2.4	19 ± 10	1071 ± 22	0.59	1.8	2.9
1-jet High	6413	46 ± 7	54 ± 28	6320 ± 50	0.69	0.9	2.8
1-jet Medium	24 576	90 ± 11	100 ± 50	24 290 ± 100	0.67	0.4	2.7
1-jet Low	73 459	125 ± 17	150 ± 70	73 480 ± 190	0.53	0.2	2.8
0-jet Very High	15 986	59 ± 11	70 ± 40	16 090 ± 90	0.55	0.4	2.6
0-jet High	46 523	99 ± 13	120 ± 60	46 190 ± 150	0.54	0.3	2.6
0-jet Medium	91 392	119 ± 14	140 ± 70	91 310 ± 210	0.46	0.2	2.7
0-jet Low	121 354	79 ± 10	90 ± 50	121 310 ± 280	0.26	0.1	2.7
VH4L	34	0.53 ± 0.05	0.6 ± 0.3	24 ± 4	0.13	2.6	2.9
VH3LH	41	1.45 ± 0.14	1.7 ± 0.9	41 ± 5	0.27	4.2	3.1
VH3LM	358	2.76 ± 0.24	3.2 ± 1.6	347 ± 15	0.17	0.9	3.0
$t\bar{t}H$	17	1.19 ± 0.13	1.4 ± 0.7	15.1 ± 2.2	0.36	9.2	3.2

Search for H→cc

Eur. Phys. J. C 82 (2022) 717

Common Selections	
Central jets	≥ 2
Signal jet p_T	≥ 1 signal jet with $p_T > 45$ GeV
c-jets	One or two c-tagged signal jets
b-jets	No b-tagged non-signal jets
Jets	2, 3 (0- and 1-lepton); 2, ≥ 3 (2-lepton)
p_T^V regions	75–150 GeV (2-lepton) > 150 GeV
$\Delta R(\mathbf{jet1}, \mathbf{jet2})$	$75 < p_T^V < 150$ GeV: $\Delta R \leq 2.3$ $150 < p_T^V < 250$ GeV: $\Delta R \leq 1.6$ $p_T^V > 250$ GeV: $\Delta R \leq 1.2$
0 Lepton	
Trigger	E_T^{miss}
Leptons	No *loose* leptons
E_T^{miss}	> 150 GeV
p_T^{miss}	> 30 GeV
H_T	> 120 GeV (2 jets), > 150 GeV (3 jets)
min $\lvert\Delta\phi(\boldsymbol{E}_T^{miss}, \mathbf{jet})\rvert$	$> 20°$ (2 jets), $> 30°$ (3 jets)
$\lvert\Delta\phi(\boldsymbol{E}_T^{miss}, \boldsymbol{H})\rvert$	$> 120°$
$\lvert\Delta\phi(\mathbf{jet1}, \mathbf{jet2})\rvert$	$< 140°$
$\lvert\Delta\phi(\boldsymbol{E}_T^{miss}, \boldsymbol{p}_T^{miss})\rvert$	$< 90°$
1 Lepton	
Trigger	e sub-channel: single electron μ sub-channel: E_T^{miss}
Leptons	One *tight* lepton and no additional *loose* leptons
E_T^{miss}	> 30 GeV (e sub-channel)
m_T^W	< 120 GeV
2 Lepton	
Trigger	Single lepton
Leptons	Exactly two *loose* leptons Same flavour, opposite charge for $\mu\mu$
$m_{\ell\ell}$	$81 < m_{\ell\ell} < 101$ GeV

The shape of the potential matters

Measurements of HH can provide discrimination between different scenarios and models...

Phys. Rev. D 101, 075023

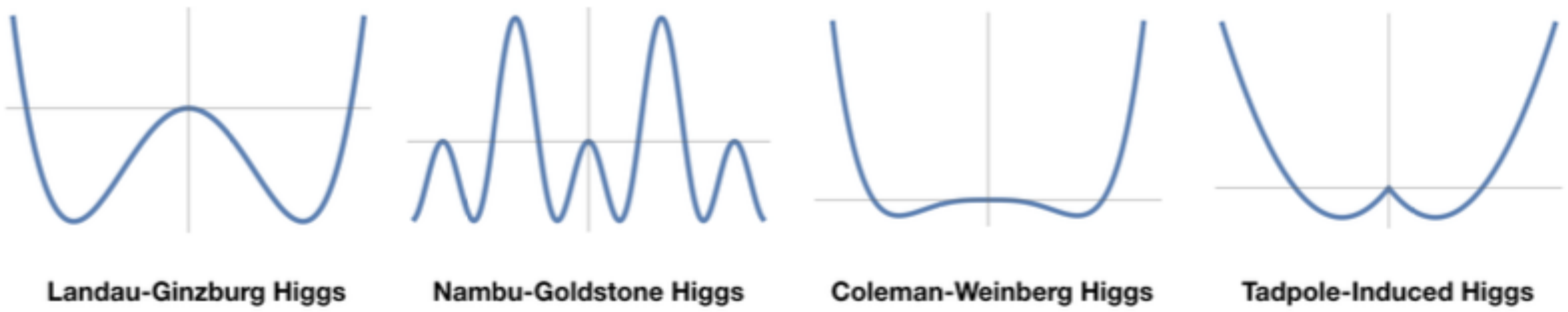

... but measuring triple-Higgs production at a future collider (e.g. 100 TeV machine) will be needed to define the exact shape of the potential.

Search for pair production of third-generation leptoquarks

arXiv:2303.01924 (Submitted to: EPJC)

- selection in $\tau_{lep}\tau_{had}$, $\tau_{had}\tau_{had}$
- PNN inputs consist of a combination of multiplicity, kinematic and angular quantities
  - $b\tau$ invariant mass, the most likely combination of the τ-lepton and a b-jet is chosen based on a mass-pairing strategy that minimises the mass difference between the two resulting LQ candidates

	$\tau_{lep}\tau_{had}$ channel	$\tau_{had}\tau_{had}$ channel
e/μ selection	= 1 'signal' e or μ $p_T^e > 25, 27$ GeV $p_T^\mu > 21, 27$ GeV	No 'veto' e or μ
$\tau_{had\text{-}vis}$ selection	= 1 $\tau_{had\text{-}vis}$ $p_T^\tau > 100$ GeV	= 2 $\tau_{had\text{-}vis}$ $p_T^\tau > 100, 140, 180$ (20) GeV
Jet selection	≥ 2 jets $p_T^{jet} > 45$ (20) GeV 1 or 2 b-jets	
Additional selection	Opposite charge e, μ, τ_{had} and τ_{had} $m_{\tau\tau}^{MMC} \notin 40 - 150$ GeV $E_T^{miss} > 100$ GeV $s_T > 600$ GeV	

Variable	$\tau_{lep}\tau_{had}$ channel	$\tau_{had}\tau_{had}$ channel
$\tau_{had\text{-}vis}$ p_T^0	✓	✓
s_T	✓	✓
N_{b-jets}	✓	✓
$m(\tau, jet)_{0,1}$		✓
$m(\ell, jet)$, $m(\tau_{had}, jet)$	✓	
$\Delta R(\tau, jet)$	✓	✓
$\Delta\phi(\ell, E_T^{miss})$	✓	
E_T^{miss} ϕ centrality	✓	✓

Measurement of tt/Z cross-section ratio at 13.6 TeV

	Category	**Uncert.** [%]		
		$\sigma_{t\bar{t}}$	$\sigma_{Z\to\ell\ell}^{m_{\ell\ell}>40}$	$R_{t\bar{t}/Z}$
$t\bar{t}$	$t\bar{t}$ parton shower/hadronisation	0.6	0.2	0.7
	$t\bar{t}$ scale variations	0.5	0.1	0.5
Z	Z scale variations	0.2	2.9	2.9
Bkg.	Single top modelling	0.6	< 0.01	0.6
	Diboson modelling	0.1	< 0.01	0.5
	Mis-Id leptons	0.6	< 0.01	0.6
Lept.	Electron reconstruction	1.6	2.3	1.1
	Muon reconstruction	1.3	2.4	0.3
	Lepton trigger	0.2	1.3	1.1
Jets/tagging	Jet reconstruction	0.2	< 0.01	0.2
	Flavour tagging	1.9	< 0.01	1.9
	PDFs	0.5	1.4	1.3
	Luminosity	10.3	9.6	1.3
	Systematic Uncertainty	10.8	10.7	4.4
	Statistical Uncertainty	1.5	0.1	1.5
	Total Uncertainty	11	10.7	4.7

Example HL-LHC expectations exceeded

ATL-PHYS-PUB-2014-016

Nature 607, 52-59 (2022)

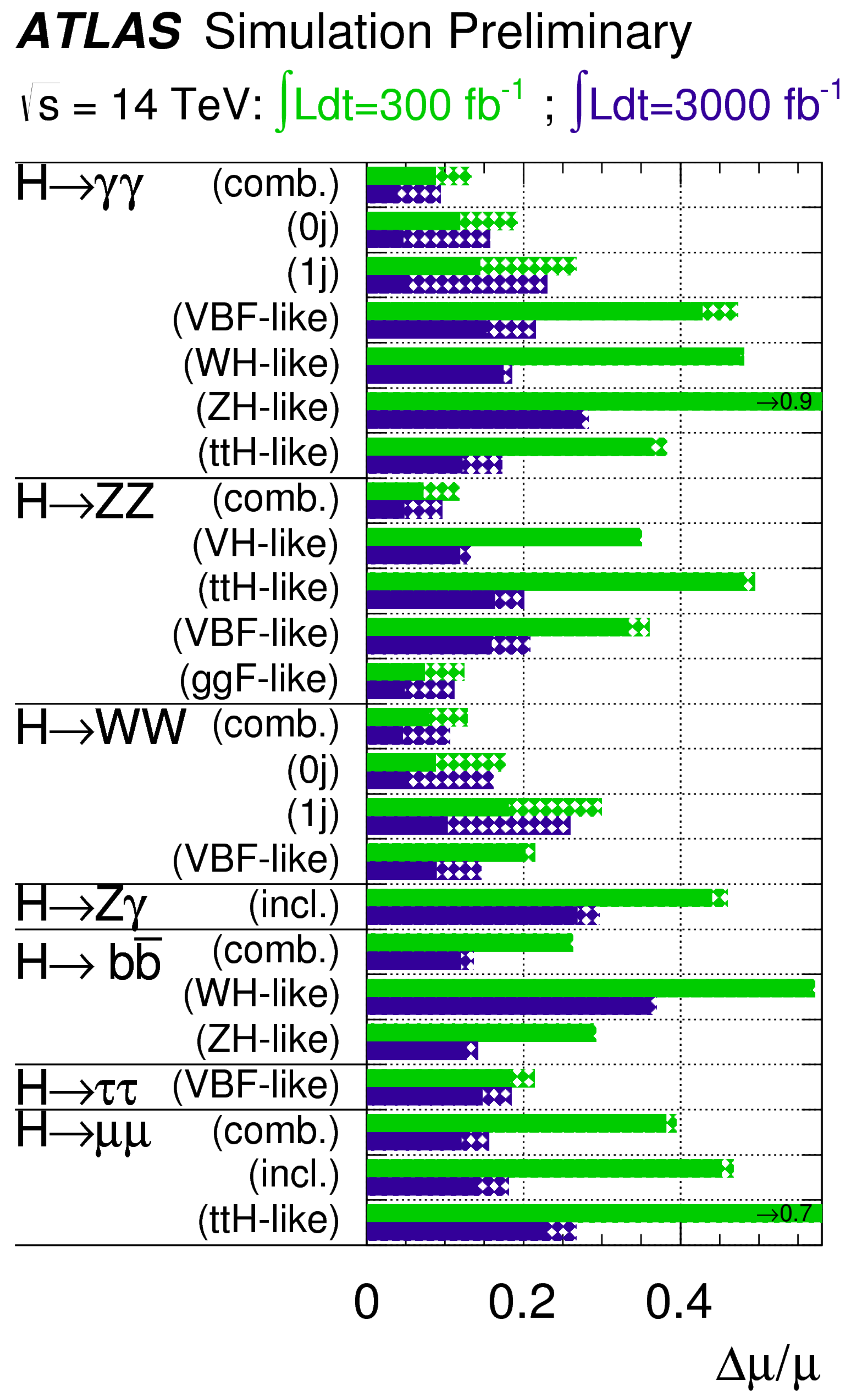

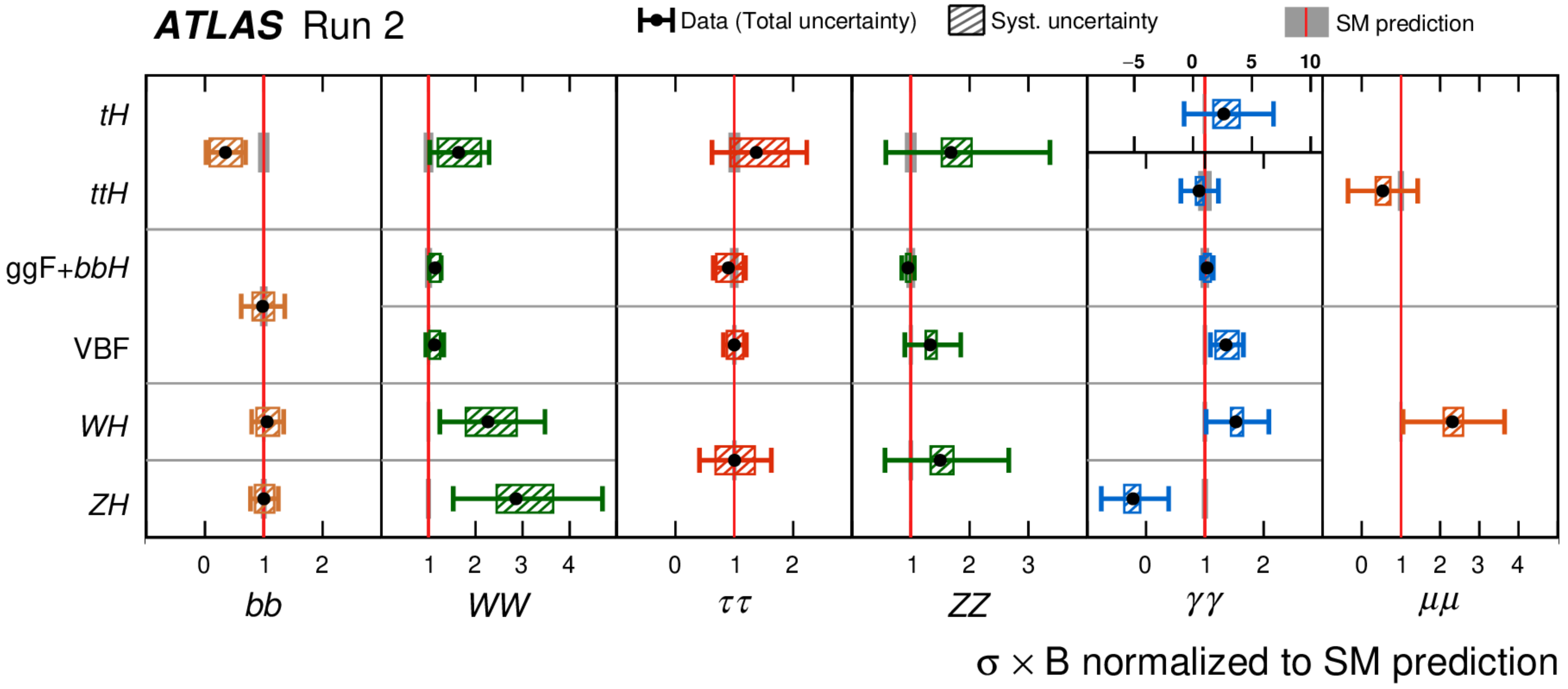

μ = 1.05 ± 0.06

= 1.05 ± 0.03 (stat.) ± 0.03 (exp.) ± 0.04 (sig.th.) ± 0.04 (bkg.th.)

- ATLAS Run 2 results comparable to 2014 HL-LHC projections!

Example HL-LHC sensitivity to κλ

ATL-PHYS-PUB-2022-053

- Combining bbγγ,bbττ,bbbb
  - Baseline - experimental uncertainties scaled, and theory uncertainties halved

Projection studies for H→ bbγγ + bbττ + bbbb

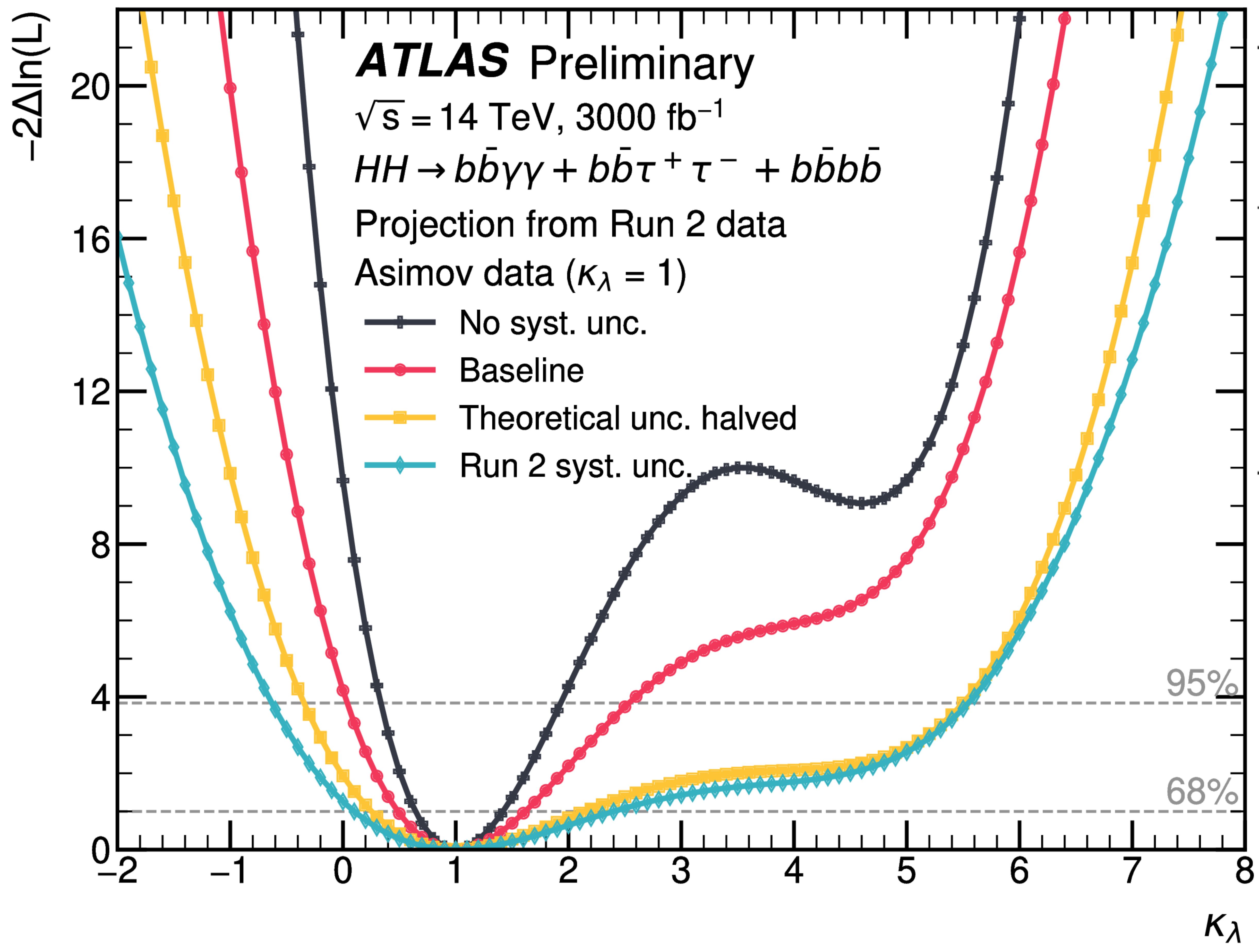

Uncertainty scenario	Significance [σ] $b\bar{b}\gamma\gamma$	$b\bar{b}\tau^+\tau^-$	$b\bar{b}b\bar{b}$	Combination	Combined signal strength precision [%]
No syst. unc.	2.3	4.0	1.8	4.9	−21/+22
Baseline	2.2	2.8	0.99	3.4	−30/+33
Theoretical unc. halved	1.1	1.7	0.65	2.1	−47/+48
Run 2 syst. unc.	1.1	1.5	0.65	1.9	−53/+65

Uncertainty scenario	κ_λ 68% CI	κ_λ 95% CI
No syst. unc.	[0.7, 1.4]	[0.3, 1.9]
Baseline	[0.5, 1.6]	[0.0, 2.5]
Theoretical unc. halved	[0.3, 2.2]	[−0.3, 5.5]
Run 2 syst. unc.	[0.1, 2.4]	[−0.6, 5.6]

Example HL-LHC sensitivity to κ_λ

Summary of the systematic uncertainty scale factors considered HL-LHC baseline scenario.

Source	**HL-LHC Scale Factor**
Experimental Uncertainties	
Luminosity	0.6
Electrons and muons efficiency	1.0
b-jet tagging efficiency	0.5
c-jet tagging efficiency	0.5
Light-jet tagging efficiency	1.0
$\tau_{\text{had-vis}}$ efficiency (statistical)	0.0
$\tau_{\text{had-vis}}$ efficiency (systematic)	1.0
$\tau_{\text{had-vis}}$ energy scale	1.0
Fake-$\tau_{\text{had-vis}}$ estimation	1.0
Jet energy scale and resolution, $E_{\text{T}}^{\text{miss}}$	1.0
κ_λ reweighting	0.0
Theoretical Uncertainties	0.5

- Combining bbγγ,bbττ,bbbb
- Scenarios:
  1. No systematic uncertainties (optimistic)
  2. Baseline - experimental uncertainties scaled, and theory uncertainties halved
  3. Theory uncertainties halved - but with Run2 experimental systematic uncertainties
  4. Run2 systematic uncertainties (conservative)